VANADIUM

Chemistry, Biochemistry, Pharmacology and Practical Applications

R-H   R-X + H$_2$O

XOH

H$^+$, X$^-$

enz(O$_3$N)V(O$_2$)   (O)V(O$_3$N)enz

H$_2$O   H$_2$O$_2$

Alan S. Tracey

Gail R. Willsky

Esther S. Takeuchi

VANADIUM

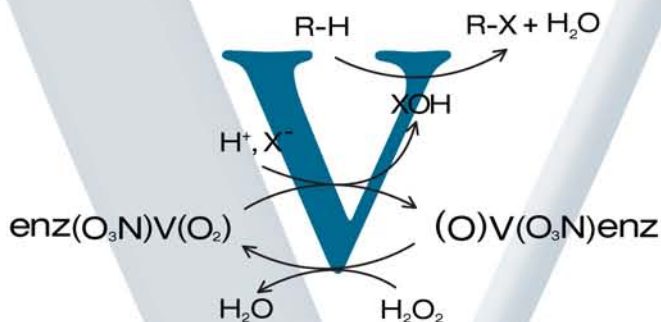**Chemistry, Biochemistry, Pharmacology and Practical Applications**

VANADIUM
Chemistry, Biochemistry, Pharmacology and Practical Applications

Alan S. Tracey
Gail R. Willsky
Esther S. Takeuchi

Preface

This book has evolved from over a quarter-century of research that concentrated on delineating the aqueous coordination reactions that characterize the vanadium(V) oxidation state. At the beginning of this time period, only a minor amount of research was being done on vanadium aqueous chemistry. However, the basic tenets of ^{51}V NMR spectroscopy were being elaborated, and some of the influences of ligand properties and coordination geometry on the NMR spectra were being ascertained. The power of NMR spectroscopy for the study of vanadium speciation had been recognized by only one or two laboratories. This would change, and the demonstration of the great value of this technique for determination of speciation, together with the discovery that vanadium in the diet of rats could be used to ameliorate the influence of diabetes, provided the impetus for rapid growth in this area of science. The discovery of the vanadium-dependent haloperoxidases, the enzymes responsible for a host of biological halogenation and oxidation reactions, added even more impetus for understanding vanadium(V) chemistry, in particular that involving hydrogen peroxide.

This book does not follow a chronological sequence but rather builds up in a hierarchy of complexity. Some basic principles of ^{51}V NMR spectroscopy are discussed; this is followed by a description of the self-condensation reactions of vanadate itself. The reactions with simple monodentate ligands are then described, and this proceeds to more complicated systems such as diols, -hydroxy acids, amino acids, peptides, and so on. Aspects of this sequence are later revisited but with interest now directed toward the influence of ligand electronic properties on coordination and reactivity. The influences of ligands, particularly those of hydrogen peroxide and hydroxyl amine, on heteroligand reactivity are compared and contrasted. There is a brief discussion of the vanadium-dependent haloperoxidases and model systems. There is also some discussion of vanadium in the environment and of some technological applications. Because vanadium pollution is inextricably linked to vanadium(V) chemistry, some discussion of vanadium as a pollutant is provided. This book provides only a very brief discussion of vanadium oxidation states other than V(V) and also does not discuss vanadium redox activity, except in a peripheral manner where required. It does, however, briefly cover the catalytic reactions of peroxovanadates and haloperoxidases model compounds.

The book includes discussion of the vanadium haloperoxidases and the biological and biochemical activities of vanadium(V), including potential pharmacological applications. The last chapters of the book step outside these boundaries by introducing some aspects of the future of vanadium in nanotechnology, the recyclable redox battery, and the silver/vanadium oxide battery. We enjoyed writing this book and can only hope that it will prove to provide at least a modicum of value to the reader.

Acknowledgments

Kenneth J. Takeuchi received his BS degree summa cum laude from the University of Cincinnati in 1975 and his PhD degree in chemistry from Ohio State University in 1981. He spent two years at the University of North Carolina at Chapel Hill conducting postdoctoral research in chemistry. In 1983, he accepted a position as assistant professor of chemistry at the State University of New York at Buffalo; he was granted tenure and promoted to associate professor in 1990 and promoted to professor in 1998. Professor Takeuchi was a consultant with ARCO Chemical for five years and has been a consultant with Greatbatch, Inc. for the past five years. He is an author or coauthor of 75 refereed articles and more than 140 presentations at various scientific meetings. His areas of research include coordination chemistry of ruthenium, ligand effects on transition metal chemistry, electrochemistry, materials chemistry, and battery related chemistry.

Amy Marschilok graduated magna cum laude with a BA degree in chemistry at the State University of New York at Buffalo (UB) in 1999, and was inducted into the Phi Beta Kappa society in 2000. She completed her PhD studies in inorganic chemistry at UB in 2004, and was recognized with the 2004 UB Department of Chemistry Excellence in Teaching Award for Outstanding Teaching Assistant. Since 2004, she has worked as a senior scientist in the Battery Research and Development Group at Greatbatch, Inc. in Clarence, NY. Since 2004, she has also served as a volunteer research assistant at UB, where she assists in training undergraduate student researchers. She is coauthor of ten peer-reviewed articles and 14 research presentations.

Authors

Dr. Alan S. Tracey's research career has concentrated on two major research areas, liquid crystalline surfactant materials and the aqueous chemistry of vanadium(V), with emphasis on biochemical applications. He is the author of 150 scientific publications. He obtained his undergraduate degree in honors chemistry from the University of British Columbia and his doctorate from Simon Fraser University. After postdoctoral fellowships in Brazil, Switzerland, and Australia, he returned to Simon Fraser University. He has recently taken early retirement.

Dr. Gail R. Willsky received a BS degree in biophysics from the Massachusetts Institute of Technology, Cambridge, and her PhD from the microbiology department of Tufts University in Boston. She spent 4 years at Harvard University, Cambridge, Massachusetts, as a National Institutes of Health (NIH) postdoctoral fellow in the biology department and a research associate in biochemistry. Willsky then moved to the biochemistry department at the State University of New York at Buffalo (UB) as an assistant professor and is currently an associate professor in that department. She has been a visiting scientist at the Laboratoire de Genetique, CNRS Strasbourg, France, and in the department of physiology at the University of Southern California School of Medicine.

Her research interests originally focused on biological cell membranes, first working on phosphate transport in *Escherichia coli* and then the plasma membrane proton ATPase in *Saccharomyces cerevisiae.* While isolating vanadate-resistant mutants in yeast, she became fascinated with work showing that oral administration of vanadium salts alleviated symptoms of diabetes and switched her research focus to that area. She has pursued the insulin-enhancing mechanism of vanadium salts and complexes in cell culture, the STZ-induced diabetic rat, and human type 2 diabetic patients. The National Institutes of Health, the American Heart Association, and the American Diabetes Association have funded the work in her laboratory. Willsky has lectured all around the world and published both research articles and book chapters in this area.

Willsky is interested in education and has mentored over 75 high school, undergraduate, medical school, or graduate students in her laboratory, while developing the undergraduate program in biochemistry at UB. She also promotes women in science and is on the Executive Committee of the Gender Institute at the University at Buffalo and is the president of the Buffalo chapter of the Association for Women in Science (AWIS). She has received a Special Achievement Award from the Buffalo Area Engineering Awareness for Minorities group for her work in the Buffalo schools (in partnership with AWIS, the Women's Pavilion Pan Am 2001, and Zonta International), developing a career day program called "Imagine yourself as a scientist!" that is integrated into the middle school curriculum.

Dr. Esther S. Takeuchi is the executive director of Battery Research and Development and the Center of Excellence at Greatbatch, Inc. Since joining Greatbatch, Takeuchi has been active in lithium battery research, particularly researching cells for implantable applications. A main focus has been the development of power sources for implantable cardiac defibrillators. Takeuchi's work has been honored by several organizations. These include the Jacob F. Schoellkopf Award, given by the WNY American Chemical Society for creative research in batteries for medical applications, the Battery Division of the Electrochemical Society Technology Award for development of lithium/silver vanadium oxide batteries, the Community Advisory Council of the State University at Buffalo for outstanding achievement in science, Woman of Distinction as recognized by the American Association of University Women, and the Achievement in Healthcare Award presented by D'Youville College. She is also a fellow of the American Institute for Medical and Biological Engineering, was inducted into the WNY Women's Hall of Fame, and is an inventor credited with 130 patents. In 2004, she was inducted into the National Academy of Engineering.

Prior to joining Greatbatch, Takeuchi received a bachelor's degree from the University of Pennsylvania, with a double major in chemistry and history, and completed a PhD in chemistry at the Ohio State University. She also completed post-doctoral work at the University of North Carolina and the State University of New York at Buffalo.

Table of Contents

1 Introduction

1.1 BACKGROUND

Vanadium is a widely dispersed element that is found in about 65 minerals and generally occurs in low concentrations. Making up about 0.014% of the Earth's crust, it is the fifth-most abundant transition metal. It can be found in deposits with ores of other metals, particularly with a titanium iron magnetite ore and with the uranium ore, carnotite. Relatively high concentrations are found in certain oil and coal deposits, and consequently, they present a significant pollution hazard when such deposits are exploited. In particular, ash from gas- and oil-burning equipment often contains more than 10% vanadium. It is also found at rather high concentrations in some freshwaters and is listed as a metal of concern by the U.S. Environmental Protection Agency. It is found in ocean waters at concentrations of about 30 nmol/L, a value that varies considerably, dependent on region. Vanadium in the metallic state is used, along with other metals, as an additive to iron to form various stainless steels and is a component of some superconducting alloys. Also, it catalyzes the disproportionation of CO to C and CO_2. The vanadium oxide, V_2O_5, is a powerful and versatile catalyst that is used extensively in industrial processes and finding recent application in nanomaterials, whereas peroxovanadates are useful oxidants often used in organic synthesis and found in naturally occurring enzymes, the vanadium-dependent haloperoxidases.

The most common oxidation states of the metal are +2, +3, +4, and +5, although oxidation states of +1, 0, and −1 are well known. The oxidation states +3 through +5 can be maintained in aqueous solution, and these three oxidation states all have known biological significance, even though the function might not be understood.

Until recently, probably the best understood oxidation state of vanadium was V(IV). This situation changed with the advent of high field nuclear magnetic resonance (NMR) spectrometers, which provided the means to obtain a detailed understanding of the V(V) oxidation state. Indeed, the past 2 decades have seen the redrawing of the landscape of V(V) science, particularly where the aqueous phase is involved.

Much of the recent impetus for the studies of vanadium(V) chemistry derives from the fact that there is marked diversity in biochemical activity associated with this oxidation state. Vanadium(V) occurs naturally in vanadium-dependent haloperoxidases, but beyond this, various complexes of V(V) have powerful influences, inhibiting the function of a large range of enzymes and promoting the function of others. Additionally, vanadium oxides have a marked insulin-mimetic or insulin-enhancing effect in diabetic animals. Despite intensive investigation, the specific function or functions of the metal that leads to this behavior are not known. A great deal of research has gone into obtaining highly potent insulin-mimetic

compounds. A number of compounds have essentially the same activity, and this suggests the function is at a level not yet understood. It seems quite likely that the insulin-mimetic effect derives from the simultaneous modification of the function of a number of enzymes and that the role of the ligands is to ensure vanadium is transported effectively to the appropriate sites. The situation is somewhat different with peroxovanadates. These complexes are often exceedingly effective insulin-mimetics, at least in cell cultures. They are good oxidizing agents and function by means of an oxidative mechanism. However, unless selectivity of function can be built into them, they will probably not achieve success in animal models.

The potentially serious aspects of vanadium pollution, the function of biologically occurring enzyme systems, the role of vanadium on the function of numerous enzymes, and the associated role in the insulin-mimetic vanadium compounds are inextricably linked. The key to our understanding all such functionality relies on understanding the basic chemistry that underlies it. This chemistry is determined to a significant extent by the V(IV) and V(V) oxidation states but clearly is not restricted to these states. Indeed, the redox interplay between the vanadium oxidation states can be a critical aspect of the biological functionality of vanadium, particularly in enzymes such as the vanadium-dependent nitrogenases, where redox reactions are the basis of the enzyme functionality.

1.1.1 VANADIUM(V)

The V(V) oxidation state is the major focus of this book, which concentrates particularly on the aqueous chemistry of the V(V) oxoanion, vanadate, but also describes applications in biochemistry, pharmacology, and technology. The chemistry described includes the self-condensation reactions of vanadate and its reactions with a number of mono- and oligodentate ligands and the associated coordination geometries. Mixed ligand chemistry is of particular interest and is an integral part of this discussion. Various aspects of the coordination chemistry are then drawn together, and it is shown that electron-donating properties of ligands have a significant and systematic influence on vanadium coordination and reactivity. Vanadium in its higher oxidation states has a significant effect on numerous biological processes and has various biological, nutritional, and pharmacological influences, including potential applications in treating diabetes and cancer. Possible mechanisms leading to this behavior are described. The vanadium-dependent haloperoxidases are briefly discussed, and model compounds that mimic some of the functionality of these enzymes are described. Also covered is the distribution of vanadium in the biosphere and its occurrence in terrestrial and marine organisms.

Developing technologies in vanadium science provide the basis for the last two chapters of this book. Vanadium(V) in various forms of polymeric vanadium pentoxide is showing great promise in nanomaterial research. This area of research is in its infancy, but already potential applications have been identified. Vanadium-based redox batteries have been developed and are finding their way into both large- and small-scale applications. Lithium/silver vanadium oxide batteries for implantable devices have important medical applications.

1.1.2 VANADIUM(II), (III), AND (IV)

The V(II), V(III), and V(IV) vanadium oxidation states are not discussed in detail in this book. These oxidation states have an important and well-developed chemistry, and additionally, all have biological significance. Perhaps the most widely recognized function associated with these oxidation states is the accumulation of vanadium by ascidians where vanadium, in its V(V) oxidation state, is enriched by means of a reductive mechanism by a factor of six orders of magnitude from its concentration in seawater and incorporated as V(III) into modified blood cells called vanadocytes. There are extensive research programs directed toward understanding the biochemistry and biological significance of V(III) both in the marine tunicates [1–3] and the polychaete worms [4]. The most important biochemical role of these oxidation states may lie in their utilization in nitrogen-fixing enzymes. Both the V(III) and V(II) oxidation states have a critical function in the redox cycling of the vanadium-dependent nitrogenases. These serve as alternative nitrogen-fixing enzymes to the more prevalent molybdenum-based systems. These nitrogenases function in situations where molybdenum is deficient, but even more importantly, they are more efficient than the molybdenum enzyme when the ambient temperature is significantly reduced [5,6]. It seems likely that they play an important role in arctic and alpine environments.

The V^{2+} (aq) oxidation state is not stable in aqueous solution. The redox potential of V^{2+} (aq) is such that hydrogen ions will be reduced to hydrogen and V^{3+}(aq) formed. However, under reducing conditions, the V(II) state can be maintained. The aqua V^{2+} ion is octahedrally coordinated with six water ligands, and octahedral coordination is characteristic of this oxidation state. The nitrogen functionality, as found, for instance, in diamines [7] and pyridines [8], provides a good ligating center and serves well as a functional group in multidentate ligands. Up to four pyridines can be complexed to a V(II) center. The complexation of pyridine is stepwise and quite favorable. One molar equivalent of pyridine reacts with vanadium(II) in aqueous solution, with a formation constant of 11 M^{-1} [8]. This compares with a very weak interaction with V(V), where a bispyridine complex is observable only under high pyridine concentrations [9].

Unlike V(II), both the V(III) and V(IV) oxidation states are stable in water. However, neither the V(III) nor the V(IV) oxidation states are easily maintained in the presence of oxygen if the pH is neutral or above, although, under acidic conditions, both these states are rather easily maintained. Somewhat surprisingly, the V(IV) species is more readily oxidized by O_2 than is the V(III) species. In aqueous acidic solution, the vanadium(III) ion exists as a hexaqua octahedral complex that can deprotonate to form the 2+ and 1+ species, dependent on pH. Additionally, di, tri and tetra polymeric forms are known. Structures have been proposed and their formation constants determined [10]. The occurrence of the various polymeric forms in the presence of sulfate has also been described and is particularly relevant to concentration of vanadium by bioaccumulators [10].

Complexes of vanadium(III) typically have octahedral coordination, though other coordinations are certainly not unusual, particularly with bulky ligands where trigonal bipyramidal coordination is adopted. Nitrogen- and oxygen-containing mul-

tidentate ligands such as aminopolycarboxylates are common ligands that strongly complex V(III) [11]. Complexes of such ligands are generally monomeric, but with some ligands of appropriate structure, dimeric structures are formed. Dimerization is known to occur through oxygen to give oxo-bridged dimers. However, with appropriate tridentate ligands containing an alkoxo ligating group, dimerization can occur through two bridging alkoxo oxygens to give a cyclic [VO]$_2$ core. Sulfur-containing ligands are well known to be complexed by vanadium(III). Thiolates, for instance, are good complexation agents [12,13], whereas vanadium(III)-sulfide polymers are formed during the desulfurization of crude oils.

Sulfate itself complexes V(III) and, together with appropriate V(III) ligands such as oxalate, can form crystalline V(III)-sulfate polymers, where the sulfate acts as a bidentate bridging ligand [11]. Although the polymer dissociates in solution to predominantly give the bisoxalato V(III) complex, some sulfate complexes still occur. With ligands other than oxalate, such as with aminopyridines, sulfate complexation is much more highly favored, and it may complex either in monodentate or bidentate fashion. Vanadium is also locked into the catalytic site of the vanadium nitrogenases by iron/sulfur bonds, where V(III) is involved in the redox cycle of this enzyme. There is considerable electron delocalization within [VFe$_3$S$_4$]$^{2+}$ clusters, which makes it difficult to definitively assign the vanadium oxidation state. It is, however, most consistent with the V(III) state [14]. Unlike the V(IV) and V(V) oxidation states, strong Voxo bonds do not dominate the aqueous chemistry of V(III).

Aqua vanadium(IV), like its counterparts V(III) and V(V), exists in various ionic states dependent on the pH, including VO(H$_2$O)$_5$$^{2+}$, VO(OH)(H$_2$O)$_4$$^{+}$, and the dimer, (VOOH)$_2$(H$_2$O)$_n$$^{2+}$. In these cationic forms, which occur under acidic conditions, V(IV) is highly water soluble. However, under mildly acidic conditions, about pH 4, where it is largely non-ionic, it forms a hydrous oxide VO$_2$·nH$_2$O (K$_{sp}$ ≈ 10^{-22}) that is very insoluble and precipitates from solution, thus limiting the solution concentrations to low values. It has, however, been suggested that V$_2$O$_4$ is even more insoluble [15]. Under basic conditions, the oxide can be redissolved to form the anionic species, VO(OH)$_3$$^{-}$. Apparently, this compound is electron paramagnetic resonance (EPR) silent, which suggests it is at least a dimeric material.

The VO^{2+} moiety is critically important to the chemistry of vanadium(IV). The V=O bond is strong, typically having a bond length of about 1.6 Å, a value similar to that found in the V(V) oxide. Vanadium(IV) does not readily relinquish the bond to oxygen, and the strength of this bond has a direct bearing on heteroligand coordination. It has a strong influence on the position of attachment of ligating groups and consequently on ligand orientation within V(IV) complexes. Square pyramidal complexation is a favored coordination mode, with the VO bond projecting vertical to the plane of the remaining coordinating atoms. The open position opposite the VO bond provides a site for complexation by strongly complexing ligands so that six-coordinate species can form.

Mono-, di-, tri-, and tetradentate ligands of various types readily form complexes with VO^{2+}. Typical ligating functional groups are *O*, *N*, and *S*, so it is not surprising that this oxidation state of vanadium has been found to have a strong influence in biochemical systems. Such biochemically relevant ligands as oxidized and reduced glutathione, ascorbic acid, nucleotides, and monosaccharides are all good complex-

ation agents [16,17]. A detailed synopsis of the coordination chemistry of V(IV) that discusses the formation and structural properties of numerous V(IV) complexes is available [18]. Details of the structure of many paramagnetic complexes are difficult to obtain, particularly so if crystalline compounds cannot be prepared for x-ray analysis. This problem has been solved to an extent by utilization of frozen solutions in electron nuclear double resonance (ENDOR) spectroscopy. This technique allows the accurate measurement of hyperfine couplings and, because these couplings are dependent on distances between interacting nuclei, provides detailed structural information. Application of this experimental technique has been discussed in detail for a variety of V(IV) complexes, including those formed from ligands such as nucleotides, amino acids, porphyrins, and other organic compounds [19].

REFERENCES

1. Ueki, T., N. Yamaguchi, and H. Michibata. 2003. Chloride channel in vanadocytes of a vanadium-rich ascidian *Ascidia sydneiensis samea*. *Comp. Biochem. Physiol. B: Biochem. Mol. Biolog.* 136:91–98.
2. Michibata, H., T. Uyama, and K. Kanamori. 1998. The accumulation mechanism of vanadium by ascidians. In *Vanadium compounds. Chemistry, biochemistry and therapeutic applications*, A.S. Tracey and D.C. Crans (Eds.), American Chemical Society, Washington, D.C., pp. 248–258.
3. Smith, M.J., D.E. Ryan, K. Nakanishi, P. Frank, and K.O. Hodgson. 1995. Vanadium in ascidians and the chemistry of tunichromes. In *Vanadium and its role in life*. H. Sigel and A. Sigel (Eds.), Marcel Dekker, Inc., New York, pp. 423–490.
4. Ishii, I., I. Nakai, and K. Okoshi. 1995. Biochemical significance of vanadium in a polychaete worm. In *Vanadium and its role in life.* H. Sigel and A. Sigel (Eds.), Marcel Dekker, Inc., New York, pp. 491–509.
5. Miller, R.W. and R.R. Eady. 1988. Molybdenum and vanadium nitrogenases of Azotobacter chroococcum. Low temperature favours N_2 reduction by vanadium nitrogenase. *Biochem. J.* 256:429–432.
6. Eady, R.R. 1990. Vanadium nitrogenases. In *Vanadium in biological systems*. N.D. Chasteen (Ed.), Kluwer Academic Publishers, Dordrecht, pp. 99–127.
7. Niedwieski, A.C., P.B. Hitchcock, J.D. DaMotta Neto, F. Wypych, G.J. Leigh, and F.S. Nunes. 2003. Vanadium(II)-diamine complexes: Synthesis, UV-Visible, infrared, thermogravimetry, magnetochemistry and INDO/S characterisation. *J. Braz. Chem. Soc.* 14:750–758.
8. Frank, P., P. Ghosh, K.O. Hodgson, and H. Taube. 2002. Cooperative ligation, backbonding, and possible pyridine-pyridine interactions in tetrapyridine-vanadium(II): A visible and x-ray spectroscopic study. *Inorg. Chem.* 41:3269–3279.
9. Galeffi, B. and A.S. Tracey. 1989. 51-V NMR investigation of the interactions of vanadate with hydroxypyridines and pyridine carboxylates in aqueous solution. *Inorg. Chem.* 28:1726–1734.
10. Meier, R., M. Boddin, S. Mitzenheim, and K. Kanamori. 1995. Solution properties of vanadium(III) with regard to biological systems. *Met. Ions Biolog. Syst.* 31:45–88.
11. Kanamori, K. 2003. Structures and properties of multinuclear vanadium(III) complexes: Seeking a clue to understand the role of vanadium(III) in ascidians. *Coord. Chem. Rev.* 237:147–161.

12. Money, J.K., K. Folting, J.C. Huffman, and G. Christou. 1987. A binuclear vanadium(III) complex containing the linear $[VOV]_{4+}$ unit: Preparation, structure, and properties of tetrakis(dimethylaminoethanethiolato)oxodivanadium. *Inorg. Chem.* 26:944–948.

13. Hsu, H.F., W.C. Chu, C.H. Hung, and J.H. Liao. 2003. The first example of a seven-coordinate vanadium(III) thiolate complex containing the hydrazine molecule, an intermediate of nitrogen fixation. *Inorg. Chem.* 42:7369–7371.

14. Carney, M.J., J.A. Kovacs, Y.-P. Zhang, G.C. Papaefthymiou, K. Spartalian, R.B. Frankel, and R.H. Holm. 1987. Comparative electronic properties of vanadium-iron-sulfur and molybdenum-iron-sulfur clusters containing isoelectronic cubane-type $[VFe_3S_4]^{2+}$ and $[MoFe_3S_4]^{3+}$ cores. *Inorg. Chem.* 26:719–724.

15. Baes, C.F. and R.E. Mesmer. 1976. *The hydrolysis of cations.* Wiley Interscience, New York, pp. 193–210.

16. Baran, E.J. 1995. Vanadyl(IV) complexes of nucleotides. *Met. Ions Biolog. Syst.* 31:129–146.

17. Baran, E.J. 2003. Model studies related to vanadium biochemistry: Recent advances and perspectives. *J. Braz. Chem. Soc.* 14:878–888.

18. Maurya, M.R. 2003. Development of the coordination chemistry of vanadium through bis(acetylacetonato)oxovanadium(IV): Synthesis reactivity and structural aspects. *Coord. Chem. Rev.* 237:163–181.

19. Makinen, M.W. and D. Mustafi. 1995. The vanadyl ion: Molecular structure of coordinating ligands by electron paramagnetic resonance and electron nuclear double resonance. *Met. Ions Biolog. Syst.* 31:89–127.

2 Vanadate Speciation

2.1 TECHNIQUES

Traditionally, the principal tools for the study of vanadate speciation in aqueous solution were UV/vis and electrochemistry. Unfortunately, the complex chemistry associated with vanadate has rendered much, but certainly not all, of the earlier work obsolete. The reaction solutions often contained numerous products that, *a priori,* could not be specified. Properly describing the chemistry was somewhat like doing a jigsaw puzzle without knowing what the pieces looked like or how many there were. Only with the advent of ^{51}V NMR spectroscopy in high field NMR spectrometers was there a tool in place that allowed a coherent picture of V(V) chemistry to be fully developed. The combination of potentiometry with NMR spectroscopy has proven a certain winner. Additionally, x-ray diffraction studies have provided an invaluable source of information, but it is information that, in all cases, must be used with extreme caution when attempting to describe the chemistry in solution.

Utilization of potentiometry in the study of complex equilibria is hindered by the fact that the observed electrode response derives from all reactions occurring in solution. Characterization of the system relies on the influences of hydrogen ion and reactant concentration on the measured voltage. The chemical system is then modeled and the observations compared with those expected for the model adopted. It is not unusual that there are weak differential responses for specific equilibria so that the solution potential does not adequately differentiate between alternate equilibria, and thus potentiometry might only poorly define the system. UV/vis is basically a very poor-resolution technique that often is unusable for studying equilibria if the system is at all complex. For less-complex systems, it can provide useful information and, in certain circumstances where multiple reactions are limited, can be particularly valuable, such as in the study of tight binding ligands where very dilute reactants are required in order to probe the equilibrium reaction.

An indirect method of gathering information about solution structures is provided by electrospray ionization/mass spectrometry. This technique involves ejection of a droplet of solution into an electric field chamber. As the droplet is being ejected, it becomes highly charged and essentially explodes into numerous very small charged droplets of about 10 μm in diameter. These small droplets rapidly evaporate and, in the process, release charged ions that are drawn into the inlet of a mass spectrometer. Analysis of the resultant fragmentation data provides details of molecular weight and structure. For complexes that undergo chemical changes during a millisecond or so timescale, acidity and concentration changes within the evaporating droplet can present problems in interpretation. Diligence in recognizing such factors is key to this application. This technique has proven very valuable for the study of vanadium complexes, where it has been used principally to probe model haloperoxidases complexes based on peroxovanadates [1,2]. It is reasonable to turn the argument around and use the

evidence obtained for transient species to provide evidence for possible reaction pathways, for instance, for mechanisms of oxidation by peroxovanadates.

Vanadium-51 NMR spectroscopy is generally the method of choice for studying complex equilibria or obtaining structural data. In principle, and frequently in practice, signals for all reactant and product species are observable. An NMR spectrum showing the spectral dispersion that is typical for this nucleus is shown Figure 2.1. Variation of pH or reactant concentrations usually allows an unambiguous interpretation of the information inherent in such spectra. Combination of NMR with potentiometry adds a significant degree of accuracy and redundancy to the NMR studies. This hybrid technique is particularly powerful when there is signal overlap in the NMR spectra or when certain equilibria are highly favored so that some reactant or product concentrations are poorly defined by NMR. Potentiometry is without peer when ligated ligands have noncomplexed sidechains that undergo protonation/deprotonation reactions. Such reactions often will not be easily characterized by NMR studies alone.

Although NMR is a notoriously insensitive technique, vanadium is a highly responsive nucleus, and it is quite feasible to get spectra from a few micromolar concentration of vanadium in solution. Frequently, there is no necessity for such low concentrations, and more typically NMR studies utilize 0.5 mM, and above, total vanadium concentrations.

2.1.1   VANADIUM-51 NMR SPECTROSCOPY

Vanadium-51 is a spin 7/2 nucleus, and consequently it has a quadrupole moment and is frequently referred to as a quadrupolar nucleus. The nuclear quadrupole moment is moderate in size, having a value of -0.052×10^{-28} m^2. Vanadium-51 is about 40% as sensitive as protons toward NMR observation, and therefore spectra are generally easily obtained. The NMR spectroscopy of vanadium is influenced strongly by the quadrupolar properties, which derive from charge separation within the nucleus. The quadrupole moment interacts with its environment by means of electric field gradients within the electron cloud surrounding the nucleus. The electric field gradients arise from a nonspherical distribution of electron density about the
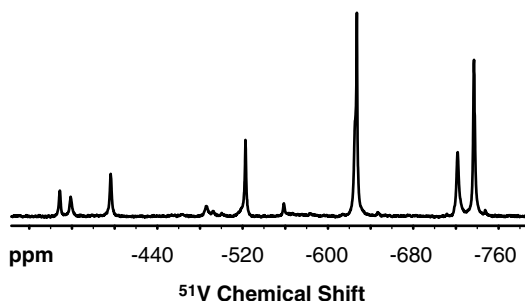
FIGURE 2.1 ^{51}V NMR spectrum showing aqueous vanadate in the presence of *N,N*-dimethylhydroxylamine and dithiothreitol. The wide spectral dispersion of the signals is characteristic of vanadium NMR spectra.

nucleus, and therefore they are influenced by ligating groups. If the electron density symmetry at the nucleus is tetrahedral or higher, the electric field gradients are zero, and there is no quadrupolar interaction.

The coordination geometry is, however, often not a good delineator of electric field gradients. Ostensibly high-symmetry molecules can give rise to significant electric field gradients at the nucleus, whereas the opposite situation may arise for low-symmetry molecules. Probably the best known, though perhaps not recognized, example of the latter behavior is the sharp NMR signals normally observed for bisperoxovanadate complexes, which typically have a pentagonal pyramidal geometry. Generally, though, it can be expected that for compounds of similar molecular weights, those with tetrahedral or higher symmetry will have sharper signals than less-symmetrical species.

The influence of the quadrupole is exhibited by efficient nuclear relaxation and, thus, broadened signals in the NMR spectrum. Because the electric field gradients will be different for every complex, signals of varying linewidth are typical of vanadium NMR spectroscopy. The variation may be small, as shown in Figure 2.1, or may be much larger, as is evident in Figure 2.2. The quadrupolar relaxation is moderated by the tumbling rate of the compound in question, so low-viscosity solvents tend to give rise to higher quality spectra. A corollary of this is that one has to be very careful in interpreting variable temperature data. Changes in linewidth as a function of temperature may well have their origin in quadrupole interactions rather than in chemical exchange. This can easily be true even if some signals within the spectrum do not undergo significant changes. Whenever possible, two-dimensional exchange spectroscopy (EXSY) should be employed to characterize exchanging systems.

Because of rapid, quadrupole-induced relaxation, NMR signals frequently are 200 or 300 Hz wide or more. This is not as severe a problem as it may at first appear because vanadium-51 has a large chemical shift range of about 3000 ppm. As illustrated in Figure 2.2, the line widths shown vary from about 130 to 1000 Hz (1.3 to 10.0 ppm with a 400 MHz spectrometer), yet the spectrum is well resolved. The fast relaxation does mean that spectra can be accumulated very rapidly. Only in atypical situations will 20 or 30 accumulations per second lead to problems of
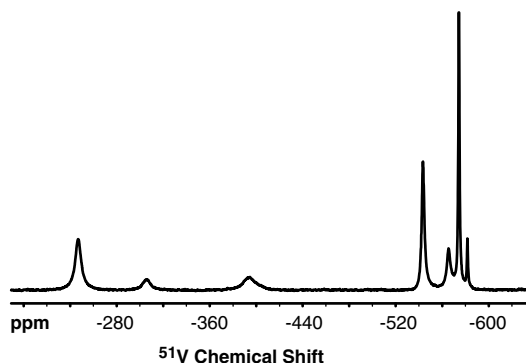
FIGURE 2.2 ^{51}V NMR spectrum showing vanadate in the presence of cysteine at pH 8.4. Signals of varying linewidth are frequently found in vanadium spectra.

perturbed signal intensity. Difficulties with very broad lines often arise if the species of interest have a high molecular weight or the solvents are of high viscosity. Both such situations slow the tumbling of the vanadium nucleus and increase the rates of quadrupole-induced relaxation. Under such conditions, it is possible that the signals are so broad that they cannot easily be observed. Molecules that for one reason or another have very large electric field gradients about the nucleus might also give atypically broad lines even in low-viscosity solvents.

It can generally be expected that spectra from samples of about 1 mmol/L concentration will be obtained within a short period of time. Spectra corresponding to concentrations of 10 or so µmol/L can be detected within a few hours if the signals are not excessively broad. Because of the linewidths of the signals, small data set sizes can routinely be used when acquiring and processing the spectra. Optimum signal to noise in a processed spectrum is obtained with a matched filter. Therefore, line-broadening factors corresponding to the linewidth at half height of the sharpest signal in the spectrum should be used. Typically, a line-broadening factor of 40 or 50 Hz serves well. When there is good signal to noise, resolution enhancement by means of a Lorentzian to Gaussian transform can provide useful information in situations where signals are partially resolved.

As a result of the short relaxation times of most vanadate species, ^{51}V 2D exchange spectroscopy is limited to dynamic processes that occur within a few tens of milliseconds. This timescale is conveniently lengthened to 1 sec or longer in cases where proton (or other) NMR spectroscopy can be employed, for instance, in ligand exchange reactions.

Because vanadium-51 has a spin of 7/2, the NMR signal generally observed is actually a composite seven-part signal deriving from transitions between all the nuclear spin states as defined by the selection rule that $\Delta m = \pm 1$. For typical solution spectra, the nuclear relaxation corresponding to the individual transitions of each chemically distinct nucleus is more or less the same, and correspondingly broadened signals are observed. However, in the slow-motion regime, the nature of the relaxation pathways between the various spin states can lead to a situation in which all transitions other than that corresponding to the $-1/2$ to $+1/2$ transition are broadened beyond observation. This occurs when the nuclear tumbling is greatly slowed, as found when vanadium is bound to proteins. This leads to the possibility of using vanadium NMR spectroscopy to directly observe and characterize complexation to proteins [3,4].

The chemical shift reference standard for ^{51}V NMR spectroscopy is $VOCl_3$, which provides a sharp signal either as a neat liquid or in nonreactive organic solvents. Unfortunately, it is not a nice compound to work with and is hydrolytically unstable. Generally, oxovanadium trichloride is used as an external reference as the neat liquid. An alternative is to calibrate a secondary reference such as a vanadate solution at pH 8 and use the signal from tetravanadate as the secondary reference frequency. Except for the preliminary calibration, this eliminates the possibility of breaking the sample of $VOCl_3$ in the NMR probe. Additionally, unless the magnetic field or the radio frequencies of the spectrometer drift significantly, the broad signals of vanadate complexes mean that little is gained by locking or even shimming the

magnet. Samples can then be prepared in protonated solvents and the spectra obtained in an unlocked mode of acquisition. This greatly expedites sample turn-around time. Note that when running in unlocked mode, the magnet cannot be shimmed, because the shim coils alter the magnetic field strength and the chemical shift calibration will then be incorrect.

There is a direct relationship between the electronegativity of ligating groups and the chemical shift. The relationship is similar for four, five, or six coordinate complexes with chemical shifts moving to higher field with increased substituent electronegativity [5]. Although apparently this is true when using a gross scale of electronegativity, it is not necessarily true when looked at under a finer scale within a series of homologous compounds, as for instance in alkyl alcohols (see Section 9.1). Also, ligands such as catechols, which give rise to low energy charge transfer bands, have a large influence on the electronic environment about the nucleus and consequently strongly influence vanadium chemical shifts. Correlations, based on the Ramsey formulation, clearly show the relationship between such charge transfer transitions and the observed chemical shifts [6].

Vanadium undergoes J-coupling interactions when suitably substituted. The interactions are often not large or are decoupled by fluctuations in the quadrupole interaction. An example of such a coupling is the ^{17}O to ^{51}V J-coupling in the vanadate trianion, which is 62 Hz [7]. J-couplings have been used in the assignment of NMR signals to complexes occurring in solution. A particularly nice example of this is found in a study of peroxovanadates, where the V to V J-coupling was used in 2D correlation spectroscopy (COSY) spectra to assign vanadium signals to the pairs of vanadiums in asymmetrically substituted peroxo divanadates [8].

2.1.2 pH-Dependence of Vanadium Chemical Shifts

A common characteristic of vanadium NMR spectra is that chemical shifts vary with pH. The source of this behavior is generally an equilibrium reaction that is dependent on pH. Such equilibria can involve ligand reactions, but generally these are slow on the ^{51}V NMR timescale. However, an equilibration that is almost always fast is the protonation/deprotonation reaction. Exceptions that might be observed will generally involve changes in coordination geometry that accompany the changes in protonation state. This equilibrium can be critical to the solution chemistry that is observed and can be written simply, as in Equation 2.1, for a generic vanadate complex, VLH.

$$\text{VLH} \rightleftharpoons \text{VL}^- + \text{H}^+ \quad [\text{VLH}]K_a = [\text{VL}^-][\text{H}^+] \qquad (2.1)$$
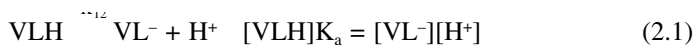
The ^{51}V NMR spectrum for this equilibrium will be characterized by a low pH limiting value, a high pH limiting value, and a pH region where the chemical shift will be sensitive to the pH of the solution. Scheme 2.1 provides a sketch of this behavior. It is evident that the chemical shift is determined by the limiting chemical shifts and the acidity constant (K_a) of VLH. This relationship can be inverted and the pH-dependence of the chemical shift used to provide the $-\log K_a$ (pK_a) of the complex of interest, as described by Equation 2.2.

$$\text{low pH} \quad \begin{matrix} \delta_l \\ | \end{matrix} \quad \bigwedge \delta_{obs} \qquad \begin{matrix} \delta_h \\ | \end{matrix} \quad \text{high pH}$$

$$\text{VLH} \qquad\qquad\qquad \text{VL}^-$$
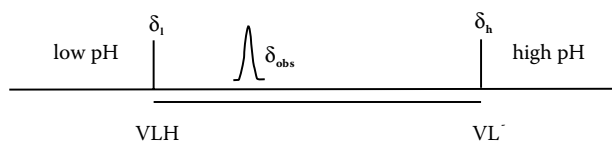
$$P(\text{VLH}) = (\delta_h - \delta_{obs})/(\delta_h - \delta_l) \qquad (P\text{VL}^-) = (\delta_{obs} - \delta_l)/(\delta_h - \delta_l)$$

SCHEME 2.1

In Scheme 2.1, P(VLH) and P(VL⁻) represent the molar fractions of the two species.

$$pH = \log((\delta_{obs} - \delta_l) / (\delta_h - \delta_{obs})) + pK_a \qquad (2.2)$$

From a pH-variation study, a plot of pH versus $\log((\delta_{obs} - \delta_l) / (\delta_h - \delta_{obs}))$ will then provide a graph with an intercept equal to the pK_a of the complex. Note that Equation 2.2 has a slope of 1. This is a useful property of this equation, as it provides a convenient check on the accuracy or interpretation of the titration experiment and can be utilized when analyzing the results of an experiment where only a partial titration curve is obtained.

A practical consequence of the pH dependence of chemical shifts is that the charge state of the various species referred to should be provided when chemical shifts are quoted. Because it is not unusual for chemical shifts to be different by 30, 40, or more ppm, dependent on protonation state, for situations of intermediate charge state, the pH of the solution should also be reported. The latter is particularly important when the pH of the medium is close to the pK_a of the species of interest.

In the context here, there is nothing special about H⁺, and in principle, Scheme 2.1 and Equation 2.2 can be applied to any fast ligation interaction by making the appropriate changes to reflect a ligand, L, rather than H⁺, i.e., –log [L] for pH and –log K for pK_a, thereby leading to Equation 2.3.

$$\log((\delta_{obs} - \delta_V) / (\delta_P - \delta_{obs})) = n \log[L] + \log K \qquad (2.3)$$

In this case, the slope will be dependent on the number of ligands required for product formation. An example of the application of this equation is provided by the reaction of acetic acid with vanadate, where there is formation of a bisacetato vanadate [9].

2.1.3 ⁵¹V 2-DIMENSIONAL NMR: CORRELATION AND EXCHANGE SPECTROSCOPIES

The magnitude of the nuclear electric quadrupolar interaction is dependent on the orientation of the molecular-fixed electric field gradient tensor in the applied magnetic field. Consequently, molecular tumbling causes fluctuations in the quadrupolar interaction. These fluctuations generally cause decoupling of the J interaction. However, under circumstances where the quadrupolar coupling is not very large because

electric field gradients about the nucleus are relatively small, the fluctuations in the quadrupolar interaction might not decouple the interaction. As a rule of thumb, if the signals have a width at half-height of less than 100 or 200 Hz, there is a reasonable chance that the J interaction is not decoupled. In this event, correlation spectroscopy can be exceedingly useful in providing chemical information. Both homonuclear (COSY) and heteronuclear (HETCOR) correlations can be observed under the appropriate circumstances.

Identification and coordination assignment to products observed in the complexation of hydrogen peroxide provides a particularly nice example of the utilization of correlation spectroscopy. Ambiguity in the assignment of signal positions of two products, one of V_2L^{3-} and the other of $V_2L_2^{3-}$ stoichiometry, presented a problem in structure assignment. The COSY spectrum clearly showed the signal positions of the individual vanadiums and a distinct molecular asymmetry. The result allowed assignments of VVL and VVL_2 stoichiometry to the two compounds [8]. With knowledge of the chemical shifts (See section 5.1) of the respective nuclei, it was evident that no peroxide bridging occurs in these molecules.

Exchange spectroscopy (EXSY) has been utilized to a much greater extent than has correlation spectroscopy. In fact, ^{51}V NMR offers itself very well to this technique for a variety of compounds. The advantage derives from the fact that many exchange rates are within the millisecond timescale. This also is the timescale frequently observed for vanadium relaxation. At the same time, the vanadium signal separation in frequency units (Hz) is generally quite large, which means fast processes can be monitored because the signals are not in coalescence. The result is that exchange data can be obtained very efficiently. Of course, if exchange is much longer than 30 ms or so, all exchange information is lost because of nuclear relaxation, and alternative procedures are required. In such circumstances, both ^{13}C and ^{1}H exchange spectroscopies can prove very useful. Vanadate and its oligomers provide a good example where exchange information is only available from ^{51}V exchange spectroscopy. This technique provides detailed information about the kinetics of oligomeric vanadate formation [10].

A problem that often needs to be addressed when utilizing exchange spectroscopy is the question of whether exchange is direct or stepwise. It is possible that magnetization can be transferred from one nucleus to a second and then further transferred to a third nucleus within the exchange (mixing) time (t_m) allowed in the 2D experiment. This could be interpreted to mean that nucleus 1 and 3 are in direct exchange even though they are not. This problem can be solved by systematically varying the mixing time to determine whether build-up of magnetization is exponential or not. If stepwise exchange occurs, then the first exchange step will show exponential behavior of the magnetization build-up, whereas the magnetization transfer in the second step will show a lag in the rate of magnetization transfer. Scheme 2.2 depicts the two types of behavior.

2.1.4 ^{1}H AND ^{13}C NMR SPECTROSCOPY

Most of the normally encountered applications of proton and carbon NMR spectroscopy have been applied in studies of vanadate complexes, complexation reactions, equilibria, and kinetics. Carbon-13 studies of the influence of complexation
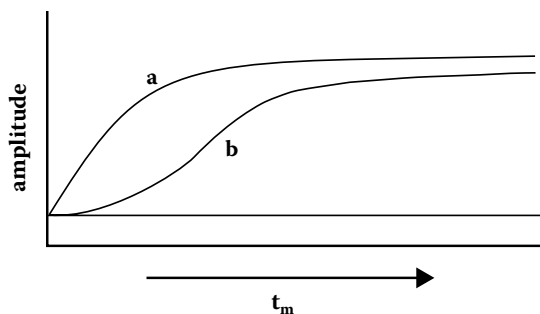
a direct transfer of magnetization
b stepwise transfer of magnetization

SCHEME 2.2

on ligand chemical shifts have proven to provide a powerful technique, particularly in situations where the ligands are multidentate. Such studies rely on the relative influence that ligand binding has on the chemical shifts of the various carbons of the ligand. Carbons near the points of ligation tend to have large induced changes in their resonance positions, whereas carbons farther removed undergo comparatively small values. The change in chemical shift is generally defined as $(\delta_C - \delta_L)$, where δ_C corresponds to the chemical shift in the complex and δ_L the corresponding chemical shift in the free ligand. The factor, $\delta_C - \delta_L$, is referred to as the chemically induced shift (CIS). Typical values of the CIS are 2 to 10 ppm for carbons near chelate positions and very small CIS values for positions distantly removed from the point of chelation. Although the CIS can be positive or negative, often the induced shifts unambiguously define the positions of coordination. Proton NMR spectroscopy can similarly be applied to good effect.

Carbon-13 complexation induced shifts have been extensively utilized. In the study of ethanolamine-derived complexes, an interesting example of its power was demonstrated by studies of the complexation of triethanolamine. The CIS values observed for this ligand showed that it complexed in a tridentate fashion when in aqueous solution, but it behaved as a tetradentate ligand in nonaqueous solvents such as methanol or acetonitrile [11]. An interesting application of coordination-induced chemical shifts is described in Section 6.1.1. An example of the power of carbon-13 EXSY experiments has been provided by the study of *N*-(phosphonom-ethyl)iminodiacetate kinetics, where the nature of the ligand allowed interconversion between enantiomeric forms of the vanadium complex to be studied [12]. Also, both ^{1}H and ^{13}C have been used in the study of ligand exchange in the dipicoline/dipi-colinatobisoxovanadium(V) system [13].

2.1.5 ^{17}O NMR Spectroscopy

Oxygen-17, like vanadium-51, is a quadrupolar nucleus. Unlike vanadium-51, the natural isotopic abundance of oxygen-17 is very low, being 0.038%. Its electric quadrupole moment is quite small, comparable to that of vanadium-51, and therefore it is a good NMR nucleus, provided isotopically enriched samples are

available. ^{17}O NMR spectroscopy has been usefully applied to delineate coordination geometry in numerous complexes. An early study demonstrated the power of this technique when it, together with ^{51}V NMR spectroscopy, was applied to the study of vanadate equilibria and the formation of vanadate oligomers [14]. Much of the power of ^{17}O NMR spectroscopy derives from the specificity of ^{17}O chemical shifts. ^{17}O, oxo oxygens, for instance, in tetrahedral vanadium complexes, have resonance positions about 500 ppm to higher field than oxo groups in octahedral coordination. Table 2.1 gives chemical shift ranges typical for different oxygen types. The sources of information for this table are quite restricted, so chemical shift ranges may well be wider than indicated.

Often, just being able to count the number of coordinated oxygen nuclei is enough to specify coordination number when the coordination of heteroligands is also known. Unfortunately, in aqueous solution, often the coordination of water cannot be ascertained because of rapid exchange kinetics. Generally, by necessity, the ^{17}O NMR signal from bulk water is very large compared to that from complexed water, and even if exchange is slow, it might not be possible to observe a signal for water tied up in a complex simply because there is not enough chemical shift separation. ^{51}V to ^{17}O heteronuclear 2D correlation experiments could well prove very useful in such circumstances, and also, of course, direct observation might be possible with the high field NMR spectrometers that are becoming more available.

2.1.6 NMR Spectroscopy in Lipophilic Solutions

There is developing interest in the nature of interactions between vanadium(V) complexes and lipids. Because of the properties of the complexes, which are frequently anionic, such interactions are restricted principally to the interfacial region between the hydrocarbon region of the lipid aggregate and the bulk water. Residence times, location, and preferential orientation in the interfacial region are all topics of interest. This region encompasses the lipid headgroup and the associated water and ionic species. Micellar solutions using surfactants as models for the lipid have been used in studies such as this. If the complex of interest does not carry a charge, then

TABLE 2.1
Oxygen-17 Chemical Shifts for Selected Coordination Types[a]

Type of Oxygen	Chemical Shift Range (ppm)
Coordinated water	75–100
Tetrahedral O or OH (acyclic, terminal)	550–720
Tetrahedral O (acyclic, bridging)	400–440
Tetrahedral O (cyclic, terminal)	928
Tetrahedral O (cyclic, bridging)	472
Octahedral O or OH (terminal)	1000–1250
Pentacoordinate O (terminal)	940–985

[a] These chemical shift ranges are derived from the work of Howarth and coworkers [14, 46, 47] and Crans and coworkers [11, 12, 48].

it will be expected to disperse more freely into the interior of the bilayer. Micelles and reversed micelles represent a special case of anisotropic liquids (liquid crystals) found typically in bilayer membranes and often in surfactant solutions.

Anisotropic solutions add an extra dimension to ^{51}V NMR spectroscopy, in that dipolar couplings (D_{ij}) and quadrupole splittings ($\Delta\nu_q$) can be directly observed. These parameters are dependent on molecular structure and molecular alignment. Their magnitudes derive directly from structural and orientational properties of the compound in the medium [15,16,17,18]. In lipid-like hydrophylic materials, they frequently depend greatly on surface interactions that influence the orientational order. For quadrupolar nuclei such as vanadium, the anisotropic spectra are almost always dominated by the quadrupole coupling. The quadrupole splitting is defined by Equation 2.4, for which e$\mathbf{Q}$ is the nuclear electric quadrupole moment, $\mathbf{V}$ is the electric field gradient tensor, and η_q is the asymmetry in $\mathbf{V}$.

$$\Delta\nu_q = \frac{e\mathbf{Q} \cdot V_{zz}}{h \cdot 2I(2I-1)}[3S_{zz} + \eta_q(S_{xx} - S_{yy})] \tag{2.4}$$

The asymmetry, η_q, is defined as $(V_{yy} - V_{xx}) / V_{zz}$, so it takes the values between 0 and 1 because $V_{zz} + V_{xx} + V_{yy} = 0$ and $|V_{zz}| \geq |V_{xx}| \geq |V_{yy}|$. The parameter e$\mathbf{Q}$ (V_{zz} / h) is the quadrupole coupling constant. The matrix of $\mathbf{S}$ values represents the order parameters, and they give the alignment of the compound with respect to the applied magnetic field. They can be, and usually are, defined in terms of a molecular-fixed coordinate system. $\mathbf{S}$ is a symmetrical 3×3 matrix, and the sum of the diagonal elements of $\mathbf{S}$ is zero, so that in a molecular-fixed coordinate system, the number of components of the $\mathbf{S}$ matrix varies from 5 for compounds with no elements of symmetry, such as chiral species, to 1 for entities with a C_3 or higher axis of symmetry.

The quadrupole coupling constant has been determined for a number of tetrahedral and octahedral species in crystalline compounds. In general, it is found that for tetrahedral species, the quadrupole coupling constant is 3 to 5 MHz, with an asymmetry parameter generally close to 1 [19,20]. For a number of six-coordinate vanadiums in polyoxometalates, octahedrally coordinated vanadium tends to have a significantly smaller quadrupole coupling constant, the value ranging from about 0.6 to 2 MHz, with η_q varying almost over its full range from 0 to 1 [21,22]. Corresponding quadrupole parameters for vanadium compounds in liquid crystalline solutions are not known, but they probably are similar. Certainly, the quadrupole coupling gives rise to splittings in the NMR spectra of V(V)-containing compounds.

Similar to the situation for quadrupole-induced relaxation, the quadrupole splitting in liquid crystals is zero if the molecular symmetry is tetrahedral or higher. Electric field gradients are zero for such symmetries so there can be no quadrupolar interaction. However, one expects to see small splittings from tetrahedral or octahedral derivatives because of structural distortions. These predominately arise from specific interactions with extraneous materials such as lipophilic headgroups in surfactant systems, as seen, for instance, in both cationic and anionic octahedral cobalt(III) species [23]. Much larger splittings will be expected from other structure

types. One must, in addition, take into account the order parameter, **S**. If the order parameter is zero, then quadrupole splittings are also zero even if the corresponding quadrupole coupling constants are large. Indeed, in isotropic solution, the order parameter is zero and the influences of the quadrupole couplings appear in the linewidths, as determined by the relaxation times.

Figure 2.3 shows an NMR spectrum obtained for vanadate in a nematic lyotropic aqueous detergent-based material liquid crystal. Signals from V_1, V_2, and V_4 are identified in the spectrum. The signal from V_1 shows a small quadrupole splitting of 200 Hz. This value is consistent with small distortions from tetrahedral symmetry, probably arising from the fact that, under the conditions used for the spectrum, V_1 carries a single proton. No quadrupole splitting is observed for V_2. This can only occur if the two order parameters for this ion are zero. In contrast to V_2, V_4 has a large quadrupole splitting of 5.36 kHz, which shows that the molecule is relatively highly aligned in this medium with a substantial order parameter. The large linewidth of the individual signals from V_4 is expected because dipole couplings between nuclei (D_{ij}) also arise in anisotropic media, so that dipolar interactions [16] between the various vanadiums of V_4 will occur (Equation 2.5). They are not seen for V_2 in the spectrum shown in Figure 2.3 because both order parameters are close to zero. In Equation 2.5, γ_i and γ_j are the magnetogyric ratios of the interacting nuclei, r_{ij} is the internuclear distance, and S_{ij} is the corresponding order parameter.

$$D_{ij} = -h\gamma_i\gamma_j S_{ij} / 4\pi r_{ij} \qquad (2.5)$$
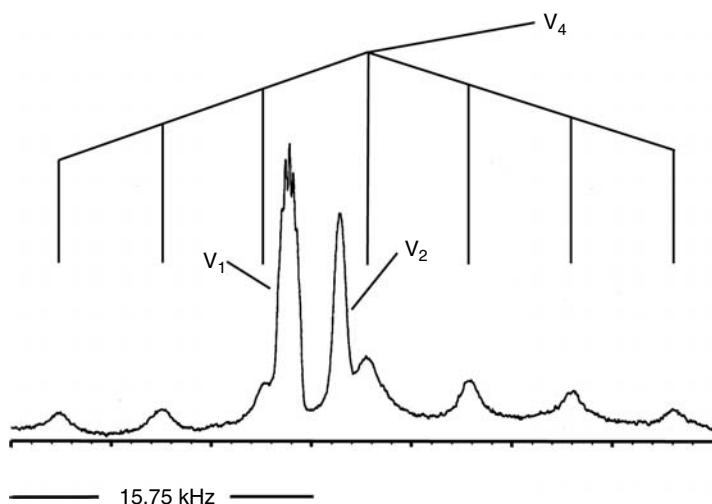
FIGURE 2.3 [51]V NMR spectrum of vanadate in a nematic lyotropic liquid crystalline solution. The spectrum shows quadrupole-split signals from V_1 and V_4, while the signal of V_2 is broadened. The quadrupole splittings are 200 Hz and 5.35 kHz for V_1 and V_4, respectively. The spectrum was obtained from a tetradecyltrimethylammonium bromide (TDTMABr) mesophase of composition: TDTMABr, 160 mg; decanol, 30 mg; D_2O, 450 mg; NaCl, 10 mg.

Interestingly, if the salt concentration in the liquid crystal sample of Figure 2.3 is increased substantially, the quadrupole splitting from V_4 approaches zero. This suggests there is some type of site-averaging process occurring in the detergent bilayer solution, causing a zero splitting. This is a well-known phenomenon for alkali metal and halide ions, but zero splittings more typically are observed in mixed detergent systems [24]. Failure to recognize this averaging process resulted in the mischaracterization of vanadate ions in liquid crystalline solution [25]. The site averaging could be as simple as exchange between surface-bound tetravanadate and tetravanadate in the bulk water. It more likely derives from averaging between two surface sites, where the S values have opposite signs, and also with the bulk water.

Dipolar interactions are dependent on the internuclear vector, say, between hydrogens H_i and H_j contained in the ligands of a vanadium complex of interest, and also are dependent on the angle between the internuclear vector and the direction of the applied magnetic field (Equation 2.5). If sufficient dipolar couplings are available for the molecule, the average alignment of that molecule in the magnetic field can be specified. Because the alignment of the surfactant is generally known, then dipolar couplings provide a powerful means of detailing lipid/molecule inter-actions. Deuteration of the molecule will provide deuterium quadrupole splittings, which can provide equivalent orientational information. An example of the latter technique shows the dependence of alkylpyridinium chain length on incorporation into cationic bilayer detergent systems [26].

There is one remaining anisotropic parameter that may turn out to be important in characterizing vanadium spectra in anisotropic media, and that is the anisotropy in the chemical shift. Anisotropy in the chemical shift simply reflects the fact that if the [51]V chemical shift were measured with, say, a VO bond aligned parallel to the magnetic field of the spectrometer and remeasured with the VO bond aligned per-pendicular to the applied field, the two values would be different. The observed anisotropy in the chemical shift, like the quadrupole splitting and dipole coupling, therefore, depend on the order parameters describing the alignment of the species being studied. The isotropic chemical shift of nucleus **i** (σ_t) normally observed in NMR spectra derives from the diagonal elements of the chemical shift tensor, as described in Equation 2.6.

$$\sigma_t = (1/3)\ (\sigma_{zzi} + \sigma_{yyi} + \sigma_{xxi}) \tag{2.6}$$

The anisotropy in the chemical shift of nucleus **i** (σ_{ia}) is related to the chemical shift tensor and the elements of the order matrix, as shown in Equation 2.7.

$$\sigma_{ia} = (2/3)\ [(S_{zz}\sigma_{zzi} + S_{yy}\sigma_{yyi} + S_{xx}\sigma_{xxi}) + S_{xz}\ (\sigma_{xzi} + \sigma_{zxi}) +$$

$$S_{yz}(\sigma_{yzi} + \sigma_{zyi}) + S_{xy}(\sigma_{xyi} + \sigma_{yxi})] \tag{2.7}$$

The observed chemical shift is simply the sum of σ_i and σ_{ia}. Vanadium has a large chemical shift range of 3000 ppm or so, so liquid crystal spectra can reasonably be expected to show significant influences of chemical shift anisotropy. Chemical

shift anisotropies known from studies of solids can be very large, 300 or 400 ppm or more, and are influenced strongly by the counterions contained in the crystal.

All the anisotropic parameters discussed above can play a role in micellar solutions. For instance, quadrupolar interactions at the vanadium nucleus will be modulated much more rapidly when a complex is tumbling freely in bulk water than when the same complex is incorporated into a lipid interface, where the tumbling will be greatly slowed. Although in both cases, no quadrupole splitting will be observed, the difference in modulation rate will have a significant influence on nuclear relaxation times. Consequently, systematic study of relaxation can provide information about lipid/complex interactions. Because relaxation studies do not give details of molecular orientation, it is necessary to model the system and ascertain whether the model is in agreement with the relaxation values observed and, of course, with whatever other information one has obtained. Relaxation has been used to probe the interactions between the vanadium(V) complex, pyridine-2,6-dicarboxylato-bisoxovanadate (VO_2dipic), and a model lipid based on inverse micelles prepared from the detergent, tetradecyltrimethylammonium bromide [27]. The studies strongly support the hypothesis that the dominant contribution to the quadrupolar relaxation derives from surface interactions arising from direct interactions.

2.2   VANADATE SELF-CONDENSATION REACTIONS

Any study of the reactions of aqueous vanadate with ligands must take into account the self-condensation reactions that vanadate undergoes. These reactions often dominate the chemistry and are highly pH-dependent [28]. Similarly, equilibria are dependent on the ionic strength of the media, and it is important that this quantity be rigorously controlled. It appears that a critical factor is that many of the equilibria involve anionic species, and such equilibria are most strongly influenced by the cation concentration, so it is important that this factor be constant. Even then, equilibrium constants determined for, say, a 1 M ionic strength solution with KCl will be different from those measured for a 1 M ionic strength solution with NaCl. A detailed study has shown how oligomer formation is influenced by the ionic strength of the medium and showed, for instance, that the formation constant for tetravanadate increased by about 200 times on changing the ionic strength from 0.02 M to 2.0 M. [29].

Occasionally, work in the scientific literature describing vanadate solution chemistry or biochemistry suggests or implies that sodium orthovanadate and sodium metavanadate are different compounds with individual properties. Although this is certainly true for the solid, where the components of sodium orthovanadate (Na_3VO_4) are discrete entities whereas sodium metavanadate ($NaVO_3$) is a polymeric compound, it is not true for aqueous solution. For the same conditions (pH, ionic strength, concentration, etc.), solutions deriving from the different solid forms are indistinguishable.

2.2.1   THE COMMONLY ENCOUNTERED VANADATES

Under very strongly basic conditions, the vanadate trianion, VO_4^{3-}, will be the only vanadate in solution. The VO_4H^{2-} ion has a pK_a of about 12. Consequently, below
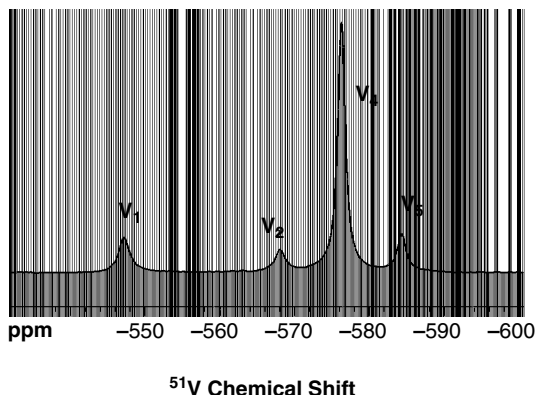
FIGURE 2.4 ^{51}V NMR spectrum obtained under slightly alkaline conditions showing a typical distribution of vanadate and its oligomers in aqueous solution. Conditions of experiment: total vanadate, 6 mmol/L; pH, 8.0; NaCl, 1.0 mol/L.

pH 12, the chemistry of vanadate rapidly increases in complexity. Two VO_4H^{2-} ions can condense with each other to release water and form the vanadate dimer, $V_2O_7^{4-}$, which in turn can be protonated in a more acidic medium. An increase in acidity to near neutral conditions also promotes formation of higher oligomers. An NMR spectrum showing a typical assortment of vanadate and its oligomers under slightly alkaline conditions is shown in Figure 2.4. The predominant species are the cyclic oligomers, a tetramer, $V_4O_{12}^{4-}$, and a pentamer, $V_5O_{15}^{5-}$. Neither of these ions has been found to protonate under increasingly acidic conditions. Other oligomers that are normally found only as minor components of an equilibrated solution are a cyclic hexamer and the linear species trimer, tetramer, and hexamer [30,31]. At elevated pH (pH 10–11) and high vanadium concentrations, these compounds can readily be observed in ^{51}V NMR spectra. Of course, the relative distribution of species concentrations is dependent on total vanadate concentration, so that lower nuclearity compounds are favored at low overall concentrations.

Below a pH of about 6, the vanadium decamer, decavanadate, is formed, and it is the predominant species when the total vanadate concentration is above about 0.2 mM. Unlike the vanadate oligomers discussed above, the decamer is strongly colored, both as a solid and in solution. This oligomer undergoes successive protonation reactions with increase in acidity, going from the 6- to 3- anion. Of these states, the 4- and 5- anions are the predominant forms. Under strongly acidic conditions, below a pH of about 2, decavanadate is replaced by the cationic species, $[VO_2(H_2O)_4]^+$ (often referred to as VO_2^+). Because of its high proton stoichiometry compared to the other vanadate derivatives, the cation is frequently the only compound in significant concentration in solution under strongly acidic conditions, even in the presence of strong-binding ligands. Figure 2.5 shows the influence of pH on the distribution of the major vanadate species for total vanadate concentrations of 0.1 and 1.0 mM. The equilibrium constants used for Figure 2.5 are for a 0.6 M NaCl solution and are taken from the work of Pettersson and his coworkers [30]. As discussed above, changes in ionic strength will influence the various equilibria and, hence, the relative
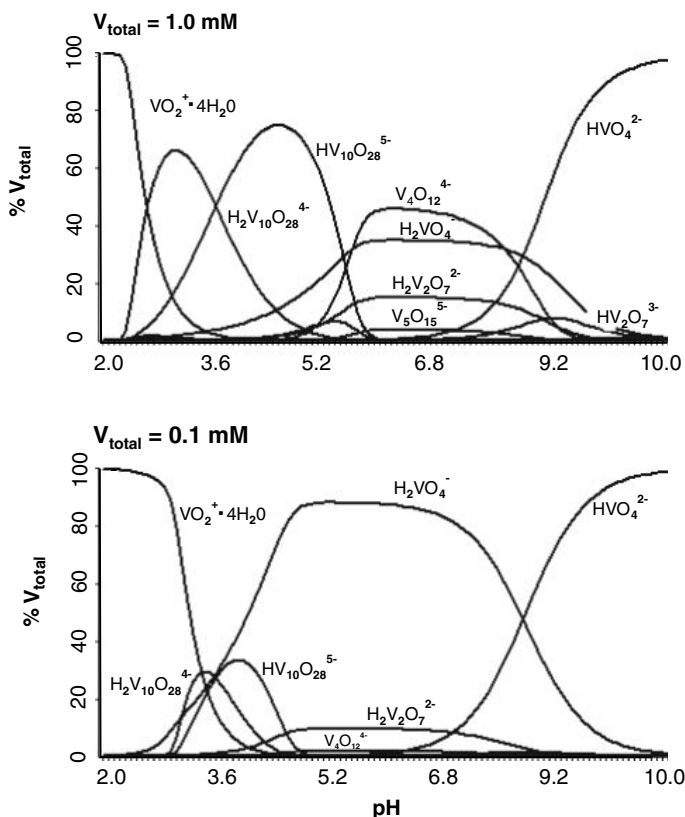
FIGURE 2.5 Species distribution diagrams for vanadate at 1.0 and 0.1 molar overall concentrations; calculated for aqueous 0.6 mol/L NaCl solutions. Formation constants are taken from Reference 30.

distribution of the various compounds. Table 2.2 gives an idea of the sensitivity of equilibria to the ionic strength of the medium.

Although there is little doubt that trianionic vanadate, VO_4^{3-}, has a tetrahedral structure, this is certainly not the only coordination adopted by vanadate. For instance, in decavanadate, there are three types of vanadium, all of octahedral coordination, whereas solid sodium metavanadate shows chains of vanadate moieties in trigonal bipyramidal coordination. In aqueous solution, the possibility arises that protonation of vanadate ions leads to a change in coordination. It has, for instance, been argued [32] that protonation of dianionic vanadate (pK_a about 8.1, dependent on ionic medium; Table 2.2) leads to a coordination change from tetrahedral geometry to a trigonal bipyramidal structure. Thermodynamic measurements have shown there is a close correspondence between the entropy and enthalpy of protonation of the vanadate dianion and the corresponding protonation of phosphate, arsenate, and chromate [29,33]. This is in contrast to the case with molybdate, where incorporation of water accompanies the protonation step, and the thermodynamic parameters show no correlation with those of the above ions. This suggests that when the vanadate dianion is protonated, there is no change in its coordination. Optimal geometry

TABLE 2.2
Formation Constants for Selected Vanadate Oligomers Determined in the Presence of Various Electrolytes and Electrolyte Concentrations

| | K_{12} $2H_2VO_4^-$ $V_2O_7^{2-}$ | K_{14} $4H_2VO_4^-$ $V_4O_{12}^{4-}$ | K_{15} $5H_2VO_4^-$ $V_5O_{15}^{5-}$ | | |
Electrolyte	K_{12}	K_{14}	K_{15}	pK_a ($H_2VO_4^-$)	Ref.
—	3.2×10^2	2.8×10^8	—	8.80	29
—	2.0×10^2	4.0×10^7	—	8.75	49
0.10 KCl	4.1×10^2	2.4×10^9	3.2×10^{11}	8.60	29
0.50 KCl	6.5×10^2	1.4×10^{10}	3.1×10^{12}	8.37	29
1.00 KCl	7.7×10^2	2.7×10^{10}	9.8×10^{12}	8.33	29
2.00 KCl	8.9×10^2	5.8×10^{10}	3.1×10^{13}	8.26	29
0.15 NaCl	4.5×10^2	1.8×10^9	1.5×10^{11}	8.17	50
0.60 NaCl	6.2×10^2	7.8×10^9	1.5×10^{12}	7.95	51
3.00 NaClO_4	6.3×10^2	1.7×10^{11}	1.4×10^{14}	8.00	28

calculations that investigated the possibility of coordinated water strongly suggested that water would be expelled from the coordination sphere and supported the assignment of tetrahedral coordination to monoanionic vanadate [34].

There is very little known about the neutral vanadate species, VO_4H_3, because it is, at best, only a minor component in aqueous solution [35]. The initial protonation of $VO_4H_2^-$ at about pH 3 is accompanied by a second protonation that cannot be separated from the first. The result is the formation of a cationic species. Thermodynamic and spectroscopic evidence [33] suggests that formation of this compound is accompanied by incorporation of water to form the octahedral derivative, $VO_2(H_2O)_4^+$, commonly referred to as VO_2^+. Theoretical calculations also support the assignment of tetrahedral coordination to the monoanion and octahedral geometry to the cationic form of vanadate [36].

Octahedral coordination is not highly favored by vanadate. Other than for the octahedral coordination of the vanadiums of decavanadate (Scheme 2.3), there is little evidence to suggest that there is a change in coordination from tetrahedral geometry when other vanadate oligomers are formed. Apparently, all such oligomers have tetrahedral vanadate as the base unit; even a crystalline tricyclic pentamer (Scheme 2.4a) has tetrahedral geometry about all the vanadiums in the structure, albeit of two different vanadium types [37]. This oligomer has a different charge state (3-) than the pentamer (5-) found in aqueous solution. If the solution pentamer were to have a similar cyclic structure, complexation of water molecules accompanied by the loss of two protons would be required. This would necessitate conversion of some of the vanadiums to a higher coordination number. It is, however, generally accepted that, in aqueous solution, the cyclic tetramer, pentamer, and hexamer are all monocyclic compounds formed from tetrahedral vanadate through VOV linkages. Such a structural form is known for a crystalline tetrameric vanadate derivative [38] and has similarly been found for the cyclic trivanadate anion, $V_3O_9^{3-}$ (Scheme 2.4b) [39]. The accepted aqueous solution structure of cationic vanadate together with common ionic vanadate species observed at pH 7 are depicted in Scheme 2.5.
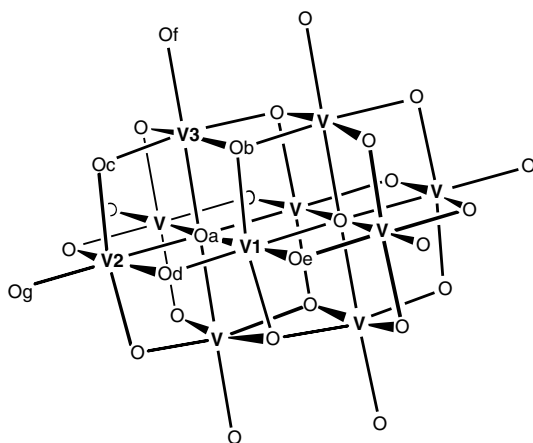
decavanadate hexaanion

SCHEME 2.3

a b
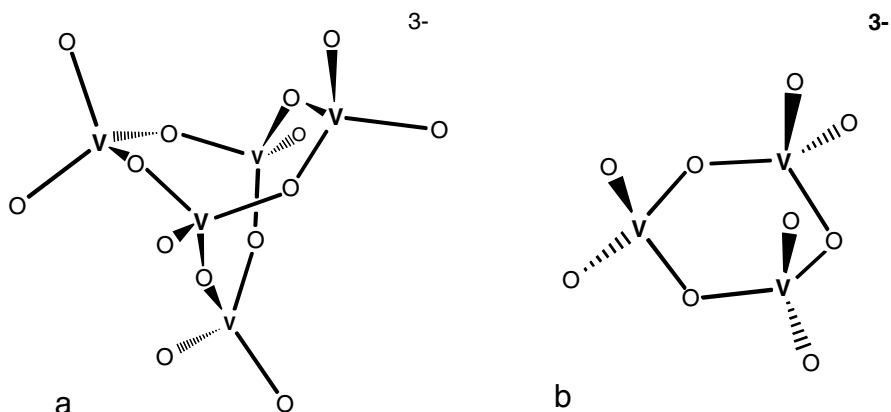
SCHEME 2.4

Although decavanadate (Scheme 2.3) is thermodynamically unstable above about pH 6, its decomposition is kinetically hindered, and the decomposition to lower oligomers and vanadate is slow, requiring in the order of hours for equilibrium to be established [40]. In contrast, the lower oligomers such as di- and tetravanadate equilibrate rapidly, requiring only a few tens of milliseconds for equilibrium conditions to be established at pH 8.6 [10]. The major exchange pathways for oligomer formation at concentrations between 5 and 20 mmol/L total vanadate are V_1 going to V_2, V_2 together with $2 V_1$ going to V_4, and V_4 plus V_1 forming V_5 [10]. Throughout this concentration range, the reaction of $2V_2$ to form V_4 is less favorable than V_2 together with $2V_1$ forming V_4. However, the rate of $2V_2 \rightarrow V_4$ is only about a factor of 5 less than $2V_1 \rightarrow V_2$.
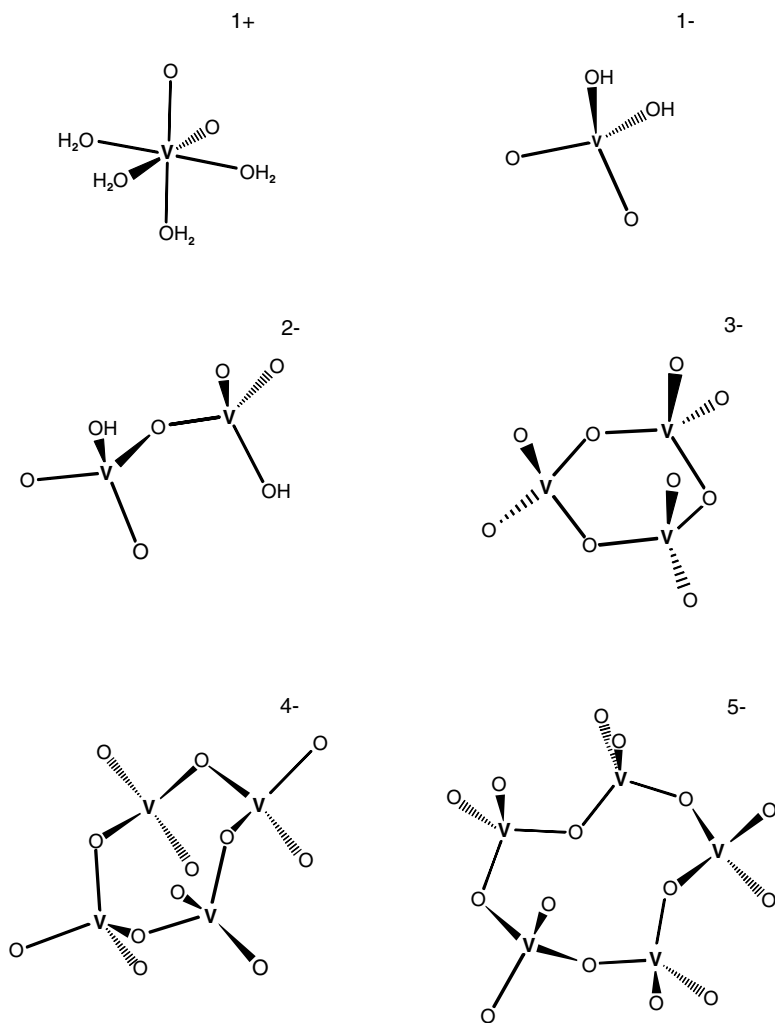
SCHEME 2.5

The linear trivanadate has been shown to undergo exchange between oxygens and also between the vanadiums [31]. In the exchange process, the terminal and central vanadiums are interconverted. The interconversion was shown not to arise from exchange with either mono- or divanadate but rather from an internal exchange process. Additionally, no exchange of *O*-17 with water was found under the conditions of the study. Because the exchange rate increased with lower pH, it was postulated that a cyclic trimer was formed as an intermediate in the equilibration. Such a trimer (Scheme 2.4a) has been characterized by x-ray diffraction [39], and this strongly supports the occurrence of such a cyclic species in the exchange process.

2.2.2 DECAVANADATE

Within the moderately acidic range of about pH 3 to pH 6, decavanadate is the preferred form of oligomeric vanadate, and it dominates the vanadium chemistry; although, of course, under dilute conditions, decavanadate dissociates to the monomer, $H_2VO_4^-$ or $VO_2(H_2O)_4^+$, dependent on pH. Decavanadate represents a significant departure in vanadium coordination geometry from the other oligomeric vanadates. Although there are three distinct types of vanadium in decavanadate, all 10 nuclei have octahedral coordination. This coordination is otherwise found only with cationic vanadate $(VO_2(H_2O)_4)^+$.

The VO bond distances of decavanadate are typical distances observed for vanadium compounds. The longest distances are to Oa atoms (Scheme 2.3), which are surrounded by six vanadium nuclei. In the hexaanion, the lengths are V1-Oa, 2.116 Å; V2-Oa, 2.316 Å; V3-Oa, 2.242 Å, and these distances change very little when decavanadate is protonated [41,42]. The bond distances to the external oxygens, Of and Og, are very short, being 1.614 Å and 1.605 Å, respectively. Such distances are typically observed for V=O bond lengths. The remaining V-O distances, varying from 1.83 to 2.03 Å, are within the range observed for V to O single bonds.

Decavanadate has ionic states varying from 3- to 6-. The multiple sharing of oxygen by the vanadium nuclei has prompted extensive studies directed toward locating the position of the hydrogen atoms of the complex. Oxygen-17 NMR studies have proven particularly enlightening [41]. Protonation of the V_{10}^{6-} anion occurs at a triply bound oxygen of decavanadate (Scheme 2.6, Ob). However, the three protons of the 3- anion are not all localized to the triply bonded oxygens, and protonation also occurs at doubly bridging oxygens (Scheme 2.6, Oc). This suggests there is not
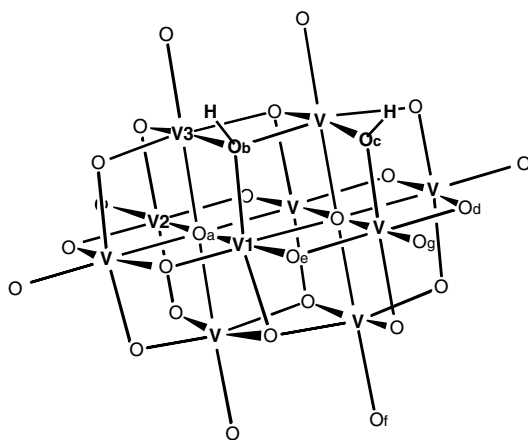
decavanadate tetraanion

SCHEME 2.6

a large difference in the basicity of these two types of oxygen. This is particularly evident from crystal structure studies, where a structure of a tetra(*n*-hexylammonium) salt of $H_2V_{10}O_{28}^{4-}$ shows hydrogens only on the triply bridging oxygens (Ob) [42], whereas a structure of the corresponding 4-ethylpyridinium salt shows the two hydrogens only on the doubly bridging oxygens (Oc) [41]. There is a difference in the hydrogen bonding network within the two crystalline materials, so it is evident that hydrogen-bonding has a strong influence on protonation positions in decavanadate. Interestingly, if methanol in moderate concentrations is included in an aqueous solution of decavanadate, the methanol oxygen preferentially replaces a triply bridging oxygen (Ob) to afford the corresponding *O*-methyldecavanadate.

Although decavanadate is thermodynamically unstable above a pH of about 6, it ($V_{10}O_{28}^{6-}$) decomposes quite slowly, having a half-life of about 9 h at pH 7.5 and 25°C. The decomposition rate increases substantially at higher pH, with the half-life being about 1.5 h at pH 12 and 25°C [43]. These rates contrast quite remarkably with decavanadate when the conditions are acidic enough to significantly protonate the polyanion. The half-life drops to about 6 s at pH 1 and 25°C [44]. Under such strongly acidic conditions, the vanadate cation, $VO_2(H_2O)_4^+$, is the thermodynamic sink. Ion-pairing has a significant influence on decavanadate throughout the pH range, and decomposition rates are dependent on the nature and on the concentration of the counterion.

2.3   VANADIUM ATOM STOICHIOMETRY OF COMPLEXES

If ligand binding is not exceptionally strong, the vanadium stoichiometry in complexes can be obtained using a rather simple technique [45]. The procedure relies on the utilization of two vanadium concentrations the second being double, triple, or even more concentrated than the first. The two spectra will be obtained under the same conditions. When the complexation constant is weak enough, changing the vanadate concentration will have only a minor influence on free ligand concentration, because the ligand will be in excess. If one works at minimal vanadate concentrations but where V_1, V_2, V_4, and possibly V_5 are observed in both spectra (a typical range is about 2 to 10 mmol/L total vanadate), then these compounds provide a convenient reference. Because the uncomplexed ligand concentration is approximately constant, product formation is directly dependent on the V_1 concentration according to the 1st, 2nd or nth power, according to the stoichiometry.

As a consequence, if the product signal of interest is scaled to the same amplitude in the two spectra and the higher concentration spectrum subtracted from the other, the residual signals corresponding to compounds with a stoichiometry lower than that of the complex of interest will be positive, those corresponding to a higher stoichiometry will be negative, and those of the same stoichiometry will have zero residual intensity. If, for instance, when the spectra are subtracted and both the signal of interest and the one deriving from the vanadate dimer are removed from the difference NMR spectrum, then the signal being investigated corresponds to a complex of V_2 stoichiometry. The residual V_1 signal will have positive relative intensity,

whereas the V_4 and V_5 signals will have negative intensity. Other product signals will correspondingly have negative or positive signal intensity, dependent on the stoichiometry. Of course, the subtraction procedure can be utilized for any signal of interest. This simple procedure provides a useful starting point for interpreting detailed titration studies.

REFERENCES

1. Bortolini, O., M. Carraro, V. Conte, and S. Moro. 1999. Histidine-containing bisper-oxovanadium(V) compounds: Insight into the solution structure by an ESI-MS and [51]V-NMR comparative study. *Eur. J. Inorg. Chem.* 1489–1495.
2. Conte, V., O. Bortolini, M. Carraro, and S. Moro. 2000. Models for the active site of vanadium-dependent haloperoxidases: Insight into the solution structure of peroxo-vanadium compounds. *J. Inorg. Biochem.* 80:41–49.
3. Butler, A. and H. Eckert. 1987. 51-V NMR as a probe of metal ion binding in metalloproteins. *J. Am. Chem. Soc.* 109:1864–1865.
4. Butler, A. and H. Eckert. 1989. 51-V NMR as a probe of vanadium(V) coordination to human apotransferrin. *J. Am. Chem. Soc.* 111:2802–2809.
5. Rehder, D., C. Weidemann, A. Duch, and W. Priebsch. 1988. 51-V shielding in vanadium(V) complexes: A reference scale for vanadium binding sites in biomole-cules. *Inorg. Chem.* 27:584–587.
6. Cornman, C.R., G.J. Colpas, J.D. Hoeschele, J. Kampf, and V.L. Pecoraro. 1992. Implications for the spectroscopic assignment of vanadium biomolecules: Structure and spectroscopic characterization of monooxovanadium(V) complexes containing catecholate and hydroxamate-based noninnocent ligands. *J. Am. Chem. Soc.* 114:9925–9933.
7. Lutz, O., W. Nepple, and A. Nolle. 1976. Indirect spin-spin coupling between [17]O and other quadrupolar nuclei in oxyanions. *Z. Naturforsch.* 31a:1046–1050.
8. Andersson, I., S.J. Angus-Dunne, O.W. Howarth, and L. Pettersson. 2000. Speciation in vanadium bioinorganic systems 6. Speciation study of aqueous peroxovanadates, including complexes with imidazole. *J. Inorg. Biochem.* 80:51–58.
9. Tracey, A.S., H. Li, and M.J. Gresser. 1990. Interactions of vanadate with mono- and dicarboxylic acids. *Inorg. Chem.* 29:2267–2271.
10. Crans, D.C., C.D. Rithner, and L.A. Theisen. 1990. Application of time-resolved 51-V 2-D NMR for quantitation of kinetic exchange pathways between vanadate mono-mer, dimer, tetramer, and pentamer. *J. Am. Chem. Soc.* 112:2901–2908.
11. Crans, D.C. and P.K. Shin. 1994. Characterization of vanadium(V) complexes in aqueous solutions: Ethanolamine- and glycine-derived complexes. *J. Am. Chem. Soc.* 116:1305–1315.
12. Crans, D.C., F. Jiang, I. Boukhobza, I. Bodi, and T. Kiss. 1999. Solution character-ization of vanadium(V) and -(IV) *N*-(phosphonomethyl)iminodiacetate complexes: Direct observation of one enantiomer converting to the other in an equilibrium mixture. *Inorg. Chem.* 38:3275–3282.
13. Crans, D.C., L. Yang, T. Jakusch, and T. Kiss. 2000. Aqueous chemistry of ammonium (dipicolinato)oxovanadate(V): The first organic vanadium(V) insulin-mimetic com-pound. *Inorg. Chem.* 39:4409–4416.

14. Heath, E. and O.W. Howarth. 1981. Vanadium-51 and oxygen-17 nuclear magnetic resonance study of vanadate(V) equilibria and kinetics. *J. Chem. Soc., Dalton Trans.* 1105–1110.

15. Diehl, P. and C.L. Khetrapal. 1969. *NMR studies of molecules oriented in the nematic phase of liquid crystals.* Springer-Verlag, Berlin.

16. Khetrapal, C.L., A.C. Kunwar, A.S. Tracey, and P. Diehl. 1975. *Lyotropic liquid crystals.* Springer-Verlag, Berlin.

17. Paulsen, K. and D. Rehder. 1982. Nuclear quadrupole perturbations in 51-V NMR spectra of oxovanadium(+V) complexes. *Z. Naturforsch.* 37a:139–149.

18. Khetrapal, C.L. and A.C. Kunwar. 1977. *NMR studies of molecules oriented in thermotropic liquid crystals.* Academic Press, New York.

19. Nielsen, U.G., H.J. Jakobsen, J. Skibsted, and P. Norby. 2001. Crystal structure of α-$Mg_2V_2O_7$ from synchrotron x-ray powder diffraction and characterization by 51V MAS NMR spectroscopy. *J. Chem. Soc., Dalton Trans.* 3214–3218.

20. Delmair, F., M. Rigole, E.A. Zhilinskaya, A. Aboukais, R. Hubaut, and G. Mairesse. 2000. ^{51}V magic angle spinning solid state NMR studies of $Bi_4V_2O_{11}$ in oxidized and reduced states. *Phys. Chem. Chem. Phys.* 2:4477–4483.

21. Huang, W., L. Todaro, P.A. Glenn, R. Beer, L.C. Francesconi, and T. Polenova. 2004. ^{51}V Magic angle spinning NMR spectroscopy of Keggin anions $[PV_nW_{12-n}O_{40}^{(3+n)-}]$: Effect of countercation and vanadium substitution on fine structure constants. *J. Am. Chem. Soc.* 126:11564–11573.

22. Huang, W., L. Todaro, L.C. Francesconi, and T. Polenova. 2003. ^{51}V Magic angle spinning NMR spectroscopy of six-coordinate Lindqvist oxoanions: A sensitive probe for the electronic environment in vanadium-containing polyoxometalates. Counterions dictate the ^{51}V fine structure constants in polyoxometalate solids. *J. Am. Chem. Soc.* 125:5928–5938.

23. Iida, M. and A.S. Tracey. 1991. ^{59}Co NMR investigation of $Co(CN)_6^{3-}$ and $Co(NH_3)_6^{3+}$ interactions in nematic liquid crystalline surfactant solution. *J. Phys. Chem.* 95:7891–7896.

24. Tracey, A.S. and T.L. Boivin. 1984. Interaction of alkali metal and halide ions in lyotropic liquid crystalline solution. *J. Phys. Chem.* 88:1017–1023.

25. Tracey, A.S. and K. Radley. 1985. A vanadium-51 nuclear magnetic resonance investigation of vanadate oxyanions in a lyotropic liquid crystalline bilayer system. *Can. J. Chem.* 63:2181–2184.

26. Weiss-Lopez, B.E., C. Gamboa, and A.S. Tracey. 1995. Location and average alignment of alkylpyridinium ions in cationic nematic lyomesophases. *Langmuir* 11:4844–4847.

27. Stover, J., C.D. Rithner, R.A. Inafaku, D.C. Crans, and N.E. Levinger. 2005. Interaction of dipicolinatodioxovanadium(V) with polyatomic cations and surfaces in reverse micelles. *Langmuir* 21:6250–6258.

28. Pettersson, L., I. Andersson, and B. Hedman. 1985. Multicomponent polyanions. 37. A potentiometric and 51-V NMR study of equilibria in the H^+-HVO_4^{2-} system in 3.0 M $Na(ClO_4)$ medium covering the range 1 <-lg[H^+] <10. *Chem. Scr.* 25:309–317.

29. Tracey, A.S., J.S. Jaswal, and S.J. Angus-Dunne. 1995. Influences of pH and ionic strength on aqueous vanadate equilibria. *Inorg. Chem.* 34:5680–5685.

30. Pettersson, L., B. Hedman, I. Andersson, and N. Ingri. 1983. Multicomponent polyanions. 34. A potentiometric and 51-V NMR study of equilibria in the H^+-HVO_4^{2-} system in 0.6 M $Na(Cl)$ medium covering the range 1 <-lg[H^+] <10. *Chem. Scr.* 22:254–264.

31. Andersson, I., L. Pettersson, J.J. Hastings, and O.W. Howarth. 1996. Oxygen and vanadium exchange processes in linear vanadate oligomers. *J. Chem. Soc., Dalton Trans.* 3357–3361.

32. Harnung, S.E., E. Larsen, and E.J. Pedersen. 1993. Structure of monovanadates in aqueous solution. *Acta Chem. Scand.* 47:674–682.

33. Cruywagen, J.J., J.B.B. Heyns, and A.N. Westra. 1996. Protonation equilibria of mononuclear vanadate: Thermodynamic evidence for the expansion of the coordination number in VO_2^+. *Inorg. Chem.* 35:1556–1559.

34. Buhl, M. 1999. Theoretical study of a vanadate peptide complex. *J. Comp. Chem.* 20:1254–1261.

35. Pettersson, L., B. Hedman, A.-M. Nenner, and I. Andersson. 1985. Multicomponent polyanions. 36. Hydrolysis and redox equilibria of the H^+-HVO_4^{2-} system in 0.6 M Na(Cl). A complementary potentiometric and 51-V NMR study at low vanadium concentrations in acid solution. *Acta Chem. Scand.* A 39:499–506.

36. Buhl, M. and M. Parrinello. 2001. Medium effects on [51]V NMR chemical shifts: A density functional study. *Chem. Eur. J.* 7:4487–4494.

37. Day, V.W., W.G. Klemperer, and O.M. Yaghi. 1989. A new structure type in polyoxoanion chemistry: Synthesis and structure of the $V_5O_{14}^{3-}$ anion. *J. Am. Chem. Soc.* 111:4518–4519.

38. Nakano, H., T. Ozeki, and A. Yagasaki. 2002. $(Et_4N)_4[V_4O_{12}]2H_2O$. *Acta Crystallogr., Sect. C* C58:m464–m465.

39. Hamilton, E.E., P.E. Fanwick, and J.J. Wilker. 2002. The elusive vanadate $(V_3O_9)^{3-}$: Isolation, crystal structure, and nonaqueous solution behavior. *J. Am. Chem. Soc.* 124:78–82.

40. Druskovich, D.M. and D.L. Kepert. 1975. Base decomposition of decavanadate. *J. Chem. Soc., Dalton Trans.* 947–951.

41. Day, V.W., W.G. Klemperer, and D.J. Maltbie. 1987. Where are the protons in $H_3V_{10}O_{28}^{3-}$? *J. Am. Chem. Soc.* 109:2991–3002.

42. Roman, P., A. Aranzabe, A. Luque, J.M. Gutierrez-Zorrilla, and M. Martinez-Ripoll. 1995. Effects of protonation in decavanadates: Crystal structure of tetrakis(*n*-hexylammonium) dihydrogendecavanadate(V). *J. Chem. Soc., Dalton Trans.* 2225–2231.

43. Murmann, R.K. and K.C. Giese. 1978. Mechanism of oxygen-18 exchange between water and the vanadium(V) oxyanion: $V_{10}O_{28}^{6-}$. *Inorg. Chem.* 17:1160–1166.

44. Clare, B.W., D.L. Kepert, and D.W. Watts. 1973. Kinetic study of the acid decomposition of decavanadate. *J. Chem. Soc., Dalton Trans.* 2479–2487.

45. Tracey, A.S. 2003. Applications of [51]V NMR spectroscopy to studies of the complexation of vanadium(V) by α-hydroxycarboxylic acids. *Coord. Chem. Rev.* 237:113–121.

46. Harrison, A.T. and O.W. Howarth. 1985. High-field vanadium-51 and oxygen-17 nuclear magnetic resonance study of peroxovanadates. *J. Chem. Soc., Dalton Trans.* 1173–1177.

47. Andersson, I., L. Pettersson, J.J. Hastings, and O.W. Howarth. 1996. Oxygen and vanadium exchange processes in linear vanadate oligomers. *J. Chem. Soc., Dalton Trans.* 3357–3361.

48. Crans, D.C., H. Chen, O.P. Anderson, and M.M. Miller. 1993. Vanadium(V)-protein model studies: Solid-state and solution structure. *J. Am. Chem. Soc.* 115:6769–6776.

49. Larson, J.W. 1995. Thermochemistry of vanadium(V+) in aqueous solutions. *J. Chem. Eng. Data* 40:1276–1280.

50. Elvingson, K., A.G. Baro, and L. Pettersson. 1996. Speciation in vanadium bioinorganic systems. 2. An NMR, ESR, and potentiometric study of the aqueous H$^+$-vanadate-maltol system. *Inorg. Chem.* 35:3388–3393.

51. Elvingson, K., M. Fritzsche, D. Rehder, and L. Pettersson. 1994. Speciation in vanadium bioinorganic systems. 1. A potentiometric and ^{51}V NMR study of aqueous equilibria in the H$^+$-vanadate(V)-L-α-alanyl-L-histidine system. *Angew. Chem., Int. Ed. Engl.* 48:878–885.

3 Monodentate Ligands of Vanadate

3.1 ALCOHOLS AND PHENOLS

Monomeric vanadate reacts rapidly and reversibly with alcohols and phenols, with reaction occurring within a few milliseconds at room temperature. The products correspond to alkoxovanadate derivatives, the mono- and diesters. The criterion is that the vanadate is protonated so that an OH can be replaced by OR or OAr with release of water. The reactions are quite weak when compared to many other ligands, formation constants (V + L ⇌ VL) being about 0.2 M^{-1} under neutral conditions for formation of ethylvanadate and about 5 times as large for phenylvanadate. The subsequent incorporation of a second ligand to form the diester proceeds with similar formation constants. Under strongly forcing conditions where no water is present, the triester can be formed from the alcohol, but it rapidly hydrolyzes in the presence of water. In nonaqueous solution, there is a marked tendency for the triesters to form dimers [1], with structures similar to those found for diol complexes (Section 4.1.1). The dimerization reaction does, however, seem to be sensitive to the steric bulk of the ligand, and triesters prepared from bulky alcohols apparently do not form dimers [2]. Interestingly enough, the oxovanadium(V) triester formed from isopropanol serves as a versatile material for generating vanadium pentoxide-based nanorods, nanowires, and nanotubes (Chapter 12).

Despite the fact that the formation of these alkoxo and aryloxo vanadates is not favored relative to many other ligated species, they can still have important influences in enzymic systems. It has, for instance, been shown that vanadate in the presence of glucose and glucose-6-phosphate dehydrogenase readily produces gluconic acid, a normal product of glucose-6-phosphate metabolism [3]. Similar reactivity has been observed with a number of enzymes that metabolize phosphate compounds [4].

The electronic properties of both alkyl [5] and aryl alcohols [6] play a clearly definable role in ester formation, with formation constants decreasing with increase in electron withdrawing ability of the ligand . For both types of ligands, the electronic influences are quite small, but the resonance effects found with the aromatic ligands indicate there are π-electron contributions to the empty d orbitals of vanadate [6]. The influences of the electronic properties of ligands on coordination mode and geometry are discussed in detail in Chapter 9.

3.1.1 PRIMARY, SECONDARY, AND TERTIARY ALIPHATIC ALCOHOLS

There is little influence of ligand bulk on alkoxovanadate formation, and reaction of vanadate with secondary alcohols is not disfavored when compared to primary

alcohols. The reason for this probably derives from the fact that the V-OR bond is quite long (~1.9 Å), and this serves to reduce steric interactions. Even the very bulky alcohol, *tert*-butanol, readily forms a vanadate alkoxide. Variable-temperature studies in aqueous ethanolic solution showed that formation of ethylvanadate occurred within milliseconds. The exchange rate constants measured were k_f[EtOH] = 0.97 $\times 10^3$ s^{-1} and k_h [H$_2$O] = 1.3 $\times 10^3$ s^{-1} at 328 K and pH 7.5 [7].

Systematic influences of ligands on alkoxovanadate ^{51}V chemical shifts have been observed [8] that appear to attach significance to the chemical shift of –559 ppm. The shifts of monoanionic primary alkyl esters are to low field of –559 ppm (–560 ppm, chemical shift of VO$_4$H$_2^-$), whereas those from secondary alkyl esters are to high field of this chemical shift. Additionally, there is an additivity of chemical shifts in the sense that the chemical shift of the bisalkoxovanadate is twice as far from –559 ppm as is that of the monoalkoxo derivative. This additivity appears to extend between ligands, so that if the chemical shifts of two monoalkoxovanadates (VR and VR′) are known, the shifts for the three bisligand complexes, VRR, VR′R′, and VRR′, can be predicted. Table 3.1 gives experimental and calculated chemical shifts for a variety of alcohols. There is not a very large body of data addressing this phenomenon, and it is likely that exceptions occur. Although the relationship applies to secondary alcohols that have been studied, it is quite possible it will not apply to bulky ligands, although the discrepancy might be mitigated by the fact that the V-O bond is quite long, in the order of 1.9 Å. Also, the additivity correlations have been shown to break down when 100 mM imidazole is present in solution [9], thus revealing that vanadium alkoxoimidazole complexes are being formed. Section 9.1 addresses this phenomenon in more detail.

It is not clear what the chemical shift of –559 ppm corresponds to. It is close to that of monoanionic vanadate, –560 ppm, but cannot be said to correspond to that chemical shift. Possibly, it corresponds to some species that in the presence of water leads to vanadate but, in aqueous alcoholic solution, also generates an alkoxovanadate.

The divanadate dianion also has two hydroxyl groups and readily forms mono- and dialkoxo derivatives. The situation is different with the cyclic tetra- and penta-vanadates, as they do not react with alcohols. The ionic states of these two oligomers preclude ester formation. However, the situation changes with decavanadate. Under appropriate conditions, decavanadate is protonated on several of its oxygens, and those OHs can be replaced by OR groups. In fact, ^{51}V NMR studies [4] have shown that the methyl group in monomethylated decavanadate is located on one of the triply bonded oxygens of decavanadate, in the same position as the hydrogens found in the diprotonated decavanadate, dihydrogendecavanadate tetraanion [10]. Deca-vanadate also forms well-characterized complexes with dipeptides, where the inter-actions are mediated via hydrogen bonds to the oxygens of decavanadate rather than by modifying the vanadium coordination shell. Although apparently rather easily formed in the solid, such complexes are not stable in aqueous solution [11].

There is little information available on the complexation of alcohols by five- or six-coordinate vanadium(V) compounds. Complexes of ethanolamine do form het-eroligand products with alcohols [12]. The formation constants for these materials are in the order of 0.2 to 0.5 M^{-1} and, therefore, are not very different from similar formation constants observed for alkoxovanadates.

TABLE 3.1
Chemical Shifts (ppm) Observed and Calculated for Monoanionic Vanadate Complexes of Aliphatic Alcohols (ROH)[a]

Ligand	δ ROVO$_2$OH$^-$	δ (RO)$_2$VO$_2^-$	δ (RO)$_2$VO$_2^-$ (Calculated)
CH$_3$OH	−551.0	−543.3	−543.0
CH$_3$CH$_2$OH	−555.0	−552.4	−551.0
(CH$_3$)$_3$COH	−574.6	−597.1[b]	−590.2
CH$_3$CHOHCH$_3$	−561.8	−564.6	−564.6
CH$_3$CHOHCH$_2$CH$_3$	−562.2	−564.8	−565.4
CH$_3$CHOHCH$_2$CH$_2$OH	—	—	—
Primary OH	−556.0	−552.9	−553.0
Secondary OH	−564.0	−569.5	−569.0
Mixed OH	—	−560.9	−561.0
CH$_2$OHCH$_2$OH	−556.1	−553.4	−553.2
CH$_3$C(CH$_2$OH)$_3$	−556.1	−553.0	−553.2
HCCCH$_2$CH$_2$OH	−557.8	−556.1	−556.6
NCCH$_2$CH$_2$OH	−561.0	−564.6	−563.0
CF$_3$CH$_2$OH	−562.9	−566.5	−566.8

[a] All chemical shifts taken from Tracey et al. [5,8].

[b] This shift is from a 50% acetone/water solution.

3.1.2 PHENOLS

The formation constants for the phenylate complexes are about 5 times larger than those for the alkoxovanadates, being about 1 M^{-1} under neutral conditions for the formation of the monoligated complex (V + L ⇌ VL). The complexation by a number of phenols has been studied with a view to probing the influences of electronic withdrawing and donating groups on phenylate ester formation [6]. The findings agreed with similar studies of aliphatic alcohols [5,9] and showed the influences of electronic donation or withdrawal were small. However, it was evident that π electron donation does influence complex formation.

3.2 AMINES AND ACIDS

3.2.1 ALIPHATIC AND AROMATIC AMINES

Vanadate reacts only very weakly with aliphatic amines such as ethylamine. As a consequence, reactions with aliphatic amines have not been extensively studied, but the information available suggests the reactions are analogous to those of alcohols. Additionally, there have been numerous studies of multidentate ligands where amino functionality is a critical component of vanadium ligation (Section 4.4).

Apparently, aromatic amines such as pyridine and imidazole react more strongly than do aliphatic amines, but even so, the reaction is weak. Although its formation is not highly favored, a well-defined pyridine complex of VL$_2$ stoichiometry is observed at high pyridine concentrations in aqueous solution, its formation constant

being similar to that of bisalkoxovanadate complexes [13]. At moderately low imidazole concentrations, formation of an imidazole complex is not observed [14]. However, the influence of imidazole on the reaction equilibria of vanadate in the presence of various alcohols is fully consistent with the formation of imidazole complexes [9]. Imidazole is much more reactive as a heteroligand towards numerous chelate complexes, including those of glycols and hydrogen peroxide.

3.2.2 CARBOXYLIC ACIDS, PHOSPHATE, ARSENATE, AND SULFATE

Acids react readily with vanadate to form the acid analogues to esters, the mixed acid anhydrides. Vanadate, of course, condenses with itself to form divanadate but similarly reacts with phosphate (P) or arsenate (As) to form phosphovanadate or arseniovanadate complexes [15]. Product formation constants determined at 1.0 M ionic strength with KCl for the reaction ($V^{1-} + L^{1-}$ ⇌ VL^{2-}) for L equal to P or As$_1$ are (64 ± 3) M^{-1} and (21 ± 2) M^{-1}, respectively [15]. Although trivanadate is known, its formation is not well favored, and similarly, the phosphovanadiophosphate, PVP, is not readily formed. However, the related compound diphosphovanadate, PPV, readily forms from pyrophosphate, as does a chelated pyrophosphate complex. The formation of such mixed anhydrides as phosphovanadates and carboxylatovanadates needs to be carefully considered when studying reaction chemistry of vanadate, because they can have a significant influence on the observed chemistry, as observed, for instance, in the vanadate-catalyzed oxidation of 5-keto-gluconic acid [16].

The reactions of vanadate, both with aliphatic acids and with phosphate monoanion, proceed significantly faster than reaction with alcohols, with condensation occurring within a millisecond. Alkylphosphates such as adenosine monophosphate (AMP) react with vanadate to form the alkylphosphatovanadate. Thus, AMP forms AMPV, the ADP analogue. The situation with the carboxylic acids is somewhat different from phosphate and arsenate, because both mono- and biscarboxylato complexes form [17]. Strong acids such as sulfate do not react unless the conditions are acidic enough for a significant degree of protonation. This is in accord with elimination of water during the condensation reaction.

Although the mechanism of ester and anhydride formation is not known, it seems very likely that a pentacoordinate transition state is involved. Some evidence for this is available from mixed reactions of vanadate in methanolic solution together with phosphate. A greatly enhanced rate of equilibration of the mono- and bismethyl esters with each other when phosphate is included in the reaction solution is in accord with rapid formation of a mixed methoxophosphatovanadate species that would be expected for a pentacoordinate intermediate [18]. Additionally, trigonal bipyramidal geometry is well known in vanadate chemistry, so formation of such a transition state structure is not unexpected. In fact, there is some evidence suggesting that an intermediate structure is formed. The reactions of long chain alkyl acids such as valeric (pentanoic) acid give rise to a ^{51}V product signal at –536 ppm. The coordination of vanadium in this complex is not known, but it clearly shows that products with other than tetrahedral coordination can be formed with alkylcarboxylic acids. Interestingly enough, imidazole [9] has an influence on exchange rates similar to, though not as effective as, that of phosphate, and it is likely that the mechanism

is the same. Phosphate and di- and triphosphate compete effectively for binding to vanadate with other ligands such as ethylene glycol, but not as well with the similar ligating groups in the ribose ring of nucleotides [19].

3.2.3 SULFHYDRYL LIGANDS

Very few studies of vanadate complexation with isolated alkylsulfhydryl ligands have been reported. In aqueous solution, there apparently is no complexation of vanadate with thiol groups unless multidentate reaction is possible. Sulfur, itself, is known to be able to replace the oxygens of vanadate to give the corresponding sulfidovanadium(V) complex (VS_4^{3-}) [20]. This chemistry has been studied in the equilibrium reactions of hydrogen sulfide with vanadate [21]. A sequential replacement of oxygen by sulfur was found for both the 2- and 3- series of sulfidovanadates, that is to say, the series VO_4^{3-}, VO_3S^{3-}, $VO_2S_2^{3-}$, VOS_3^{3-}, VS_4^{3-}, and the corresponding series deriving from VO_4H^{2-}. Somewhat surprisingly, no corresponding sulfidovanadates deriving from $VO_4H_2^-$ were found. Sulfur also replaced oxygen in tetranionic divanadate, yielding only symmetrically substituted products $O_3VSVO_3^{4-}$, $O_2SVSVO_2S^{4-}$, and $S_3VSVS_3^{4-}$. In addition to the above complexes, other sulfidovanadates were formed but not characterized. It seems likely that some corresponded to asymmetrical divanadate derivatives and possibly monoanionic sulfido vanadates.

REFERENCES

1. Priebsch, W. and D. Rehder. 1990. Oxovanadium alkoxides: Structure, reactivity, and 51-V NMR characteristics. Crystal and molecular structures of $VO(OCH_2CH_2Cl)_3$ and VOCl2(THF)2H2O. *Inorg. Chem.* 29:3013–3019.
2. Crans, D.C., H. Chen, and R.A. Felty. 1992. Synthesis and reactivity of oxovanadium(V) trialkoxides of bulky and chiral alcohols. *J. Am. Chem. Soc.* 114:4543–4550.
3. Nour-Eldeen, A.F., M.M. Craig, and M.J. Gresser. 1985. Interaction of inorganic vanadate with glucose-6-phosphate dehydrogenase. *J. Biol. Chem.* 260:6836–6842.
4. Stankiewicz, P.J. and A.S. Tracey. 1995. Stimulation of enzyme activity by oxovanadium complexes. *Met. Ions Biolog. Syst.* 31:259–285.
5. Tracey, A.S., B. Galeffi, and S. Mahjour. 1988. Vanadium(V) oxyanions. The dependence of vanadate ester formation on the pK_a of the parent alcohols. *Can. J. Chem.* 66:2294–2298.
6. Galeffi, B. and A.S. Tracey. 1988. The dependence of vanadate phenyl ester formation on the acidity of the parent phenols. *Can. J. Chem.* 66:2565–2569.
7. Gresser, M.J. and A.S. Tracey. 1985. Vanadium(V) oxyanions: The esterification of ethanol with vanadate. *J. Am. Chem. Soc.* 107:4215–4220.
8. Tracey, A.S. and M.J. Gresser. 1988. The characterization of primary, secondary, and tertiary vanadate alkyl esters by 51-V nuclear magnetic resonance spectroscopy. *Can. J. Chem.* 66:2570–2574.
9. Crans, D.C., S.M. Schelble, and L.A. Theisen. 1991. Substituent effects in organic vanadate esters in imidazole-buffered aqueous solutions. *J. Org. Chem.* 56:1266–1274.

10. Roman, P., A. Aranzabe, A. Luque, J.M. Gutierrez-Zorrilla, and M. Martinez-Ripoll. 1995. Effects of protonation in decavanadates: Crystal structure of tetrakis(*n*-hexylammonium) dihydrogendecavanadate(V). *J. Chem. Soc., Dalton Trans.* 2225–2231.

11. Crans, D.C., M. Mahroof-Tahir, O.P. Anderson, and M.M. Miller. 1994. X-ray structure of $(NH_4)_6(Gly-Gly)_2V_{10}O_{28}\cdot4H_2O$: Model studies for polyoxometalate-protein interactions. *Inorg. Chem.* 33:5586–5590.

12. Crans, D.C., H. Chen, O.P. Anderson, and M.M. Miller. 1993. Vanadium(V)-protein model studies: Solid-state and solution structure. *J. Am. Chem. Soc.* 115:6769–6776.

13. Galeffi, B. and A.S. Tracey. 1989. 51-V NMR investigation of the interactions of vanadate with hydroxypyridines and pyridine carboxylates in aqueous solution. *Inorg. Chem.* 28:1726–1734.

14. Elvingson, K., D.C. Crans, and L. Pettersson. 1997. Speciation in vanadium bioinorganic systems. 4. Interactions between vanadate, adenosine and imidazole—an aqueous potentiometric and [51]V NMR study. *J. Am. Chem. Soc.* 119:7005–7012.

15. Gresser, M.J., A.S. Tracey, and K.M. Parkinson. 1986. Vanadium(V) oxyanions: The interaction of vanadate with pyrophosphate, phosphate and arsenate. *J. Am. Chem. Soc.* 108:6229–6234.

16. Matzerath, I., W. Klaui, R. Klasen, and H. Sahm. 1995. Vanadate catalyzed oxidation of 5-keto-D-gluconic acid to tartaric acid: The unexpected effect of phosphate and carbonate on rate and selectivity. *Inorg. Chim. Acta* 237:203–205.

17. Tracey, A.S., H. Li, and M.J. Gresser. 1990. Interactions of vanadate with mono- and dicarboxylic acids. *Inorg. Chem.* 29:2267–2271.

18. Tracey, A.S., M.J. Gresser, and B. Galeffi. 1988. Vanadium(V) oxyanions. Interactions of vanadate with methanol and methanol/phosphate. *Inorg. Chem.* 27:157–161.

19. Geraldes, C.F.G.C. and M.M.C.A. Castro. 1989. Multinuclear NMR studies of the interaction of vanadate with mononucleotides, ADP and ATP. *J. Inorg. Biochem.* 37:213–232.

20. Do, Y., E.D. Simhon, and R.H. Holm. 1985. Tetrathiovanadate(V) and tetrarhenate(VII): Structures and reactions, including characterization of the VFe_2S_4 core unit. *Inorg. Chem.* 24:4635–4642.

21. Harrison, A.T. and O.W. Howarth. 1986. Vanadium-51 nuclear magnetic resonance study of sulphido- and oxosulphido-vanadate(V) species. *J. Chem. Soc., Dalton Trans.* 1405–1409.

4 Aqueous Reactions of Vanadate with Multidentate Ligands

Tetrahedral coordination is the coordination geometry most frequently found in vanadate and its oligomers and in reaction products with monodentate ligands. The situation changes with bidentate ligands, where pentacoordination is most frequently encountered with monoligated species, whereas hexacoordination is generally encountered with bisligated vanadates, if the latter products form. An example of unusually high coordination is afforded by amavadin that has been oxidized to the V(V) state. This V(V) complex is eight-coordinate [1] and is also unusual in that there is no V-oxo group.

4.1 GLYCOLS, α-HYDROXYCARBOXYLIC ACIDS, AND DICARBOXYLIC ACIDS

Glycols, α-hydroxycarboxylic acids, and dicarboxylic acids react readily with vanadate to form products that generally have pentacoordinate geometry. The increase in coordination number is frequently accomplished by the formation of a dimeric product centered about a cyclic $[VO]_2$ core. This structural element is one of the defining properties of vanadate coordination, and the bridge is formed through oxo, alkoxo, or even peroxo oxygens in the manner depicted in Scheme 4.1. The VO bond lengths within the core typically are not very different, although they can be. Generally, the oxygens involved in core formation do not derive from the oxygens of the VO_2 oxo grouping. The VO bond lengths of the VO_2 are quite short, typically about 1.6 Å. In the examples in which a V-oxo bond is found in the $[VO]_2$ core, a short bond to the primary vanadium is maintained. This is observed, for instance, in a salicylic acid Schiff base complex (Scheme 4.1a), where the VO bond length to one vanadium is 1.678 Å, whereas it is 2.445 Å to the other [2]. These distances compare to the VO bond length of 1.605 Å to the oxo oxygen not involved in the core. Long VO bonds within the core of the crystalline complex suggest that the dimeric complex will not be maintained when the crystalline material is in aqueous solution, and indeed, solution dimers of this type have not been reported.

In the situation with 1,2-diols, such as depicted in Scheme 4.1b, where the oxygens of the VO_2 grouping are not incorporated into the core, the dimeric structure of the complex is highly favored in aqueous solution. For a nucleoside complex, the VO bond of the VO_2 moiety are 1.625 lengths and 1.626 Å, whereas the individual VO bonds of the core are 2.036 Å and 1.983 Å in length [3]. Dimeric structures,
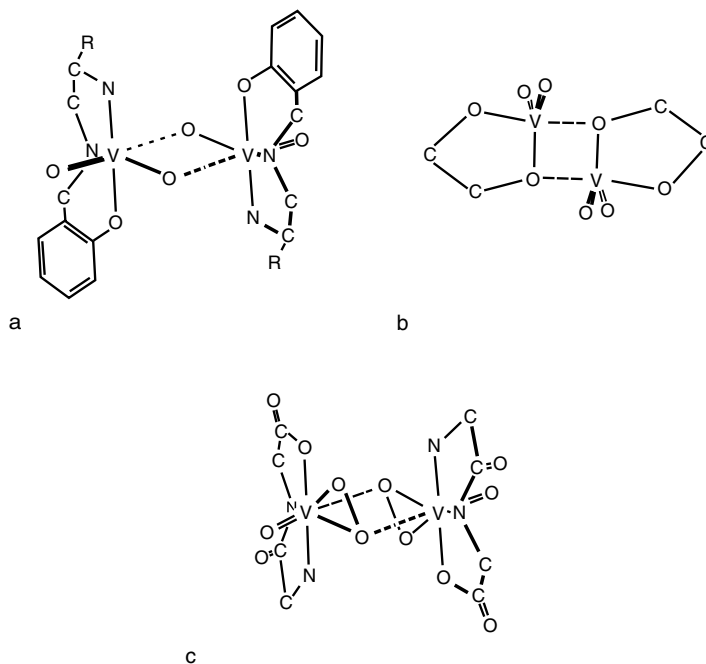
SCHEME 4.1

similar to those deriving from glycols, are also observed for α-hydroxycarboxylate complexes, where comparable VO bond lengths, 1.605 and 1.617 Å for the VO_2 and 1.973 Å and 1.984 Å for the core, are found [4]. Other dimeric complexes that appear to maintain their structure in aqueous solution have similar bond lengths.

The core itself tends to be very close to planar, and this may reflect a dominating influence of the VO_2 functionality. Planarity is not necessary, and significant deviations from planarity have been found in some vanadium peroxo complexes with chiral hetero ligands, where one oxygen of the VO_2 group has been replaced with a peroxo group to afford a $VO(O_2)$ grouping [5].

Formation of the cyclic core structure can also directly involve oxygens of peroxo groups, as depicted in Scheme 4.1c for a dipeptidoperoxovanadate complex. The situation depicted here is somewhat similar to the situation with Schiff bases. The vanadium to oxygen distances of the directly ligated peroxo group are 1.877 and 1.892 Å. This compares to the distances to the adjacent peroxo oxygens of the core, which are much longer, 2.573 and 2.660 Å. As for the Schiff base complex, the dimer is not maintained in solution [6].

4.1.1 GLYCOLS: CYCLOHEXANE DIOLS, CARBOHYDRATES, AND NUCLEOSIDES

Vanadate reacts with ethylene glycol and other 1,2-diols such as carbohydrates and nucleosides (nucleotides) to form two predominant types of products. Reaction can

occur at the hydroxyl group in a monodentate fashion to form vanadate esters at the individual hydroxyl groups. As for other alcohols, formation constants corresponding to such reactions are small. Incorporation of the second hydroxyl into the vanadium coordination sphere leads to a secondary reaction and a dimeric product is formed. Although data is highly limited, evidence from studies of nucleosides and β-methyl riboside suggest the dimerization constant is in the order of 10^6 to 10^7. Such a large dimerization constant means the observation of the monomeric precursor is difficult, although its presence in solution has been inferred from vanadate/nucleoside equilibrium studies [7,8] and from dissolution studies of the crystalline adenosine complex [3]. The magnitude of the dimerization constant reflects the stability afforded by the $[VO]_2$ core that is generated in the dimerization reaction.

X-ray structure analysis of glycolato-derived dimeric complexes has established the pentacoordinate arrangement of ligands about the vanadium nucleus in an approximate trigonal bipyramidal geometry [3,9]. Dissolution studies are fully consistent with retention of that geometry in aqueous solution. There is, however, an interesting dynamic process that occurs that can be readily observed when ligands are chiral. The processes depicted in Scheme 4.2 are in accord with observations. With a chiral ligand complex of the type in Scheme 4.2a, the two ligands of the complex are interconverted by a rotation of the complex and, therefore, are equivalent. If the bonds V′–O′ and V″–O″ break, then a macrocyclic compound Scheme 4.2b is formed. The macrocycle can regenerate the original complex or undergo a sideways motion of the reactive groups, then recyclize to form a second symmetrical product, an isomer of **a**, Scheme 4.2c. An alternative reaction is that if the V″–O′ and V′–O″ bonds of the original complex, Scheme 4.3a, break as depicted in Scheme 4.3b to form the two monomers. If one monomer rotates 180º with respect to the second monomer and dimerization reoccurs, then a third isomeric product, Scheme 4.3c, is formed. The two ligands of **c** are not equivalent and such a compound will give two sets of NMR signals. Subsequent bond breakage and recyclization of the type depicted in Scheme 4.2a–c will interconvert the two ligands of the complex in Scheme 4.3c. Although the macrocycle proposed for the equilibration described above has not been reported for hydroxo-containing complexes, a macrocycle with this structure has been characterized for a dimeric chlorovanadium complex with ethylene glycol [10]. This crystal structure provided strong support for the two types of isomerization reactions described above and the reactions were invoked in order to explain the observation of four adenosine NMR signals and also the isomerization between them that was observed after dissolution of a crystalline adenosine complex [3].

There is a marked stereospecificity for product formation that is observed with cyclic 1,2-glycols, for instance, cyclohexane diols [11] and pyranose monosaccharides [11–13]. With ligands of this type, complex formation when the hydroxyls are trans to each other is disfavored compared to the situation with cis hydroxyl groups. For instance, for similar conditions, there is a factor of about 10 between product formation with cis cyclohexane diol compared to the trans ligand. It is, however, with furanose rings that product formation is very highly favored. With furanose rings, the cis hydroxyls can easily align in a close-to-parallel fashion with each other, and this geometry promotes formation of the five-membered ring that is generated as the complex forms. This is revealed in product formation constants, where for-
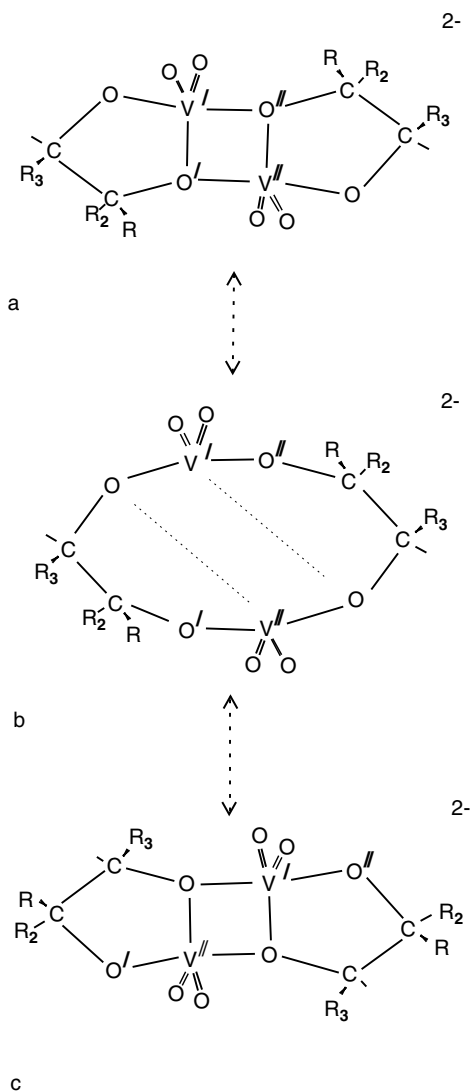
SCHEME 4.2

mation of complexes with nucleosides is 3 orders of magnitude larger than product formation with cis 1,2-cyclohexanediol.

An interesting reaction is observed with galactose α-methylpyranoside. In addition to the dimeric compounds (–521 ppm) of the type described above, an additional product (–502 ppm) with similar V_2L_2 stoichiometry is formed. This product is distinct in the NMR spectrum and has the property of being able to incorporate at least one additional ligand [11]. It seems likely that the galactoside can function as a trident ligand, where the C_6 hydroxyl group participates in the complexation reaction. In the absence of the stabilizing influence of the 1,2-cis glycol functionality
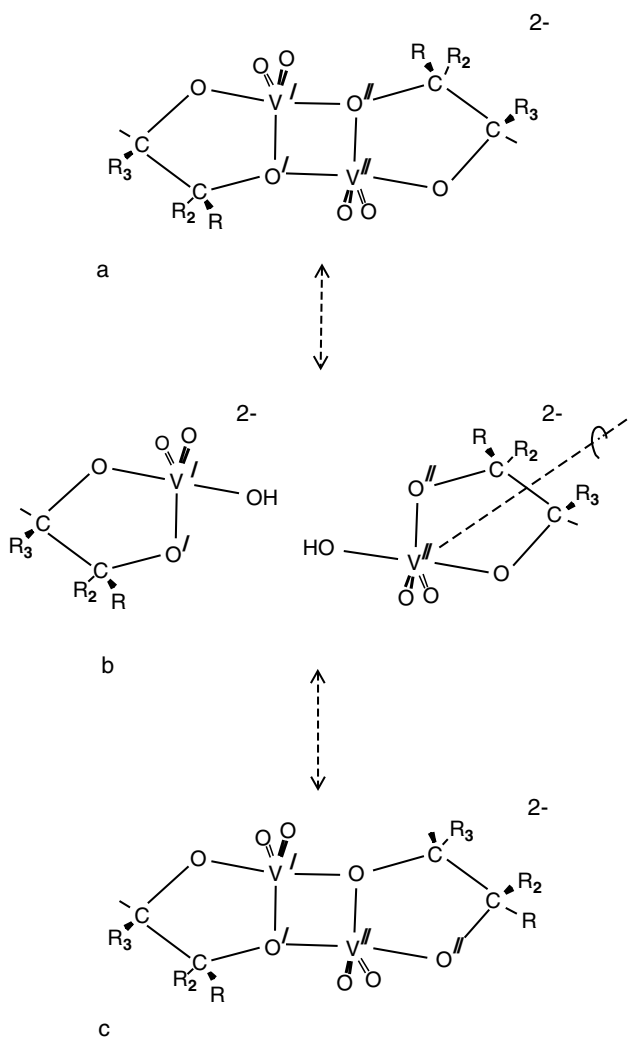
SCHEME 4.3

of the galactoside, complexation involving the C_6 hydroxyl would not be expected because this corresponds to 1,3 diol complexation, which is not favored. Considering the structure of the dimer (–521 ppm), which has pentacoordinate geometry, it is highly likely that the –502 ppm product has octahedral coordination about the vanadiums. Additionally, an apparent mixed coordination product (–517, –544 ppm) of V_2L_2 stoichiometry is readily formed that possibly involves complexation with the C_6 hydroxyl group. If complexation does involve the C_6 hydroxyl, then similar products cannot form with the related monosaccharides, α–methylmannopyranoside and α-methylglucopyranoside, and they are not observed.

   Although they have been looked for, no bidentate complexes of 1,3-glycols have been found in aqueous solution. This suggests their formation is energetically very

unfavorable. Doubtless, under appropriate conditions, they will be observed. They can be formed in nonaqueous solution as heterocomplexes with other ligands, but even as heterocomplexes, they hydrolyze when in an aqueous environment [14]. 1,3-Diol chelates require a six-membered ring for their formation, and it seems clear that this is not a favored ring size. When there are additional stabilizing interactions, 1,3-chelates can form as with the triol, 1,1,1-tris(hydroxymethyl)ethane, and similarly with Tris buffer, tris(hydroxymethyl)aminomethane. As found for the 1,2-diols, these complexes are binuclear in vanadium and contain two ligands [15]. It seems reasonable that coordination would be somewhat similar to that of the 1,2 diols except that there very likely is bridging between vanadium centers by one of the hydroxymethyl groups, perhaps after the fashion suggested by Scheme 4.4. The bridging would provide the stabilization necessary for formation of significant amounts of these products. The formation constant for the 1,1,1-tris(hydroxymethyl)ethane complex for the reaction $2V + 2L \rightleftharpoons V_2L_2$ is $(1.4 \pm 0.1) \times 10^2$ M^{-3} at pH 7.5. This formation constant is 4 to 5 orders of magnitude smaller than formation constants found for 1,2-diols that have a favorable orientation of the hydroxyl groups such as the nucleosides [7] but not very different from other 1,2-diol ligands.

Tris(hydroxymethyl)aminomethane (Tris buffer) reacts as a heteroligand with complexes of 1,2-diols [7,15]. This heteroligand reaction suggests amine functionality is important for formation of mixed diol/heteroligand complexes. It is unlikely that there is a specific requirement for the amine functionality, but certainly even the monodentate amine, imidazole, readily forms a mixed ligand complex in the vanadate/adenosine/imidazole (V/Ad/Im) mixed ligand system [16]. An interesting facet of this reaction is the large shift in equilibrium from the dimeric diol complex, where VAd monomers are relatively disfavored, to high proportions of at least two products of VAdIm stoichiometry, albeit under fairly high relative concentrations of imidazole. Presumably, the observation of multiple VAdIm products indicates there
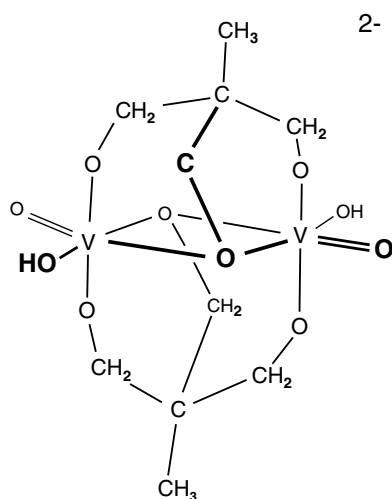
SCHEME 4.4

is formation of geometrical isomers. Schiff base heteroligands with diol complexes readily form, and in these types of complexes, there is direct bonding of the amine functionality [17].

4.1.2 α-HYDROXY CARBOXYLIC ACIDS, MALTOL

Oxidation of one of the hydroxyl groups of a 1,2 glycol to form an α-hydroxy carboxylic acid increases the complexity of the vanadate chemistry. Mono, di, tri and higher nuclearity compounds are formed with α-hydroxycarboxylic acids. Except for the dimeric products, the structures adopted by these compounds are not known with any degree of certainty.

The dimeric compounds are structurally similar to those formed with 1,2-glycols. However, their chemistry is somewhat simpler. This is because an alkoxo oxygen can participate in the formation of bonds to two different vanadiums (Scheme 4.2), while the carboxyl oxygen forms bonds to only one vanadium. The principal consequence of this is that isomer formation is restricted so that, although three dimeric complexes are possible with 1,2-glycolato-derived ligands, only one dimer is expected for α-hydroxycarboxylato ligands. Because of this, the dynamic process depicted in Scheme 4.2 does not function. A number of crystal structures [18,19] have revealed this selectivity of structure and, correspondingly, NMR spectroscopy has shown the formation of only one dimeric complex in solution, as opposed to three isomers with glycolato type ligands.

In crystal structures of numerous α-hydroxy carboxylate complexes, the core is close to being planar, with the V-alkoxo bond lengths typically being about 2.00 Å for the ligand alkoxo VO bond and 1.96 Å for the bridging VO bond [18]. Therefore, these lengths are different by only about 3%. The VO oxo bond length is considerably shorter, normally being about 1.62 Å. The core has a distinct rhomboidal shape, with the OVO angle within the range of 71 to 72°, whereas the VOV angle is 108 to 109°. Bond distances and angles for dimeric complexes of a number of different ligands are summarized in Table 4.1. It is interesting to note how similar the structure of the diol complexes are to those of the α-hydroxy carboxylate derivatives. The major difference is that the OVO angle is slightly compressed by about 2° in the diol complexes compared to the α-hydroxy carboxylate complexes. As is evident from Table 4.1, in the crystalline matrix, the core can be distorted from a perfect rhomboidal structure by the crystal forces. There is no reason to expect those distortions to persist if the compound is put into solution. Certainly, there is no evidence for such deformations from any NMR studies.

In contrast to the situation with 1,2-glycolato ligands, the reaction with α-hydroxy carboxylato ligands to form monomeric products is relatively highly favored, being about 20–30 M^{-1} for the reaction $V^- + L^- \rightleftharpoons VL^{2-}$. The dimerization constant is, however, comparatively much smaller, being about 3 orders of magnitude smaller for α-hydroxyisobutyric acid than for nucleoside ligands. The coordination about vanadium in the monomers is not known, although because lower coordination numbers tend to be favored, they most likely are pentacoordinate. The fact that the VL complexes can incorporate an additional ligand without a significant change in ^{51}V chemical shift between VL (~ –503 ppm) and VL_2 (~ –518 ppm) suggests there

TABLE 4.1
Bond Distances and Angles for the $[VO]_2$ Core of Various Dimeric Vanadate Complexes of Diols and α-Hydroxycarboxylic Acids

	Ligand [a]				
	Aden	**Man**	**Glyc**	**Lac**	**Cit**
Bond Length					
V_1–O_{oxo}	1.625(2)	1.610(7)	1.614(2)	1.635(5)	1.634(3)
	1.626(3)	1.630(7)	1.614(2)	1.617(4)	1.618(3)
V_2–O_{oxo}	1.633(3)	1.596(8)	—[b]	1.599(5)	—[b]
	1.630(2)	1.631(7)	—[b]	1.605(4)b	—[b]
V_1–O_1	2.036(2)	2.002(8)	1.998(2)	1.998(4)	2.017(2)
V_1–O_2	1.983(2)	2.014(6)	1.944(2)	1.949(3)	1.970(2)
V_2–O_2	2.042(2)	2.061(7)	b2.004(4)	—[b]	
V_2–O_1	1.976(2)	1.995(6)	b1.965(3)	—[b]	
Angle					
O_1–V_1–O_2	69.20(8)	69.3(3)	71.14(7)	71.6(1)	70.9(1)
V_1–O_1–V_2	110.68(9)	107.4(8)	108.86(7)	108.4(2)	109.1(1)
O_{oxo}–V_1–O_{oxo}	109.3(1)	108.9(4)	107.87(11)	107.9(2)	106.9(2)
O_1–V_2–O_2	69.21(8)	68.3(3)	—[b]	71.19(14)	—[b]
V_1–O_2–V_2	110.18(9)	104.4(3)	—[b]	108.8(2)	—[b]
O_{oxo}–V_2–O_{oxo}	107.9(1)	108.2(5)	—[b]	108.8(3)	—[b]
References	[3]	[9]	[18]	[18]	[23]

[a] Abbreviations: **aden**, adenosine; **man**, methyl- 4,6-*O*-benzilidine-α-**D**-mannopyranoside; **glyc**, glycolic acid; **lac**, lactic acid; **cit**, citric acid.

[b] Bond lengths or angles are related by crystal lattice symmetry to those already quoted.

is no change in coordination geometry when the second ligand is incorporated into the complex.

An additional complex that under appropriate conditions can be the major product in solution has a V_3L_2 stoichiometry. The available evidence shows that two of the vanadiums, each with an attached ligand, are interconverted by a rotation whether or not the ligands are chiral. Two of the most likely coordination modes are depicted in Scheme 4.5. Both of these coordination modes allow for isomers. When the ligand is chiral structure, **a** can have endo and exo forms, whereas for **b** there is the possibility of isomeric forms whether or not the ligand is chiral. As yet, there are no reports of more than one V_3L_2 complex. There is some evidence that a tetranuclear complex is also formed. However, it is a minor product, and it has not been well characterized [20]. Structure **a** leads more naturally to a tetranuclear product. The chemical shifts, –533 and –550 ppm for the lactate complex (and similar for other ligands), also seem more consistent with the octahedral/tetrahedral vanadiums of **a**. However, the evidence in support of either coordination is not at all definitive.

Considering the ease of formation of the trinuclear complex, it is somewhat surprising that a corresponding complex was not reported for the vanadiocitrate
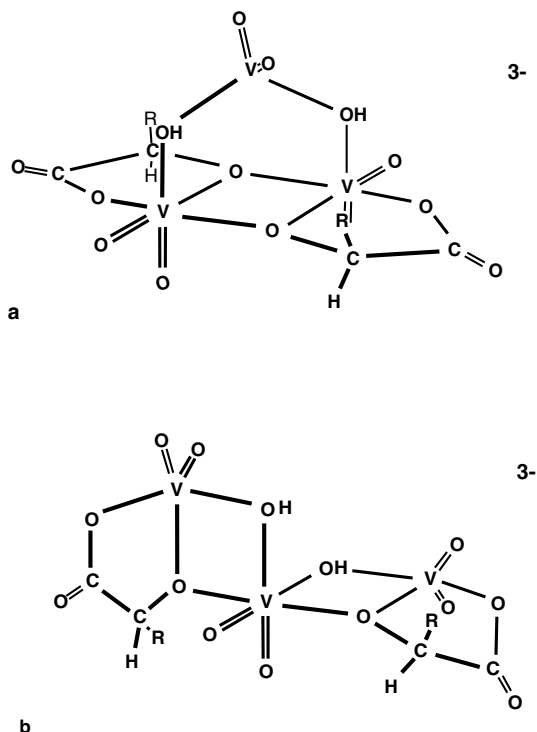
SCHEME 4.5

system. The equilibria, however, are very complex, and components found in the simpler α-hydroxycarboxylate equilibria might not be observable. Of considerable interest in the citrate system was the formation of a V_2L product. The central V_2O_2 core can form in such a complex if both terminal carboxyl groups and the central hydroxyl are involved in complex formation [21]. This is unique because such a complex does not require the carboxylate group adjacent to the hydroxyl; that is to say, it is a β-hydroxy not an α-hydroxy complex. However, as found in the crystal structures [19,22,23] and by solution studies [21], the dimeric α-hydroxy complexes are well represented with the citrate ligand and also with the closely related homocitrate [24]. Below pH values of about 7, 2R,3R-tartaric acid efficiently complexes tetravanadate with which it forms a unique complex of V_4L_2 stoichiometry. In this complex, each vanadium is pentacoordinate (see Section 8.1).

Somewhat surprisingly, maltol (2-methyl-3-hydroxy-4-pyrone), an aromatic analogue to α-hydroxy carboxylic acids, shows little inclination toward formation of dimeric complexes. Rather, the chemistry is more in parallel with that of oxalate, and an x-ray structure of the bismaltolato complex [25] shows a cis octahedral coordination similar to that found for the oxalate complex. Under mildly acidic to moderately basic solution, the major complexes are mono- and bisligand derivatives. The corresponding vanadium chemical shifts are –509 and –496 ppm, respectively [25,26]. The closely related amines, 2-methyl-3-hydroxy-4-pyridinone and its N-

TABLE 4.2
^{51}V Chemical Shifts and Formation Constants for Selected 2-Methyl-3-Hydroxy 4-Pyrone and 4-Pyridinone Complexes of Vanadate at pH 7.0

Ligand	Chemical Shift (ppm)	K_f	Ref.
$V_1 + L$ VL			
2-Methyl-3-hydroxy-4-pyrone	−509	$(4.0 \pm 0.4) \times 10^2$ M^{-1}	25, 26
2-Methyl-3-hydroxy-4-pyridinone	−505	$(7.9 \pm 0.4) \times 10^3$ M^{-1}	—
2-Methyl-3-hydroxy-4-(N-methyl)pyridinone[a]	−504	$(1.2 \pm 0.1) \times 10^4$ M^{-1}	—
$V_1 + 2L$ VL_2			
2-Methyl-3-hydroxy-4-pyrone[a]	−496	$(5.1 \pm 0.4) \times 10^6$ M^{-2}	25, 26
2-Methyl-3-hydroxy-4-pyridinone	−481	$(9.2 \pm 1.0) \times 10^6$ M^{-2}	—
2-Methyl-3-hydroxy-4-(N-methyl)pyridinone[a]	−478	$(1.9 \pm 1.0) \times 10^7$ M^{-2}	—

[a] Unpublished work of A.S. Tracey and H. Li.

methylated derivative, 2-methyl-3-hydroxy-4-(N-methyl)pyridinone, also form two major products. Table 4.2 gives chemical shifts and formation constants for various products for pH 7.0. The pyridinone ligands give rise to additional complexes (–490, –520 ppm and –489, –519 ppm for the N-H and N-methyl ligands, respectively) that cannot readily be associated with the major maltol and pyridinone products. Unfortunately, they have not been adequately characterized, but it may be that they are binuclear complexes similar to those formed from α-hydroxy carboxylic acids.

It has been shown that the monomaltolato complex has a pK_a of about 10.0 [25,26], whereas the bisligated species does not have a pK_a except under strongly acidic conditions where it is protonated. It therefore seems that the bismaltolato complex in solution retains the structure found in the solid (Scheme 4.6a). It is difficult to judge what the structure of the monoligated complex is. Because it has a pK_a, it has an ionizable proton, as expected from its charge state of –1. This would imply a pentacoordinate geometry. However, it is possible that the vanadium center is hydrated, thus generating a hexacoordinated vanadium center. It can be determined from Table 4.1 that the formation constant for the reaction V + L   VL is not greatly different from that for the reaction VL + L VL_2. This lack of strong cooperativity in the two reactions may indicate that, in this reaction sequence, there is a stepwise change in coordination from tetrahedral to pentacoordinate to octahedral coordination. Also, transfer of electrons from the oxygen of ligated water to the vanadium nucleus should make the bound water a stronger acid, not a weaker one, as is suggested by a pK_a of 10. On these bases, the monomaltolato complex will have pentacoordinate geometry as depicted in Scheme 4.6b. Certainly, though, an octahedral coordination (Scheme 4.6c) cannot definitively be ruled out and this is the coordination that has previously been proposed [25,26].
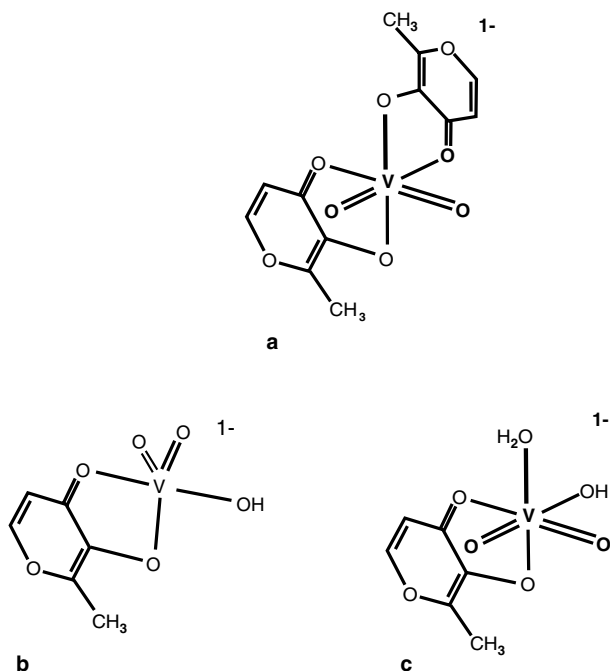
SCHEME 4.6

4.1.2.1 Heteroligand Complexes

An interesting facet of complexes of vanadate with diols and α-hydroxycarboxylates is their reaction with heteroligands. Unfortunately, this aspect of vanadate chemistry has not been well investigated. The reactions can lead both to mononuclear and binuclear products. Vanadate in the presence only of excess diol apparently does not give rise to products additional to those described above, whereas excess α-hydroxycarboxylate can give rise to a mononuclear complex containing two ligands at the expense of the binuclear complex [27], so it is evident that potential for coordination of heteroligands does exist. It has been shown, for instance, that some amino alcohols can react with complexes of 1,2-diols with elimination of one diol ligand [7,15]. In this regard, the bidentate ligand, ethanol amine, was found to be ineffective, whereas tris(hydroxymethyl)aminomethane forms a binuclear complex of V_2LL' stoichiometry. It seems from this observation that for amino alcohols, being a tridentate ligand is a minimum requirement for formation of significant amounts of heteroligand vanadate/diol complexes. On the other hand, high imidazole concentrations have been shown to convert significant amounts of the dimeric adenosine complex to a monomeric VLL′ derivative [16].

1,2-Diols derived from substituted monosaccharides have also been shown to bind as chelated heteroligands to L-amino acid-derived Shiff base complexes [17]. The coordination about vanadium in these complexes is octahedral, with the sixth coordination site occupied by an oxo ligand. Vanadium-5 NMR spectra from nonaqueous solvent show the coordination is retained in solution. Evidently, the compound is stable

in the presence of water, as adding D_2O to the NMR sample did not destroy the complex. An interesting aspect of these compounds was the finding that one of the hydroxyls of the diol ligand did not lose its proton on complexation. Possibly a similar type of hydroxo functionality would be important to diol V_2L_2 complexes such as the complex with adenosine, where it has been shown that protonation of the $V_2Ad_2^{2-}$ occurs to form $V_2Ad_2^{1-}$ [16]. In $V_2Ad_2^{2-}$, both oxygens of the ligand are deprotonated, but presumably one of the oxygens that is shared with the adjacent vanadium nucleus is protonated when $V_2Ad_2^{1-}$ is formed under more highly acidic conditions, the pK_a for the deprotonation step being 4.21. This would explain why a second protonation step was not observed, as a substantial increase in acidity of $V_2Ad_2^0$ compared to $V_2Ad_2^{1-}$ would be expected. It has, however, been proposed that the protonation occurs at the N1 nitrogen of an adenosine ligand [16].

4.1.3 DICARBOXYLIC ACIDS: OXALIC, MALONIC, AND SUCCINIC ACIDS

Detailed investigations of the aqueous reactions of vanadate with oxalate (Ox) have been carried out and two major products identified [27,28]. Unlike the major complexes formed with 1,2-glycols and α-hydroxycarboxylic acids, the oxalate derivatives are monomeric with VL and VL_2 stoichiometry. There is little doubt that in solution, the bis oxalato complex is cis coordinated in octahedral geometry, as found in the solid state [29,30]. Additionally, arguments based on ^{13}C and ^{17}O NMR studies have been used to assign a pentacoordinate geometry to the monoligated product [30]. Despite the apparent difference in coordination geometry between these two complexes, the vanadium chemical shifts are quite close together, being within a few ppm of –536 ppm: VOx^- (–533 ppm) and VOx_2^{3-} (–536 ppm).

Because of the cis octahedral structure of the bisoxalato complex, the two carboxyl groups of oxalate are not equivalent. Carbon-13 NMR spectroscopy has been used to study the kinetics of interconversion of the carboxyl groups [31]. The results of the study were consistent with breakage of one VO bond of one of the oxalate ligands to form a five-coordinate intermediate. A rotation about the remaining VO bond followed by recyclization would then afford the isomeric product. Because no exchange with free oxalate was observed, the kinetics of the dissociation/reassociation reaction must be significantly slower than internal rotation and cyclization of an oxalate group. It is interesting that even with such a strong binding ligand as oxalate, a pentacoordinate structure is rather easily obtained.

Unlike glycols, where no 1,3 complexation has been observed in aqueous solution, 1,3 complexation readily occurs with malonic acid. Although under similar conditions it is not as strong a complexation agent as oxalate, complexation of vanadium by malonic acid is favorable. With longer chain diacids, complexation is much less favored. In terms of such ligands, succinate is different with three complexes being formed; one product (–541 ppm) of VL_2 stoichiometry, but in rapid chemical equilibrium, is presumably coordinated similarly to acetate, whereas the other two (–536, –548 ppm) are of VL stoichiometry and unknown coordination. Both pentane 1,5 and hexane 1,6 dicarboxylic acids give product ^{51}V NMR signals

at –536 ppm. It is expected that the products corresponding to this chemical shift are of similar coordination to those formed with valerate and succinate.

The structure of the –536 ppm products of VL stoichiometry is one of conjecture. The fact that the products are in slow exchange on the ^{51}V NMR timescale while existing in the presence of fast-exchanging products suggests that the –536 ppm products have other than tetrahedral geometry. Electron withdrawing groups tend to favor an increase in coordination number. The series 2-methylsuccinate, succinate, and 2-chlorosuccinate shows a systematic increase in formation constant for the –536 ppm product (1.4, 7.3, 16.7 M^{-1}, respectively), whereas the –541 ppm fast exchanging products show a systematic decrease in formation constant (9.1, 5.8, < 0.2 M^{-2}), respectively. It is most likely that the –541 ppm complexes have tetrahedral coordination. If so, it is reasonable to expect that the –536 ppm compounds have either penta- or hexacoordinate geometry. If they are pentacoordinate, the coordination must be different from that in the transition state for formation of the acid anhydrides, and this raises the possibility that the carboxylate group is complexed in a bidentate fashion. Octahedral coordination does, however, seem the more likely possibility.

The remaining complex (–548 ppm) observed with succinic acid may well represent participation of both carboxyl groups in complexation and formation of an octahedral product. In view of the complexity of these carboxylic acid reactions, they, and succinic acid reactions in particular, deserve more study.

4.2 HYDROXAMIC ACIDS

The hydroxamic acids offer an interesting problem in the chemistry of their complexation. Do they complex as the hydroxamate or as the hydroximate? Both forms of reaction are known. Complexation of a salicylhydroxamide ligand leads to the formation of a trimeric cluster where the ligands complex as the hydroximates [32]. The cluster, unfortunately, is not stable in aqueous solution. However, the complexation of aqueous vanadate by hydroxamates is a highly favorable reaction that provides the basis for a number of analytical procedures. Even the very simple hydroxamate, N-hydroxyacetamide, readily forms complexes of VL and VL$_2$ stoichiometry throughout a wide pH range [33]. Scheme 4.7 depicts possible coordination modes for the N-hydroxyacetamide ligand for various protonation states. There seems little doubt that VL corresponds to a hydroxamate complexes of the form depicted in Scheme 4.7a–c. Heteronuclear chemical shift correlation experiments showed the presence of a proton J-coupled to ^{15}N in a benzohydroxamic acid complex [34]. This is not possible with a hydroximate complex, where no proton is attached to nitrogen. In contrast, an x-ray structure of a mixed catocholate/salicyl-hydroxamate complex clearly showed the hydroximate rather than the hydroxamate form for the salicylhydroxamic acid ligand [35].

This type of complex undergoes a series of protonation/deprotonation reactions with change in pH. Table 4.3 gives the ^{51}V chemical shifts for the N-hydroxyacetamide complexes. It can be seen from the table that the VL signal position changes in a consistent manner as it goes through its successive deprotonation steps, its value changing little for the first deprotonation but changing significantly for the second.
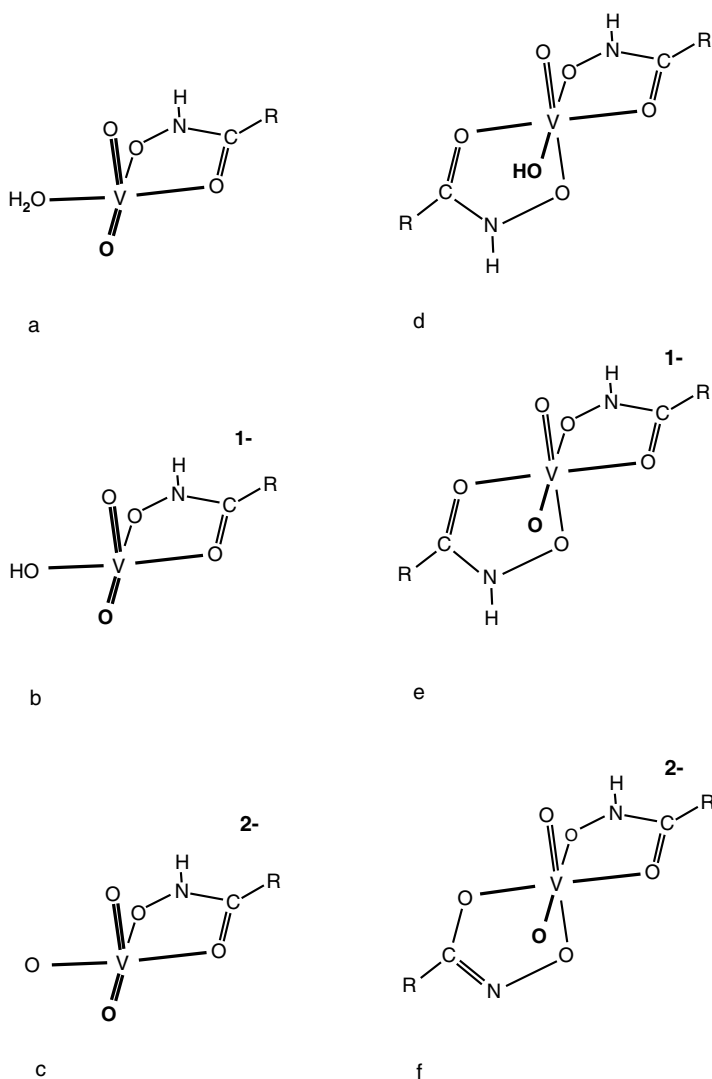
SCHEME 4.7

The situation is quite different with VL_2 (Scheme 4.7d–f), where the direction of change in chemical shift of the first deprotonation is opposite to that for the second deprotonation, whereas the magnitude of the change is large in both cases. It has been suggested that the second deprotonation of VL_2 leads via a coordination change to a complex in which one ligand is not chelated [33]. Loss of chelation is certainly possible. However, a chelate can be retained if deprotonation occurs at the nitrogen. In this case an electronic rearrangement provides a mixed ligand hydroximate/hydroxamate complex (Scheme 4.7f).

TABLE 4.3
^{51}V Chemical Shifts for Selected Hydroxamate Complexes of Vanadate

Ligand	Complex	Chemical Shift (ppm)	pK$_a$	Ref.
N-Hydroxyacetamide[a]				33
	VL^0	~ −512	4.8	33
	VL^{1-}	−517	8.4	—
	VL^{2-}	~ −478	—	—
	VL$_2{}^0$	~ −430	3.5	—
	VL$_2{}^{1-}$	−503	7.4	—
	VL$_2{}^{2-}$	~ −460	—	—
2-Amino-N-Hydroxypropanamide				81
	VL^{1+}	−525	4.4	—
	VL^0	−513	7.3	—
	VL^{1-}	−482	—	—
	VL$_2{}^{2+}$	−420	2.6	—
	VL$_2{}^{1+}$	−503	~7.4	—
	VL$_2{}^0$	−421	—	—

[a] Chemical shift recalculated using the data in Reference 33 assuming a pK$_a$ of 4.8.

An interesting series of hydroxamates studied at pH 7.5 [34] have revealed exceedingly large differences in relative formation constants for the reactions, V + L ⇌ VL (K$_1$) and VL + L ⇌ VL$_2$ (K$_2$). The ratio, K$_1$/K$_2$, varies by about 4 orders of magnitude from 2300 to 0.13. Even the closely related compounds PheCH$_2$CONHOH and CH$_3$CONHOH have very different formation constants: K$_1$, K$_2$ of 440 M^{-1}, 3400 M^{-1}, and 2100 M^{-1}, 410 M^{-1}, respectively. Although there are very large differences in K$_1$/K$_2$ for the various ligands, the products of the formation constants, K$_1$K$_2$, are within a factor of 10 of each other. This means that the overall formation of VL$_2$ is insensitive to ligand and suggests that there is a stepwise change in coordination geometry, with VL having a different geometry than VL$_2$, as suggested by Scheme 4.7.

4.3 THIOLATE-CONTAINING LIGANDS

4.3.1 β-Mercaptoethanol and Dithiothreitol

Despite the assertion over a number of years that vanadate is rapidly reduced in the presence of ligands such as β-mercaptoethanol and dithiothreitol, it is now known that this assertion is subject to qualification. Solution studies have shown that the vanadium(V) complexes of β-mercaptoethanol [36] and dithiothreitol [37] can be quite stable in solution. At pH 7.1, reduction of vanadium in the dithiothreitol complex occurs in a timescale of about 90 min, and even at pH 6.2, significant production of V(IV) is not observed for about 20 min. When the crystalline vanadium(V) complex of β-mercaptoethanol was dissolved in water, it was shown to
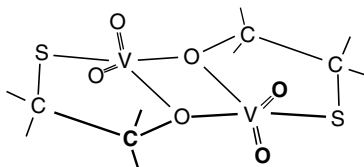
SCHEME 4.8

persist in solution for several days [36]. Acid conditions do, however, promote a rapid reductive process. This is not surprising, because vanadate is a good electron acceptor under acidic conditions [38]. No detailed studies of the reductive process have been reported. It may, however, be conjectured that reduction involves inter-mediates or side products in the complexation reaction. The β-mercaptoethanol complex in acetonitrile, for instance, is quite stable, and here there will be little dissociation of the complex. In water, the complex will dissociate and regenerate, so the vanadium is not as stable to reduction.

In contrast to the above assertions, other investigators have stated that reduction of vanadate by both β-mercaptoethanol and dithiothreitol is rapid [39]. However, that work treated the reactants with a high concentration of HCl before analysis of the reaction mixture. Strongly acidic conditions promote rapid reduction. However, a very interesting result concerning reduction by glutathione was also reported in that work. After treatment for 1 h at 37°C at pH 7.4 followed by the addition of HCl, only about 3% reduction of vanadate by glutathione was observed. This clearly showed that glutathione did not reduce vanadium as quickly as either β-mercapto-ethanol or dithiothreitol where, for comparable conditions, reduction was almost complete.

Only one β-mercaptoethanol complex of vanadate (–362 ppm) has been reported (Scheme 4.8). Superficially, the coordination about vanadium is indistinguishable from that observed for 1,2-diol and α-hydroxy acid ligands. In the solid, the complex is dimeric of V_2L_2 stoichiometry [36]. Both the oxygen and sulfur of the ligand are ligated, but only the oxygen is involved in the bridging reaction. Consequently, the complex is characterized by the central $[VO]_2$ core as found for the diol and hydrox-ycarboxylate ligands. Dissolution studies are fully consistent with retention of this structure in aqueous solution. Apparently, the structurally analogous compound, 2-aminoethanethiol, is not a good ligand for vanadate [40]. This reveals the inability of the amine nitrogen to simultaneously complex two vanadiums in a manner similar to a hydroxyl oxygen.

Dithiothreitol is a more complex ligand than β-mercaptoethanol, and there is a corresponding increase in complexity of the solution chemistry. Two binuclear products (–352, –362 ppm; –399, –526 ppm), both of V_2L stoichiometry, have been identified. The individual vanadiums of each product are chemically distinct. The NMR studies [37] show that in one of the complexes, both vanadiums have a single coordinated sulfur. In the second complex, one of the two vanadiums has sulfur coordinated, whereas the second of the two has only oxygen in the coordination sphere. Neither of these compounds have been characterized by x-ray diffraction
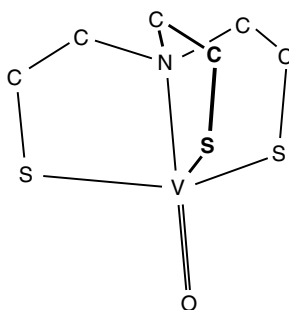
SCHEME 4.9

studies but model building studies revealed that two complexes, each appropriately substituted and each having a central [VO]$_2$ core, can be readily formed.

4.3.2 BIS(2-THIOLATOETHYL)ETHER, TRIS(2-THIOLATOETHYL)AMINE, AND RELATED LIGANDS

Reactions of these ligands have not been studied in aqueous solution. However, their complexes are readily synthesized and are stable but reactive towards heteroligands [41,42]. The reported structures all show the vanadium coordinated in monomeric units after the fashion depicted in Scheme 4.9. The multidentate thiolato complexes with tri- or tetradentate functionality are sufficient to satisfy the coordination requirements of the vanadium nucleus. Structurally, the compounds are not much different from analogous complexes formed with oxygen ligands (Section 4.4.2).

4.3.3 CYSTEINE, GLUTATHIONE, OXIDIZED GLUTATHIONE, AND OTHER DISULFIDES

Cysteine is a fairly effective reducing agent for vanadate, but even so, under neutral conditions, the V(V) lifetime is sufficiently long that vanadium NMR spectra can be obtained. Four products (–243, –309, –393, and –405 ppm) have been reported. Of these complexes, the –243 and –309 ppm NMR signals apparently correspond to products containing two thiolate groups in the coordination sphere, whereas the –393 and –409 ppm products have one thiolate ligand [43].

Although glutathione may not be quite as effective as a reducing agent, as is frequently suggested, particularly under mildly basic conditions, over time it does lead to the formation of V(IV) and the disulfide linkage of oxidized glutathione. The redox process is much more efficient under even mildly acidic conditions, where formation of V(IV) is favored.

The oxidized glutathione forms a complex with vanadate through the disulfide functionality [44]. The parent disulfide, H$_2$S$_2$, complexes vanadate in a well-characterized side-on fashion to afford η-complexed products [45], and it seems quite likely that this mode of complexation is followed with oxidized glutathione.

4.4 AMINO ALCOHOLS AND RELATED LIGANDS

4.4.1 BIDENTATE AMINO ALCOHOLS AND DIAMINES

Unlike ethylene glycol, α-hydroxycarboxylic acids, and β-mercaptoethanol, ligands such as ethanolamine, ethylenediamine, amino acids, and 2-aminoethanethiol do not form V_2L_2 complexes with vanadate [46]. However, weakly formed products of VL stoichiometry ($\sim$ –546 ppm, $\sim$ –556 ppm) are observed with a number of α-amino acids [47]. Because the amine functionality in amino acids is not suitable for formation of the cyclic $[VN]_2$ core expected for a dimer, then one or the other of these VL compounds may correspond to the monomeric precursor to such a dimeric product. Certainly, with the α-hydroxycarboxylic acids, the monomeric complex can be a major component in solution. Similar VL complexes have not been reported for the amino alcohols. Perusal of the available reports suggests that the amine derivatives were studied under conditions where the nitrogen functionality was protonated, so the results may be somewhat misleading.

4.4.2 POLYDENTATE AMINO ALCOHOLS: DIETHANOLAMINE AND DERIVATIVES

Diethanolamine reacts favorably with vanadate to yield a single product (–488 ppm) of VL stoichiometry. The amino and both hydroxyl functionalities are necessary for complex formation [46]. Replacement of the NH of $(HOCH_2CH_2)_2NH$ by NCH_3 has minimal influence on the reactivity of the ligand. The ^{51}V chemical shifts for complexes derived from these and similar ligands vary little from each other and are generally within the range of –480 to –490 ppm. The related ligand, triethanolamine $(HOCH_2CH_2)_3N$ (–483 ppm), complexes with two of the hydroxyethyl groups coordinated, whereas the other remains uncoordinated so that the complex is like that formed with $(HOCH_2CH_2)_2NCH_3$ (–481 ppm). Although these compounds have octahedral coordination in the solid, this is generally not true for the aqueous species. Triethanolamines and similar ligands in aqueous solution have been extensively studied in order to delineate the requirements for five- versus six-coordinate complexes. Carbon-13 and oxygen-17 NMR studies proved exceptionally fruitful, and these, in combination with x-ray structure studies of the crystalline materials, showed that although octahedral complexes occurred in the solid and in nonaqueous solution, in aqueous solution, coordination reverted to a pentacoordinate structure. This was demonstrated most graphically by ^{17}O NMR spectra, which showed two oxo (VO) signals in a 1:1 intensity ratio. The signals arise from one oxo trans to the amine nitrogen and from a second oxo in a cis arrangement with respect to the nitrogen [40,48]. Replacement of the amino group in diethanolamine by oxygen provides a more weakly coordinating ligand, with complex (–519 ppm) formation being less favored by about 2 orders of magnitude. If the NH is replaced by a noncoordinating CH_2 group, no complex is formed. The product complexes are all monomeric and have a single negative charge. The evidence is fully consistent with an *N*- and *O*-coordinated bicyclic structure, such as depicted in Scheme 4.10a. Table 4.4 gives
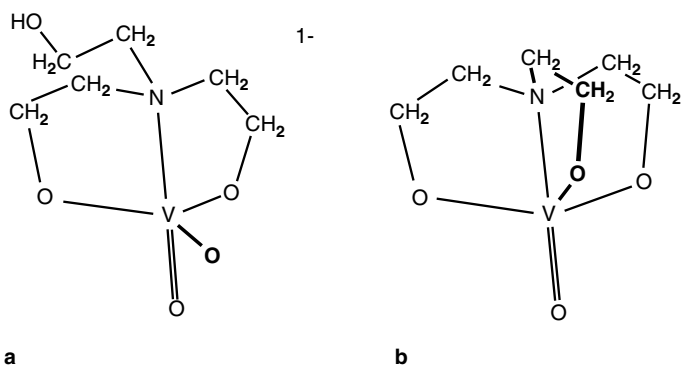
SCHEME 4.10

TABLE 4.4
Selected ^{51}V and ^{17}O Chemical Shifts for Complexes of Ethanolamine-Derived Ligands, $R_1R_2R_3N$

R_1	R_2	R_3	^{51}V (ppm)	^{17}O (ppm)	Ref.
CH$_2$CH$_2$OH –	CH$_2$CH$_2$OH	H	488[a]		40
CH$_2$CH$_2$OH –	CH$_2$CH$_2$OH	CH$_2$CH$_2$OH	483[a]	954, 980	40, 48
CH$_2$CH$_2$OH –	CH$_2$CH$_2$OH	CH$_2$CHOHCH$_3$	487[a]		40
CH$_2$CHOHCH$_3$	CH$_2$CHOHCH$_3$	CH$_2$CHOHCH$_3$	–488[a]	940, 985	40, 48
CH$_2$CH$_2$OH	CH$_2$CH$_2$OH	CH$_2$CO$_2^-$	–484[a], –508[b]		40
CH$_2$CH$_2$OH	CH$_2$CO$_2^-$	CH$_2$CO$_2^-$	–499[a]	1038, 1038	40, 82
CH$_2$CH$_2$OH	CH$_2$CO$_2^-$	CH$_2$CO$_2^-$	–520[b]	1140, 1085	40, 82
CH$_2$CH$_2$OH	CH$_2$CH$_2$OH	CH$_3$	–477[a]		50
CH$_2$CO$_2^-$	CH$_2$CO$_2^-$	CH$_3$	–513[b]		40
CH$_2$CO$_2^-$	CH$_2$CO$_2^-$	CH$_2$CO$_2^-$	–507[b]		40
CH$_2$CO$_2^-$	CH$_2$CO$_2^-$	CH$_2$CONH$_2$	–506[b]		40
CH$_2$CH$_2$OH	CH$_2$CH$_2$OH –	2CH$_2$–pyr[c]	–500[b]		49
CH$_2$CO$_2^-$	CH$_2$CO$_2^-$	2–CH$_2$–pyr[c]	–503[b]		49
CH$_2$CO$_2^-$	2–CH$_2$–pyr[3]	2–CH$_2$–pyr[c]	–494[d]		54
CH$_2$CH$_2$OH	CH$_2$CH$_2$OH	2–CH$_2$–bzim[c]	–488[1], –540[b]		49
CH$_2$CO$_2^-$	CH$_2$CO$_2^-$	2–CH$_2$–bzim[c]	–540[b]		49

[a] Observed in high pH region (~pH 8–12).
[b] Observed in low pH region (~pH 5–8).
[c] Abbreviations: pyr, pyridine; bzim, benzimidazole.
[d] Chemical shift from acetonitrile-d_3 solution.

^{51}V and ^{17}O chemical shifts that have been reported for a number of complexes derived from ethanol-amine-type ligands.

Interestingly enough, in nonaqueous solution, the third arm of triethanolamine reacts, and this ligand behaves as a tetradentate ligand to form a neutrally charged complex (Scheme 4.10b) [46,48]. It is not known whether this coordination would be

obtained if a very hydrophobic cation that would allow the anionic complex to be dissolved in nonaqueous solvent were utilized during the preparation of the complex. Replacement of one of the ethylhydroxy groups with pyridyl, (2-CH$_2$Pyr), and similar *N*-heterocyclic functionality does provide octahedral complexes, in which the ligands complex in a tetracoordinate fashion, even in aqueous solution [49].

Evidently, from Table 4.4, there are specific influences on chemical shifts that can be identified. The incorporation of the pyridine functionality of the ligand, ((HOCH$_2$CH$_2$)$_2$N(2–CH$_2$ –pyr)), into the coordination sphere of vanadium to form the tetradentate complex (–500 ppm) causes only a small change in vanadium NMR chemical shifts when compared to the shifts (–480 to –500 ppm) of other amino alcohol ligand complexes. Similarly, replacement of the hydroxyethyl functionality with acetyl has only a small influence on vanadium chemical shifts. However, replacement of the 2-CH$_2$-pyridine functionality by 2-CH$_2$-benzimidazole causes a –40 ppm change in chemical shift. It does not seem that this phenomenon can be explained in terms of variation in pK_a of the ligand ligating groups because, in all cases, there are substantial changes on pK_a of all ligating functionalities after substitution of one group by another. It is possible that the effect derives from different π-bond contributions to vanadium from the ligating nitrogen of pyridyl compared to the nitrogen of benzimidazole.

Investigation of a variety of multidentate amino alcohols revealed that there is a significant dependence of ligand pK_a on formation of product complexes. Ligands with a pK_a of about 8 are much better at coordinating the vanadate monoanion (VO$_4$H$_2^-$) than those with either a higher or lower pK_a [50]. This shows that the ability of vanadate to share electrons with ligands is sensitive to the balance between a ligand strongly donating its electrons, high pK_a, or significantly withdrawing them, low pK_a. Only weak donation, as indicated by the value of 8 for the ligand pK_a, leads to highly favored complex formation. Perhaps it is not coincidental that the pK_a of the vanadate anion is also 8. Of course, other factors including steric bulk and electronic resonance are important for ligation.

When the three ethylhydroxyl groups of triethanolamine are replaced by a tris(hydroxymethyl)methane to give (HOCH$_2$)$_3$CNH$_2$ (Tris buffer), there is a significant increase in complexity of the reaction chemistry, with complexes of VL (–530 ppm), VL$_2$ (–500 ppm), V$_2$L(-527, -540 ppm at pH 9.0) and V$_2$L$_2$ (–534 ppm) stoichiometry being formed [15]. A V$_2$L$_2$ complex (–518 ppm) is also formed with (HOCH$_2$)$_3$CCH$_3$, so it is evident that here, like with the ethanolamines, complex formation involving the nitrogen favors VL stoichiometry. Because 1,3 glycols do not easily form bidentate complexes in aqueous solution, the hydroxymethyls of these V$_2$L$_2$ complexes must be coordinated in a tridentate fashion. The amine functionality is required for formation of VL so it, presumably, is also coordinated in a tridentate fashion, the amine nitrogen together with oxygens of two of the three hydroxymethyl groups.

The diaminohydroxybenzylate ligand, *N*-(*ortho*-hydroxybenzyl)-*N*′-(2-hydroxyethyl)ethylenediamine, forms a dimeric water-stable complex with vanadate [51]. The dimer (Scheme 4.1a) has the [VO]$_2$ central core found in many other V(V) complexes. The complex is unique in that the coordination about each vanadium is octahedral. In addition, each core oxygen is an oxo oxygen, a situation different

from that found for the glycols and hydroxycarboxylates, where each oxygen of the core is an alkoxo oxygen. Each of the bridging oxygens has very different bond lengths to the two vanadiums to which it is attached, being very short (1.681 Å) to one vanadium and very long to the other (2.283 Å). The compound is soluble in water. The two very long VO distances provide an obvious position for bond breakage and suggest that in aqueous solution, the complex exists predominantly as a monomeric pentacoordinate complex that crystallizes out of solution as the dimer.

4.5 AMINO ACIDS AND DERIVATIVES

Oxidation of one of the hydroxyls of 1,2 glycols to give the α-hydroxyacid leads to a favorable reaction chemistry and an increase in its complexity. The situation is not as clear when amino alcohols are oxidized to the amino acid. This is perhaps not too surprising because, unlike ethylene glycol, ethanolamine is a poor ligand for vanadate. Glycine, histidine, and most other α-amino acids react only weakly with vanadate. Other types of amino acids are also poor ligands. However, derivatization of amino acids that adds such additional functionality as carboxylate, *o*-hydroxy phenylate, and pyridinate leads to complexation reactions where tri- and tetradentate coordination in octahedral coordination is highly favored.

4.5.1 ETHYLENE-*N,N′*-DIACETIC ACID AND SIMILAR COMPOUNDS

Ethylene-*N,N′*-diacetic acid (EDDA) and similar ligands form well-characterized octahedral complexes in aqueous solution where C-13 coordination-induced chemical shifts, [51]V and ^{17}O NMR spectroscopy has been utilized in their study [40]. X-ray crystal structure analysis showed formation of the β-cis isomer, whereas NMR studies clearly showed two complexes in solution. The ^{17}O NMR studies [40] were fully consistent with retention of octahedral coordination by both of the isomers, and these two compounds were assigned as the α- and β-cis isomers, which are depicted in Scheme 4.11. The study of these isomers in water (α-cis, −514 ppm; β-
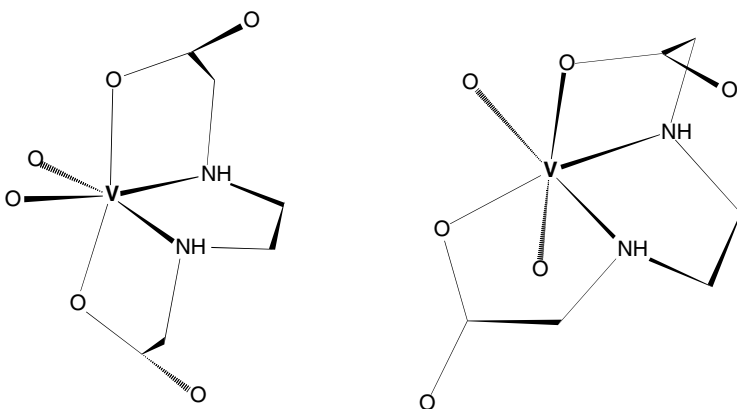
SCHEME 4.11

cis, –503 ppm) and other solvents showed a significant solvent-dependence on the isomer concentration ratio [52]. In water, the α-cis isomer is slightly more favored than the β-cis by about a factor of 1.1:1, and this ratio increases in mixed aqueous methanol, dimethylsulfoxide, and formamide solvents. However, inclusion of electrolytes in the medium reversed the trend, and the β-cis isomer was preferred. The influences on isomer ratio seem to derive from the effects that changes in the solvent have on the solvation spheres of the isomers. A related ligand with an o-hydroxyphenyl group replacing one H of each of the glycine residues of EDDA provided a similar octahedral complex, but here coordination is through the ortho oxygens of the phenyl rings [53]. The ^{51}V chemical shift (–546 ppm) of this complex is 30 to 40 ppm to high field of EDDA type complexes, and this is clearly indicative of a different functional group coordination.

The amino tris acetate, $N(CH_2CO_2)_3$ (chemical shift of complex, –506 ppm), and related ligands with one or two hydroxyethyl groups instead of acetyl are strong complexers of vanadate [40]. In general, these types of ligands complex in an octahedral fashion although there is a greater tendency toward five-coordinate compounds when there are fewer carboxylates in the coordination sphere. Table 4.4 gives vanadium chemical shifts for various complexes of this type.

A complex (–503 ppm) is readily formed when one acetate is replaced with the pyridyl functionality (2-Cyr). These complexes have octahedral coordination in the solid state, and unlike the complexes described above, this coordination is retained in aqueous solution [49]. The ligand is complexed in a tetradentate fashion, and here, as similarly observed for the analogous amino alcohol complexes, the presence of pyridine in the coordination sphere has little influence on ^{51}V NMR chemical shifts. Other complexes with similar tetradentate ligands have also been found to retain octahedral coordination when in aqueous medium [54].

An interesting variant of the amino triacetic acid ligand, in which one of the acetate functionalities was replaced by a phosphonomethyl group, forms a tetradentate complex trianionic octahedral complex (–526 ppm) that is quite stable in aqueous solution except under strongly acidic conditions [55]. In this complex, the two carboxylate groups are interconverted in an exchange reaction. Studies of the exchange kinetics suggest that the two carboxylate groups exchange positions relative to the V-oxo groups via a pentacoordinate vanadium, where one carboxylate group dissociates to form the intermediate. Presumably, the structure of the intermediate is analogous to that of the complex formed with triethanolamine in water.

4.5.2 PYRIDINE CARBOXYLATES, PYRIDINE HYDROXYLATES, AND SALICYLATE

Picolinic acid (pyridine 2-carboxylic acid) is the prototype for this type of ligand. Pyridine itself does not react favorably with vanadate, nor do the 3 and 4 pyridine carboxylates. At first sight, one would expect that 2-hydroxypyridine would react favorably with vanadate, but this is not true. There are two likely explanations for this. First, the 2-hydroxypyridine exists predominantly as the keto tautomer, so the effective concentration of the hydroxylate is low. The keto form of the ligand can be expected to be much less reactive than the hydroxyl form. Second, the formation
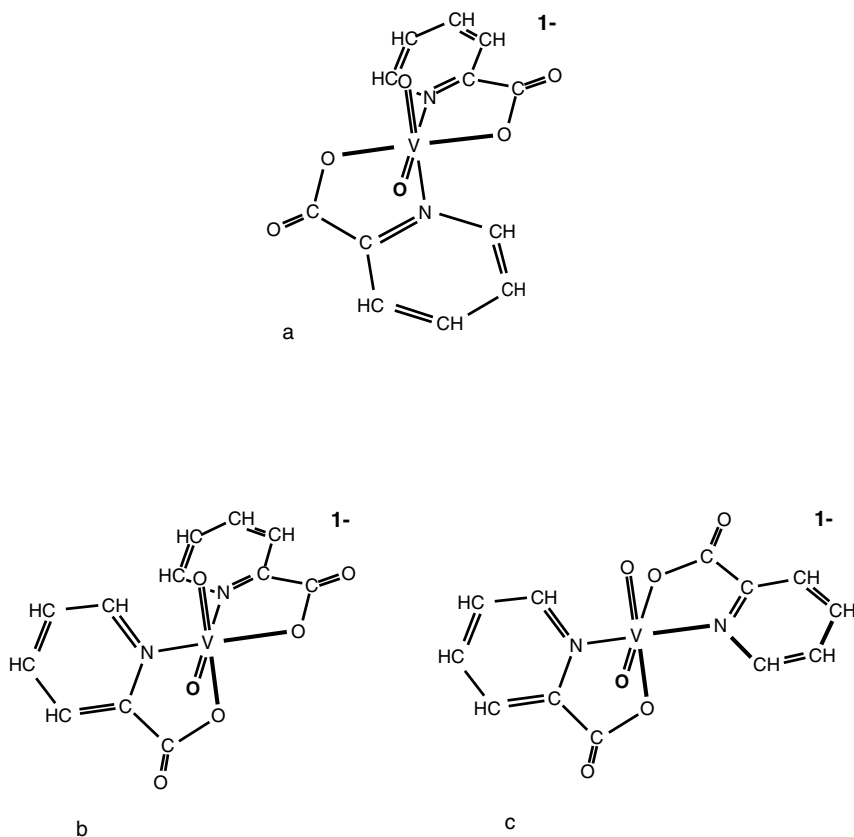
SCHEME 4.12

of a product requires a four-membered chelate, and in general, this will not be a favorable reaction compared to formation of five-membered chelate rings when the potential complexing groups are similar.

2-Hydroxybenzoic acid (salicylic acid) does form a complex, although its formation is not favored when compared to that of the picolinato ligand. Presumably this, at least to an extent, reflects the fact that the chelate formed with salicylate has a six-membered ring, and six-membered chelates are much less favored than the five-membered analogue.

In aqueous solution, picolinic acid binds tightly to vanadate to form three complexes (–513 ppm, –529 ppm, –552 ppm) of VL_2^- stoichiometry and one complex (–550 ppm) of VL^- stoichiometry [56]. The x-ray structure of a bispicolinato complex shows the picolinate groups oriented in a cis fashion in octahedral coordination [57]. The three NMR signals may well correspond to the three ligand orientations possible for octahedral products of VL_2 stoichiometry. The orientations of the ligands within the crystalline complex are depicted in Scheme 4.12a, whereas Scheme 4.12b and Scheme 4.12c show the other two possibilities. Dissolution of the crystalline bis picolinate complex into D_2O provided ^{51}V NMR signals at –515 and –554 ppm [58].

Unfortunately, a time course study was not reported in that work, so it is not known whether the crystalline compound corresponds to the –513 or –552 ppm signal of the solution study. However, it seems most likely that the –515 ppm signal corresponds to the bisligand compound of the crystal structure and the –554 ppm signal to the partially hydrolyzed product. Chemically, it seems likely that partial hydrolysis rather than isomerization occurs on dissolution. Additionally, isomerization of VL_2 would be expected to provide three NMR signals not just two, whereas two signals would be expected from partial hydrolysis.

The tendency for carboxylate coordination is that these groups are oriented perpendicular to the cis dioxo (VO_2) functionality of the vanadate complex. Given that the –513 ppm signal corresponds to the octahedral coordination found in the crystal structure (Scheme 4.12a), then it seems probable that the –529 ppm signal corresponds to the isomer with one carboxylate oriented perpendicular to the cis dioxo group (Scheme 4.12b). The –552 signal then can be assigned to the complex where the picolinate nitrogens rather than the carboxylates occupy the two perpendicular positions (Scheme 4.12c). The formation constant for the –552 ppm compound ($(1.5 \pm 0.3) \times 10^4$ M^{-1}) is about one third that of the –529 ppm complex and one sixth that of the –513 ppm complex.

The influence of the relative orientation of ligating atoms on bond lengths is significant in the bispicolinato complex. The carboxylate VO bond length for the oxygen oriented perpendicular to both oxygens of the VO_2 grouping is 1.989 ±0.002 Å, compared to 2.125 ±0.003 Å for the ligating oxygen of the second carboxylate group. The situation is similar for the pyridyl nitrogens, where the VN bond distances are 2.126 ±0.002 Å and 2.314 ±0.002Å, respectively, for the two orientations. The orientation factor in this complex then corresponds to a bond-length change of 0.136 Å for oxygen and 0.188 Å for nitrogen. In contrast, the VO bond lengths of the VO_2 groups are indistinguishable, being 1.638 ± 0.002 Å and 1.637 ± 0.002 Å, even though, as seen in Scheme 4.12, one VO bond has a carboxylate oxygen in the trans position and the other has a trans aromatic nitrogen.

The remaining picolinato complex has VL stoichiometry. This complex very likely is pentacoordinate in trigonal bipyramidal geometry, as depicted in Scheme 4.13. A structure of a closely related hexamethylphosphate triamide (HMPT) derivative where the HMPT residue is located in an axial position of the complex has been determined by x-ray diffraction studies [59].

Pyridine 2,6-dicarboxylic acid (dipic) also reacts favorably in a tridentate manner with vanadate to form a distorted trigonal bipyramidal complex [60]. Multinuclear NMR studies of the complex in aqueous solution were consistent with the formation of only one complex (–533 ppm) that was monoanionic and had VL stoichiometry and a solution structure that corresponded to the crystalline compound [61]. A pH variation study of a sample (10 mM in H_2O) prepared from the crystalline material showed that this complex is stable over a very wide pH range. Although it was almost fully dissociated at pH 7.3, the complex regenerated at lower pH and was almost fully formed at pH 6. At pH 0.4, it was partially dissociated to cationic vanadate but was still about half formed at pH 0.3 [61]. One of the reasons for the extended range under strongly acidic conditions is the fact that the complex can be protonated and has a pK_a very close to 0. This compound is a well-known insulin-
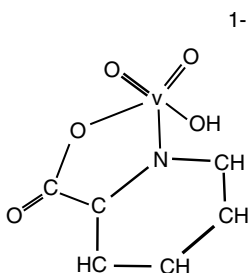
SCHEME 4.13

mimetic [61] and, in combination with hydrogen peroxide, has been used as a model for studies of vanadium-dependent haloperoxidase activity (see Section 5.1 and Section 10.4.2).

4.5.3 AMIDES

Simple amides such as acetamide are not known to form complexes with vanadate. Reaction at the amide nitrogen requires ancillary ligating groups. Complexation seems to require at least three ligating groups, as found, for instance, in dipeptides (see Section 4.6.2), where ligation occurs at the terminal carboxylate, the amino nitrogen, and the amide nitrogen in its deprotonated form [47,62]. Deprotonation at the amide nitrogen has also been observed in other amide complexes [63], and apparently such deprotonation is characteristic of amide complexation.

4.6 α-AMINO ACIDS AND DIPEPTIDES

There is a very large difference in reactivity between α-amino acids and small peptides derived from them. Even the presence of functional sidechains on amino acids has minimal influence on their reactivity. In contrast, with peptides the sidechains on the amino acid residues can strongly influence reactivity and lead to a variety of different complexes. The sidechains are critically important in vanadium-binding enzymes, where they are essential to the binding process. Furthermore, judicious use of appropriate groups in affinity chromatography can provide exceedingly effective methods for isolation and purification of enzymes [64].

4.6.1 α-AMINO ACIDS

Although α-amino acids generally do not complex vanadate at all well, they do give rise to a number of products that can be observed in vanadium NMR spectra. Products seem to fall into three categories, one of VL_2 stoichiometry and two others of VL stoichiometry. Only with glycine has the VL_2 product (–523 ppm) been reported. This may simply mean that steric interactions limit formation of similar products with other amino acids, where sidechains replace a hydrogen of the CH_2 group. For a number of amino acids, the VL products give rise to [51]V NMR chemical shifts within a few ppm of –544 ppm, corresponding to one type of product, and a

few ppm of –557 ppm for the second type of product [47,65]. The formation constants for both types of VL derivatives (V + L ⇌ VL) are in the order of 0.5 M^{-1} under neutral conditions and are not very dissimilar from formation constants for reactions with alcohols to form vanadate esters.

The identities of the two VL complexes are not known with certainty, but the available evidence suggests the –557 ppm-type products arise from monodentate reaction at the carboxylate group, whereas the –544 ppm products derive from monodentate reaction at the nitrogen functionality. Additional products from amino acids with reactive sidechains, as found in serine or aspartic acid, have not been reported. ^{51}V chemical shifts for products formed with histidine are similar to those observed for other amino acids, except that an additional signal (–571 ppm) has been observed [66].

The reaction chemistry is quite different with cysteine. Under neutral conditions, cysteine reduces vanadate within an hour or so, but vanadate also rapidly forms relatively highly favored complexes with the cysteine that can be studied by NMR spectroscopy within the reduction time. All the complexes studied have sulfur in the coordination sphere. Four such complexes have been identified (Figure 2.2), two bisligand (–243 ppm, –309 ppm) and two monoligand (–393 ppm, 405 ppm) complexes [43]. These complexes have not been structurally characterized, but it is quite likely that they are octahedral complexes with a coordination similar to that depicted in Scheme 4.14. Because vanadium(V) displays a general propensity toward five-membered rather than six-membered chelates, coordination of the type depicted in Scheme 4.14b with a nitrogen rather a carboxylate oxygen in the coordination shell seems most likely.

4.6.2 DIPEPTIDES

Amino acids fall naturally into two main classes, those for which the sidechain residues are not functionalized, as found, for instance, in alanine or leucine, and those for which the sidechains are functionalized, as in serine or histidine. Not surprisingly, the reactions of vanadate with peptides are often dependent on the sidechains of the amino acid residues. This is particularly true with proteins where the chemistry is dominated by the sidechains. For instance, the protein tyrosine phosphatases have an active site designed to promote hydrolysis of aryl phosphates. The amino acid sidechains within the active site are arranged to stabilize a phosphate transition state structure. The same arrangement of groups is conducive to strong interactions with vanadate, and vanadate is tightly complexed by this group of enzymes. Many other classes of enzymes that are involved with phosphate metabolism react strongly with vanadate or vanadate derivatives. The vanadium-dependent haloperoxidases also bind vanadate by sidechain interactions, but these enzymes are unique in that the arrangement of sidechains is critical to the peroxidase activity. Binding of vanadate by enzymes is not, however, restricted to systems such as this, and numerous other proteins bind vanadate very tightly.

Glycylglycine ($NH_2CH_2C(O)NHCH_2CO_2H$) is the prototypical nonfunctional-ized dipeptide. This, and related dipeptides, forms minor product complexes (~ –555 ppm) that have VL stoichiometry and a small formation constant, about 0.3 ± 0.1
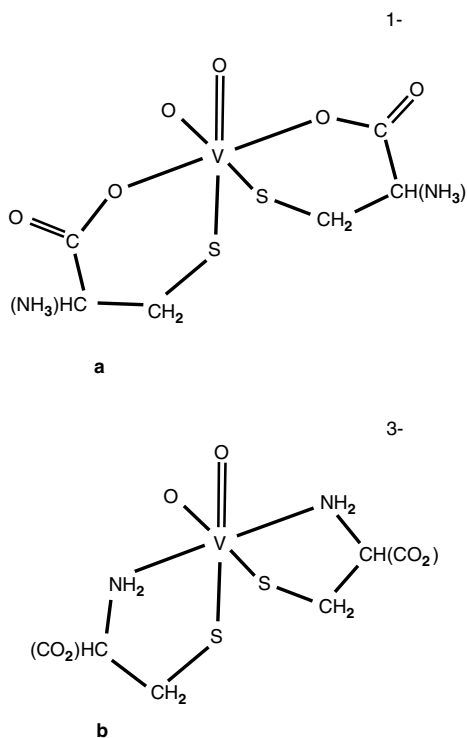
SCHEME 4.14
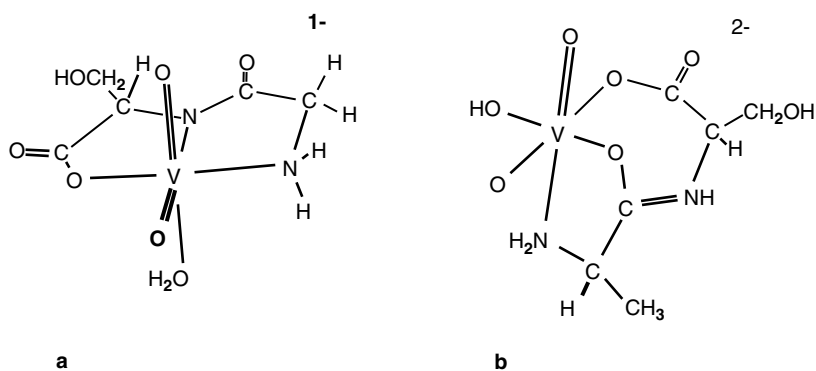
SCHEME 4.15

M^{-1} for the reaction V + L $\rightleftharpoons$ VL at pH 7. This product most likely arises from monodentate reaction at the carboxylate group. The major product (–505 ppm) also has VL stoichiometry but a much larger formation constant, 17 ± 1 M^{-1}. Blocking any of the amine nitrogen, amide nitrogen, or carboxylate oxygen prevents the formation of the major glycylglycine complex. Taken together, these observations suggest that complexation occurs in a tridentate manner, with loss of a proton at the

amide nitrogen. ^{15}N NMR studies have shown a 66 ppm coordination-induced change in chemical shift of the amide nitrogen [67], a value fully consistent with such a deprotonation reaction as the complex is formed. Scheme 4.15 presents coordination modes that have been proposed, with Scheme 4.15a representing the generally accepted structure. However, molecular dynamics simulations are not in accord with this depiction of the geometry. In the simulations six-coordinated species derived from incorporation of water are energetically unfavored when compared to the five-coordinate structure [68]. The anionic form, though, is favored, with deprotonation of the neutral compound occurring very quickly in the simulations.

Complexation does not necessarily require a carboxylate group, and it can be substituted by a hydroxyl group. For instance, glycylserine gives rise to three major products, two deriving from complexation through alkoxo oxygen (–494 ppm and –504 ppm) and one through the carboxylate oxygen (–507 ppm), with formation constants of 2.9 ± 0.8 M^{-1}, 0.4 ± 0.4 M^{-1}, and 63 ± 4 M^{-1}, respectively, at pH 7. Blocking of the carboxylate group eliminates one complex, leaving products of chemical shift –484 ppm and –501 ppm (formation constants, 2 ± 1 M^{-1} and 39 ± 4 M^{-1}, respectively, at pH 7). These products all carry a single negative charge at the vanadium center and can lose an additional proton at elevated pH [47,66,69]. However, under neutral conditions, the hydroxyl of the ligand will retain its proton, whereas the carboxylate will be deprotonated, so therefore, the overall charge states of the two complexes are different, dependent on whether complexation occurs through the hydroxyl (2- charge on complex) or carboxyl (1- charge on complex) oxygen. Equation 4.1 describes the equilibrium reaction that characterizes these complexes (V^{1-}, $H_2VO_4^{1-}$; P^0, neutral peptide; VP, product complex).

$$V^{1-} + P^0 \quad VP^{(n+1)-} + nH^+$$

$$\text{(4.1)}$$

$$VP^{(n+2)-} + H^+$$
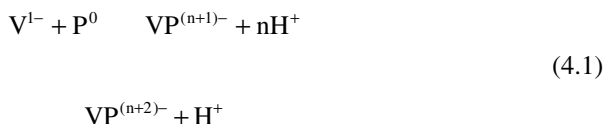
Table 4.5 provides [51]V chemical shifts for a number of peptide chelates. If one considers only the carboxylate-derived chelates, [51]V chemical shifts from chelates deriving from peptides with aromatic sidechains average about 5 ppm to higher field than those from peptides with aliphatic sidechains. Despite this, the full range of shifts is less than 20 ppm. If an alkoxo oxygen replaces the carboxylato oxygen, as in serine- or threonine-based dipeptides, there typically is a shift to lower field of about 14 ppm. These observations suggest all the dipeptides are coordinated in the same manner. The exception is the minor product from glycylserine, which would not be expected to follow the pattern because it has a different structure. A similar minor product has not been reported for other serine-based dipeptides, and this suggests the sidechain of the amino acid, X, in XSer restricts formation of this minor product.

Although it would not be expected that alanylserine would behave much differently from glycylserine, a recent study has utilized ^{13}C chemical shifts in order to assign a coordination of the type displayed in Scheme 4.15b [70]. The proposed

TABLE 4.5
51V Chemical Shifts of Vanadium Dipeptide Chelates in Aqueous Solution

Peptide	Chemical Shift (ppm)	Ref.
Aliphatic Sidechains		
Glygly	−504	62, 47
Glyasp	−508	62
Glyglu	−505	62
Glugly	−500	83
Gluglu	−516	83, 69
Glulys	−513	69
Glythr	−597, −511	69
Glytyr	−510	84
Glyser	−493, −504, −506	62, 47
Glyval	−510	47
Valgly	−506	47
Valasp	−513	47
Leuleu	−512	47
Progly	−493	62, 47
Glypro	no product	62, 47
Glysar	no product	62, 47
Glyglycinamide	no product	47
Glyglygly	−505	47
Glyglysar	no product	69
Aromatic Sidechains		
Glyhis	−511	69
Alahis	−518	66
Glytyr	−509	62, 69
Tyrgly	−513	69
Hisgly	−513	69
Hisser	−503, −517	69
Pheglu	−515	84, 69
Glytrp	−510	69
Trpgly	−511	69
Trpphe	−519	69
Trptrp	−518	69
Trptyr	−520	69
Tyrtyr	−519	69
Glyhisgly	no product	69
Tyrglygly	no product	69
Tryglygly	no product	69

coordination was based on observations of ^{13}C coordination shifts of the α and β carbons of the serine. This seems an interesting coordination because it involves formation of a seven-membered ring, coordination of a carbonyl-like oxygen in that ring, and isomerization of a double bond from NC=O to OC=N. Individually, each is plausible but overall quite unlikely. A close look at the assignment of the carbon
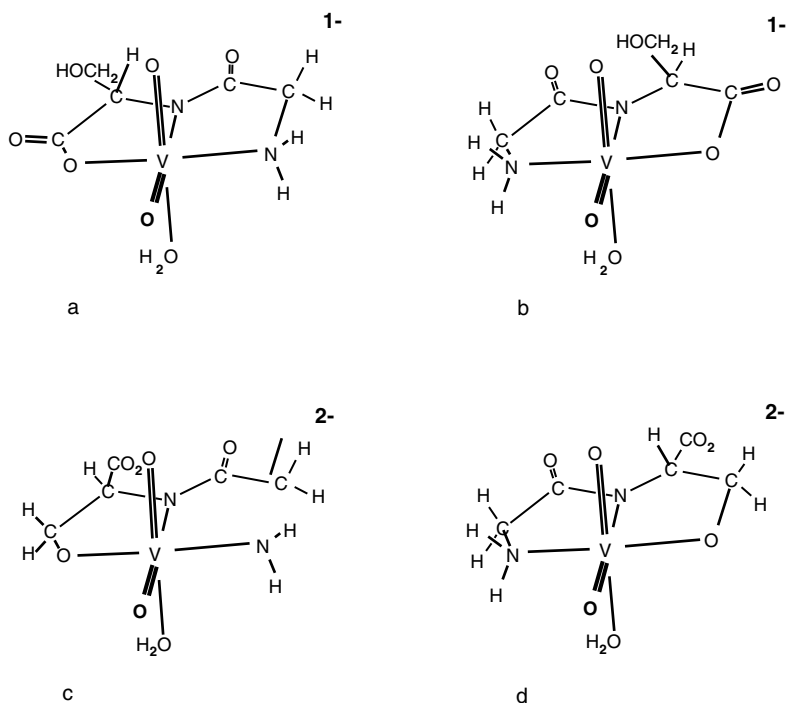
SCHEME 4.16

resonances suggested that the α and β carbons were incorrectly assigned. Compendiums of the ^{13}C chemical shifts of amino acids residues in peptides [71,72] indicate the chemical shifts had been reversed. With the revised assignment of the α and β carbon chemical shifts, there seems little reason to adopt the coordination in Scheme 4.15b. Coordination modes similar to those proposed for glycylserine, Scheme 4.16, are adequate to explain the observations. Theoretical calculations also support these two coordination modes [73]. Table 4.6 gives coordination-induced changes in ^{13}C chemical shifts for a number of vanadate/peptide complexes.

A ^{13}C NMR study [69] of the pH dependence of chemical shifts for the histidylserine complex has shown that coordination-induced chemical shifts are not sensitive to pH except for the carbons on either side of the peptide nitrogen. The coordination-induced shifts for both these carbons decrease as the pH is raised through the pK_a range from pH 7.14 to pH 8.63; for the adjacent C-terminal carbon, 4.1, 3.8, 3.3 ppm; for the adjacent N-terminal carbon, 8.1, 6.1, 4.7 ppm, respectively. Neither the carbon adjacent to the N-terminal nitrogen nor that to the carboxylate carbon shows a significant dependence of coordination-induced chemical shift on pH. One might be inclined to draw unwarranted conclusions from this, such as there being a pH-dependent influence on the strength of the V to N bond. However, closer observation reveals that the pH-dependency of the chemical shift derives from variation in the chemical shifts of the free peptide carbons, not from those of the ligated peptide. This demonstrates that care must be exercised when interpreting

TABLE 4.6
Coordination-Induced C-13 Chemical Shifts in Vanadium(V) Dipeptide Complexes
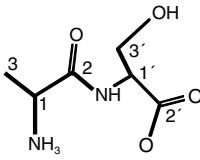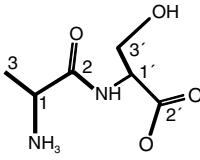
Ligand (pH, ^{51}V ppm)	C	Dipeptide	Complex	Complexation Shift
GlyTyr (7.10, -509)	1	43.3	49.5	6.2
	2	169.2	181.1	11.9
	1′	59.5	69.4	9.9
	2′	180.6	183.6	3.0
	3′	39.3	38.9	0.4
	4′	131.1	131.1	1.0
	5′	133.2	133.7	0.5
	6′	118.1	117.9	0.2
	7′	156.9	157.1	0.2
AlaSer (7.33, -516)	1	59.6	64.6	5.0
	2	173.2	183.8	10.6
	3	18.9	20.6	1.7
	1′	51.5	56.3	4.8
	2′	178.1	185.3	7.2
	3′	64.1	70.1	6.1
AlaSer (8.52, -503)	1	59.2	71.8	12.6
	2	178.4	182.0	3.6
	3	21.8	77.6	−2.8
	1′	52.4	57.0	4.6
	2′	180.1	185.2	6.7
	3′	20.4	77.6	1.5
AlaHis (7.2, -519)	1	52.9	57.6	4.7
	2	180.1	186.8	6.7
	3	20.4	21.9	1.5
	1′	58.5	68.4	9.9
	2′	174.7	184.7	10.4
	3′	31.7	31.9	0.2
	4′	138.4	137.8	−0.6
	5′	120.8	121.6	0.8
	6′	135.2	133.5	−1.7

TABLE 4.6 (continued)
Coordination-Induced C-13 Chemical Shifts in Vanadium(V) Dipeptide Complexes
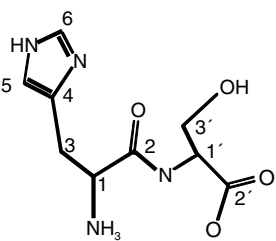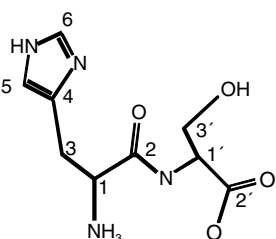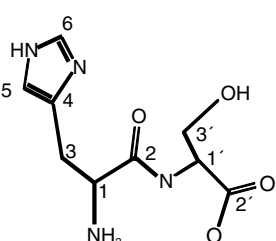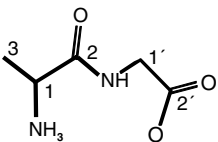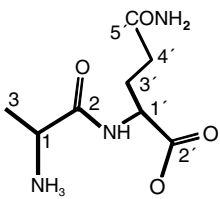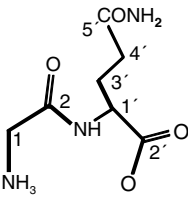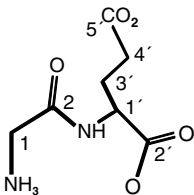
Ligand (pH, ^{51}V ppm)	C	Dipeptide	Complex	Complexation Shift
HisSer (7.14, -517)	1	60.1	70.6	10.5
	2	174.2	182.3	8.1
	3	31.8	32.3	0.5
	4	132.6	134.4	1.8
	5	120.9	120.1	-0.8
	6	138.6	138.7	0.0
	1′	56.2	60.3	4.1
	2′	178.6	185.6	7.0
	3′	64.7	65.4	0.7
HisSer (8.63, -517)	1	59.7	70.6	10.9
	2	178.0	182.7	4.7
	3	33.8	32.8	-1.0
	4	134.7	135.4	0.7
	5	121.1	120.0	-1.1
	6	138.9	138.9	0.0
	1′	57.2	60.5	3.3
	2′	178.7	185.7	7.0
	3′	64.9	65.5	0.6
HisSer (8.63, -503)	1	59.7	72.6	12.9
	2	178.0	183.6	5.6
	3	33.8	31.7	-2.1
	4	134.7	135.7	1.0
	5	121.1	120.2	-0.9
	6	138.9	139.2	0.3
	1′	57.2	61.4	4.2
	2′	178.7	182.5	3.8
	3′	64.9	78.3	13.4
AlaGly (7.00, -513)	1	50.2	54.8	4.6
	2	171.8	183.7	11.9
	3	17.4	18.4	1.0
	1′	44.2	55.9	11.7
	2′	177.2	186.7	9.5

TABLE 4.6 (continued)
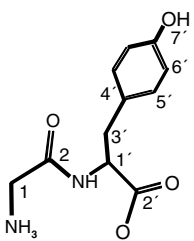**Coordination-Induced C-13 Chemical Shifts in Vanadium(V) Dipeptide Complexes**

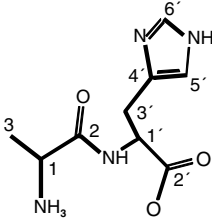| Ligand (pH, ^{51}V ppm)	C	Dipeptide	Complex	Complexation Shift
	1	50.1	55.1	5.0
	2	171.8	182.4	11.1
	3	17.4	19.3	1.9
	1′	55.9	65.5	9.6
	2′	178.5	185.1	6.6
	3′	28.4	29.1	0.7
	4′	32.5	31.0	−1.5
AlaGln (7.0, -517)	5′	179.5	179.7	0.2
	1	41.5	47.9	6.4
	2	167.5	180.8	13.3
	1′	55.7	65.5	9.8
	2′	178.8	185.2	6.4
	3′	28.5	29.1	0.6
	4′	32.5	31.0	−1.5
GlyGln (7.0, -509)	5′	179.5	179.5	0.0
	1	41.9	48.0	6.1
	2	168.6	180.5	11.9
	1′	56.2	65.8	9.6
	2′	179.5	185.5	6.0
	3′	29.2	30.2	1.0
	4′	34.9	33.1	−1.9
GlyGlu (7.0, -508)	5′	182.9	183.3	0.4

coordination-induced chemical shifts. Scheme 4.16 provides some possible structural isomers for complexes of glycylserine. There is little evidence to suggest that the proteins are restricted to the water ligand as shown; indeed, it seems likely that they are fluxional.

It is curious that two chelate products are formed with glycylserine when complexation occurs through the hydroxyl oxygen and only one when complexation is through the carboxylate oxygen. It is possible to rationalize this in the following manner: If Scheme 4.16a represents a structure corresponding to the carboxylate-derived complex, then a similar structure would be expected for the hydroxyl-derived product (Scheme 4.16b). In either case, an end-to-end flip (exo/endo interconversion) of the ligand would provide a second complex (Scheme 4.16c). However, only one signal for carboxylate-derived products is observed for numerous dipeptides [47,69], and only one hydroxyl- and one carboxyl-derived complex is observed with either glycylthreonine and histidylserine. In a somewhat analogous situation, with a Schiff

TABLE 4.7
Equilibrium Constants for Selected Dipeptide Chelate Complexes of Vanadate

Ligand	Chemical Shift (ppm)	Equilibrium Constant	pK$_a$	Ref.
Equilibrium equation	$V^{1-} + P^0$	VP^{1-}	pK$_a$ (VP^{1-})	
Glygly	−505	$(1.9 \pm 0.1) \times 10^1$ M^{-1}	10.9	47
Glyser	−507	$(7.2 \pm 0.6) \times 10^1$ M^{-1}	9.4	47
Alaser	−516	$(2.6 \pm 0.1) \times 10^2$ M^{-1}	8.2	70
Trptyr	−520	$(2.1 \pm 0.7) \times 10^2$ M^{-1}	8.5	69
Trptrp	−518	$(2.2 \pm 0.3) \times 10^2$ M^{-1}	8.1	69
			pK$_a$ (VP^0)	
Glyhis	−511	$(1.1 \pm 0.2) \times 10^2$ M^{-1}	7.0	69
Alahis^c	−518	$(3.6 \pm 0.4) \times 10^2$ M^{-1}	6.9	66
Hisgly	−513	$(2.0 \pm 0.3) \times 10^2$ M^{-1}	6.7	69
Hisser	−517	$(1.5 \pm 0.4) \times 10^2$ M^{-1}	7.5	69
	$V^{1-} + P^0$	$VP^{2-} + H^+$	pK$_a$ (VP^{2-})	
Glyser^a	−494	$(3.3 \pm 0.8) \times 10^{-7}$	9.8	47
Glyser^a	−504	$(5.3 \pm 0.6) \times 10^{-8}$	—	47
	$V^{1-} + P^+$	$VP^{1-} + H^+$	pK$_a$ (VP^{1-})	
Hisser^a	−503	$(4.8 \pm 1.9) \times 10^{-6}$	7.8	69

^{a} These values correspond to complexes that are chelated through the serine sidechain hydroxyl group.

base complex [74] where only carboxylate-derived products were possible, two NMR signals (–546 ppm, –560 ppm) were observed from an aqueous acetonitrile solution. The observation of either one or two product signals for each coordination mode can be rationalized as simply a reflection of small changes in relative energy, as reflected in the magnitudes of the formation constants. This can easily make the minor products difficult to observe. Also, it is by no means certain what the coordination geometry of the dipeptide complexes is or what the rates of internal interconversions such as proton transfer are, so structural arguments must be treated with care.

As suggested by Table 4.7, sidechains on the amino acid residues of the dipeptides favor product formation. There does not appear to be a systematic change in the formation constants, except that it is evident that dipeptides with larger sidechain residues tend to more readily form complexes. For instance, at pH 7, glycyltyrosine has a formation constant of 144 M^{-1} compared to 570 M^{-1} for tryptophyltyrosine [66,69]. It may simply be that bulkier sidechains favor a ligand conformation that leads to a more facile reaction. There does appear to be a somewhat systematic behavior of the product pK$_a$ values. Peptides with aliphatic sidechains have product (either hydroxo- or carboxylato-derived) pK$_a$ values above 9; those with aromatic

sidechains range from 6.7 to 8.5 (Table 4.7). Detailed studies [66,69] have shown that aromatic sidechains, including those of histidine, are not involved in complex formation.

The complex with glycylglycine has a pK_a higher than 10, whereas those of the glycylserine chelates have pK_a values of about 9.5, leading to 2- (–507 ppm, pK_a 9.4) or 3- (–494 ppm, pK_a 9.8) complexes. The latter pK_a shows an interesting behavior as it drops considerably with aromatic sidechains to 8.5 for trptyr (–520 ppm), 8.1 for trptrp (–518 ppm), 7.8 for hisser (–503 ppm [3- because of noncomplexed carboxylate]), 7.5 for hisser (–517 ppm), 7.0 for glyhis (–511 ppm), and 6.7 for hisgly (–513 ppm).

The presence of a pK_a is critical to the assignment of a coordination environment about the vanadium nucleus and suggests there is water in the coordination sphere as depicted in Schemes 4.15 and 4.16. In the absence of water, the only source of protons would be the RNH_2-V functionality. Theoretical studies have suggested that the hydrated form is significantly higher in energy than the nonhydrated form of the complex [73,75]. Even if the protons of the bound water are redistributed after the manner depicted in Scheme 4.17b, the calculations still suggest this is a disfavored state [75]. Furthermore, molecular dynamics simulations suggest water would rapidly be expelled from the coordination sphere, and the favored product will be five-coordinate and anionic [68]. However, there is a second pK_a. If the monoanionic complex under neutral conditions is not hydrated, then one is forced to conclude either that deprotonation occurs at the amine group or that the second pK_a involves a simultaneous hydration/deprotonation step (i.e., there is a coordination change). It seems somewhat unlikely that the amine is deprotonated, so hydration leads to the alternative structure. There is little change in vanadium chemical shift on deprotonation, so it is unlikely, but certainly it is not excluded, that a coordination change accompanies the deprotonation step. However, it seems most likely that one or another of the coordinations described by Scheme 4.17a and b are reasonable representations of the possible structure of these complexes. Because of the lack of change in chemical shift, structure b of this scheme seems a little less likely. Hopefully, further experimental and computational work will enable this question of structure to be resolved.

SCHEME 4.17

a

b
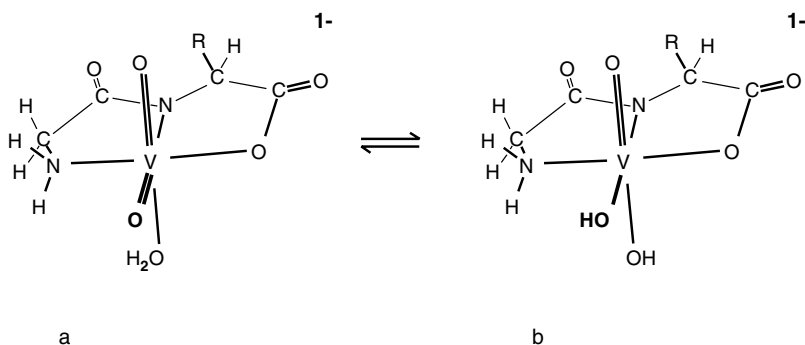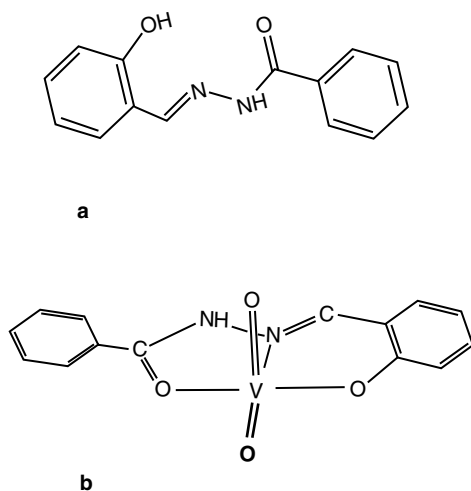
SCHEME 4.18

4.7 OTHER MULTIDENTATE LIGANDS

The chemistry already described is reproduced by numerous ligands that have not specifically been addressed in the previous discussion. The *N*-salicylidenehydrazides (Scheme 4.18a) and related compounds provide a good example. The structure [76] of a typical complex, represented in Scheme 4.18b, is not very different from that proposed for the solution structures of dipeptide complexes (Scheme 4.17). Interestingly, other similar complexes, based on Schiff base-derived ligands, form dimeric [VO]$_2$ core complexes (Scheme 4.1) via two long (~2.4 Å) VO bonds [2]. The cyclic core is not necessary for dimer formation, and a dimer can form via a linear VOV bond [77]. These complexes otherwise are not significantly different in their vanadium coordination from that depicted in Scheme 4.18b.

The salicylidene hydrazides provide useful templates for heteroligand reactions. For instance, they react with 1,3-diols such as 1,3-propane diol to form the corresponding 1,3-chelated product (Scheme 4.19a). However, given the choice, as in glycerol, a 1,2,3-triol, the five-membered chelate (Scheme 4.19b) preferentially forms [14]. For both types of complexes, the coordination is octahedral, with one oxygen of the glycol opposite to the N of the hydrazide. The VO bond distance for this oxygen is quite short, about 1.78 Å. This shows a remarkable contrast with the second glycolic oxygen, which is opposite to the V=O and has a VO bond length in the order of 2.34 Å for the two coordinations (Scheme 4.19a and b). These values compare with more typical VO bond lengths for single bonds of about 1.9 Å and shows that although one oxygen of the glycol is tightly complexed, the second oxygen of the pair is only weakly bound. The long bond length is even more exaggerated in a similar complex with mannopyranoside, for which the VO length
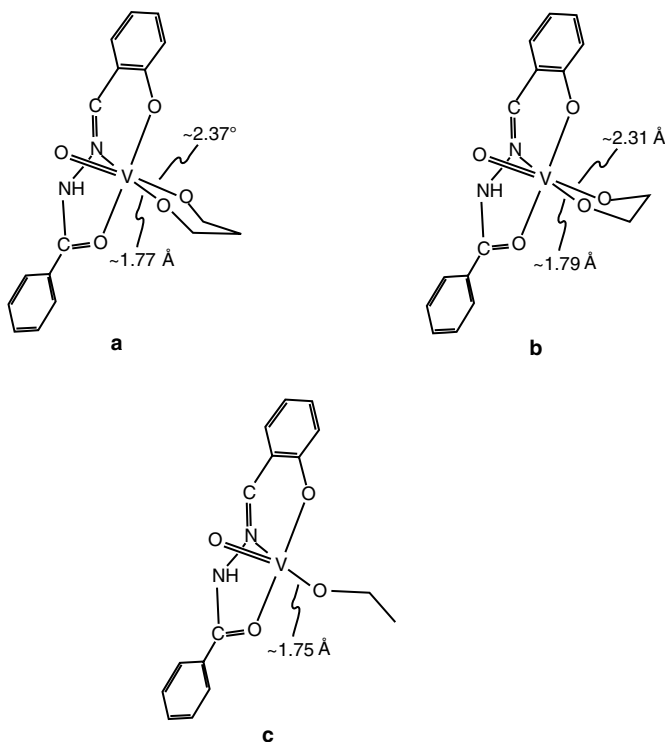
SCHEME 4.19

is 2.514 Å [78]. This weak binding to one oxygen of the ligand suggests that hydrolysis will occur in aqueous solution, and it has been found that partial hydrolysis occurs even in organic solvents if the solvents are not dry [14]. Similar observations have been made for diol complexes with other salicylidene-derived complexes [79]. The observation that the five-membered diol chelate preferentially forms over the six-membered one is in accord with studies of unligated vanadate, where only 1,2-diol complexes have been observed in aqueous solution.

The weak binding to the second oxygen of the glycol suggests that complexes should readily form with aliphatic alcohols. They do form [77], and the alkoxo oxygen lies in the base of a square pyramidal structure and has a VO bond length close to those of the corresponding diols (Scheme 4.19c). Like the glycolato complexes, the alkoxo ligands are readily hydrolyzed. Unfortunately, no detailed studies have been carried out in order to ascertain the formation constants for either the alkoxo or the glycolato complexes in aqueous solution.

Although square pyramidal coordination is frequently observed for these tridentate types of ligands, distortions toward a trigonal bipyramidal coordination are observed with salicylaldehyde-derived Schiff bases of 8-aminoquinoline [80]. The distortions from the square pyramidal coordination about vanadium presumably have their origins in the rigid structure of the quinoline ring and are imposed on the geometry through ligation of the aromatic nitrogen of the quinoline ring.

REFERENCES

1. Armstrong, E.M., R.L. Beddoes, L.J. Calviou, J.M. Charnock, D. Collison, N. Ertok, J.H. Naismith, and C.D. Garner. 1993. The chemical nature of amavadin. *J. Am. Chem. Soc.* 115:807–808.

2. Li, X., M.S. Lah, and V.L. Pecoraro. 1988. Vanadium complexes of the tridentate Schiff base ligand *N*-salicydene-*N′*-(2-hydroxyethyl)ethylenediamine: Acid-base and redox conversion between vanadium(IV) and vanadium(V) imino phenolates. *Inorg. Chem.* 27:4657–4664.

3. Angus-Dunne, S.J., R.J. Batchelor, A.S. Tracey, and F.W.B. Einstein. 1995. The crystal and solution structures of the major products of the reaction of vanadate with adenosine. *J. Am. Chem. Soc.* 117:5292–5296.

4. Hambley, T.W., R.J. Judd, and P.A. Lay. 1992. Synthesis and crystal structure of a vanadium(V) complex with a 2-hydroxy acid ligand: A structural model of both vanadium(V) transferrin and ribonuclease complexes with inhibitors. *Inorg. Chem.* 31:343–345.

5. Schwendt, P., P. Svancarek, I. Smatanova, and J. Marek. 2000. Stereospecific formation of α-hydroxycarboxylato oxo peroxo complexes of vanadium(V). Crystal structure of $(NBu_4)_2[V_2O_2(O_2)(L-lact)_2]\cdot 2H_2O$ and $(NBu_4)_2[V_2O_2(O_2)_2(D-Lact)(L-lact)]\cdot H_2O$. *J. Inorg. Biochem.* 80:59–64.

6. Einstein, F.W.B., R.J. Batchelor, S.J. Angus-Dunne, and A.S. Tracey. 1996. A product formed from glycylglycine in the presence of vanadate and hydrogen peroxide: The (glycylde-*N*-hydroglycinato-K^3N^2,N^N,O^1)oxoper oxovanadate(V) anion. *Inorg. Chem.* 35:1680–1684.

7. Tracey, A.S., J.S. Jaswal, M.J. Gresser, and D. Rehder. 1990. Condensation of aqueous vanadate with the common nucleosides. *Inorg. Chem.* 29:4283–4288.

8. Tracey, A.S. and C.H. Leon-Lai. 1991. 1-H and 51-V NMR investigation of the complexes formed between vanadate and nucleosides. *Inorg. Chem.* 30:3200–3204.

9. Zhang, B., S. Zhang, and K. Wang. 1996. Synthesis, characterization and crystal structure of cyclic vanadate complexes with monosaccharide derivatives having a free adjacent diol system. *J. Chem. Soc., Dalton Trans.* 3257–3263.

10. Crans, D.C., R.A. Felty, O.P. Anderson, and M.M. Miller. 1993. Structure and solution properties of a dimeric tetrahedral vanadium(V) chloride alkoxide complex. *Inorg. Chem.* 32:247–248.

11. Tracey, A.S. and M.J. Gresser. 1988. Vanadium(V) oxyanions. Interactions of vanadate with cyclic diols and monosaccharides. *Inorg. Chem.* 27:2695–2702.

12. Geraldes, C.F.G.C. and M.M.C.A. Castro. 1989. Interaction of vanadate with monosaccharides and nucleosides: A multinuclear NMR study. *J. Inorg. Biochem.* 35:79–93.

13. Noleto, G.R., C.A. Tischer, P.A.J. Gorin, M. Iacomini, and M.B.M. Oliveira. 2003. Complexes of sodium vanadate(V) with methyl α-**D**-mannopyranoside, methy α- and β-**D**-galactopyranoside, and selected *O*-methylated derivatives: A ^{51}V and ^{13}C NMR study. *Carbohydrate Research* **338**:1745–1750.

14. Rath, S.P., K.K. Rajak, S. Mondal, and A. Chakravorty. 1998. Synthesis and structure of vanadate esters of glycerol and propane-1,3-diol. *J. Chem. Soc., Dalton Trans.* 2097–2101.

15. Tracey, A.S. and M.J. Gresser. 1988. Vanadium(V) oxyanians: Interactions of vanadate with 1,1,1-tris(hydroxymethyl)ethane and with the buffer tris(hydroxymethyl)aminomethane. *Inorg. Chem.* 27:1269–1275.

16. Elvingson, K., D.C. Crans, and L. Pettersson. 1997. Speciation in vanadium bioinorganic systems. 4. Interactions between vanadate, adenosine and imidazole—an aqueous potentiometric and ^{51}V NMR study. *J. Am. Chem. Soc.* 119:7005–7012.

17. Rajak, K.K., S.P. Rath, S. Mondal, and A. Chakravorty. 1999. Carbohydrate binding to VO^{3+}, sugar vanadate esters incorporating L-amino acid Schiff bases as coligands. *Inorg. Chem.* 38:3283–3289.

18. Biagioli, M., L. Strinna-Erre, G. Micera, A. Panzanelli, and M. Zema. 2000. Molecular structure, characterization and reactivity of dioxo complexes formed by vanadium(V) with α-hydroxycarboxylate ligands. *Inorg. Chim. Acta* 310:1–9.

19. Wright, D.W., P.A. Humiston, W.H. Orme-Johnson, and W.M. Davis. 1995. A unique coordination mode for citrate and a transition metal: K$_2$[V(O)$_2$(C$_6$H$_6$O$_7$)]•4H$_2$O. *Inorg. Chem.* 34:4194–4197.

20. Pettersson, L., I. Andersson, and A. Gorzsas. 2003. Speciation in peroxovanadium systems. *Coord. Chem. Rev.* 237:77–87.

21. Ehde, P.M., I. Andersson, and L. Pettersson. 1989. Multicomponent polyanions. 43. A study of aqueous equilibria in the vanadocitrate system. *Acta Chem. Scand.* 43:136–143.

22. Zhou, Z.-H., H.-L. Wan, S.-Z. Hu, and K.-R. Tsai. 1995. Synthesis and structures of the potassium-ammonium dioxocitratovanadate(V) and sodium oxocitratovanadate(IV) dimers. *Inorg. Chim. Acta* 237:193–197.

23. Kaliva, M., T. Giannadaki, A. Salifoglou, C.P. Raptopoulou, and A. Terzis. 2002. A new dinuclear vanadium(V)-citrate complex from aqueous solutions. Synthetic, structural, spectroscopic and pH-dependent studies in relevance to aqueous vanadium(V)-citrate speciation. *Inorg. Chem.* 41:3850–3858.

24. Wright, D.W., R.T. Chang, S.K. Mandal, W.H. Armstrong, and W.H. Orme-Johnson. 1996. A novel vanadium(V) homocitrate complex: Synthesis, structure, and biological relevance of [K$_2$(H$_2$O)$_5$][(VO$_2$)$_2$(R,S-homocitrate)$_2$]·H$_2$O. *J. Biol. Inorg. Chem.* 1:143–151.

25. Caravan, P., L. Gelmini, N.R. Glover, F.G. Herring, H. Li, J.H. McNeill, S.J. Rettig, I.A. Setyawati, E. Shuter, Y. Sun, A.S. Tracey, V.G. Yuen, and C. Orvig. 1995. Reaction chemistry of BMOV, bis(maltolato)oxovanadium(IV)—a potent insulin mimetic agent. *J. Am. Chem. Soc.* 117:12759–12770.

26. Elvingson, K., A.G. Baro, and L. Pettersson. 1996. Speciation in vanadium bioinorganic systems. 2. An NMR, ESR, and potentiometric study of the aqueous H$^+$-vanadate-maltol system. *Inorg. Chem.* 35:3388–3393.

27. Tracey, A.S., M.J. Gresser, and K.M. Parkinson. 1987. Vanadium(V) oxyanions. Interactions of vanadate with oxalate, lactate, and glycerate. *Inorg. Chem.* 26:629–638.

28. Ehde, P.M., I. Andersson, and L. Pettersson. 1986. Multicomponent polyanions. 40. A potentiometric and 51-V NMR study of equilibria in the H$^+$-H$_2$VO$_4^-$-C$_2$O$_4^{2-}$ system in 0.6 M Na(Cl) medium. *Acta Chem. Scand.* A40:489–499.

29. Scheidt, W.R., C. Tsai, and J.L. Hoard. 1971. Stereochemistry of dioxovanadium(V) complexes, I. The crystal and molecular structure of triammonium bis(oxalato)dioxovanadate(V) dihydrate. *J. Am. Chem. Soc.* 93:3867–3872.

30. Ehde, P.M., L. Pettersson, and J. Glaser. 1991. Multicomponent polyanions. 45. A multinuclear NMR study of vanadate(V)-oxalate complexes in aqueous solution. *Acta Chem. Scand.* 45:998–1005.

31. Lee, M.-H. and K. Schaumburg. 1991. Coordination-site exchange and solid-state 13-C NMR studies of bis(oxalato)dioxovanadate(V) ion. *Magn. Reson. Chem.* 29:865–869.

32. Pecoraro, V.L. 1989. Structural characterization of [VO(salicylhydroximate)(CH$_3$OH)]$_3$: Application to the biological chemistry of vanadium(V). *Inorg. Chim. Acta* 155:171–173.

33. Yamaki, R.T., E.B. Paniago, S. Carvalho, O.W. Howarth, and W. Kam. 1997. Interaction of *N*-hydroxyacetamide with vanadate in aqueous solution. *J. Chem. Soc., Dalton Trans.* 4817–4821.

34. Bell, J.H. and R.F. Pratt. 2002. Formation and structure of 1:1 complexes between aryl hydraxamic acids and vanadate at neutral pH. *Inorg. Chem.* 41:2747–2753.

35. Cornman, C.R., G.J. Colpas, J.D. Hoeschele, J. Kampf, and V.L. Pecoraro. 1992. Implications for the spectroscopic assignment of vanadium biomolecules: Structure and spectroscopic characterization of monooxovanadium(V) complexes containing catecholate and hydroxamate-based noninnocent ligands. *J. Am. Chem. Soc.* 114:9925–9933.

36. Bhattacharyya, S., R.J. Batchelor, F.W.B. Einstein, and A.S. Tracey. 1999. Crystal structure and solution studies of the product of the reaction of β-mercaptoethanol with vanadate. *Can. J. Chem.* 77:2088–2094.

37. Paul, P.C. and A.S. Tracey. 1997. Aqueous interactions of vanadate and peroxovanadate with dithiothreitol. Implications for the use of this redox buffer in biochemical investigations. *J. Biol. Inorg. Chem.* 2:644–651.

38. Baes, C.F. and R.E. Mesmer. 1976. *The hydrolysis of cations.* Wiley Interscience, New York.

39. Li, J., G. Elberg, D.C. Crans, and Y. Shechter. 1996. Evidence for the distinct vanadyl(+4)-dependent activating system for manifesting insulin-like effects. *Biochemistry* 35:8314–8318.

40. Crans, D.C. and P.K. Shin. 1994. Characterization of vanadium(V) complexes in aqueous solutions: Ethanolamine- and glycine-derived complexes. *J. Am. Chem. Soc.* 116:1305–1315.

41. Davies, S.C., D.L. Hughes, Z. Janas, L.B. Jerzykiewicz, R.L. Richards, J.R. Sanders, J.E. Silverston, and P. Sobota. 2000. Vanadium complexes of the N(CH$_2$CH$_2$S)$_3$$^{3-}$ and O(CH$_2$ CH$_2$S)$_2$ ligand with coligands relevant to nitrogen fixation processes. *Inorg. Chem.* 39:3485–3498.

42. Nanda, K.K., E. Sinn, and A.W. Addison. 1996. The first oxovanadium(V)-thiolate complex [VO(SCH$_2$)$_3$N]. *Inorg. Chem.* 35:1–2.

43. Bhattacharyya, S., A. Martinsson, R.J. Batchelor, F.W.B. Einstein, and A.S. Tracey. 2001. N,N-Dimethylhydroxamidovanadium(V). Interactions with sulfhydryl-containing ligands: V(V) equilibria and the structure of a V(IV) dithiothreitol complex. *Can. J. Chem.* 79:938–948.

44. Cohen, M.D., A.C. Sen, and C.-I. Wei. 1987. Ammonium metavanadate complexation with glutathione disulfide: A contribution to the inhibition of glutathione reductase. *Inorg. Chim. Acta* 138:91–93.

45. Emirdag-Eanes, M. and J.A. Ibers. 2001. Synthesis and characterization of new oxidopolysulfidovanadates. *Inorg. Chem.* 40:6910–6912.

46. Crans, D.C. and P.K. Shin. 1988. Spontaneous and reversible formation of vanadium(V) oxyanions with amine derivatives. *Inorg. Chem.* 27:1797–1806.

47. Jaswal, J.S. and A.S. Tracey. 1991. Stereochemical requirements for the formation of vanadate complexes with peptides. *Can. J. Chem.* 69:1600–1607.

48. Crans, D.C., H. Chen, O.P. Anderson, and M.M. Miller. 1993. Vanadium(V)-protein model studies: Solid-state and solution structure. *J. Am. Chem. Soc.* 115:6769–6776.

49. Crans, D.C., A.D. Keramidas, S.S. Amin, O.P. Anderson, and S.M. Miller. 1997. Six-coordinated vanadium(IV) and -(V) complexes of benzimidazole and pyridyl-containing ligands. *J. Chem. Soc., Dalton Trans.* 2799–2812.

50. Crans, D.C. and I. Boukhobza. 1998. Vanadium(V) complexes of polydentate amino alcohols: Fine-tuning complex properties. *J. Am. Chem. Soc.* 120:8069–8078.

51. Colpas, G.J., B.J. Hamstra, J.W. Kampf, and V.L. Pecoraro. 1994. Preparation of VO(3+) and VO$_2$(+) complexes using hydrolytically stable, asymmetric ligands derived from Schiff base precursors. *Inorg. Chem.* 33:4669–4675.

52. Crans, D.C., A.D. Keramidas, M. Mahroof-Tahir, O.P. Anderson, and M.M. Miller. 1996. Factors affecting solution properties of vanadium(V) compounds: x-ray structure of β–*cis*-NH$_4$[VO$_2$(EDDA)]. *Inorg. Chem.* 35:3599–3606.

53. Bonadies, J.A. and C.J. Carrano. 1986. Vanadium phenolates as models for vanadium in biological systems. 1. Synthesis, spectroscopy, and electrochemistry of vanadium complexes of ethylenebis[(*o*-hydroxyphenyl)glycine] and its derivatives. *J. Am. Chem. Soc.* 108:4088–4095.

54. Hamstra, B.J., G.J. Colpas, and V.L. Pecoraro. 1998. Reactivity of dioxovanadium(V) complexes with hydrogen peroxide: Implications for vanadium haloperoxidase. *Inorg. Chem.* 37:949–955.

55. Crans, D.C., F. Jiang, I. Boukhobza, I. Bodi, and T. Kiss. 1999. Solution characterization of vanadium(V) and -(IV) *N*-(phosphonomethyl)iminodiacetate complexes: Direct observation of one enantiomer converting to the other in an equilibrium mixture. *Inorg. Chem.* 38:3275–3282.

56. Galeffi, B. and A.S. Tracey. 1989. 51-V NMR investigation of the interactions of vanadate with hydroxypyridines and pyridine carboxylates in aqueous solution. *Inorg. Chem.* 28:1726–1734.

57. Sergienko, V.S., V.K. Borzunov, and A.B. Illyukhin. 1995. Synthesis and crystal and molecular structure of dioxobis(pyridine-2-carboxylato)vanadate(V) ammonium dihydrate, NH$_4$[VO$_2$(pic)$_2$]·2H$_2$O: A rare exception to the self-consistency rule. *Russ. J. Coord. Chem.* 21:107.

58. Melchior, M., K.H. Thompson, J.M. Jong, S.J. Rettig, E. Shuter, V.G. Yuen, J.H. McNeill, and C. Orvig. 1999. Vanadium complexes as insulin mimetic agents: Coordination chemistry and *in vivo* studies of oxovanadium(IV) and dioxovanadium(V) complexes formed from naturally occurring chelating oxazolinate, thiazolinate, or picolinate units. *Inorg. Chem.* 38:2288–2293.

59. Mimoun, H., L. Saussine, E. Daire, M. Postel, J. Fischer, and R. Weiss. 1983. Vanadium(V) peroxo complexes. New versatile biomimetic reagents for epoxidation of olefins and hydroxylation of alkanes and aromatic hydrocarbons. *J. Am. Chem. Soc.* 105:3101–3110.

60. Nuber, B., J. Weiss, and K. Wieghardt. 1978. Schwingungsspecktrum und kristallstrucktur des fünffach-koordinierten *cis*-dioxo-dipicolinato-vanadat(V)-anions. *Z. Naturforsch.* 88b:265–267.

61. Crans, D.C., L. Yang, T. Jakusch, and T. Kiss. 2000. Aqueous chemistry of ammonium (dipicolinato)oxovanadate(V): The first organic vanadium(V) insulin-mimetic compound. *Inorg. Chem.* 39:4409–4416.

62. Rehder, D. 1988. Interaction of vanadate (H$_2$VO$_4^-$) with dipeptides. Investigated by ^{51}V NMR spectroscopy. *Inorg. Chem.* 27:4312–4316.

63. Cornman, C.R., K.M. Geiser-Bush, and P. Singh. 1994. Structural and spectroscopic characterization of a novel vanadium(V)-amide complex. *Inorg. Chem.* 33:4621–4622.

64. Skorey, K.I., N.A. Johnson, G. Huyer, and M.J. Gresser. 1999. A two-component affinity chromatography purification of *Helix pomatia* arylsulfatase by tyrosine vanadate. *Prot. Expr. Purif.* 15:178–187.

65. Fritzsche, M., V. Vergopoulos, and D. Rehder. 1993. Complexation of histidine and alanylhistidine by vanadate in aqueous medium. *Inorg. Chim. Acta* 211:11–16.

66. Elvingson, K., M. Fritzsche, D. Rehder, and L. Pettersson. 1994. Speciation in vanadium bioinorganic systems. 1. A potentiometric and ^{51}V NMR study of aqueous equilibria in the H$^+$-vanadate(V)-L-α-alanyl-L-histidine system. *Angew. Chem., Int. Ed. Engl.* 48:878–885.

67. Crans, D.C., H. Holst, A.D. Keramidas, and D. Rehder. 1995. A slow exchanging vanadium(V) peptide complex: Vanadium(V)-glycine-tyrosine. *Inorg. Chem.* 34:2524–2534.

68. Buhl, M. 2005. Molecular dynamics of a vanadate-dipeptide complex in aqueous solution. *Inorg. Chem.* 44:6277–6283.

69. Tracey, A.S., J.S. Jaswal, F. Nxumalo, and S.J. Angus-Dunne. 1995. Condensation reactions between vanadate and small functionalized peptides in aqueous solution. *Can. J. Chem.* 73:489–498.

70. Gorzsas, A., I. Andersson, H. Schmidt, D. Rehder, and L. Pettersson. 2003. A speciation study of the aqueous H$^+$/H$_2$VO$_4$/L-α-alanyl-L-serine system. *J. Chem. Soc., Dalton Trans.* 1161–1167.

71. Schwarzinger, S., G.J.A. Kroon, T.R. Foss, P.E. Wright, and H.J. Dyson. 2000. Random coil chemical shifts in acidic 8M urea: Implementation of random coil shift data in NMR view. *J. Biomol. NMR* 18:43–48.

72. Wishart, D.S., C.G. Bigam, R.S. Hodges, and B.D. Sykes. 1995. ^{1}H, ^{13}C and ^{15}N random coil NMR chemical shifts of the common amino acids. I. Investigation of the nearest-neighbor effects. *J. Biomol. NMR* 5:67–81.

73. Buhl, M. 2000. Density-fluctional study of vanadate-glycylserine isomer. *J. Inorg. Biochem.* 80:137–139.

74. Vergopoulos, V., W. Priebsch, M. Fritzsche, and D. Rehder. 1993. Binding of L-histidine to vanadium. Structure of exo-[VO$_2${N-(2-oxidonaphthal)-His}]. *Inorg. Chem.* 32:1844–1849.

75. Buhl, M. 1999. Theoretical study of a vanadate peptide complex. *J. Comp. Chem.* 20:1254–1261.

76. Plass, W., A. Pohlmann, and H.-P. Yozgatli. 2000. *N*-Salicylidenehydrazides as versatile tridentate ligands for dioxovanadium(V) complexes. *J. Inorg. Biochem.* 80:181–183.

77. Diamantis, A.A., J.M. Frederikson, M.A. Salam, M.R. Snow, and E.R.T. Tiekink. 1986. Structures of two vanadium(V) complexes with tridentate ligands. *Aust. J. Chem.* 39:1081–1088.

78. Rajak, K.K., B. Baraub, S.P. Rath, and A. Chakravorty. 2000. Sugar binding to VO^{3+}. Synthesis and structure of a new mannopyranoside vanadate. *Inorg. Chem.* 39:1598–1601.

79. Mondal, S., S.P. Rath, K.K. Rajak, and A. Chakravorty. 1998. A family of (*N*-salicylidene-α-amino acidato)vanadate esters incorporating chelated propane-1,3-diol and glycerol: Synthesis, structure and reaction. *Inorg. Chem.* 37:1713–1719.

80. Asgedom, G., A. Sreedhara, J. Kivikoski, E. Kolehmainen, and C.P. Rao. 1996. Structure, characterization and photoreactivity of monomeric dioxovanadium(V) Schiff-base complexes of trigonal-bipyramidal geometry. *J. Chem. Soc., Dalton Trans.* 93–97.

81. Yamaki, R.T., E.B. Paniago, S. Carvalho, and I.S. Lula. 1999. Interaction of 2-amino-*N*-hydroxypropanamide with vanadium(V) in aqueous solution. *J. Chem. Soc., Dalton Trans.* 4407–4412.

82. Mahroof-Tahir, M., A.D. Keramidas, R.B. Goldfarb, O.P. Anderson, M.M. Miller, and D.C. Crans. 1997. Solution and solid state properties of [*N*-(2-hydroxyethyl)imi-nodiacetato)vanadium(IV), -(V) and -(IV/V) complexes. *Inorg. Chem.* 36:1657–1668.

83. Rehder, D., C. Weidemann, A. Duch, and W. Priebsch. 1988. 51-V shielding in vanadium(V) complexes: A reference scale for vanadium binding sites in biomolecules. *Inorg. Chem.* 27:584–587.

84. Rehder, D., H. Holst, W. Priebsch, and H. Vilter. 1991. Vanadate-dependent bromo/iodoperoxidase from ascophyllum nodosum also contains unspecific low-affinity binding sites for vanadate(V): A 51-V NMR investigation, including the model peptides Phe-Glu and Gly-Tyr. *J. Inorg. Biochem.* 41:171–185.

85. Durupthy, O., A. Coupe, L. Tache, M.-N. Rager, J. Maquet, T. Coradin, N. Steunou, and J. Livage. 2004. Spectroscopic investigation of interactions between dipeptides and vanadate(V) in solution. *Inorg. Chem.* 43:2021–2030.

5 Coordination of Vanadate by Hydrogen Peroxide and Hydroxylamines

The reactions of hydrogen peroxide with vanadate have been of interest for many years. Much of the early work was concerned with the function of peroxovanadates as oxygen transfer agents. Alkenes and similar compounds such as allyl alcohols can be hydroxylated or epoxidized. Even alkanes can be hydroxylated, whereas alcohols can be oxidized to aldehydes or ketones and thiols oxidized to sulphones or sulphoxides. Aromatic molecules, including benzene, can be hydroxylated. The rich chemistry associated with the peroxovanadates has, therefore, led to extensive studies of their reaction chemistry. To this end, x-ray diffraction studies have successfully provided details of a number of peroxovanadate structures.

Many peroxovanadates have potent insulin-mimetic properties [1,2]. Apparently, this functionality derives from the ability of these compounds to rapidly oxidize the active site thiols found in the group of protein tyrosine phosphatases that are involved in regulating the insulin receptor function [3]. The discovery of vanadium-dependent haloperoxidases in marine algae and terrestrial lichens provided an additional stimulus in research toward obtaining functional models of peroxidase activity, and there is great interest in duplicating the function of these enzymes (see Section 10.4.2).

Because of the asymmetry of hydroxylamines and the fact that they are complexed by vanadate in a side-on fashion similar to hydrogen peroxide, they provide details of the chemistry not otherwise easily accessible. Further interest in these compounds arises from both their *in vivo* and *in vitro* insulin-mimetic properties. Animal studies have shown that the bis(*N,N*-dimethyl)hydroxamidohydroxooxovanadate is as effective as other insulin-mimetics such as bis(maltolato)oxovanadium(IV). Unlike the peroxo complexes, the hydroxylamine complexes influence enzyme activity by a nonoxidative mechanism [4,5].

These two types of ligands readily undergo reactions with vanadate to form, among other products, both mono- (VL) and bisligand (VL$_2$) complexes. The formation of the complexes is highly favorable and not very dependent on ligand type. The reactions are more intricate than what might be expected. Reactions of hydrogen peroxide lead to compounds being formed where no equivalent complex with hydroxylamines has been reported. The opposite is also true. Hydrogen peroxide in aqueous solution is not chemically stable in the presence of vanadate, although the rate of decomposition is highly dependent on the pH of the medium. Under mod-

erately to strongly acidic conditions, hydrogen peroxide disproportionates to O_2 and water, but it is progressively more stable at higher pH. In aqueous solution, under moderately basic conditions, hydroxylamine slowly forms ammonia, nitrogen, and water. *N*-methyl and *N,N*-dimethylhydroxylamine are much less labile. Vanadate complexes of these types of ligands are highly reactive toward numerous heteroligands (X), both VLX and VL$_2$X complexes readily being formed. Reaction of chelating ligands such as dipeptides with peroxovanadate leads to slow formation of monoperoxoheteroligand complexes and effectively prevents the disproportionation of hydrogen peroxide.

The hydrogen peroxide and hydroxylamine ligands are unique in that, although the commonly encountered complexes are bischelates, they have properties of mono-ligated derivatives. For instance, rapid rotational isomerization that exchanges the *N* and *O* positions in hydroxylamine complexes occurs [6]. This isomerization, which occurs within a few milliseconds, is much faster than hydrolysis, for which a few hours are required. This suggests that the rotational process does not involve *N*-only or *O*-only coordinated intermediates, because complexes of this type would be expected to rapidly dissociate. Apparently, the vanadate in the intermediate complex retains bonding to both *N* and *O* during the rotational process. Doubtless, a similar isomerization occurs with peroxo complexes, and in principal, it could be observed with ^{17}O NMR spectroscopy.

The ^{51}V NMR spectra of bis(*N*-methylhydroxylamine) complexes show signals for methyl groups in orientations assignable to the possible positions available on the nitrogen [7,8]. Unfortunately, detailed kinetics experiments have not been carried out. It would be of interest to know whether the end-for-end rotation is correlated with methyl group reorientation.

5.1 HYDROGEN PEROXIDE

The use of ^{51}V NMR spectroscopy has proven particularly fruitful for the delineation of the various peroxovanadates found in aqueous solution, whereas kinetics studies have provided details of the mechanisms leading to product formation. The most commonly encountered complexes of hydrogen peroxide have VL, VL$_2$, VL$_3$, and V$_2$L$_4$ stoichiometry. Table 5.1 gives the chemical shifts for various oxoperoxo complexes of vanadate. The complexes generally are anionic, although under strongly acidic conditions some neutral or cationic forms can be generated. The bisperoxovanadate is formed over a very wide pH range from 1 (monoanionic) to above 10 (dianionic), where it is normally the dominant species when there is little excess peroxide in solution. Although the anionic character of the peroxo compounds has been well established, they are sometimes reported as being cationic compounds [9,10]. If there is a large excess of hydrogen peroxide, the equilibrium is shifted toward-the-trisperoxovanadate-dianion. A detailed study of the peroxovanadate system over an extended pH range, which took into account the vanadium-catalyzed decomposition of hydrogen peroxide, has provided product formation constants for numerous peroxovanadates [11], and these formation constants have been used in Figure 5.1 and Figure 5.2. Figure 5.1 shows the influence of hydrogen peroxide concentration on product distribution for the major products for pH 5.0, 7.0, and

TABLE 5.1
^{51}V Chemical Shifts for Aqueous Oxoperoxovanadate Complexes

Complex	Chemical Shift (ppm)	pK_a	Ref.
$VO(OO)(H_2O)_3^{1+}$	−540		28
$VO(OH)_2(OO)^{1-}$	−602	6.2	29
$VO_2(OH)(OO)^{2-}$	−625		11, 29
$VOH(OO)_2(H_2O)^0$	−702	0.43	28
$VO(OO)_2(H_2O)^{1-}$	−692	7.42[a], 7.67[a]	11, 28, 30
$VO(OO)_2(OH)^{2-}$	−765		11, 30
$V(OH)(OO)_3^{2-}$	−733		11, 30
$(VO(OO)_2)_2OH^{3-}$		−756	11, 30
			11
Complexes of Quoted Vanadate to Ligand Stoichiometry[b]			
$V_2L_3^0$	−669 (−671, −674)		22
VVL_2^{3-}	−737 (VL$_2$), −555 (V)		
$VLVL^{3-}$	−634		
VVL^{3-}	−622 (VL), −563 (V)		

[a] The pK_a values obtained were for 1.0 M ionic strength KCl (pK_a 7.42): for 0.15 M NaCl (pK_a 7.67).

[b] These complexes were observed at high total vanadate (80 mmol/L) and total ligand (80 mmol/L) concentrations where they are minor species.

9.0. Minor products that are not shown in the figure include anionic V_2L, VVL_2, and V_2L_3 (Section 8.1).

Detailed kinetics studies have been carried out on the mechanism of formation of monoperoxovanadates. Such studies have been carried out using multidentate ligands such as pyridine-2,6-dicarboxylic acid (dipic), *N,N*-bis(2-pyridylmethyl)glycine (hbpg), and similar ones. These form complexes that lead to monoperoxovanadate derivatives after reaction with hydrogen peroxide [12–14]. To a large extent, this eliminated the analytical problems deriving from the occurrence of additional products in the reaction sequence. The studies that were carried out for aqueous solutions were fully consistent with the occurrence of two processes for monoperoxovanadate generation. Under fixed acidity conditions, formation of the monoperoxo complex is first order in the concentration of the reactant vanadium complex and also first order in hydrogen peroxide. However, the dependence of product formation on the acidity of the medium suggested that both proton-dependent and proton-independent reactions generated the peroxo product. It is not surprising that acidic conditions speed product formation, because the proton-dependent pathway is faster than the proton-independent one by about 1000 times [13]. Furthermore, it was shown that the reaction, to an extent, is regulated by the influence of the electron-donating properties of the ligand [13]. Interestingly, one kinetics study with the picolinato ligand [12] concluded that the vanadium(V) bis(oxo)dipicolinato reactant was trimeric, a rather surprising conclusion, because no mention of this is made in an alternate kinetics study with the same reactant [13], and no evidence for such a stoichiometry has been reported from NMR studies. In fact, a study using potentiometry and both ^{1}H and ^{51}V NMR spectroscopy showed only the formation of a
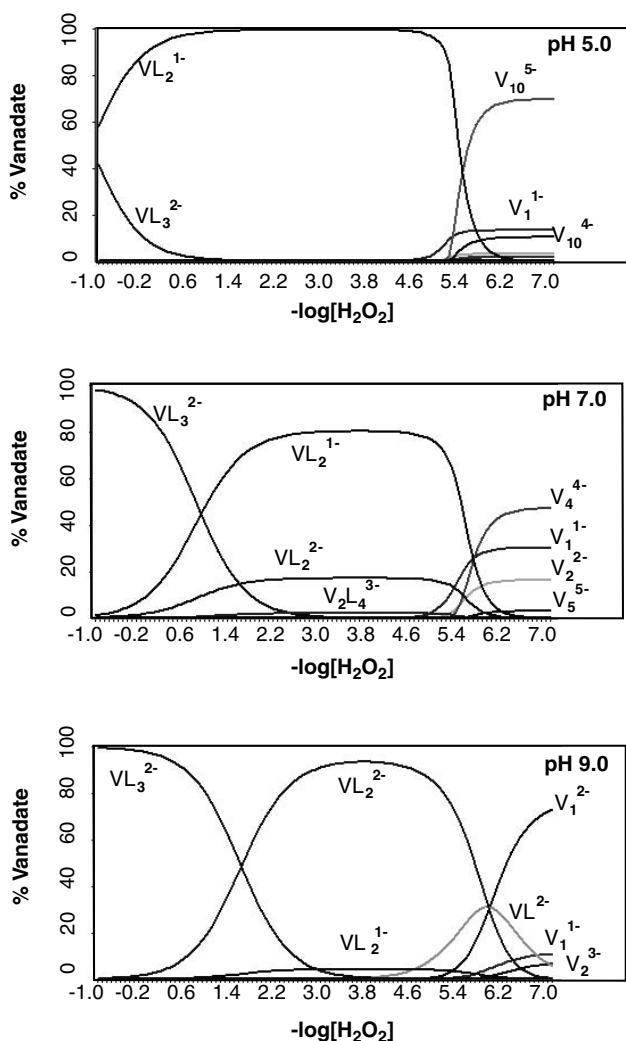
FIGURE 5.1 Distribution diagram showing the formation of vanadate and peroxovanadate species as a function of the concentration of hydrogen peroxide and of pH. Conditions for the simulation: 2mmol/L total vanadate; 0.1 μmol/L to 10 mmol/L total hydrogen peroxide; 0.15 mol/L ionic strength with NaCl; pH values, as indicated. The formation constants are from reference 11.

monomeric complex [15]. It is not evident why there is this disparity. In the trimer case, the crystalline dipicolinato complex was used, whereas in the other studies, the complex was prepared *in situ*. This may simply mean that the solutions being studied were not in thermodynamic equilibrium.

Kinetics studies carried out in acetonitrile solutions provided a similar picture for the mechanism of peroxidation. Studies were carried out for three related tertiary amine-derived ligands: *N,N*-bis(2-pyridylmethyl)glycine, *N*-(2-pyridylmethyl)imin-odiacetic acid, and *N*-(2-amidomethyl)iminodiacetic acid [14]. The kinetics studies
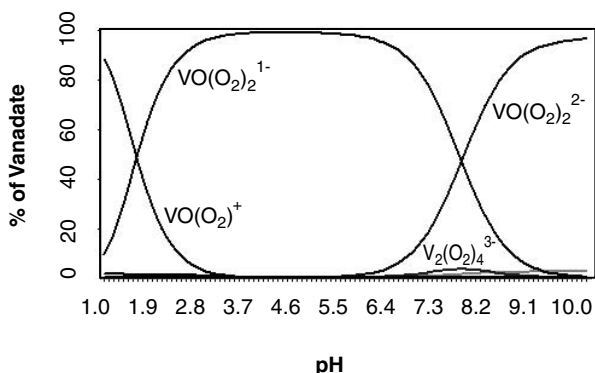
FIGURE 5.2 Diagram showing the distribution of peroxovanadium species as a function of pH. Simulation conditions: total vanadate, 2.0 mmol/L; total hydrogen peroxide, 4.0 mmol/L; ionic strength, 0.15 mol/L with NaCl; pH range, 1 to 10. Formation constants are from reference 11.

consistently paint a picture of an associative reaction of peroxide with the vanadium complex, followed by elimination of hydroxyl or water and rearrangement to the final product. Although the occurrence of end-on coordinated hydrogen peroxide does not appear to have been reported, such a compound has been suggested from [51]V NMR studies of hydroxylamines [6,7], and of course, similar coordination is well known for alcohols and phenols. Following the lead from the kinetics studies and incorporating the proposal of initial end-on coordination of the peroxide, Scheme 5.1 is thought to provide a reasonable picture of the proton-dependent and proton-independent reaction pathways for formation of the peroxo product. It is quite possible that alternate reaction sequences occur for other types of ligands. For instance, strongly electron-donating ligands may well favor an initial dissociative reaction of OH^- or H_2O followed by incorporation of hydrogen peroxide.

The most-well-known-cationic peroxovanadate is the monoperoxide, $VO(O_2)(H_2O)_3^{1+}$, which is a red vanadate derivative often utilized in a test for the presence of vanadium. Figure 5.2 shows the pH dependence of product distribution for the major peroxovanadates under a fixed overall concentration ratio of 2 mmol/L vanadate to 4 mmol/L hydrogen peroxide. It is evident from this diagram that any significant proportion of the cationic complex occurs only below pH 3. The bisperoxide is the dominant product throughout the pH range to at least pH 10.

5.2 HYDROXYLAMINES

Coordination of vanadate by hydroxylamines is similar in many respects to coordination by hydrogen peroxide. Various hydroxylamine complexes are known, although only detailed studies of the aqueous chemistry have been carried out with hydroxylamine and its *N*-methyl and *N,N*-dimethyl derivatives. *N*-substitution apparently has only a small influence on product formation. There is, however, scope for a wider range of isomeric forms with the *N*-methylated ligand compared to the unsubstituted and dimethylated ligands, and a number of isomers have been observed

SCHEME 5.1

[7]. Complexes of VL and VL_2 stoichiometry are the predominant forms. However, as for the hydrogen peroxide case, the minor complexes V_2L_3 and V_2L are also formed. Considering the observation of the last two forms, it is somewhat surprising that V_2L_2 and V_2L_4 have not been reported as solution complexes. The latter complex, in a nonionic form, is readily prepared as a crystalline compound that hydrolyzes upon dissolution in water. It will almost certainly be observed when concentrations are appropriate. The most likely reason for nonobservation of these compounds is that their ^{51}V NMR signals lie under those of VL or VL_2. From Table 5.2, it can be seen that the individual signals of V_2L_3 (VLVL$_2$) and V_2L (VVL) are very close to the corresponding signal of VL or VL_2.

There are two distinct types of bisligand complexes formed. Neither type carries a charge under neutral pH conditions. One type is protonated under mildly acidic conditions, whereas the other is deprotonated under mildly basic conditions (Table 5.2). There also are two forms of the monoligated complex that presumably are structurally related to the bisligand complexes.

TABLE 5.2
Aqueous Phase ^{51}V Chemical Shifts for Hydroxamido Complexes of Vanadate

Complex	Chemical Shift (ppm)	pK$_a$	Complex	Chemical Shift (ppm)	Ref.
Hydroxylamine					
VL	−569				
VL^{1-}	−670, −674 [a]				6, 7
VL$_2$$^{1+}$ [b]	−801	5.92	VL$_2$^{0} [b]	−823	7
VL$_2$$^{1+}$ [b]	−815	6.60	VL$_2$^{0} [b]	−848	7
VL$_2$^{0} [c]	−852	7.4 [c]	VL$_2$$^{1-}$ [c]	−852 [c]	7
VL$_2$^{0} [c]	−861	7.4 [c]	VL$_2$$^{1-}$ [c]	−861 [c]	7
N-Methylhydroxylamine					
VL	−571				
VL^{1-}	−651, −655 [a]				6, 7
VL$_2$ [c]	−751, −758, −766, −779, −798	6.1 [d]			7
VL$_2$ [d]	−789, −794, −803, −808, −810	7.8 [e]			7
N,N-Dimethylhydroxylamine					
VL	−571				
VL^{1-}	−630, v635 [a]				6, 7, 21
VL$_2$$^{1+}$ [g]	−696	3.35	VL$_2$^{0} [g]	−725	6
VL$_2$$^{1+}$ [g]	v693	3.80	VL$_2$^{0} [g]	−740	6
		9.0 [h]	VL$_2$$^{1-}$ [g, h]	−690	6, 21
VL$_2$^{0} [i]	−750				
V$_2$L [j]	v567 (V), −632 (VL)				21
V$_2$L$_3$ [j]	−648 (VL), −712 (VL$_2$)				21

[a] No pK$_a$ has been reported for the monoligated species [6, 7]

[b] Complexes with broad NMR signals and having chemical shifts dependent on protonation state [7]

[c] Complexes having sharp NMR signals with no chemical shift dependence on protonaion state. No difference between pKa's reported [7]

[d] Acidity constant reported is an average value for the broad signal products. These signals have pH-dependent chemical shifts [7]

[e] Acidity constant reported is an average value for the sharp signal complexes. These signals have little or no dependence of chemical shift on pH [7]

[f] This compound has a pKa above 11 [21]

[g] Broad signal NMR complexes with a chemical shift dependence on pH [6]

[h] This pKa is an averaged value because of coalescence of the broad -725 ppm and -740 ppm signals [21]

[i] Sharp NMR signal product; a signal for a second complex has not been reported

[j] Chemical shifts for pH 8.54 [21]

5.3 COORDINATION GEOMETRY OF PEROXO AND HYDROXAMIDO VANADATES

Crystal structures for both oxobispero [16] and oxobishydroxamido (bis(*N,N*-diethylhydroxamido) [17]) and (bis(*N,N*-dimethylhydroxamido) [6]) vanadates have been reported. In both the peroxo and hydroxamido cases, the complexes occur as dimers
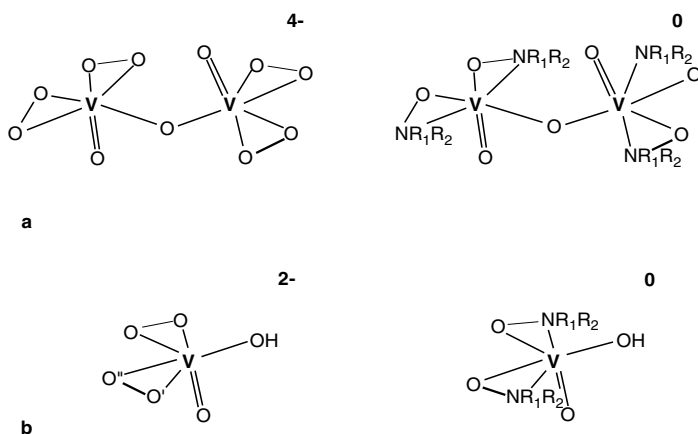
SCHEME 5.2

with a VOV linkage. The hydroxamido ligand complexes to the vanadium via an anionic oxygen and an uncharged nitrogen, whereas the peroxoligand complexes through two oxygens, both of which are anionic. Consequently, although the charge states of the peroxo and hydroxamido complexes are very different, this has little influence on coordination geometry, and the two types of complexes are quite similar.

Scheme 5.2a gives structural representations of the bisligand complexes. Hydrolysis could reasonably be expected to yield the corresponding monomeric forms depicted in Scheme 5.2b. Numerous solid-state structures have been obtained for peroxo complexes and a few for hydroxamido complexes. Some common structural parameters are summarized in Table 5.3. It is evident from this table that V to peroxo O bond lengths are not really distinguishable from the VO lengths in the hydroxamido complexes, the VO average for bisperoxo complexes being 1.889 Å compared to 1.909 Å for the bishydroxamido compounds, with much overlap of bond distances. The V-to-N bond length is, however, a little longer, the average value being 1.992 Å for the complexes given in the table. Of the crystal structures reported for bishydroxylamine complexes, only two show the nitrogens being adjacent each other [18,19]; all others show them being opposite, as depicted in Scheme 5.2. The VO_{oxo} bond length averages 1.598 Å for the complexes in the table, and there is no discernible difference between the peroxo and hydroxamido complexes.

A third peroxovanadate that is found in solution is the trisligand complex, hydroxotrisperoxovanadium(V). In the bisperoxo and bishydroxamido complexes, the two three-component rings are close to coplanar. In the tris derivative, any two of the three rings have a similar arrangement, except that the angle between the planes of the rings is 120° rather than close to 180°. Conversely, the rings can be thought of as all being mutually parallel to the symmetry axis (V-OH bond) with a slight twist of the ring plane with respect to this axis [20]. If bonding to the peroxoligand is formally considered as unidentate, then the coordination of this complex is very close to tetrahedral. In the solid state and in solution, this complex is doubly anionic. The complex is somewhat unique in that it represents one of the few instances where the V-oxo bond is lost. In solution, the trisperoxide has not

TABLE 5.3
Selected VO and VN Bond Lengths (Å) for Various Vanadium Peroxo and Hydroxamido Complexes

Complex[a]	VO_{oxo}	VO'_{peroxo} [b]	VO''_{peroxo} [c]	Ref.
$NH_4[VO(O_2)_2(NH_3)]$	1.599(3)	1.872(3)	1.871(3)	31
		1.872(3)	1.871(3)	
$ImH[VO(O_2)_2(im)]$	1.603(2)	1.866(2)	1.884(2)	19
		1.865(2)	1.922(2)	
$K_2[VO(O_2)_2(pic)]$	1.599(4)	1.899(4)	1.881(4)	32
		1.917(4)	1.895(4)	
$K_3[VO(O_2)_2(ox)]$	1.622(4)	1.934(4)	1.866(4)	33
		1.911(4)	1.856(3)	
$(NH_4)_4[O\{VO(O_2)_2\}_2$	1.601(3)	1.896(3)	1.884(3)	16
		1.914(3)	1.875(3)	
$NH_4[VO(O_2)(dipic)]$	1.579(2)	1.870(2)	1.872(2)	34
$[VO(O_2)(pic)(bipyr)]$	1.604(5)	1.887(5)	1.862(5)	7
$[NEt_4][VO(O_2)(glygly)]$	1.599(4)	1.890(4)	1.874(4)	36

	VO_{oxo}	$VO_{hydroxamido}$	$VN_{hydroxamido}$	Ref.
$[VO(H_2NO)_2(H_3NO)]Cl$	1.579(9)	1.892(9)	1.955(11)	18
	1.929(9)	1.965(10)		
$[VO(H_2NO)_2(gly)]$	1.603(2)	1.898(2)	2.021(2)	19
	1.901(2)	2.008(2)		
$[VO(H_2NO)_2(im)_2]Cl$	1.606(3)	1.927(3)	1.992(4)	19
	1.916(3)	1.993(3)		
$[VO(H_2NO)(dipic)(H_2O)]$	1.587(3)	1.903(3)	2.007(3)	37

[a] Et, ethyl; im, imidazole; pic, pyridine-2-carboxylato; dipic, pyridine-2,6-dicarboxylato; ox, oxalato; bipyr, 2,2'-bipyridine; gly, glycinato; glygly, glycylglycinato

[b] For the bisperoxo complexes, these bond distances correspond to the type VO' of Scheme 5.2.

[c] For the bisperoxo complexes, these bond distances correspond to the type VO'' of Scheme 5.2.

been observed to either accept or release protons [11]. Figure 5.3 depicts the coordination of this compound.

Vanadium-5 NMR spectroscopy has shown there are a number of complexes of varying stoichiometry and coordination formed in aqueous solution. These can clearly be seen in Figure 5.4 for the *N,N*-dimethylhydroxylamine ligand. Of the complexes formed, two chelate complexes have VL stoichiometry (~ –670 ppm). These compounds are both monoanionic at neutral pH, and one complex, if not both complexes, can give up an additional proton under basic conditions [21]. The observation of two chelate monoligand products clearly shows that there are two distinct coordination geometries for the VL complexes. Presumably, these are based on the coordination of the VL$_2$ complexes. An additional monohydroxylamine complex that apparently is coordinated end-on via the hydroxylamine OH has been found [6,7].
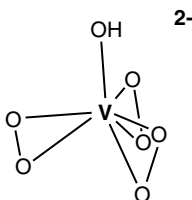
FIGURE 5.3 Diagrammatic representation of the structure of the oxotrisperovanadium(V) dianion. Detailed information for structure provided by F.W.B. Einstein [20].
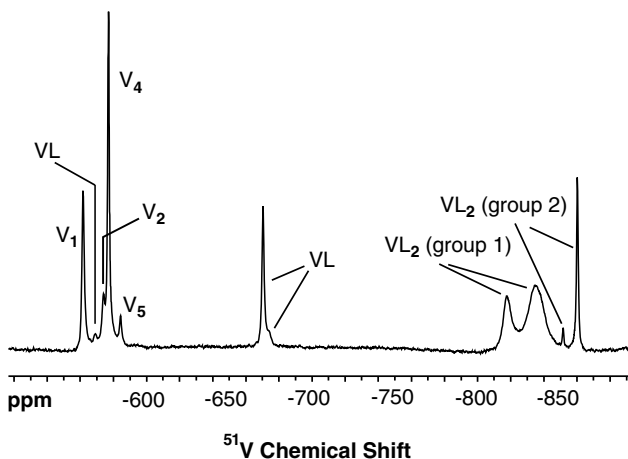

FIGURE 5.4 Vanadium NMR spectrum showing the formation of various hydroxamidova-nadium(V) complexes. Experimental conditions: 3.0 mM total vanadate, 5.0 mM total hydrox-ylamine, 20 mM HEPES buffer, 1.0 M KCl, pH 6.9.

This is a ubiquitous, though not highly favored, type of complex, and a similar complex quite likely is formed with the hydrogen peroxide ligand.

The bisligand complexes of hydroxylamines are clearly of two distinct types that have different proton reactivities and different properties in their vanadium NMR spectra. The two groups are indicated in Figure 5.4. Within each group, structural isomers occur that correspond to the relative orientations of the hydroxylamines within the complex (and, in the case of N-methylhydroxylamine, also to the relative orienta-tions of the methyl groups in the ligand [8], see Section 7.2). Although, in principle, for N,N-dimethyl and hydroxylamine itself, three such isomers are possible, NMR signals corresponding to only two of the three isomers have been identified. Two cis isomers (hydroxamido oxygens adjacent to each other [6,17,19] and nitrogens adjacent to each other [18,19]) have been found in crystal structures, but so far the trans orientation has not been reported. In aqueous solution, one isomer is favored over the other; however, the isomeric ratio is not particularly sensitive to ligand variation throughout the sequence of 0, 1, or 2 methyls on the nitrogen of the hydroxylamine. It seems very likely that the selectivity derives from electronic rather than steric factors. Scheme 5.3 depicts one isomer of each group and the observed charge states.
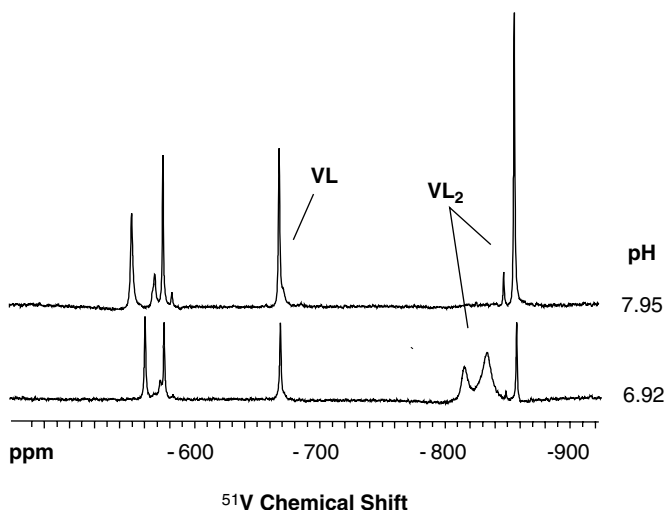
1+   0   1-

O—NR$_1$R$_2$ O—NR$_1$R$_2$ O—NR$_1$R$_2$

O—V   O—V   O—V

NR$_1$R$_2$ OH$_2$ NR$_1$R$_2$ OH   NR$_1$R$_2$ O

O   O   O

a Group I

0   1-

H$_2$O   H$_2$O

O—NR$_1$R$_2$ O—NR$_1$R$_2$

O—V   O—V

NR$_1$R$_2$ OH   NR$_1$R$_2$ O

O   O

b Group II

SCHEME 5.3

Dissolution of crystalline μ-oxo-bis(bis(*N,N*-dimethylhydroxamido)oxovanadate) in a mixed acetone/water solvent gives only one form (Group I, two isomers) of the monomer. Equilibrium studies in aqueous solution have established that, under neutral conditions, Group I complexes do not carry a charge and apparently correspond to the monomer of the crystalline complex, i.e., bis(*N,N*-dimethylhydroxamido)hydroxooxovanadate, Scheme 5.3a, neutral species. This compound can take up a proton to form a cationic complex. There is also evidence that suggests it can release a proton if conditions are sufficiently basic to form an anionic complex (Group 1 anion) [21]. Compounds of the second group of VL$_2$ complexes (Group II) are also uncharged under neutral conditions but have relatively much sharper NMR signals. They lose a proton under mildly basic conditions but are not readily protonated. Consequently, under slightly acidic conditions, only Group I complexes are observed. As shown in Figure 5.5, both types of complexes are found under neutral conditions, whereas under moderately basic conditions, Group II compounds are dominant. Additionally, Group I complexes display rather large changes (about 30 ppm) in their [51]V NMR chemical shifts as the protonation state varies, whereas the Group II complexes undergo little or no variation in chemical shift. Group II complexes must have a coordination that is different from that of Group I, and presumably this change in coordination is a result of incorporation of water into the coordination sphere. Scheme 5.3b depicts such a coordination mode if one water ligand is incorporated. If the Group I complexes have a structure similar to that of the crystalline precursor [6] as suggested by the dissolution studies, then the vanadium is out of the plane of the base ligands of the pentagonal pyramid. If the bonding to the hydroxamido ligand is formally treated as unidentate, the Group I complexes have close to tetrahedral coordination. The change depicted in Scheme 5.3, then, represents a change from tetrahedral coordination (Group I) to

FIGURE 5.5 NMR spectrum illustrating the influence of pH on product distribution of the two types of bishydroxylamine complexes of vanadate. Conditions for the experiments: 3.0 mM total vanadate, 5.0 mM total hydroxylamine, 1.0 M KCl, 20 mM HEPES buffer, indicated pH.

trigonal bipyramidal coordination (Group II). The latter coordination has been observed in a pentagonal bipyramidal hydroxylamine complex, where water is complexed in the axial position [18].

There is further evidence for the assignment of coordination geometry to the two groups of hydroxylamine complexes. The two types of compounds (Scheme 5.3) have very different properties in their ^{51}V NMR spectra (Figure 5.4). Group I compounds give rise to much broader signals than Group II compounds do. Reaction of hydroxylamine complexes with bidentate heteroligands such as glycine, cysteine, or glycylglycine provides products with NMR signals that are comparable in linewidth with those of the Group II complexes. Additionally, their chemical shifts are in the same chemical shift region as the Group II complexes. These observations strongly suggest there is a close structural correspondence. Furthermore, in the solid state, such heteroligand complexes have pentagonal bipyramidal coordination, as known from crystal structure studies of complexes formed with glycine, serine, and glycylglycine [6,19]. A further observation is that the signals from the Group II complexes and their heteroligand products are not significantly affected by the concentration of the heteroligand. However, the signals from the Group I compounds can be strongly influenced and come into coalescence with each other, as observed for some amino acids [21]. This is readily explained if the Group I complexes are more susceptible to attack by a heteroligand than are the Group II complexes. Attack by the ligand then leads to an intermediate structure, or possibly even a product, that rapidly reverts to starting materials and, by going through this cycle, catalyzes the exchange process. The pentagonal pyramidal structure proposed for the Group I complexes would be more susceptible to such behavior than the Group II pentagonal bipyramidal complexes of Group II, thus supporting such an assignment of coordination.

Studies of vanadate ligation by peroxide have not suggested there is more than one type of bisperoxo complex. A number of studies have been directed at determining the aqueous structure of this complex. NMR studies using ^{17}O-labelled water have suggested the presence of two complexed water molecules in the bisperoxo mono- and dianionic complexes, and an eight-coordinate geometry has been proposed [22]. This coordination has been disputed and pentagonal pyramidal geometry assigned to the monoanionic complex on the basis of Raman spectroscopy [23]. This latter work and the proposed geometry are compelling, although water in the axial position trans to the oxo ligand might not be adequately defined by the Raman work because of its rather long VO bond length. *Ab initio* calculations have supported the pentagonal pyramidal coordination description of the coordination [24,25]. Despite these arguments against complexed water, it is exceedingly difficult to dismiss the *O*-17 NMR studies. Additionally, the hydroxylamine complexes are clearly of two different coordination geometries, and this suggests incorporation of water into the bisperoxide is quite possible.

The ^{17}O NMR studies of the peroxovanadates strongly suggest there is at least one water molecule in the coordination sphere of dianionic bisperoxovanadate [22]. The ^{17}O NMR evidence is somewhat less compelling for the monoanionic derivative. Additionally, the vanadium NMR signals from oxobisperoxovanadate are close in linewidth to those of the Group II hydroxylamine derivatives, and this suggests these complexes are similar in structure. However, besides the Raman studies and theoretical calculations, there is a chemical argument against coordinated water. Overall, the peroxo functionality, O_2^{2-}, is a stronger base than the corresponding hydroxamido functionality, R_2NO^-. Therefore, the peroxo group has a greater tendency to donate electron density to the vanadium nucleus. The vanadium peroxo complexes will consequently have less of a tendency to draw ligands into the coordination sphere. Although complexes of two coordination numbers are observed for the hydroxylamine ligands, only one type of product is observed with the peroxoligand, and following the above argument, the shift should be toward the less highly coordinated complex. This may also explain why bisperoxovanadate has a tendency to complex bidentate heteroligands in a unidentate fashion. Although bishydroxamidovanadate complexes heteroligands, such as amino acids and related compounds, in a bidentate fashion, bisperoxovanadate ligates through either of the functional groups but not through both simultaneously. This is seen even more dramatically in imidazole complexation. Bishydroxamidovanadate complexes two imidazoles in a pentagonal bipyramidal coordination, whereas bisperoxovanadate complexes only one imidazole in a pentagonal pyramidal coordination [19]. In agreement with the crystal studies, incorporation of only one imidazole ligand into bisperoxovanadate has been observed in aqueous solution [11,26]. Bidentate coordination of ligands by bisperoxovanadate is generally accompanied by the elimination of one peroxo group.

When taken together, the evidence suggests that the Group I (Scheme 5.3a) bishydroxamidovanadates and the bisperoxovanadate complexes are similarly coordinated in aqueous solution, so that the pentagonal pyramidal coordination of hydroxooxobisperoxovanadate depicted in Scheme 5.2b is correct. If this is true, then the ^{17}O NMR studies are faulty, and there is no water in the coordination sphere of the bisperoxovanadate. It is equally clear that NMR spectroscopy has the potential

of unequivocally answering the question of whether water is or is not coordinated. If chemical exchange of complexed water with bulk water is sufficiently slow, there is a good chance that a ^{51}V-to-^{17}O J-coupling interaction can be used in a heteronuclear correlation NMR experiment to unambiguously resolve this question.

If the vanadium bonding to the peroxo group is considered as being formally unidentate, then the pentagonal pyramidal structure really can be considered as little more than a distorted tetrahedral coordination. If this is true, and because vanadate itself has tetrahedral geometry, it then seems evident that monoperoxovanadates will also have tetrahedral coordination or distorted square pyramidal coordination for formally bidentate peroxo groups. The question of coordination geometry is more problematic for the monohydroxamidovanadates. The observation of two vanadium signals clearly indicates that two coordination geometries occur, presumably geometries deriving from those of the bisligand derivatives. The ratio of the two mono-ligated products is in the order of 1:10 and apparently is insensitive to pH. Presumably, the major monohydroxamidovanadate will have square pyramidal coordination and the minor product square bipyramidal coordination, but there is little evidence for such an assignment.

The preceding arguments would suggest that the cationic monoperoxidovanadate has octahedral coordination (again assuming formally unidentate coordination of peroxide) because cationic vanadate is, itself, octahedral. *Ab initio* calculations support an octahedral geometry for this peroxide ion, although the calculations suggest the water trans to the Voxo bond is only weakly held [27]. It is also interesting to note that the hydroxotrisperoxovanadate dianion also can be considered to have tetrahedral geometry [20]. Scheme 5.4 displays possible coordination geometries for a number of the less common peroxovanadates that have been found in aqueous solution. The V_2L_3 derivative is formed under quite strongly acidic solutions and does not carry a charge. It is of particular interest because two ^{51}V NMR signals (–671 and –674 ppm, Table 5.1) that are very close in resonance position to each other virtually precludes the possibility of a $VLVL_2$ coordination for the vanadiums. Rather, bridging between vanadiums by an oxo- and one of the peroxoligands is suggested. If the remaining two peroxoligands are in the plane of the bridging groups, then two distinguishable, but almost identical, vanadiums occur that could well give rise to chemical shifts that are very close to each other. The structural representation in Scheme 5.4b provides a plausible structure that agrees with the NMR studies and also is in accord with the charge state of the complex. It is also possible that two symmetrical structural isomers, each similar to that depicted, are formed in approximately equal proportions and give rise to the two signals.

Bisperoxovanadate in aqueous solution has been represented as a cationic species, with one of the peroxo groups complexed in a side-on fashion and the second peroxo group attached in a unidentate manner [9,10]. This charge and coordination assignment is not in accord with the known properties of this complex, as discussed above. In fact, even under very strongly acid conditions, no cationic bisperoxide has been observed, rather the monoanionic species persists to below a pH of 1 [11].

a

b

c

SCHEME 5.4

REFERENCES

1. Shaver, A., D.A. Hall, J.B. Ng, A.-M. Lebuis, R.C. Hynes, and B.I. Posner. 1995. Bisperoxovanadium compounds: Synthesis and reactivity of some insulin mimetic complexes. *Inorg. Chim. Acta* 229:253–260.
2. Posner, B.I., R. Faure, J.W. Burgess, A.P. Bevan, D. Lachance, G. Zhang-Sun, I.G. Fantus, J.B. Ng, D.A. Hall, B. Soo Lum, and A. Shaver. 1994. Peroxovanadium compounds. *J. Biol. Chem.* 269:4596–4604.
3. Huyer, G., S. Liu, J. Kelly, J. Moffat, P. Payette, B. Kennedy, G. Tsaprailis, M.J. Gresser, and C. Ramachandran. 1997. Mechanism of inhibition of protein-tyrosine phosphatases by vanadate and pervanadate. *J. Biol. Chem.* 272:843–851.
4. Cuncic, C., S. Desmarais, N. Detich, A.S. Tracey, M.J. Gresser, and C. Ramachandran. 1999. Bis(N,N-dimethylhydroxamido)hydroxooxovanadate inhibition of protein tyrosine phosphatase activity in intact cells: Comparison with vanadate. *Biochem. Pharmacol.* 58:1859–1867.
5. Cuncic, C., N. Detich, D. Ethier, A.S. Tracey, M.J. Gresser, and C. Ramachandran. 1999. Vanadate inhibition of protein tyrosine phosphatases in Jurkat cells: Modulation by redox state. *J. Biol. Inorg. Chem.* 4:354–359.

6. Paul, P.C., S.J. Angus-Dunne, R.J. Batchelor, F.W.B. Einstein, and A.S. Tracey. 1997. Reactions of vanadate with N,N-dimethylhydroxylamine: Aqueous equilibria and the crystal structure of the uncharged oxygen-bridged dimer of bis(N,N-dimethylhydroxamido)hydroxooxovanadate. *Can. J. Chem.* 75:429–440.

7. Angus-Dunne, S.J., P.C. Paul, and A.S. Tracey. 1997. A ^{51}V NMR investigation of the interactions of aqueous vanadate with hydroxylamine. *Can. J. Chem.* 75:1002–1010.

8. Paul, P.C., S.J. Angus-Dunne, R.J. Batchelor, F.W.B. Einstein, and A.S. Tracey. 1997. Reactions of hydroxamidovanadate with peptides: Aqueous equilibria and crystal structure of oxobis(hydroxamido)glycylglycinatovanadium(V). *Can. J. Chem.* 75:183–191.

9. Rao, A.V.S., N.S. Islam, and T. Ramasarma. 1997. Reactivtiy of μ-peroxo-bridged dimeric vanadate in bromoperoxidation. *Arch. Biochem. Biophys.* 342:289–297.

10. Sarmah, S., D. Kalita, P. Hazarika, R. Borah, and N.S. Islam. 2004. Synthesis of new dinuclear and mononuclear peroxovanadium(V) complexes containing biogenic co-ligands: A comparative study of some of their properties. *Polyhedron* 23:1097–1107.

11. Andersson, I., S.J. Angus-Dunne, O.W. Howarth, and L. Pettersson. 2000. Speciation in vanadium bioinorganic systems 6. Speciation study of aqueous peroxovanadates, including complexes with imidazole. *J. Inorg. Biochem.* 80:51–58.

12. Wieghardt, K. 1978. Preparation and characterization of dipicolinatovanadium(V) complexes. Kinetics and mechanism of their reactions with hydrogen peroxide in acidic media. *Inorg. Chem.* 17:57–64.

13. Funahashi, S., K. Haraguchi, and M. Tanaka. 1977. Reactions of hydrogen peroxide with metal complexes. 2. Kinetic studies on the peroxo complex formation of nitrilotriacetatodioxovanadate(V) and dioxo(2,6-pyridinedicarboxylato)vanadate(V). *Inorg. Chem.* 16:1349–1353.

14. Hamstra, B.J., G.J. Colpas, and V.L. Pecoraro. 1998. Reactivity of dioxovanadium(V) complexes with hydrogen peroxide: Implications for vanadium haloperoxidase. *Inorg. Chem.* 37:949–955.

15. Crans, D.C., L. Yang, T. Jakusch, and T. Kiss. 2000. Aqueous chemistry of ammonium (dipicolinato)oxovanadate(V): The first organic vanadium(V) insulin-mimetic compound. *Inorg. Chem.* 39:4409–4416.

16. Stomberg, R., S. Olson, and I.-B. Svensson. 1984. The crystal structure of ammonium μ-oxo-bis(oxodiperoxovanadate)(4-), $(NH_4)_4[O\{VO(O_2)_2\}_2]$. A refinement. *Acta Chem. Scand.* A 38:653–656.

17. Saussine, L., H. Mimoun, A. Mitschler, and J. Fisher. 1980. Molybdenum(VI) and vanadium(V) N,N-dialkylhydroxylamino complexes: Synthesis, x-ray structure, and reactivity towards olefins. *Nouv. J. Chim.* 4:235–237.

18. Shao, M., J. Leng, and Z. Pan. 1990. Crystal structure of hydrated (bis-hydroxylamino)(hydroxylamine)oxovanadium(V) chloride $[VO(NH_2O)_2(NH_3O)H_2O]Cl$. *J. Inorg. Chem. (Chinese)* 6:443–447.

19. Keramidas, A.D., W. Miller, O.P. Anderson, and D.C. Crans. 1997. Vanadium(V) hydroxylamido complexes: Solid state and solution properties. *J. Am. Chem. Soc.* 119:8901–8915.

20. Drew, R.E., F.W.B. Einstein, J.S. Field, and D. Begin. 1975. *Angew. Chem., Int. Ed. Engl.* 31A:S135.

21. Bhattacharyya, S., A. Martinsson, R.J. Batchelor, F.W.B. Einstein, and A.S. Tracey. 2001. N,N-dimethylhydroxamidovanadium(V). Interactions with sulfhydryl-containing ligands: V(V) equilibria and the structure of a V(IV) dithiothreitol complex. *Can. J. Chem.* 79:938–948.

22. Harrison, A.T. and O.W. Howarth. 1985. High-field Vanadium-51 and Oxygen-17 Nuclear Magnetic Resonance Study of Peroxovanadates. *J. Chem. Soc., Dalton Trans.* 1173–1177.

23. Schwendt, P. and M. Pisarcik. 1990. Raman spectral study on the structure of vanadium(V) oxodiperoxo complexes in aqueous solution. *Spectrochim. Acta* 46A:397–399.

24. Conte, V., O. Bortolini, M. Carraro, and S. Moro. 2000. Models for the active site of vanadium-dependent haloperoxidases: Insight into the solution structure of peroxovanadium compounds. *J. Inorg. Biochem.* 80:41–49.

25. Buhl, M. and M. Parrinello. 2001. Medium effects on ^{51}V NMR chemical shifts: A density functional study. *Chem. Eur. J.* 7:4487–4494.

26. Tracey, A.S. and J.S. Jaswal. 1993. Reactions of peroxovanadates with amino acids and related compounds in aqueous solution. *Inorg. Chem.* 32:4235–4243.

27. Bagno, A., V. Conte, F. Di Furia, and S. Moro. 1997. *Ab initio* calculations on water-peroxovanadium clusters, $VO(O_2)(H_2O)_n^+$ (n = 1–5). Implications for the structure in aqueous solution. *J. Phys. Chem. A* 101:4637–4640.

28. Conte, V., F. Di Furia, and S. Moro. 1994. ^{51}V NMR investigation on the formation of peroxo vanadium complexes in aqueous solution: Some novel observations. *J. Mol. Catal.* 94:323–333.

29. Jaswal, J.S. and A.S. Tracey. 1991. Formation and decomposition of peroxovanadium(V) complexes in aqueous solution. *Inorg. Chem.* 30:3718–3722.

30. Tracey, A.S. and J.S. Jaswal. 1992. An NMR investigation of the interactions occurring between peroxovanadates and peptides. *J. Am. Chem. Soc.* 114:3835–3840.

31. Drew, R.E. and F.W.B. Einstein. 1972. The crystal structure of ammonium oxodiperoxoamminevanadate(V). *Inorg. Chem.* 11:1079–1083.

32. Shaver, A., J.B. Ng, D.A. Hall, B. Soo Lum, and B.I. Posner. 1993. Insulin-mimetic peroxovanadium complexes: Preparation and structure of potassium oxodiperoxo(pyridine-2-carboxylato)vanadate(V), $K_2[VO(O_2)_2(C_5H_4NCOO)]\cdot2H_2O$, and potassium oxodiperoxo(3-hydroxypyridine-2-carboxylato)vanadate(V), $K_2[VO(O_2)_2(OHC_4H_3NCOO)]\cdot3H_2O$, and their reactions with cysteine. *Inorg. Chem.* 32:3109–3113.

33. Begin, D., F.W.B. Einstein, and J. Field. 1975. An asymmetrical coordinated diperoxo compound. Crystal structure of $K_3[VO(O_2)_2(C_2O_4)]\cdot H_2O$. *Inorg. Chem.* 14:1785–1790.

34. Drew, R.E. and F.W.B. Einstein. 1973. Crystal structure at −100° of ammonium oxoperoxo(pyridine-2,6-dicarboxylato)vanadate(V) hydrate, $NH_4[VO(O_2)(H_2O)(C_5H_3N(CO_2)_2)]\cdot xH_2O$ (x ≈ 1.3). *Inorg. Chem.* 12:829–835.

35. Szentivanyi, H. and R. Stomberg. 1983. The crystal structure of (2,2'-bipyridine)oxoperoxo(pyridine-2-carboxylato)vanadium(V) hydrate, $[VO(O_2)(C_5H_4NCOO)(C_{10}H_8N_2)]\cdot H_2O$, at −100°C. *Acta Chem. Scand.* A37:709–714.

36. Einstein, F.W.B., R.J. Batchelor, S.J. Angus-Dunne, and A.S. Tracey. 1996. A product formed from glycylglycine in the presence of vanadate and hydrogen peroxide: The (glycylde-*N*-hydroglycinato-*K*$^3N^2$,N^N,*O*^{1})oxoper oxovanadate(V) anion. *Inorg. Chem.* 35:1680–1684.

37. Nuber, B. and J. Weiss. 1981. Aqua(dipicolinato)(hydroxlamido-*N,O*)oxovandium. *Acta Crystallogr.* B37:947–948.

6 Reactions of Peroxovanadates

Both the peroxovanadates and the hydroxamidovanadates readily undergo reactions with heteroligands. Such ligands may be either mono- or bidentate, and often bidentate ligands react in a monodentate fashion with the individual functional groups. Heteroligand reactions frequently occur without displacement of the peroxo- or hydroxamido groups, but certainly displacement of a ligand can occur. There is little evidence to suggest that monodentate heteroligands cause a change in coordination geometry from that of the parent complex. However, complexation of bidentate heteroligands may result in expansion of the coordination sphere rather than in expulsion of a peroxo (or hydroxamido) ligand. The chemistry of the peroxovanadates can be significantly different from that of the hydroxamidovanadates, particularly with ligands susceptible to oxidation. For instance, unlike hydroxamidovanadate, peroxovanadate very rapidly oxidizes thiolate groups, apparently with formation of a sulfinic acid [1].

6.1 HETEROLIGAND REACTIONS OF BISPEROXOVANADATES

6.1.1 COMPLEXATION OF MONODENTATE HETEROLIGANDS

There are surprisingly few detailed studies of the reaction of peroxovanadates with monodentate ligands. Perhaps the best characterized is the reaction of imidazole (Im) with bisperoxovanadate. Detailed studies of the aqueous solution equilibria have been reported, and a crystal structure has also been determined. Solution studies show the formation of complexes of stoichiometry $VLIm^{1-}$, VL_2Im^{1-}, and $V_2L_4Im^{3-}$ [2,3]. Under the conditions of the studies, the oxobisperoxoimidazolevanadate was found to be the dominant complex. Interestingly, it was found that the complex did not have a pK_a. This is in accord with expectations if the complex in solution retains the structure found in the crystalline material [4] and depicted in Scheme 6.1. The coordination in this structure is not significantly different from that reported for the oxobisperoxoamminevanadate [5]. Furthermore, Raman studies of the ammine complex strongly suggest that it does not change coordination when in aqueous solution [6]. Histidine and histidine-like imidazole-derived ligands have also been studied by a combination of ^{51}V NMR spectroscopy and electrospray ionization mass spectrometry [7]. From the fragmentation pattern, information about the mechanism of decomposition of the complexes was obtained. In particular, it was suggested that
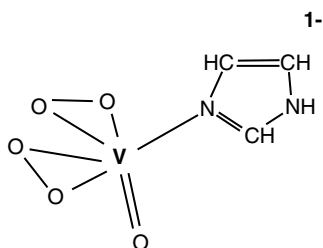
SCHEME 6.1

the *N*-derived heteroligandbisperovanadate, corresponding to the solution structure, fragments through decomposition of the peroxoligands to give a trisoxo intermediate.

Other monodentate ligands such as acetate and ethylamine react quite readily with bisperoxovanadate. Interestingly, ligands such as amino acids and dipeptides also react but, rather than in a bidentate fashion, do so in a monodentate manner, with ligation occurring independently at both the amine and carboxylate functionalities [3,8,9]. Histidine-containing dipeptides do not react to a significant extent in a multidentate fashion with bisperoxovanadate; rather, predominant products derive from reaction with the imidazole group to form monodentate imidazole-derived bisperoxovanadate complexes [8,10,11]. Characterization of complex formation with glycylhistidine by ^{13}C NMR spectroscopy clearly revealed complexation at the imidazole group of the histidine residue [8], as did ^{1}H and ^{13}C NMR spectroscopic studies of the alanylhistidine analogue [11]. With alanylhistidine and other imidazole-containing ligands such as glycylhistidine, histidylglycine, and histidylserine, two complexes have been observed. For the systems that have been studied, there is a significant influence of coordination on the chemical shifts of the two CH protons of the imidazole ring but only a small influence on the chemical shifts of all other protons [8,11].

Table 6.1 summarizes the imidazole ring ^{1}H chemical shifts of the ligand and the influence of coordination on them. As is evident from the ^{1}H NMR data in particular, the formation of the two products is consistent with coordination at each of the chemically distinct nitrogens of the imidazole ring [3]. Table 6.2 gives ^{51}V chemical shifts for a variety of oxobisperoxovanadium complexes with monodentate heteroligands, whereas Table 6.3 provides a number of formation constants for the reaction VL$_2$ + X ⇌ VL$_2$X. Interestingly enough, proton NMR studies of ligands such as glycylhistidine and glycylhistidylglycine have revealed that, in addition to two slowly exchanging complexes, a minor product that undergoes quite rapid equilibration is formed [8]. Significant chemical exchange broadening of the imidazole proton NMR signals of the ligand, but not of the protons of the above two complexes, occurs. This suggests that complexation of the minor product involves an imidazole nitrogen, but that the complex does not derive from either of the complexes. It therefore seems that this complex is an imidazole nitrogen-derived chemically labile compound with another unknown coordination geometry that is quite different from the other complexes.

TABLE 6.1
^{1}H NMR Chemical and Coordination-Induced Shifts for the Two Protons of the Imidazole Ring in Aqueous Oxobisperoxovanadate Histidine-Derived Complexes of VOL$_2$X Stoichiometry

Heteroligand (X)	Chemical Shift (ppm)				Ref.
	[51]V	Imidazole	Product	Coordination-Induced	
Histidine (pH 7.0)	−737	7.20	7.40	0.20	3
	—	8.02	8.12	0.10	—
	−748	7.20	7.45	0.25	—
	—	8.02	8.35	0.33	—
Alanylhistidine (pH 7.45)	−739[a]	—	—	—	11
	−750	7.05	7.29	0.24	—
	—	7.92	8.22	0.30	—
Glycylhistidylglycine (7.0)	−740	7.27	7.37	0.10	8
	—	8.19	8.10	−0.09	—
	−751	7.27	7.40	0.13	—
	—	8.19	8.31	0.12	—

[a] Protein data not reported.

The divanadiotetraperoxo complex of imidazole ($V_2L_4Im^{3-}$) presents an interesting structural problem. The proton NMR spectrum of the imidazole in the complex [3] was consistent with a symmetrical compound. In accord with the proton results, only one ^{51}V NMR signal was found for this compound, despite searching for a second signal [2]. Scheme 6.2 provides two alternatives for the coordination in this complex. A crystal structure [12] of a phosphate derivative has revealed that the phosphate group in $(VL_2O)_2PO_2$ bridges between the two bisperoxovanadate moieties in a manner similar to that depicted in Scheme 6.2a for imidazole. Even more intriguing is the finding that phosphate can provide a bridge between four oxobisperoxovanadate groups $((VL_2O)_4P)$ through the phosphate, with each of the four phosphate oxygens attached to a single oxobisperoxovanadate moiety [13]. Although the structure depicted in Scheme 6.2b represents a structural alternative for the imidazole complex, in the sense that it is based on the known structure of V_2L_4, the complex does not carry the correct charge. However, it might possibly form under basic conditions. The information available is consistent with the structure depicted in Scheme 6.2a, and this structure provides a viable representation of the coordination in the imidazole bis(oxobisperoxovanadate) complex.

Like other amines, pyridines and anilines readily form hetero complexes, and this has provided a means of studying the influence of substituent electronegativity on vanadium chemical shifts. Hammett plots for a number of anilines and pyridines revealed a linear relationship between substituent electronegativity and chemical shifts and showed, for both classes of ligands, that ^{51}V chemical shifts became more

TABLE 6.2
^{51}V Chemical Shifts of Selected Aqueous Oxobisperoxovanadate Heteroligand Complexes of VL$_2$X Stoichiometry

Heteroligand (X)	Chemical Shift (ppm)	Ref.
Monodentate coordination through oxygen		
Water	−765	2, 3, 9
Phenol	−731	8
Acetate	−720	9
Glycine	−712	3
Glycylglycine	−713	9
Prolylglycine	−713	9
Glycylglutamic acid	−716, −720	8
Valylaspartic acid	−714, −719	9
Glycyltyrosine	−715[a], −731[b]	8
Monodentate coordination through nitrogen		
Ammonia	−750	9
Ethylamine	−744	9
Triethylamine	−739	9
Glycine	−758	3
Glycinamide	−749	3
Glycylglycine	−747	9
Prolylglycine	−728, −750	9
Valylaspartic acid	−757	9
Glycyltyrosine	−744	8
Imidazole	−750	2, 9
N-Methylimidazole	−750	3
Glycylhistidine	−742[c], −746[d], −751[c]	8, 10
Histidylglycine	−739[c], −749[c]	8
Aniline	−710	14
Pyridine	−712	3, 14

[a] Chemical shift corresponds to reaction at the carboxylate oxygen.
[b] Chemical shift corresponds to reaction at the phenolate oxygen.
[c] Chemical shifts correspond to reaction at imidazole nitrogens.
[d] Chemical shift corresponds to reaction at the glycyl amine functionality.

positive with increase in electron-withdrawing ability of the ligand [14]. Unfortunately, no correlations with formation constants of the product bisperoxoheteroligand complexes were reported. However, other work has shown there is a linear correlation between the acidity constant of the conjugate acid (pK$_a$) of aliphatic ligands and product formation constants (log K$_f$) [9]. This free energy correlation suggests that the formation of products is highly favored by increased electron-donating ability of the ligand. The linearity encompasses amines, phenols, and carboxylic acids, as displayed in Figure 6.1. Extrapolation of this graph to aliphatic alcohols suggests that, in agreement with observation, they will complex only very weakly at pH 7. On the basis of the graph (Figure 6.1), the formation constant for the reaction VL$_2^-$ + RO$^-$ ⇌ VL$_2$OR^{2-} is large for alcohols (in the order of 2 × 10^5 M^{-1}). However,

3-

a

5-

b
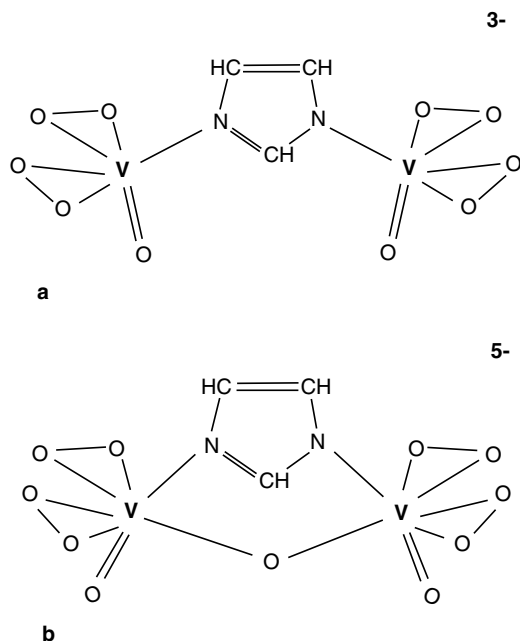
SCHEME 6.2
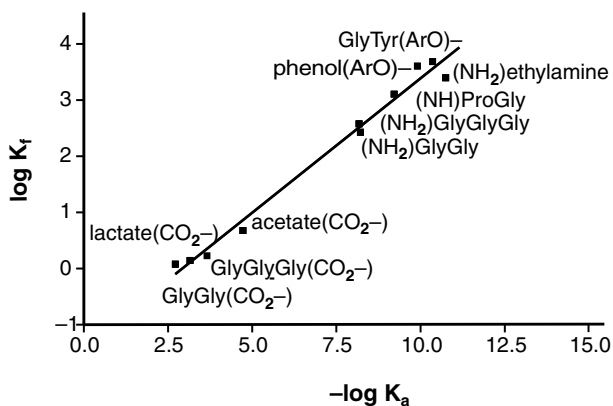
FIGURE 6.1 A graphical representation of the relationship between the pK_a of various ligands and product formation constants for reaction with oxobisperoxovanadate ($VL_2^- + R^{(n-)}$ $VL_2R^{(n+1)-}$). The straight line is defined by the equation $\log K_f = 0.48 \, (-\log K_a) - 1.39$. The information for the graph was taken from Tracey and Jaswal [9], Jaswal and Tracey [8], and, for lactate, Gorzsas and coworkers [53].

TABLE 6.3
Equilibrium Constants for Selected Monodentate Heteroligand Complexes of Bisperoxovanadate[9]

Ligand	Chemical Shift (ppm)	Equilibrium Constant (M^{-1})	Ref.
Equilibrium equation	$VL_2^- + RCO_2^{n-}$	$VL_2X^{(n+1)-}$	
Acetate[1−]	−720	4.8 ± 0.5	9
Lactate[1−]	−721	1.7 ± 0.3	53
Glycine[0]	−712	0.7 ± 0.1	3
Alanine[0]	−714	0.8 ± 0.2	3
Glycylglycine[0]	−713	1.2 ± 0.5	9
Prolylglycine[0]	−713	1.4 ± 0.5	9
Glycyltyrosine[0]	v715	1.1 ± 0.3	8
Equilibrium equation	$VL_2^- + HOArR^{n-}$	$VL_2X^{(n+1)-}$	
Phenol[0]	−731	$(4.9 \pm 0.3) \times 10^3$	8
Glycyltyrosine[0]	−731	$(1.9 \pm 0.2) \times 10^4$	8
Equilibrium equation	$VL_2^- + NH_2R^{n-}$	$VL_2X^{(n+1)-}$	
Ethylamine[0]	−744	$(2.5 \pm 0.3) \times 10^3$	9
N-Methylimidazole[0]	−750	$(6.3 \pm 0.6) \times 10^3$	3
Pyridine[0]	−712	$(1.0 \pm 0.2) \times 10^2$	3
Glycine[1−]	−758	$(4.0 \pm 0.5) \times 10^3$	3
Alanine[1−]	−766	$(3.6 \pm 0.5) v 10^3$	3
Glycylglycine[1−]	v747	$(2.7 \pm 0.4) \times 10^2$	9
Glycyltyrosine[1−]	−744	$(2.4 \pm 0.7) \times 10^2$	8
Alanylhistidine[0]	−750[a]	$(1.6 \pm 0.3) v 10^3$	11
Alanylhistidine[0]	−739[a]	$(2.0 \pm 0.4) v 10^2$	11

[a] Products correspond to reaction at imidazole nitrogens.

the concentration of the alkoxide is exceedingly low so that overall product formation is disfavored. Similar correlations have also been found for reactions of vanadate, itself, with alkyl alcohols and with phenols (Section 3.1), but the dependence of product formation on ligand acidity is not as pronounced as found for the peroxovanadates.

6.1.2 COMPLEXATION OF OXOBISPEROXOVANADATE BY MULTIDENTATE HETEROLIGANDS

Although amino acids and related compounds frequently react in a monodentate fashion with bisperoxovanadate, they can react in a bidentate manner, but the products are often not bisperoxo complexes; rather, one peroxide is eliminated in the condensation reaction. This is not necessarily true for all conditions, and bisperoxo-heterobidentate-ligand complexes are known, although in the solid state where a number of x-ray structures have been reported. In this case, one coordination site is an apical position, and a pentagonal bipyramidal product is formed, in the fashion of the oxalato [15] and picolinato (pyridine-2-carboxylato) [16] complexes, as represented diagrammatically in Scheme 6.3. There seems to be no detailed study of these and similar complexes in aqueous solution. Preliminary studies [17,18] of the
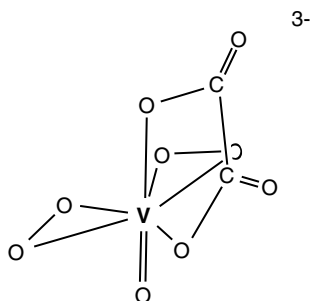
SCHEME 6.3

picolinato complex have shown that the species distribution tends to the picolina-tooxobisperoxovanadate under neutral and moderately basic conditions with twofold excess peroxide in solution. Whether or not this complex has bidentate coordination under the conditions of the study is not known. This coordination is assumed in investigations of the catalytic properties of this complex, where potentiometric studies provided a value of 4.41 ±0.02 for the pK_a of the monoanionic complex [19].

There is little evidence available to show that bidentate coordination of bisper-oxovanadate by a heteroligand is retained on dissolution of the complex in aqueous solution, although studies with alanine have shown, in addition to the *N*- and *O*-derived products already discussed, there is formation of two additional products, both apparently being in rapid exchange. Somewhat surprisingly, the two fast exchanging complexes were found to require both the amino and carboxylato for their formation [3]. For the picolinato complex, the [51]V chemical shift of –745 ppm lies in the range of chemical shifts of bisperoxo monodentate heteroligand complexes, as seen in Table 6.2. This chemical shift is to higher field than typically observed for carboxylate-derived complexes (–712 to –720 ppm) but, although within the range of amino-derived complexes, is significantly higher than that of the pyridine complex (–712 ppm). This suggests (but certainly does not prove) that, in aqueous solution, the bisperoxovanadate coordinates the picolinato ligand in a bidentate fashion. Study of coordination-induced ^{13}C chemical shifts would, perhaps, go a long way to providing an answer. Certainly, however, the propensity is toward elimination of one peroxo group to give rise to a monoperoxovanadate with the heteroligand having bidentate or higher coordination, and with the picolinato ligand, these are the predominant compounds under acidic conditions [17,18].

There is evidence from Raman studies that oxalate coordinates in a bidentate manner without elimination of a peroxo group [6]. Possibly here, as for the picolinate complex, the question of the coordination could be more definitively answered by observation of ^{13}C coordination-induced NMR chemical shifts. The x-ray structure for the oxalate complex shows that the two VO_{ox} bond distances are very different. The VO distance to the equatorial oxalato oxygen is 2.060(4) Å compared to 2.251(4) Å to the apical oxygen [15]. Similarly long distances are found in the picolinato complex (VO_{pic} 2.290 Å [16]) and other complexes [20]. These distances are indicative of relatively weak bonds to the apical oxygens, and dissociation of that bond

from the vanadium center to form a monodentate complex is quite possible. Detailed aqueous solution studies to determine the relative stability of various oxalate complexes have not been made.

6.2 REACTIONS OF MONOPEROXOVANADATES WITH HETEROLIGANDS

A number of x-ray structures of monoperoxoheteroligand complexes of vanadate have been reported. The heteroligands have included picolinate, dipicolinate, dipeptides, and a number of α-hydroxycarboxylate. Solution NMR studies have been carried out for several of these systems, and various solution products described. Table 6.4 gives the ^{51}V NMR chemical shifts for a number of products that have been studied. This table covers a variety of types of complexes, and the chemical shifts range over about 100 ppm, from about –580 to –680 ppm.

6.2.1 COMPLEXATION BY AMINO ACIDS, PICOLINATE, AND DIPEPTIDES

Picolinic acid forms both mono- and bisligand heterocomplexes with monoperoxovanadate. However, for amino acids, only bisheteroligand complexes have been reported. Blocking of either the amine or carboxylate groups prevented formation of products. The amino acid-derived bisheteroligand complexes are of two different forms. In the less favored form, one of the heteroligands is complexed in a monodentate fashion through the nitrogen functionality [3]. A second form could be a similar complex, where the second ligand is complexed through a carboxylate oxygen rather than the nitrogen. However, an alternative is that in the predominant complex, the second heteroligand is also bidentate, as depicted in Scheme 6.4. This is a coordination mode found for the bispicolinate complex in the solid state [21] and also seen for the corresponding bisoxalate [22] and the dipyridinate picolinato mixed ligand complex [20]. Although this clearly is a viable solution coordination mode for these ligands, solution studies of the amino acid complexes have shown that the major product has a pK_a and thus must have an ionizable proton. A structure of the monopicolinate complex has shown coordination of two water molecules [23], so in the bisamino acid complex, monodentate coordination of the second amino acid together with a single water is quite feasible. This suggests coordination modes similar to that displayed in Scheme 6.5 are adopted by monoperoxovanadate complexes.

Amino acids (L) have also been shown to form a dimeric-type complex of $(VO(OO)_2L)_2(OO)L$ coordination, for which it has been proposed that one peroxo group and the carboxylate group of one amino acid form a bridge between the two vanadium nuclei, after the fashion displayed in Scheme 6.6 [24]. The complex was found not to retain its integrity when dissolved in aqueous solution.

Dipeptides complex in a trident fashion to form oxoperoxodipeptido products. The rate of complexation by these ligands is quite slow. Even the vanadium-catalyzed disproportionation of hydrogen peroxide occurs quickly when compared to the rate of complexation by dipeptides. The formation of the dipeptide complex is interesting, in the sense that the ligand is tridentate, and complex formation involves loss of a

TABLE 6.4
**^{51}V NMR Chemical Shifts of Selected Aqueous
Oxoperoxovanadate Heteroligand (V:L:X) Complexes**

Heteroligand	Stoichiometry (V:L:X)	Chemical Shift (ppm)	Ref.
Picolinic acid	VLX^0	–600	17, 18
	VLX$^{1-/2-}$	–658	17
	VLX$_2^{1-}$	–611, –616, –632[a]	17, 18
Glycolic acid	VLX	–574	37
	V$_2$L$_2$X$_2$	–583	37
Lactic acid	V$_2$L$_2$X$_2$	–596	17, 40
	V$_2$LX$_2$	–521, –592[b]	17
	V$_2$LX$_2$	–519, –590[b]	17
Mandelic acid	V$_2$L$_2$X$_2$	–588	37
Glycine	VLX$_2^{1-/2-}$	–662	3
	VLX$_2^{1-/2-}$	–674	3
Glycylglycine	VLX^{1-}	–649[c]	8, 25
Phenol	VLX^{2-}	–605	8
Glycyltyrosine	VLX^{2-}	–604	8

[a] Three signals presumably corresponding to three structural isomers.

[b] Two compounds, each with two signals.

[c] A number of dipeptide complexes show chemical shifts for VLX derivatives within two or three separate ranges: –620 to –632 ppm; –644 to –657 ppm; and –663 to –675 ppm (Reference 3).

1-
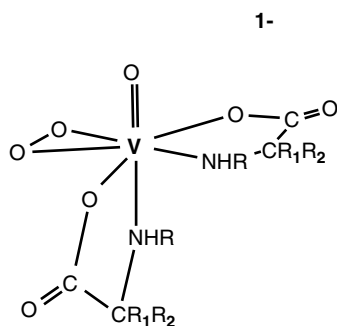
Chelate complexation through both amine
and carboxylate

SCHEME 6.4

proton from the amide NH of the peptide linkage (Scheme 6.7). NMR studies have established this for the reaction in aqueous solution [8], whereas the x-ray structure clearly shows this coordination mode in the solid [25]. Other ligands such as dipicolinate form complexes that are structurally similar to those of the dipeptide complexes [26,27]. The x-ray structure of the dipeptide complex suggests that two isomeric forms of the complexes should be observed if the structure is retained in
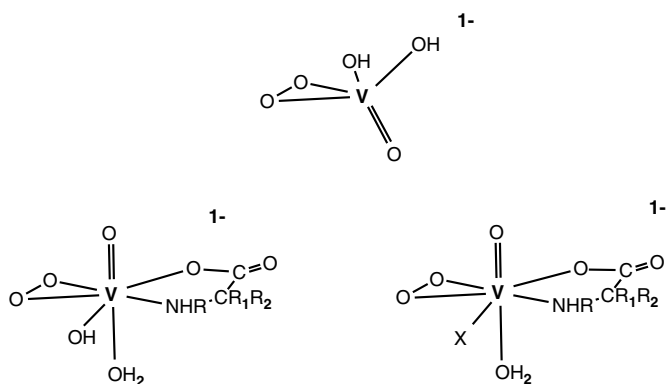
X-ligand complexation through amine, N, and carboxylate, O

SCHEME 6.5

SCHEME 6.6

a

b
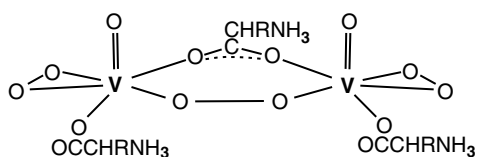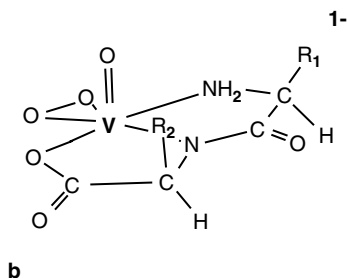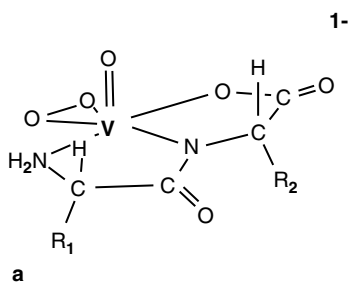
SCHEME 6.7

aqueous solution. As depicted in Scheme 6.7, the isomers derive from the presence of the sidechain of the amino acid residues and result from an end-for-end rotation of the ligand that moves the sidechain from being exo (Scheme 6.7a) to the V = O to being in an endo (Scheme 6.7b) orientation. Two isomers would be expected from dipeptides such as valylglycine, tryptophylglycine, tryptophyltryptophan, glutamyl-glutamate, and others. On the other hand, glycylglycine would be expected to form only one isomer. In line with expectations, vanadium NMR spectroscopy for a number of complexes has shown the occurrence of isomeric forms. Table 6.5 gives ^{51}V NMR chemical shifts for a variety of dipeptidomonoperoxovanadates.

If the dipeptides have a sidechain suitable for chelation to monoperoxovanadate, then it is possible to observe more than one type of product complex. Table 6.5 gives the ^{51}V NMR chemical shifts of products observed for several such systems. The complexes formed with glycylthreonine provide a good example of such behavior [8]. Under neutral to slightly acidic conditions, two complexes (–632 ppm, –650 ppm) arising from chelation at the *N*-terminal nitrogen, the amide nitrogen and carboxylate oxygen, are observed. Upon raising the pH, two additional signals (–637 ppm, –656 ppm) are observed. The two sets of signals are readily assigned to involvement of the carboxylate in the product chelate (–632 ppm, –650 ppm) and replacement of the carboxylate oxygen by a hydroxyl oxygen (–637 ppm, –656 ppm). The different proton requirements for product formation readily distinguish the two types of complexes. Protons are given up when reaction occurs at the hydroxyl group, so such products are doubly negative because the uncomplexed carboxylate group also carries a negative charge. Except for the change in charge state, there seems little reason to suspect a structure that is different from those suggested in Scheme 6.7. Similar types of products are observed when dipeptides are complexed by vanadate (see Section 4.6.2).

It is interesting that the study of the alanylserine/monoperoxovanadate system showed ^{51}V NMR signals corresponding to only three product complexes (Table 6.5 [28]) rather than the four expected from the above arguments. Also, it was found that the product corresponding to a –659 ppm NMR signal had a pK_a. The products corresponding to Scheme 6.7 would not be expected to have a pK_a. However, if the –569 ppm signal is a composite signal deriving, in the one case, from complexation at carboxylate oxygen and, in the second case, from complexation at the hydroxyl oxygen, then the different proton stoichiometries and the subsequent pattern of dependence of overall product formation on pH could easily be misinterpreted as a product pK_a. It seems quite possible that such an error has been made. If so, products corresponding to reaction at carboxylate (singly negative complexes) have chemical shifts of –656 and –659 ppm, whereas products deriving from reaction at the hydroxyl oxygen (doubly negative complexes) have chemical shifts of –659 and –677 ppm.

Histidine-containing dipeptides show a more complex chemistry than found for the dipeptides discussed above. Three complexes of monoperoxovanadate are formed, two of which have the characteristics of the complexes described above. The clearly obvious difference of the third type of complex from the others, as exemplified in Table 6.5, is that they have a pK_a. The pK_a values that have been measured are significantly different from that of the imidazole of the histidine

TABLE 6.5
^{51}V NMR Chemical Shifts of Selected Aqueous Oxoperoxovanadate Dipeptide (V:L:X) Complexes

Heteroligand	^{51}V Chemical Shift (ppm)	pK$_a$	Ref.
Glycylglycine	–649	—	8
Valylglycine	–643, 657	—	8
Glycyltryptophan	–620, –651	—	8
Tryptophylglycine	–652, –656	—	8
Tryptophyltryptophan	–623, –648	—	8
Tryptophyltyrosine	–628, –644	—	8
Glycylthreonine	–632, –650[a]	—	8
	–637, –656[a]	—	8
Alanylserine	–656	—	28
	–659[b], –677[c]	—	—
Glycylglutamate	–625, –647, –651	—	8
Alanylhistidine	–627, –v660	—	11
	–627 → –683[d]	5.92	—
Glycylhistidine	–650	—	8
	–649 → –673[d]	6.9	—
Hiystidylglycine	–651	—	8
	–664 → –675[d]	6.2	—
Histidylserine	–652	—	8
	–660 → –663[d]	—	—

[a] Complexes at –632 and –650 ppm have been assigned to chelation involving the threonine carboxylate group (single negative charge), whereas the –637 and –656 ppm signals have been assigned to hydroxyl-derived chelates (doubly negative charge), Reference 8.

[b] It seems quite likely that the assignment of this chemical shift to a single product should be revised to a chemical shift corresponding to two overlapped signals corresponding to complexes of singly and doubly negative charges (see text).

[c] This chemical shift corresponds to a complex carrying a doubly negative charge so probably derives from chelation through the hydroxyl oxygen rather than through a carboxylate oxygen.

[d] pH-dependent limiting chemical shifts going from low to high pH.

sidechain. For instance, the pK$_a$ of alanylhistidine (imidazole) is 6.72, whereas the pK$_a$ of the complex in question is 5.92 [11]. Only one complex with a pK$_a$ has been reported for the ligand systems that have been studied. This suggests that only one type of such a complex is formed. Additionally, blocking the *N*-terminal position prevents product formation. An alternative arrangement that has the peptide nitrogen, the *C*-terminal carboxylate oxygen, and imidazole nitrogen available for complexation, as in glycylhistidylglycine, does not give rise to products. Taken together, these support an assignment of these compounds to tridentate complexes with coordination to the *N*-terminal amine, the peptide nitrogen, and the α-nitrogen of the imidazole ring, somewhat as depicted in Scheme 6.8. This leaves an imidazole *N*
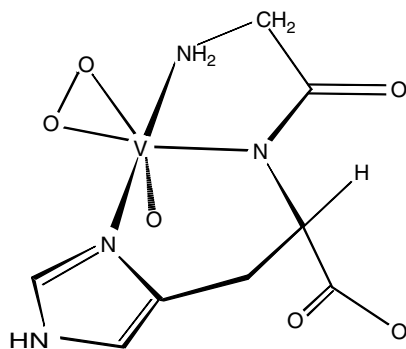
SCHEME 6.8

that can undergo a protonation/deprotonation reaction to account for the pK_a observed for this complex. Imidazole, by itself, has been shown to react with monoperoxovanadate, but only very weakly [2].

An interesting facet of the reaction of dipeptides in peroxovanadate solution is their ability to effectively prevent the vanadium-catalyzed disproportionation of hydrogen peroxide to water and oxygen. It makes sense that formation of any complex will depopulate alternative reaction pathways and thus change, for instance, the overall rate of a chemical reaction. In the case with dipeptides, it has been found that the rate of vanadium-catalyzed disproportionation in the absence of dipeptides is much faster than the rate of formation of the dipeptide monoperoxovanadate complex. Despite this, little or no decomposition of hydrogen peroxide occurs, even after extended periods of time [8,9,17]. These findings suggest that an intermediate peroxovanadium complex lying on the decomposition pathway is effectively trapped by the dipeptide ligand and progress along this path prevented. The trapped intermediate then reverts back to its starting components, with perhaps some of it converting to the peptidomonoperoxovanadate complex. Alternatively, the observed peptide complex may well form through an independent reaction pathway. Finally, however, the formation of the peptide product locks the vanadium into a complex that does not promote hydrogen peroxide lability.

It is very unlikely that the disproportionation is stopped only by peptide complexes; rather, it seems probable that other ligands will behave in a similar fashion. The efficiency of inhibition apparently is quite dependent on whether the ligand is bidentate or tridentate. Amino acids, for instance, are not very effective when compared to dipeptide ligands.

6.2.2 COMPLEXATION BY α-HYDROXYCARBOXYLIC ACIDS

The reactions of α-hydroxycarboxylic acids with monoperoxovanadate are strikingly similar to those with vanadate itself. The predominant products are dimers that have the characteristic $[VO]_2$ cyclic core. Structurally, the major difference between the two types of complexes is simply that one of the oxo groups (Scheme 6.9a) is replaced by a peroxo group to give a structure similar to that depicted in Scheme
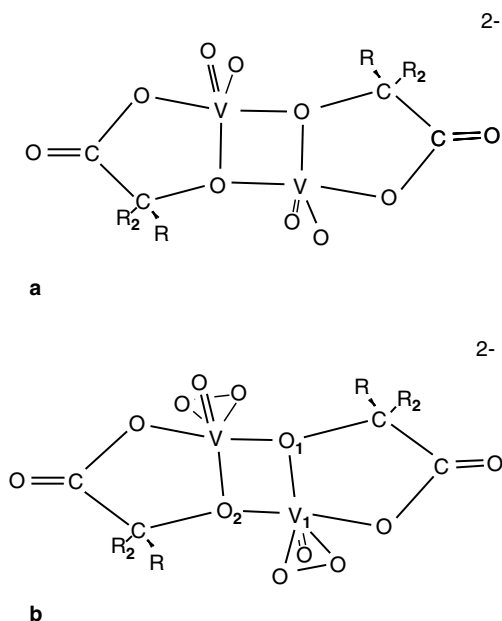
SCHEME 6.9

6.9b. In the case of chiral ligands such as R and S lactate, x-ray studies have revealed that the central $[VO]_2$ core structure can be nonplanar when there is an S,S (R,R) ligand combination of ligands but be planar when the combination is R,S [29]. With an achiral ligand, such as glycolic acid, the central core is planar [30]. This latter is not a necessary requirement because, in principle, the structural arrangement can be such that the two oxo groups of the dimer are in a cis (nonplanar core) arrangement or in a trans (planar core) arrangement about the $[VO]_2$ center. The VOV angles within the core typically are within the range 108 to 110°, whereas the corresponding OVO angles are in the order of 69 to 71°. These angles are essentially the same as those of the corresponding oxovanadate complexes (see, for instance, Table 4.1).

As clearly seen in Scheme 6.9, there are two distinct types of VO bonds in the core region. Bonds of the type V_1–O_1 tend to be shorter than those of the type V_1–O_2, often by up to 0.10 Å or more, though smaller differences of 0.02 to 0.04 Å are more generally found. Table 6.6 gives a selection of such VO bond lengths obtained from x-ray diffraction studies. Of course, it is the V_1–O_2 type bonds that break when dissociation to the monomer occurs.

If the α-hydroxylic acid has a functional group attached, as in malic acid ($HO_2CCH(OH)CH_2CO_2H$), the dependent CH_2CO_2H arm can also complex, but in a nonbridging fashion. However, this is a pH-dependent phenomenon, and the malic acid can function as either a bidentate (pH about 4) or tridentate ligand (pH about 7), as suggested by crystallization of the compound from solution [31]. Such a change in structure in aqueous solution has not been verified from solution studies.

TABLE 6.6
VO Bond Lengths and Angles in the Cyclic $[VO]_2$ Core of Selected Dimeric Monoperoxovanadate α-Hydroxycarboxylato Complexes

Ligand	VO_a	VO_b	$\angle VOV$	$\angle OVO$	Ref.
Planar $[VO]_2$					
Glycolato	1.923(4)	2.011(4)	110.3(2)	69.7(2)	30
R,S-Lactato	1.927(6)	2.025(6)	110.0(3)	70.0(3)	29
R,S-Malato	2.009(1)	2.030(1)	108.1(1)	71.9(1)	33
	2.005(2)	2.025(2)	107.7(1)	72.3(1)	31
	1.986(2)	2.021(2)	108.6(1)	71.4(1)	31
Nonplanar $[V_1O_1V_2O_2]$					
S,S-Lactato	1.918(6)	2.049(6)	109.3(3)	69.8(3)	29
	1.927(6)	2.037(5)	109.4(3)	69.3(2)	29
S,S-Mandelato	1.975(4)	2.035(3)	109.92(16)	69.25(14)	38
	1.967(3)	1.990(4)	108.44(150	70.32(14)	38

In the solid, the $[VO]_2$ core is retained in both complexes, and the vanadium coordination simply goes from six to seven [32,33]. Interestingly enough, a vanadium(IV) complex of citrate shows a similar pH-dependent phenomenon, and here also a cyclic $[VO]_2$ core is retained [34]. Unlike the oxoperoxovanadium(V) malato complex, the oxoperoxo complex of citric acid ($HO_2CC(OH)(CH_2CO_2H)_2$), a more complex α-hydroxylic acid with two CH_2CO_2H arms, shows bridging from one vanadium center to the other [35]. Such bridging is not necessary, and a dimeric complex in which no bridging occurs has also been studied [36]. In both types of complexes, the $[VO]_2$ core is retained.

It has been proposed that there is an additional oxo bridging between the two vanadiums of the dimeric glycolato complex [37]. Although x-ray diffraction studies have shown there can be water bridging for crystalline complexes with mandelic acid [38] and tartaric acid [39], the VO bonds are exceedingly long (2.475(2) Å and 2.398(6) Å, respectively), and it seems unlikely that such bridging would be retained in aqueous solution. Certainly with mandelic acid, dimeric complexes with or without the additional bridging group are formed [38]. No O-17 NMR signal for such a bridging oxygen was detected in the glycolic acid study [40]. It seems quite likely that the structures found in the solid state for glycolate [30], lactate [29], malate [31], and other ligands are maintained in aqueous solution (Scheme 6.9b). A monomeric form of the glycolate, lactate, and malate complexes has been reported for acidic conditions. It seems unlikely that the dimer simply splits apart to give the monomer: more probably, dissociation of the dimer is accompanied by protonation and incorporation of water. Both mono- and bis(aquo)oxoperoxocarboxylato complexes have been suggested [37].

6.3 OXYGEN TRANSFER REACTIONS OF PEROXOVANADATES

The efficacy of peroxovanadium complexes as oxidative catalysts is very well known. These compounds promote a variety of one- and two-electron transfer reactions [41–43]. Many of the applications have been directed toward synthesis in organic chemistry. This is not surprising, because peroxovanadate complexes react with substrates ranging from alkyl hydrocarbons to hydroxylic, olefinic, and aromatic compounds. They carry out hydroxylation, expoxidation, and sulfoxidation reactions. These reactions frequently are stereospecific and regioselective, and the chemistry can be directed by choices for a heteroligand. Indeed, with appropriate chiral heteroligands, asymmetric induction can be promoted. Peroxovanadates can also oxidize halides, and it is this reaction that characterizes the vanadium-dependent haloperoxidases, where peroxovanadium is an essential cofactor for vanadium-dependent haloperoxidases activity. It is, therefore, not surprising that both these enzymes and the peroxovanadates catalyze many similar reactions. As a consequence, there is much effort put towards efficient functional models of the haloperoxidase active site (see Section 10.4.2).

Olefins undergo a two-step oxidative process, with the first step leading to an epoxide that, in the presence of excess oxidant, subsequently is cleaved to afford aldehydes or ketones, dependent on the position of the olefinic bond. Oxidative reactions by peroxovanadates tend to be retarded by protic solvents such as water or methanol. For instance, oxidation of norbornene by picolinatooxomonoperoxovanadate in acetonitrile affords 22% of the product epoxide in 9 min. After 120 min in methanol solvent, only 1.8% yield was obtained. In dichloromethane, even cyclohexane is oxidized faster than this, giving 4% cyclohexanol and 9% cyclohexanone in 120 min, whereas benzene in acetonitrile yields 56% of phenol [23].

6.3.1 HALIDE OXIDATION

Peroxovanadates based on numerous complexes obtained from a variety of types of heteroligands are effective oxidants. However, the properties of the heteroligand can directly influence the mechanism of oxidation. The ligands based on substituted amino acids such as N-(2-hydroxyethyl)iminodiacetic acid and N,N-bis(2-pyridylmethyl)glycine provide an example of ligands that allow effective oxidation of halides and halogenation of suitable substrates via a two-electron transfer process. The ligands are tetradentate and give rise to oxoperoxoligand products of approximately pentagonal bipyramidal geometry, which appear to be stable in aqueous solution under the conditions under which they were studied [44]. Interestingly, as suggested by the use of methanol mentioned above, the compounds are ineffective oxidants of bromide in water but rapidly oxidize iodide and bromide in acidified acetonitrile. It was suggested that this lack of reactivity arises from an inability to protonate the complex under conditions where it would remain intact. If a suitable organic substrate is available, these compounds can catalyze halogenation according to the reaction cycle of Equation 6.1 [44].

$$VO_2L + H_2O_2 \rightarrow VO(O_2)L + H_2O \qquad (6.1)$$

$$VO(O_2)L + X^- + H^+ \rightarrow VO_2L + XOH$$

$$RH + XOH \rightarrow RX + H_2O$$

$$VO_2L + H_2O_2 \rightarrow VO(O_2)L + H_2O$$
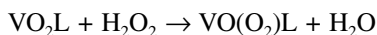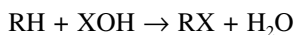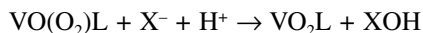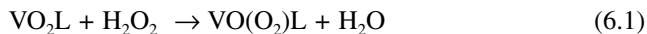
Despite the fact that protic solvents generally retard or even effectively prevent the oxidative process by peroxovanadate, binuclear peroxo complexes do catalyze the oxidation of bromide and do so in an efficient manner. Under conditions of acidic hydrogen peroxide with catalytic amounts of ammonium vanadate, the rate of bromide oxidation is second order in V(V) and shows a complicated dependence on hydrogen peroxide concentration. Analysis of the results in terms of various peroxo complexes in solution suggested the oxidation was catalyzed by a dimeric product such as $(VO)_2(O_2)_3$ [45]. It seems likely that the oxidant is a peroxo-bridged complex, perhaps $(O_2)OVOOVO(O_2)$ or $(O_2)OVO(OO)VO(O_2)$, for which both the peroxo and oxo groups bridge. A structurally similar peroxo-bridged compound in which each vanadium has a glycine as a heteroligand has been found to be a very powerful oxidant of bromide in aqueous solution, even without acidifying the medium [46]. Other similar amino acid-based peroxo complexes function in an analogous manner, whereas monomeric bisperoxovanadates with an amino acid heteroligand do not oxidize under similar conditions [24]. These binuclear complexes are also effective bromination agents of aromatic substrates such as aniline and *o*-methoxyphenol.

A binuclear tetraperoxo complex, $(O_2)_2OVOOVO(O_2)H_2O$, can be rather readily prepared in the crystalline state, where it is stable for extended periods of time. The structure of this compound is unique. As depicted in Scheme 6.10, the two oxygens of the bridging peroxo group are bound to one vanadium center and simultaneously one oxygen is bound to the second vanadium. Surprisingly, the asymmetric character of this complex persists for some time in aqueous solution [47]. It is reasonable to expect that the bridging peroxo group in such a complex would be activated towards oxidative reactions. This type of bridging could well occur as a transient structure in other peroxo-bridging dimeric complexes and be involved in their oxidative reactions.
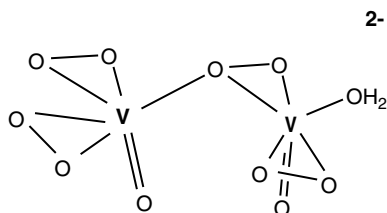
SCHEME 6.10

6.3.2 SULFIDE OXIDATION

Studies of the oxidation of organic sulfides with amino acid-derived ligands in acetonitrile revealed very little difference between the mechanism of their oxidation and that of halides, except for one major exception. Despite the fact that acid conditions are still required for the catalytic cycle, hydroxide or an equivalent is not produced in the catalytic cycle, so no proton is consumed [48]. As a consequence, there is no requirement for maintenance of acid levels during a catalyzed reaction. Peroxo complexes of vanadium are well known to be potent insulin-mimetic compounds [49,50]. Their efficacy arises, at least in part, from an oxidative mechanism that enhances insulin receptor activity, and possibly the activity of other protein tyrosine kinases activity [51]. With peroxovanadates, this is an irreversible function. Apparently, there is no direct effect on the function of the kinase, but rather there is inhibition of protein tyrosine phosphatase activity. The phosphatase regulates kinase activity by dephosphorylating the kinase. Oxidation of an active site thiol in the phosphatase prevents this down-regulation of kinase activity. Presumably, this sulfide oxidation proceeds by the process outlined above.

Both nucleophilic and electrophilic reactions are known, and the reaction sequence can be directed by a suitable choice for a heteroligand [41,52]. As suggested by Scheme 6.11a, the ability of the heteroligand to direct electrophilic or nucleophilic attack by the peroxocomplex can provide an important tool in oxidative reactions, where selectivity of action is required. A second mode of electrophilic reaction chemistry is available through attack of sulfur electrons at the vanadium center to give a transient anion/cation radical pair via formation of V(IV) and $S\cdot^+$ (Scheme 6.11b).

Although oxidative catalysis by monoperoxovanadates is slow in protic solvents, it seems that this is less true for the bisperoxo complexes, and they can be much more effective oxidants. An example of this is provided by the oxidation of Co(III) thiolate (($en)_2Co(SCH_2CH_2NH_2)$), where the rate of oxidation by a bisperoxide is about 1000 times that of a monoperoxide. However, like the monoperoxides, the bisperoxo complexes are better oxidents when protonated. For instance, $HVO(O_2)_2(pic)^{1-}$ oxidizes the above sulfide substrate 7 times faster than does $VO(O_2)_2(pic)^{2-}$ [19].

a nucleophilic oxidation / electrophilic oxidation

b electrophilic oxidation via radical cation/anion pairs

SCHEME 6.11

REFERENCES

1. Paul, P.C. and A.S. Tracey. 1997. Aqueous interactions of vanadate and peroxovanadate with dithiothreitol. Implications for the use of this redox buffer in biochemical investigations. *J. Biol. Inorg. Chem.* 2:644–651.

2. Andersson, I., S.J. Angus-Dunne, O.W. Howarth, and L. Pettersson. 2000. Speciation in vanadium bioinorganic systems 6. Speciation study of aqueous peroxovanadates, including complexes with imidazole. *J. Inorg. Biochem.* 80:51–58.

3. Tracey, A.S. and J.S. Jaswal. 1993. Reactions of peroxovanadates with amino acids and related compounds in aqueous solution. *Inorg. Chem.* 32:4235–4243.

4. Keramidas, A.D., W. Miller, O.P. Anderson, and D.C. Crans. 1997. Vanadium(V) hydroxylamido complexes: Solid state and solution properties. *J. Am. Chem. Soc.* 119:8901–8915.

5. Drew, R.E. and F.W.B. Einstein. 1972. The crystal structure of ammonium oxodiperoxoamminevanadate(V). *Inorg. Chem.* 11:1079–1083.

6. Schwendt, P. and M. Pisarcik. 1990. Raman spectral study on the structure of vanadium(V) oxodiperoxo complexes in aqueous solution. *Spectrochim. Acta* 46A:397–399.

7. Bortolini, O., M. Carraro, V. Conte, and S. Moro. 1999. Histidine-containing bisperoxovanadium(V) compounds: Insight into the solution structure by an ESI-MS and [51]V-NMR comparative study. *Eur. J. Inorg. Chem.* 1489–1495.

8. Jaswal, J.S. and A.S. Tracey. 1993. Reactions of mono- and diperoxovanadates with peptides containing functionalized side chains. *J. Am. Chem. Soc.* 115:5600–5607.

9. Tracey, A.S. and J.S. Jaswal. 1992. An NMR investigation of the interactions occurring between peroxovanadates and peptides. *J. Am. Chem. Soc.* 114:3835–3840.

10. Guevara-Garcia, J.A., N. Barba-Behrens, R. Contreras, and G. Mendosa-Diaz. 1998. Bis-peroxo-oxovanadium(V) complexes of histidine-containing peptides as models for vanadium haloperoxidases. In *Vanadium Compounds: Chemistry, Biochemistry and Therapeutic Applications*. A.S. Tracey and D.C. Crans (Eds). American Chemical Society, Washington, D.C. 126–35.

11. Schmidt, H., I. Andersson, D. Rehder, and L. Pettersson. 2001. A potentiometric and [51]V NMR study of the aqueous $H^+/H_2VO_4^-/H_2O_2$ /L-α-alanyl-L-histidine system. *Chem. Eur. J.* 7:251–257.

12. Schwendt, P., J. Tyrselova, and F. Pavelcik. 1995. Synthesis, vibrational spectra, and single-crystal x-ray structure of the phosphato-bridged dinuclear peroxovanadate $(NH_4)_5[V_2O_2(O_2)_4PO_4]\cdot H_2O$. *Inorg. Chem.* 34:1964–1966.

13. Schwendt, P., A. Oravcova, J. Tyrselova, and F. Pavelcik. 1996. The first tetranuclear vanadium(V) peroxo complex: Preparation, vibrational spectra and x-ray crystal structure of $K_7[V_2O_4(O_2)_8(PO_4)]$ $9H_2O$. *Polyhedron* 15:4507–4511.

14. Conte, V., F. Di Furia, and S. Moro. 1995. Studies directed toward the prediction of the oxidative reactivity of vanadium peroxo complexes in water. Correlations between the nature of the ligands and the [51]V-NMR chemical shifts. *J. Mol. Catal. A* 104:159–169.

15. Begin, D., F.W.B. Einstein, and J. Field. 1975. An asymmetrical coordinated diperoxo compound. Crystal structure of $K_3[VO(O_2)_2(C_2O_4)]\cdot H_2O$. *Inorg. Chem.* 14:1785–1790.

16. Shaver, A., J.B. Ng, D.A. Hall, B. Soo Lum, and B.I. Posner. 1993. Insulin-mimetic peroxovanadium complexes: Preparation and structure of potassium oxodiperoxo(pyridine-2-carboxylato)vanadate(V), $K_2[VO(O_2)_2(C_5H_4NCOO)]\cdot 2H_2O$, and potassium oxodiperoxo(3-hydroxypyridine-2-carboxylato)vanadate(V), $K_2[VO(O_2)_2 (OHC_4H_3 NCOO)]\cdot 3H_2O$, and their reactions with cysteine. *Inorg. Chem.* 32:3109–3113.

17. Pettersson, L., I. Andersson, and A. Gorzsas. 2003. Speciation in peroxovanadium systems. *Coord. Chem. Rev.* 237:77–87.

18. Conte, V., F. Di Furia, and S. Moro. 1994. [51]V NMR investigation on the formation of peroxo vanadium complexes in aqueous solution: Some novel observations. *J. Mol. Catal.* 94:323–333.

19. Ghiron, A.F. and R.C. Thompson. 1990. Comparative kinetic study of oxygen atom transfer reactions of diperoxo and monoperoxo complexes of oxovanadium(V) in aqueous solution. *Inorg. Chem.* 29:4457–4461.

20. Szentivanyi, H. and R. Stomberg. 1983. The crystal structure of (2,2'-bipyridine)oxoperoxo(pyridine-2-carboxylato)vanadium(V) hydrate, [VO(O$_2$)(C$_5$H$_4$NCOO)(C$_{10}$H$_8$N$_2$)] ·H$_2$O, at –100˚C. *Acta Chem. Scand.* A37:709–714.

21. Sergienko, V.S., M.A. Porai-Koshits, V.K. Borzunov, and A.B. Illyukhin. 1993. Crystal structure of three VO(O$_2$)$^+$ compounds with pyridine-2-carboxylate ions and *o*-phenanthroline. Structural features of pseudooctahedral vanadium(V) oxoperoxo complexes. *Koord. Khim.* 19:767–781.

22. Stomberg, R. 1986. The crystal structures of potassium bis(oxalato)oxoperoxovanadate(V) hemihydrate, K$_3$[VO(O$_2$)(C$_2$O4)$_2$]·1/2H$_2$O, and potassium bis(oxalato)dioxovanadate(V) trihydrate, K$_3$[VO$_2$(C$_2$O$_4$)]·3H$_2$O. *Acta Chem. Scand.* A 40:168–176.

23. Mimoun, H., L. Saussine, E. Daire, M. Postel, J. Fischer, and R. Weiss. 1983. Vanadium(V) peroxo complexes. New versatile biomimetic reagents for epoxidation of olefins and hydroxylation of alkanes and aromatic hydrocarbons. *J. Am. Chem. Soc.* 105:3101–3110.

24. Sarmah, S., D. Kalita, P. Hazarika, R. Borah, and N.S. Islam. 2004. Synthesis of new dinuclear and mononuclear peroxovanadium(V) complexes containing biogenic coligands: A comparative study of some of their properties. *Polyhedron* 23:1097–1107.

25. Einstein, F.W.B., R.J. Batchelor, S.J. Angus-Dunne, and A.S. Tracey. 1996. A product formed from glycylglycine in the presence of vanadate and hydrogen peroxide: The (glycylde-*N*-hydroglycinato-K^3N^2,N^N,O^1)oxoper oxovanadate(V) anion. *Inorg. Chem.* 35:1680–1684.

26. Wieghardt, K. 1978. Preparation and characterization of dipicolinatovanadium(V) complexes. Kinetics and mechanism of their reactions with hydrogen peroxide in acidic media. *Inorg. Chem.* 17:57–64.

27. Drew, R.E. and F.W.B. Einstein. 1973. Crystal structure at –100˚ of ammonium oxoperoxo(pyridine-2,6-dicarboxylato)vanadate(V) hydrate, NH$_4$[VO(O$_2$)(H2O)(C$_5$H$_3$N(CO$_2$)$_2$)·xH2O (x ≈ 1.3). *Inorg. Chem.* 12:829–835.

28. Gorzsas, A., I. Andersson, H. Schmidt, D. Rehder, and L. Pettersson. 2003. A speciation study of the aqueous H$^+$/H$_2$VO$_4$/L-α-alanyl-L-serine system. *J. Chem. Soc., Dalton Trans.* 1161–1167.

29. Schwendt, P., P. Svancarek, I. Smatanova, and J. Marek. 2000. Stereospecific formation of α-hydroxycarboxylato oxo peroxo complexes of vanadium(V). Crystal structure of (NBu$_4$)$_2$[V$_2$O$_2$(O$_2$)(L-Lact)$_2$]·2H$_2$O and (NBu$_4$)$_2$[V$_2$O$_2$(O$_2$)$_2$(D-Lact)(L-lact)] ·H$_2$O. *J. Inorg. Biochem.* 80:59–64.

30. Svancarek, P., P. Schwendt, J. Tatiersky, I. Smatanova, and J. Marek. 2000. Oxo peroxo glycolato complexes of vanadium(V). Crystal structure of (NBu$_4$)2[V$_2$O$_2$(O$_2$)$_2$(C$_2$H$_2$O$_3$)$_2$] H$_2$O. *Monat. Chemie.* 131:145–154.

31. Kaliva, M., T. Giannadaki, A. Salifoglou, C.P. Raptopoulou, A. Terzis, and V. Tangoulis. 2001. pH-dependent investigations of vanadium(V)-peroxo-malate complexes from aqueous solutions. In search of biologically relevant vanadium(V)-peroxo species. *Inorg. Chem.* 40:3711–3718.

32. Kaliva, M., T. Giannadaki, A. Salifoglou, C.P. Raptopoulou, and A. Terzis. 2002. A new dinuclear vanadium(V)-citrate complex from aqueous solutions. Synthetic, structural, spectroscopic and pH-dependent studies in relevance to aqueous vanadium(V)-citrate speciation. *Inorg. Chem.* 41:3850–3858.

33. Djordjevic, C., M. Lee-Renslo, and E. Sinn. 1995. Peroxo malato vanadates(V): Synthesis, spectra and structure of the $(NH_4)_2[VO(O_2)(C_4H_4O_5)]_2 2H_2O$ dimer with a rhomboidal V_2O_2(hydroxyl) bridging core. *Inorg. Chim. Acta* 233:97–102.

34. Tsaramyrsi, M., M. Kaliva, A. Salifoglou, C.P. Raptopoulou, A. Terzis, V. Tangoulis, and J. Giapintzakis. 2001. Vanadium(IV)-citrate complex interconversions in aqueous solutions. A pH-dependent synthetic, structural, spectroscopic and magnetic study. *Inorg. Chem.* 40:5772–5779.

35. Djordjevic, C., M. Lee, and E. Sinn. 1989. Oxoperoxo(citrato)vanadates(V): Synthesis, spectra, and structure of a hydroxyl oxygen bridged dimer, $K_2[VO(O_2)(C_6H_6O_7)]$ $2H_2O$. *Inorg. Chem.* 28:719–723.

36. Wright, D.W., P.A. Humiston, W.H. Orme-Johnson, and W.M. Davis. 1995. A unique coordination mode for citrate and a transition metal: $K_2[V(O)_2(C_6H_6O_7)] \bullet 4H_2O$. *Inorg. Chem.* 34:4194–4197.

37. Justino, L.L.G., M.L. Ramos, M.M. Caldeira, and V.M.S. Gil. 2000. Peroxovanadium(V) complexes of glycolic acid as studied by NMR spectroscopy. *Inorg. Chim. Acta* 311:119–125.

38. Ahmed, M., P. Schwendt, J. Marek, and M. Sivak. 2004. Synthesis, solution and crystal structures of dinuclear vanadium(V) oxo monoperoxo complexes with mandelic acid: $(NR_4)_2[V_2O_2(O_2)_2(mand)_2]xH_2O$ [R = H, Me, Et; mand = mandelato(2-) = $C_8H_6O_{32}^-$]. *Polyhedron* 23:655–663.

39. Schwendt, P., P. Svancarek, L. Kuchta, and J. Marek. 1998. A new coordination mode for the tartrato ligand. Synthesis of vanadium(V) oxo peroxo tartrato complexes and the x-ray crystal structure of $K_2[\{VO(O_2)(L\text{-}tartH_2)\}_2(\mu\text{-}H_2O)]\cdot5H_2O$. *Polyhedron* 17:2161–2166.

40. Justino, L.L.G., M.L. Ramos, M.M. Caldeira, and V.M.S. Gil. 2000. Peroxovanadium(V) complexes of L-lactic acid as studied by NMR spectroscopy. *Eur. J. Inorg. Chem.* 7:1617–1621.

41. Ligtenbarg, A.G.L., R. Hage, and B.L. Feringa. 2003. Catalytic oxidations by vanadium compounds. *Coord. Chem. Rev.* 237:89–101.

42. Butler, A., M.J. Clague, and G.E. Meister. 1994. Vanadium peroxide complexes. *Chem. Rev.* 94:625–638.

43. Bonchio, M., V. Conte, F. Di Furia, G. Modena, S. Moro, and J.O. Edwards. 1994. Nature of the radical intermediates in the decomposition of peroxovanadium species in protic and aprotic media. *Inorg. Chem.* 33:1631–1637.

44. Colpas, G.J., B.J. Hamstra, J.W. Kampf, and V.L. Pecoraro. 1996. Functional models for vanadium haloperoxidase: Reactivity and mechanism of halide oxidation. *J. Am. Chem. Soc.* 118:3469–3478.

45. Clague, M.J. and A. Butler. 1995. On the mechanism of *cis*-dioxovanadium(V)-catalyzed oxidation of bromide by hydrogen peroxide: Evidence for a reactive, binuclear vanadium(V) peroxo complex. *J. Am. Chem. Soc.* 117:3475–3484.

46. Rao, A.V.S., N.S. Islam, and T. Ramasarma. 1997. Reactivity of μ-peroxo-bridged dimeric vanadate in bromoperoxidation. *Arch. Biochem. Biophys.* 342:289–297.

47. Schwendt, P. and K. Liscak. 1996. Spectral investigation of stability of the peroxo complexes $M_2[V_2O_2(O_2)_4H_2O]$ aq (M = $N(CH_3)_4$, $N(C_4H_9)_4$) in solutions. *Coll. Czech. Chem. Commun.* 61:868–876.

48. Smith, T.S. and V.L. Pecoraro. 2002. Oxidation of organic sulfides by vanadium haloperoxidase model complexes. *Inorg. Chem.* 41:6754–6760.

49. Posner, B.I., C.R. Yang, and A. Shaver. 1998. Mechanism of insulin action of peroxovanadium compounds. In *Vanadium compounds: Chemistry, biochemistry and therapeutic applications.* A.S. Tracey and D.C. Crans (Eds.). American Chemical Society, Washington, D.C. 316–28.

50. Posner, B.I., R. Faure, J.W. Burgess, A.P. Bevan, D. Lachance, G. Zhang-Sun, I.G. Fantus, J.B. Ng, D.A. Hall, B. Soo Lum, and A. Shaver. 1994. Peroxovanadium compounds. *J. Biol. Chem.* 269:4596–4604.

51. Krejsa, C.M., S.G. Nadler, J.M. Esselstyn, T. Kavanagh, J.A. Ledbetter, and G.L. Schieven. 1997. Role of oxidative stress in the action of vanadium phosphotyrosine phosphatase inhibitors. *J. Biol. Chem.* 272:11541–11549.

52. Ballistreri, F.P., G.A. Thomaselli, R.M. Toscano, V. Conte, and F. Di Furia. 1991. Application of the thianthrene 5-oxide mechanistic probe to peroxometal complexes. *J. Am. Chem. Soc.* 113:6209–6212.

53. Gorzsas, A., I. Andersson, and L. Pettersson. 2003. Speciation in the aqueous $H^+/H_2VO_4^-/H_2O_2/L-(+)$-lactate system. *J. Chem. Soc., Dalton Trans.* 2503–2511.

7 Aqueous Reactions and NMR Spectroscopy of Hydroxamidovanadate

7.1 INTERACTIONS OF HYDROXAMIDOVANADATES WITH HETEROLIGANDS

Few studies of the reaction chemistry of hydroxamidovanadates with heteroligands have been carried out. Available studies have concentrated on reactions of biochemically relevant ligands such as amino acids, small peptides, and thiolates. The aqueous chemistry observed is somewhat different from that found with peroxovanadates. For instance, reaction of the vanadate bisperoxide with glycylglycine rapidly forms monodentate complexes deriving from reaction at the *N* and *O* terminal groups. This is followed by a slow reaction, where a peroxo group is lost and a tridentate complex formed. In this product, the diglycine complexes through the terminal amine, a depronated peptide nitrogen, and a terminal carboxylate oxygen (see Scheme 6.5). This chemistry compares with that of the bishydroxamido vanadate, where glycylglycine rapidly forms a glycylglycinatobishydroxamido complex (Scheme 7.1), in which the glycylglycine is complexed in a bidentate fashion through the terminal amine group and the adjacent carbonyl oxygen to yield a zwitterionic complex with the positive charge at vanadium [1,2]. Similar coordination is found for other small peptides [1] and for amino acids [1,2], except that with amino acids, the complex is not zwitterionic. Interestingly, a bisimidazole complex has also been characterized by x-ray diffraction, and the coordination about vanadium is similar to that of peptides and amino acids, except, of course, there is no chelate ring and two imidazoles are complexed. Dissolution of the complex leads to loss of imidazole with one equivalent of ligand released to the medium [2]. It can be expected that incorporation of excess imidazole into the medium will regenerate the bis imidazole complex.

Hydroxylamine complexes display internal dynamics that are not generally observable with similar peroxo complexes. There is the possibility of end-for-end rotation of the hydroxylamine group. This rotation gives rise to isomers that, in principle and in practice, are observable. In fact, for the imidazole complexes, dynamics studies have shown there is rapid exchange between the various isomeric complexes that arises from end-for-end rotation of the hydroxylamine groups and from imidazole dissociation and reassociation [2].

The available evidence suggests that alkyl alcohols; 1,2 diols; and aliphatic carboxylic acids do not readily form complexes with hydroxamidovanadate. Also, in spite of the facile complexation of peptides, amino acids do not as readily form
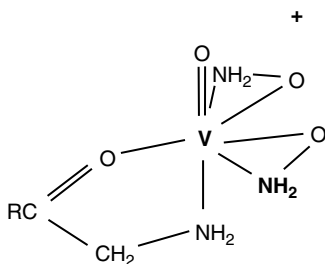
SCHEME 7.1

heteroligand complexes. For instance, glycine was observed to form complexes with the bis(*N,N*-dimethylhydroxamido)vanadate complex with an overall formation constant of about 5 M^{-1} for the reaction VL$_2$ + gly ⇌ VL$_2$gly at pH 8.5 [3]. This formation constant does not increase substantially at lower pH and is about 3 orders of magnitude smaller than observed for the corresponding reaction with the dipeptide, glycylglycine, at pH 7.0 ((3.3 ± 0.5) × 10^3 M^{-1}) [1]. Complexes also form if the amino acid sidechain contains sulfur, as in cysteine. Thiolates do not readily complex in a monodentate fashion but do so if a five-membered chelate can be formed. Both amine, *N*, and hydroxyl, *O,* are favorable ligating groups to accompany the thiolate. For instance, cysteine forms two complexes of approximately equal proportions that derive from *S,O* and from *S,N* coordination [3,4]. Interestingly, although hydroxyls lose a proton when ligated, the amine and thiol groups retain their hydrogens. Mono and bishydroxamidovanadates both form heteroligand complexes with cysteine, β-mercaptoethanol, and dithiothreitol [3]. Of course, vanadate itself similarly complexes these ligands (Section 4.3).

Monohydroxamido complexes with heteroligands tend to be unfavored solution products compared to the bishydroxamido complexes, and consequently, few such complexes have been characterized in detail. Picoline (pyridine-2-carboxylic acid) reacts readily with oxobishydroxamidovanadate and has provided a crystallographically characterized bishydroxamido complex that structurally is very similar to those formed from amino acids and dipeptides. However, the related dipicolinato (pyridine-2,6-dicarboxylato) complex contains a single hydroxamido group, and the dipicoline is ligated in a tridentate fashion [5]. The dipicolinato and hydroxamido groups are in the equatorial plane of a pentagonal bipyramidal structure. The oxo ligand is in one axial position, whereas a water molecule occupies the second axial position. The V to O$_{aqua}$ distance is 2.240(3) Å, a distance similar to other VO bond lengths, where the ligand oxygen is opposite a VO$_{oxo}$ bond. The two equatorial VO bond distances are 2.031(3) Å and 2.039(3) Å, also typically observed distances for equatorial ligands.

7.2 VANADIUM NMR SPECTROSCOPY OF HYDROXAMIDO COMPLEXES

The ^{51}V chemical shifts of hydroxamidovanadates and their heterocomplexes appear to be useful as diagnostic tools. Table 7.1 gives the chemical shifts of a number of

TABLE 7.1
^{51}V Chemical Shifts of Selected Aqueous Hydroxamidovanadate Complexes

Complexes with hydroxylamine

Heteroligand (X)	Stoichiometry	Chemical Shift (ppm)	Ref.
	VL^-	−670	6
	VL_2^+	−801, −815[a,b]	6
	VL_2^0	−823, −848[a,b]	6
	VL_2^-	−840, −860[a,b]	6
Glycine	VL_2X	−843, −854[b]	2
Serine	VL_2X	−847, −850, −861	2
Imidazole	VL_2X	−850, −858, −868[b]	2
Glycylglycine	VL_2X^0	−839, −848, −861[b]	1

Complexes with *N*-methylhydroxylamine

	VL^-	−651	6
	VL_2^0	−751, −758, −766, −779, −798[c,d]	6
	VL_2^0	−789, −794, −803, −808, −810[c,d]	6
Glycylglycine	VL_2X^0	−770, −779, −785, −796, −804, −809[c]	1

Complexes with *N,N*-dimethylhydroxylamine

	VL^-	−630	7
	VL_2^+	−696, −694[e]	7
	VL_2^0	−724, −740[e,f]	7
	VL_2^0	−750[f]	7
Glycine	VL_2X	−700, −724, −734[g]	3
Serine	VL_2X	−730, −736, −741[g]	4
β-Mercaptoethanol	VLX	−487[h]	3
β-Mercaptoethanol	VL_2X	−629[h]	3, 4
Dithiothreitol	VLX	−485, −517[g]	3
Dithiothreitol	VL_2X	−626[h]	3
Mercaptoacetic acid	VL_2X	−680[h]	4
Cysteine	VLX	−496[h]	3
Cysteine	VL_2X	−729, −734, −741[g]	3, 4
Cysteine	VL_2X	−632, −636[h]	3, 4
Glutathione (GluCysGly)	VL_2X	−731, −737, −743[g]	4
Glutathione (GluCysGly)	VL_2X	−633, −635[h]	4

[a] The −801 and −823 ppm signals correspond to the same complex but of different protonation states. Similarly, the −815 and −848 ppm signals are for different protonation states of a stereoisomer of the first pair. The −840 and −860 ppm signals derive from stereoisomers that have a different coordination number than the above pairs.

[b] Structural isomers deriving from relative orientations of the two hydroxamido ligands.

[c] Structural isomers deriving both from the relative orientations of the two *N*-methyl hydroxamido ligands and from the relative methyl group orientations.

[d] The two sets of chemical shifts correspond to two groups of isomers of different coordination number.

[e] The −696, −724 ppm chemical shift pair and the −694, −740 ppm chemical shift pair correspond to different protonation states of the same complex. The two pairs of complexes are stereoisomers.

[f] The −750 ppm signal corresponds to a complex of different coordination number than the −724 and −740 ppm complexes.

[g] *N, O* coordination.

[h] *N, S* and *O, S* coordination.

complexes. The range of chemical shifts is similar to that of the peroxovanadates, and like them, there is a substantial difference between the shifts of the mono- and bisligated vanadates, about 100 ppm, dependent on the particular hydroxylamine ligand. Mono anionic monohydroxamidovanadate (VL$^-$) has a chemical shift of –670 ppm compared to –801 to –860 for variously charged bishydroxamido complexes. With the *N,N*-dimethylhydroxylamine complex, the chemical shifts range from –630 ppm for the VL$^-$ derivative to –694 to –750 ppm for the corresponding bisligand complexes. Thus, a systematic influence of ligand number on chemical shifts is represented by these values.

Other factors also strongly influence the chemical shifts. For instance, the chemical shift ranges from –670 to –651 to –630 ppm, respectively, for the sequence of 0, 1, and 2 methyl groups on the hydroxamido nitrogen of VL$^-$. A similar variation is found for the bishydroxamido complexes. It is evident, then, that substitution of a methyl for a hydrogen on the nitrogen leads to a 20 to 30 ppm positive change in chemical shifts for each hydrogen that has been replaced. Additionally, as seen from the entries for the mono *N*-methylated hydroxylamine ligand in Table 7.1 and depicted in Figure 7.1, methyl group orientation also has a substantial influence on chemical shifts. It is not possible to know from Table 7.1 what the magnitude of the effect is because the appropriate pairs of isomers are not known. Clearly, though, the methyl orientation has a 10 to 20 ppm influence on chemical shifts. The mechanism of methyl group reorientation is not known but it seems likely that the methyl reorientation is coupled to the end-for-end rotation of the hydroxamido ligand after the fashion depicted in Scheme 7.2.
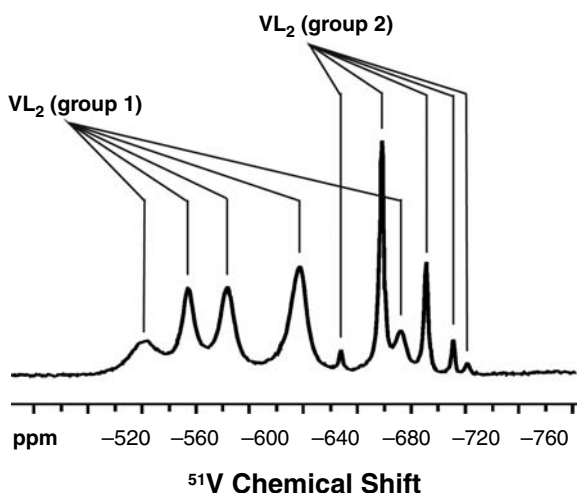
FIGURE 7.1 Partial ^{51}V NMR spectrum of vanadate in the presence of *N*-methylhydroxylamine showing the VL$_2$ region of the spectrum. The presence of two types of complexes with five observable isomers for each type of complex is revealed. Experimental conditions: 3.1 mM total vanadate, 4.1 mM total *N*-methylhydroxylamine, 1.0 M KCl, 20 mM HEPES buffer, pH 6.6.
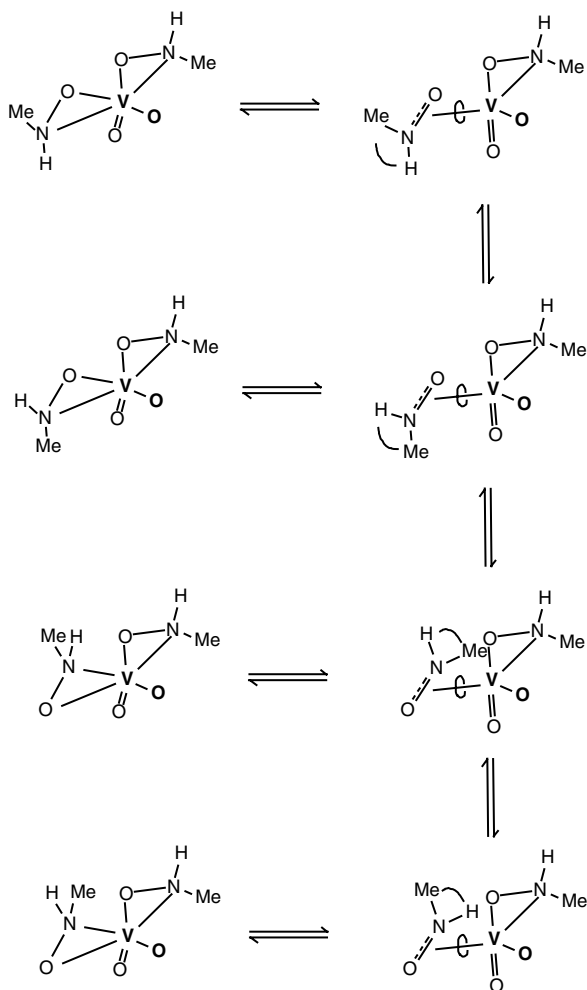
SCHEME 7.2

There can be a significant influence on vanadium chemical shifts that results from changes in the protonation state of the complex. For instance, protonation of specific bishydroxamido complexes leads to a positive change in chemical shifts of 22 to 28 ppm. However, this applies to the six-coordinate bisligand complex only. The seven-coordinate bishydroxamido complex (−840 ppm, −860 ppm, Table 7.1) can be deprotonated under moderately alkaline conditions; however, no change in chemical shift was found to accompany the change in protonation state [6]. Similarly, the corresponding bis(*N*,*N*-dimethylhydroxamido) complex shows no change in chemical shift [7].

Heteroligand chelate complexes with *N* or *O* coordination by such ligands as imidazole or amino acids have only a small influence on the chemical shifts. For
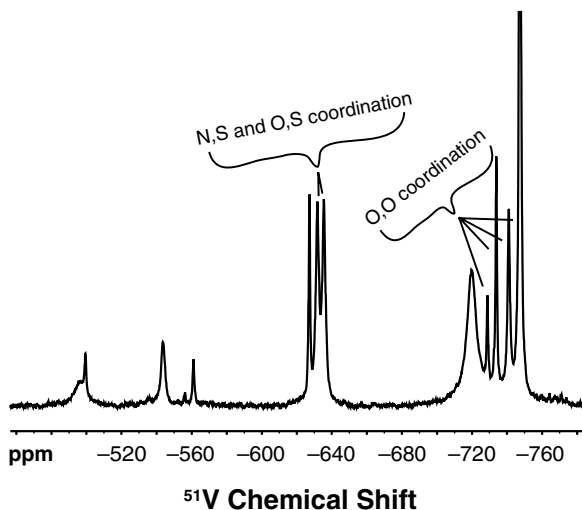
FIGURE 7.2 NMR spectrum showing the large influence of coordination of *S*-containing heteroligands on ^{51}V chemical shifts compared to similar *O* coordinated ligands in bis(*N,N*-dimethylhydroxylamine)(heteroligand)vanadium(V) complexes at pH 8.50. Experimental conditions: total vanadate, 5.0 mM; total *N,N*-dimethylhydroxylamine, 40 mM; total cysteine, 90 mM; KCl, 1.0 M; pH, 8.5.

instance, the vanadium signals for amino acid, dipeptide, and imidazole heteroligand complexes fall within the region of the parent hydroxamido complex (Table 7.1). Only the signal of the picolinato complex occurs outside the range and then by only about –13 ppm, which is probably not significant. The dipicolinic acid ligand similarly has only a small influence on vanadium chemical shifts.

However, the situation is very different when sulfur is coordinated (Table 7.1). Coordination of a single sulfur in a chelate complex causes a change in chemical shift of +100 or more ppm, as indicated in Figure 7.2 for heteroligand cysteine complexes of *N,N*-dimethylhydroxamidovanadate [3,4]. Additional coordinated sulfurs cause a corresponding further change in chemical shift. Also, as can be seen from Figure 7.3, similar changes are observed when vanadate, itself, is coordinated by sulfur ligating groups.
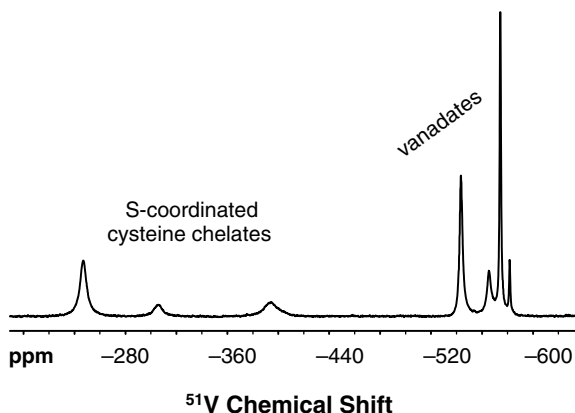
FIGURE 7.3 ^{51}V NMR spectrum showing vanadate in the presence of cysteine at pH 8.4. Signals at high field derive from vanadate and its various oligomers. The low field signals are from *S*-coordinated cysteine complexes.

REFERENCES

1. Paul, P.C., S.J. Angus-Dunne, R.J. Batchelor, F.W.B. Einstein, and A.S. Tracey. 1997. Reactions of hydroxamidovanadate with peptides: Aqueous equilibria and crystal structure of oxobis(hydroxamido)glycylglycinatovanadium(V). *Can. J. Chem.* 75:183–191.
2. Keramidas, A.D., W. Miller, O.P. Anderson, and D.C. Crans. 1997. Vanadium(V) hydroxylamido complexes: Solid state and solution properties. *J. Am. Chem. Soc.* 119:8901–8915.
3. Bhattacharyya, S., A. Martinsson, R.J. Batchelor, F.W.B. Einstein, and A.S. Tracey. 2001. N,N-dimethylhydroxamidovanadium(V). Interactions with sulfhydryl-containing ligands: V(V) equilibria and the structure of a V(IV) dithiothreitol complex. *Can. J. Chem.* 79:938–948.
4. Nxumalo, F. and A.S. Tracey. 1998. Reactions of vanadium(V) complexes of N,N-dimethylhydroxylamine with sulfur-containing ligands: Implications for protein tyrosine phosphatase inhibition. *J. Biol. Inorg. Chem.* 3:527–533.
5. Nuber, B. and J. Weiss. 1981. Aqua(dipicolinato)(hydroxylamido-*N,O*)oxovandium. *Acta Crystallogr.* B37:947–948.
6. Angus-Dunne, S.J., P.C. Paul, and A.S. Tracey. 1997. A ^{51}V NMR investigation of the interactions of aqueous vanadate with hydroxylamine. *Can. J. Chem.* 75:1002–1010.
7. Paul, P.C., S.J. Angus-Dunne, R.J. Batchelor, F.W.B. Einstein, and A.S. Tracey. 1997. Reactions of vanadate with N,N-dimethylhydroxylamine: Aqueous equilibria and the crystal structure of the uncharged oxygen-bridged dimer of bis(N,N-dimethylhydroxamido)hydroxooxovanadate. *Can. J. Chem.* 75:429–440.

8 Reactions of Oligovanadates

8.1 THE SMALLER OLIGOMERS

The chemistry discussed here is largely restricted to the complexes in which the basic backbone structure of the oligomers is not changed, such as by generation of multiple bonds between the vanadium centers. The coordination number and geometry of the individual vanadiums, however, might well be influenced by coordination. In this sense, then, the oligovanadates do not generally display the rich chemistry found with the monomer. One of the reasons for this is that in order for, for instance, divanadate to form, two VOH bonds condense, with the elimination of water and formation of the VOV linkage. The result is the loss of a reactive center at each vanadium. To an extent, this may be compensated for by expansion of the coordination sphere. Many of the known V_2 complexes have pentacoordinate geometry and a $[VO]_2$ cyclic core that distinguishes such complexes from divanadate, where the vanadiums have tetrahedral coordination and are linked through a single bridging oxygen. Complexes having the cyclic core have previously been discussed (Section 4.1). Divanadate displays much of the chemistry associated with monodentate ligation of the monomer with reaction occurring at the OH functionalities. Thus, for instance, alcohols replace hydroxyl groups in a systematic manner to give alkyldivanadates [1]. Unfortunately, divanadate chemistry generally is difficult to study in detail because reactants are not specific to divanadate, and almost invariably the chemistry of the monomer dominates.

Hydrogen peroxide forms V_2 complexes of VVL^{3-}, VVL_2^{3-}, $VLVL^{3-}$, and $VL_2VL_2^{3-}$ stoichiometry [2]. These compounds have ^{51}V chemical shifts of -563 and -622 ppm for the two vanadiums of VVL and -555 and -737 ppm for those of VVL_2. A third complex of VLVL stoichiometry has a single signal at -634 ppm, whereas VL_2VL_2 has a shift of -755 ppm for its two vanadiums. Table 8.1 provides chemical shifts observed for these peroxovanadates and for related hydroxamido complexes. Taken together, these chemical shifts clearly suggest that all these compounds are based on a divanadate-like structure, as depicted in Scheme 8.1 and seen in the x-ray structure of the tetraperoxodivanadate complex ($V_2L_4^{4-}$) [3].

In solution, a tetraperoxide (V_2L_4) has been characterized as carrying a triply negative charge [2]. In this case, a proton is required in the $V_2L_4^{4-}$ structure depicted in Scheme 8.1. The location of such a proton is problematic, but presumably the bridging oxo would protonate to form a bridging hydroxo group. The chemical shift of the compound is -755 ppm, which is close to that of VL_2^{2-} (-765 ppm) and about 65 ppm from that of VL_2^{1-} (-691 ppm). The chemical shift, therefore, agrees with

TABLE 8.1
^{51}V chemical shifts for aqueous peroxo and hydroxamido divanadium(V) complexes

Complex	Chemical shift (ppm)			
Peroxo complexes	V	VL	VL$_2$	VL$_x$
V$^-$	−560			
VL$^-$		−625		
VL$_2{}^{2-}$			−765	
VVL^{3-}	−563	−622		
VVL$_2{}^{3-}$	−555		−737	
VLVL^{3-}		−634		
VL$_2$VL$_2{}^{3-,b}$			−755	
V$_2$L$_3{}^0$				−669
N,N-Dimethylhydroxamido complexes				
VL$^-$		−630		
VL$_2{}^0$			−724, −740, −750	
VVL	−567	−632		
VLVL$_2$		−648	−712	

^{a} These complexes were observed at high total vanadate (80 mmol/L) and total ligand (80 mmol/L) concentrations where they are minor species [2].

^{b} See arguments in text concerning charge state of this complex [14].

protonation of the oxo group. This complex is favored by basic conditions and is a very minor component.

The divanadium trisperoxo complex (V$_2$L$_3{}^0$) represents an interesting variant on the structures of the above complexes. Its charge state and ligand stoichiometry signifies there is bridging between the two vanadiums by one of the peroxo groups. Additionally, only one ^{51}V NMR signal was found for the complex [2]. The structure in Scheme 8.1 is in accord with the properties of this complex. A somewhat similar complex has been observed when imidazole is included in solution. A complex in which imidazole bridges between two peroxovanadium groups has been reported, albeit this is a minor solution product [4].

The N,N-dimethylhydroxylamine complex of V$_2$L$_3$ stoichiometry should provide two NMR signals irrespective of the coordination, because the two vanadium nuclei are not equivalent, even if there is bridging by a ligand. The positions of the signals (−648, −712 ppm, Table 8.1) suggest that bridging does not occur with this ligand, so that this product most likely has a VLVL$_2$ coordination with oxo bridging only. In principle, this product should have a number of isomers. However, only one has been found, and therefore, there is high selectivity toward a single isomer.

Although linear vanadate oligomers, up to V$_6$, have been identified as minor products in aqueous solution, little is known of their chemistry. Presumably, they will undergo monodentate and other reactions that involve only one vanadium center similar to those observed for V$_2$. A V$_3$L$_2$ complex has been found for an α-hydroxy-

SCHEME 8.1

carboxylic acid ligand. This compound has multiple bridging between vanadiums, and the compound is discussed more fully in Section 4.1.

In addition to the linear oligomers, cyclic derivatives ($V_3{}^{3-}$, $V_4{}^{4-}$, $V_5{}^{5-}$) are also known (see Section 2.2). The latter two are readily formed and are ubiquitous components of aqueous solutions. These compounds are relatively inert to complexation reactions that preserve their cyclic structure; rather, the equilibria shift towards products of other vanadium stoichiometry. Presumably, one way to generate complexes of these oligomers would be to protonate one or more oxygens so that the reactivity is increased. However, neither protonated V_4 nor V_5 has been identified in solution, nor has there yet been any indication from studies in alcoholic solution that an alkoxo group can replace an oxo ligand, as might be expected if protonation occurs.

Under anhydrous conditions, tetranuclear vanadium clusters such as $[V_4O_4\{(OCH_2)_3CCH_3\}_3(OC_2H_5)_3]$ can be generated in alcoholic solutions with 1,1,1–tris(hydroxymethyl)ethane. The coordination does vary somewhat with the alcohol utilized in the preparation, but all retain the tetranuclear structure. Each vanadium nucleus in the complex has octahedral coordination. The clusters are not stable to hydrolysis and decompose in chloroform solution in the presence of just a few equivalents of water [5].

Despite the general observations that tetravanadate does not react favourably in aqueous solution with available ligands, it certainly does so with tartaric acid [6]. $2R,3R$-tartrate reacts very favorably in vanadate solution to form a number of products including a complex formed with V_4^{4+} that has V_4L_2 stoichiometry and a structure for which each vanadium has an approximately square pyramidal pentacoordinate geometry. The product is also unique in that the $[VO]_4$ ring is not a chair-like with the four vanadiums being approximately coplanar, but rather the ring has a boat conformation for which an adjacent pair of vanadiums is arranged in a perpendicular fashion to the second pair (Scheme 8.2). This product is highly favoured at pH values lower than about 7 and is the predominant solution product to about pH 2. Another complex with V_2L_2 stoichiometry probably has a structure similar to that found with complexes of other α-hydroxycarboxylic acids (Section 4.1).

The tetramer can also react with other metal centers without destruction of the cyclic structure. It has, for instance, been found to act as a ligand toward a cationic bisphenanthrene cobalt complex ($[Co(phen)_2]^{2+}$). Two V-oxo groups on adjacent vanadium centers ligate a cobalt through the oxygens, whereas oxo groups on the second pair of vanadiums similarly ligate a second cobalt to form a biscobalt tetravanadate derivative ($[\{Co(phen)_2\}_2V_4O_{12}]$) [6]. In this cluster, the tetravanadate can be thought of as an anion bridging between two cationic centers. Although this compound was obtained in crystalline form from aqueous solution, little is known about its solution chemistry.

8.2 DECAVANADATE

There have been very few studies of the reactions of decavanadate with organic ligands. Most that have been carried out simply reveal that the ligand behaves much like a counterion and interacts via hydrogen bonds [8,9]. An interesting example of this is a complex formed between decavanadate and the dipeptide, glycylglycine $((NH_4)_6(glygly)_2V_{10}O_{28}$, where the peptide complexes in its zwitterionic form. In the
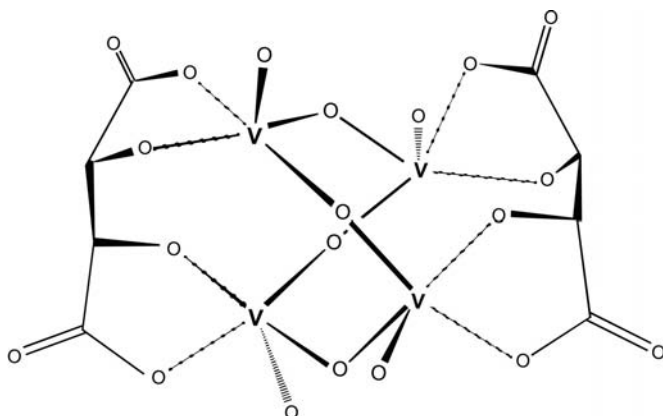
SCHEME 8.2
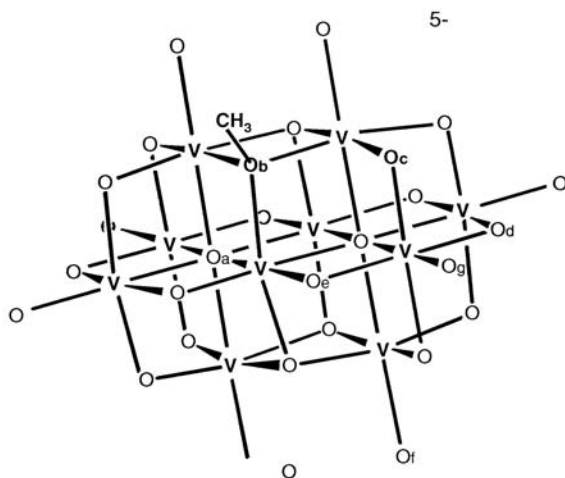
a methoxodecavanadium(V)
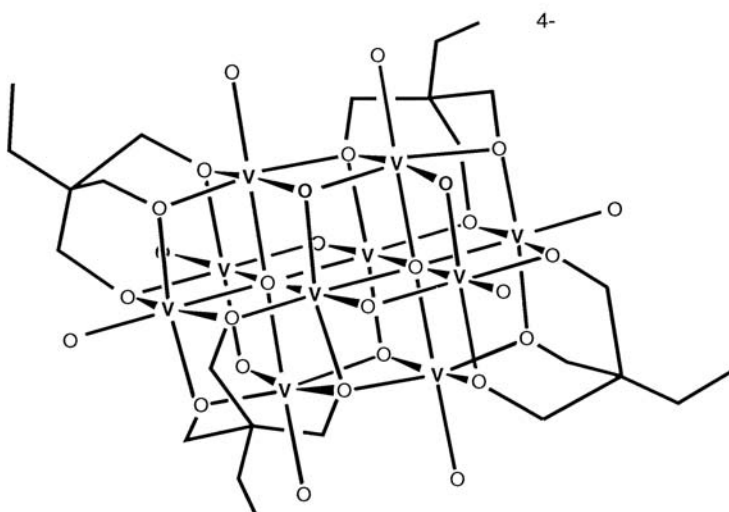
b tetra{1,1,1-tris(oxomethyl)propane}decavanadium(IV)

SCHEME 8.3

structure, six ammonium ions and the two ammonium groups of GlyGly hydrogen bond to the decavanadate core. In effect, decavanadate, together with its hydrogen bonded complement, is cationic. The carboxylates of the two glycylglycines are directed away from the decavanadate core toward nearby ammonium groups of an adjacent decavanadate and serve to neutralize the positive charge. Attempts to study this compound in aqueous solution were not successful, and no evidence for retention of the crystal structure coordination on dissolution was obtained [8].

Very little work related to the insertion of ligands into the decavanadate core has been reported. Methanol, contained in aqueous solution with decavanadate, has been found to insert in a stereospecific manner in the fashion depicted in Scheme 8.3a. The situation changes dramatically for the reaction of decavanadate under forcing conditions with 1,1,1-tris(hydroxymethyl)propane. This remarkable reaction does not lead to insertion into decavanadate but rather insertion into a similar decavanadium structure (Scheme 8.3b), in which all vanadiums have been reduced to vanadium(IV) [10].

Oxides of molybdenum and tungsten can readily be inserted into the V_{10} structure to form heteropoly vanadates. A decavanadate-like structure is retained if the degree of substitution is low. However, incorporation of high proportions of the hetero species often leads to hexanuclear derivatives [11,12]. Other structural forms are also known [13]. Both W_6 and W_{12} polyoxometalates of tungsten readily undergo displacement reactions by vanadate, and W_5V, $W_{11}V$, $W_{10}V_2$, and W_9V_3 materials are well known. Compounds of this type are finding applications in nanomaterials because they appear to have unique electro, optical, and thermal properties.

REFERENCES

1. Tracey, A.S. and M.J. Gresser. 1988. The characterization of primary, secondary, and tertiary vanadate alkyl esters by 51-V nuclear magnetic resonance spectroscopy. *Can. J. Chem.* 66:2570–2574.
2. Andersson, I., S.J. Angus-Dunne, O.W. Howarth, and L. Pettersson. 2000. Speciation in vanadium bioinorganic systems 6. Speciation study of aqueous peroxovanadates, including complexes with imidazole. *J. Inorg. Biochem.* 80:51–58.
3. Stomberg, R., S. Olson, and I.-B. Svensson. 1984. The crystal structure of ammonium μ-oxo-bis(oxodiperoxovanadate)(4-), $(NH_4)_4[O\{VO(O_2)_2\}_2]$. A refinement. *Acta Chem. Scand.* A 38:653–656.
4. Tracey, A.S. and J.S. Jaswal. 1993. Reactions of peroxovanadates with amino acids and related compounds in aqueous solution. *Inorg. Chem.* 32:4235–4243.
5. Crans, D.C., F. Jiang, J. Chen, O.P. Anderson, and M. Miller. 1997. Synthesis, x-ray structures, and solution properties of $[V_4O_4\{(OCH_2)_3CCH_3\}_3(OC_2H_5)_3]$ and $[V_4O_4\{(OCH_2)_3CCH_3\}_2(OCH_3)_6]$: Examples of new ligand coordination modes. *Inorg. Chem.* 36:1038–1047.
6. Schwendt, P., A. S. Tracey, J. Tatiersky, J. Gáliková and Z. Zák. 2006. Vanadium (V) Tartrato Complexes: Speciation in the $H_3O^+(OH^-)/H_2VO_4^-/(2R,3R)$-tartrate System and X-ray Crystal Structures of $Na_4[V_4O_8(rad\text{-}tart)_2] \cdot 12H_2O$ and $(NEt_4)_4[V_4O_8(R,R\text{-}tart)_2] \cdot 6H_2O$ (tart = $C_4H_2O_6^{4-}$). Submitted for publication.
7. Kucsera, R., R. Gyepes, and L. Zurkova. 2002. The crystal structure of the cluster complex $[\{Co(phen)_2\}2V_4O_{12}]$ H_2O. *Cryst. Res. Technol.* 37:890–895.
8. Crans, D.C., M. Mahroof-Tahir, O.P. Anderson, and M.M. Miller. 1994. X-ray structure of $(NH_4)_6(Gly\text{-}Gly)_2V_{10}O_{28}.4H_2O$: Model studies for polyoxometalate-protein interactions. *Inorg. Chem.* 33:5586–5590.
9. Averbuch-Pouchot, M.T. 1995. Crystal structure of hexakis(2-ammonium-2-methyl-1-propanol) decavanadate $(C_4H_{12}NO)_6(V_{10}O_{28})$. *Z. Krist.* 210:371–372.

10. Ishaque Khan, M., Q. Chen, D.P. Goshorn, H. Hope, S. Parkin, and J. Zubieta. 1992. Polyoxo alkozides of vanadium: The structures of the decanuclear vanadium(IV) clusters $[V_{10}O_{16}\{CH_3CH_2C(CH_2O)_3\}_4]^{4-}$ and $[V_{10}O_{13}\{CH_3CH_2C(CH_2O)_3\}_5]^-$. *J. Am. Chem. Soc.* 114:3341–3346.
11. Howarth, O.W. and J.J. Hastings. 1990. Monotungstononavanadate and *mer*-tritungstotrivanadate. *Polyhedron* 9:143–146.
12. Flynn Jr., C.M. and M.T. Pope. 1971. Tungstovanadate heteropoly complexes. I. Vanadium(V) complexes with the constitution $M_6O_{19}^{n-}$ and V:W less than or equal to 1:2. *Inorg. Chem.* 10:2524–2529.
13. Howarth, O.W. 1990. Vanadium-51 NMR. *Prog. Nucl. Magn. Reson. Spectrosc.* 22:453–485.
14. Bhattacharyya, S., A. Martinsson, R.J. Batchelor, F.W.B. Einstein, and A.S. Tracey. 2001. N,N-dimethylhydroxamidovanadium(V). Interactions with sulfhydryl-containing ligands: V(V) equilibria and the structure of a V(IV) dithiothreitol complex. *Can. J. Chem.* 79:938–948.

9 Influence of Ligand Properties on Product Structure and Reactivity

As has been seen in the earlier discussion, vanadate readily complexes numerous ligands varying from simple monodentate ligands to large multidentate ones that impose a greatly expanded coordination sphere on the metal. Often bi- and tridentate ligands enhance or confer reactivity to vanadate that is not found to an appreciable extent in the parent. Despite the reactivity of vanadate toward numerous and chemically diverse ligands, there are subtleties in the chemistry that are not obviously apparent but, in the final analysis, have a remarkably consistent influence throughout the aqueous chemistry. Phenomenological aspects of the aqueous chemistry have been described previously, but various components are re-examined here, with the objective of identifying some underlying influences and to provide a basis for them.

9.1 ALKYL ALCOHOLS

A study of the formation of a number of mono- and bisligand vanadate complexes of aliphatic alcohols revealed that ^{51}V chemical shifts of the singly charged anionic complexes were related to a chemical shift of –559 ppm (Section 3.1.1). The observation was that if the chemical shift difference between –559 ppm and that of the monoligated complex was known, then doubling this difference gave the chemical shift of the bisligated derivative [1]. Furthermore, this behavior extended to mixed aliphatic alcohols, so if the chemical shifts of the two monoligand complexes were known, then the shifts of the two homo bisligand complexes and that of the hetero bisligand complex could be predicted. In a separate study [2] where imidazole was contained in solution, the findings were not as clear-cut as described above. However, those authors found that imidazole was having a significant influence on the reactions. Table 9.1 lists various chemical shifts observed and the corresponding calculated shifts. From this table, it is evident that the calculated values are very close to the observed signal positions. This intriguing phenomenon suggests that, to the extent that the chemical shifts are related to the electron density about the vanadium nucleus, the coordination of the second ligand was independent of the complexation of the first. In fact, considering the systematic variation in chemical shifts for the various ligands with respect to whether they are primary or secondary alcohols, it might be argued that complexation is having, at best, only a small influence on electron distribution at the vanadium center. This is quite surprising, considering that the aliphatic alcohols encompass a range of K_a values of about 8 orders of

TABLE 9.1
^{51}V chemical shifts (ppm) observed for selected heteroligand bisperoxovanadate complexes

Ligand	$RO_2VO(O_2)_2$ [a]	Ligand	$RNH_nVO(O_2)_2$ [a]	Ref.
		Ammonia	−750	13
		Ethylamine	−744	13
		Picolinic acid	−745[b]	26
		Imidazole	−749	27, 28
Acetic acid	−720			13
Lactic acid	−721			8
Glycine	−712	Glycine	−758	12
CBz-glycine	−714	Glycine-OEt	−736	12
Glycylglycine	−713	Glycylglycine	−747	13
Alanylserine	−714[b]	Alanylserine	−743[b]	28
		Glycylhistidine	−742, −746, −751[c]	28
Alanylhistidine	−712[b]	Alanylhistidine	−739, −750	30

[a] Charge state is variable depending on ligand. Reaction of $VO(O_2)_2(H_2O)^-$ with RCO_2^- or RNH_2 occurs without loss of protons.

[b] These chemical shifts were reported but not assigned to specific products.

[c] Chemical shifts of −742 and −751 ppm correspond to reaction at the imidazole nitrogens, that of −746 to the *N*-terminal nitrogen.

magnitude. Additionally, despite this variation in K_a, there is only a small overall influence on product formation constants [3].

A convenient probe for testing the above proposal is provided by the pK_a values of the various monoligated products that are formed. The bisligand complexes, not being protonated, do not have a pK_a. If complexation of an alcoholic ligand has an insignificant influence on the electron distribution at vanadium, then changing the electron-donating property of the alcohol should influence the pK_a of the product complex in a quantifiable manner. As seen in Figure 9.1, there is a distinct relationship between the chemical shift of the alkylvanadate and its pK_a. However, this dependence is a complicated one that apparently centers on whether the pK_a of the complex is greater or less than about 8.3. The behavior observed is dependent on the pK_a of the alcohol giving rise to the vanadate derivative. Figure 9.2 shows the relationship between the pK_a's of the parent alcohols and their vanadate complexes.

It is remarkable that despite a change of almost 6 orders of magnitude in K_a of the alcohols between methanol and hexafluoroisopropanol, the pK_a's of the corresponding complexes vary somewhat less than half a pK_a unit. However, with the alcohols having a pK_a greater than methanol where the ligand pK_a's increase by about 1.8 pK_a units, the pK_a's of the product complexes vary linearly by up to 1.1 pK_a unit. This behavior suggests that the vanadium center carries a preferential electron density that derives from the coordinating ligands. Associated with this electron density is a saturation effect.

The more acidic alcohols are most effective as electron-withdrawing groups. To compensate for the electron withdrawal, some electron density is pulled away from
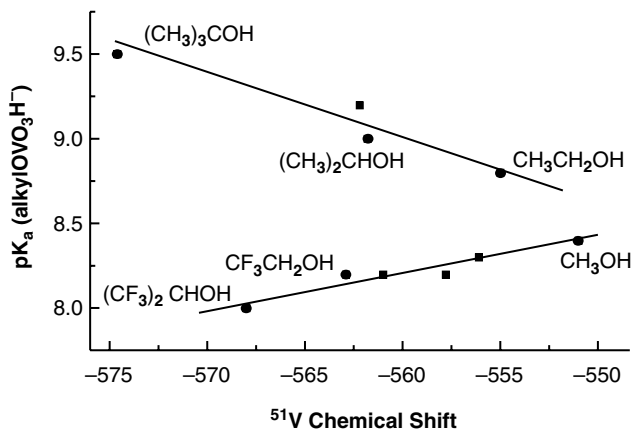
FIGURE 9.1 The ^{51}V chemical shifts of monoanionic alkoxovanadates are shown as a function of their pK$_a$ values. Only a selection from all the alkoxo ligands is identified. The solid lines provide a guide for viewing the data, which was taken from the work of Tracey and coworkers [3].
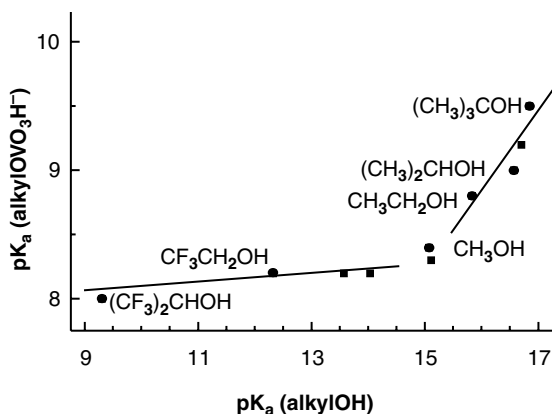
FIGURE 9.2 The pK$_a$ values of a variety of monoanionic alkoxovanadates are plotted as a function of the pK$_a$ of the parent alcohols. The solid lines are provided as an aid in viewing the data and have no theoretical significance. Not all alcohols are identified in the graph. The data was taken from the work of Tracey and coworkers [3].

the vanadate oxygens, including the OH, and the pK$_a$ of the complex drops a little. On the other hand, more basic alcohols donate electrons to the vanadate center. However, the ability to handle the extra electron density is exhausted with alcohols that have a pK$_a$ of about 15, for instance, methanol. Vanadate compensates for this by transferring the extra electron density to its other ligands. By doing so, the pK$_a$ of the complex is increased by an incremental amount that is virtually the same as the increment in basicity of the alcohol. It is, therefore, fortuitous that the chemical shifts of Figure 9.1 fold back the way they do to clearly show that there are two major contributions to the changes in chemical shifts observed for the alkylvanadate
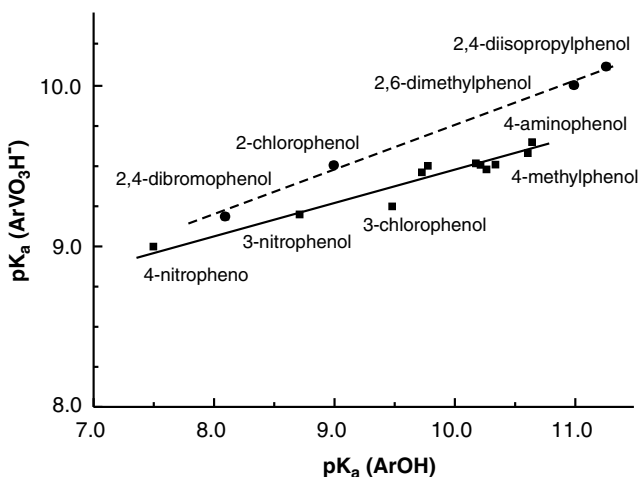
FIGURE 9.3 The relationship between the pK_a's of various ortho-($\bullet$) and *meta*- and *para*-($\blacksquare$) substituted phenols and the pK_a's of the corresponding arylvanadates. The values are for 42% vol/vol acetone/water solutions. For the various phenolic solutions, the pK_a of vanadate ($VO_4H_2^-$) is about 9.5 and dependent on solution properties. A correction to a value of 9.55 was made for all solutions. Data taken from Galeffi and Tracey [4]. Not all phenols have been identified in the figure.

complexes, one deriving from desaturation of the electron density at the vanadium, the other from changes in electron density at the OH, and presumably the other oxygens, of the complex.

It is now evident why the formation of the alkylvanadates is insensitive to the pK_a of the parent alcohol. The electron density about vanadate is close to optimal, so small changes arising from variation in the ability of the ligand to donate or withdraw electrons are relatively unimportant components of complexation of the alcohols. It would be expected, and is also observed, that both resonance and inductive effects are small for the reaction of vanadate with phenols [4]. Considering that the pK_a values of the various substituted phenols are considerably lower than 15, an approximately linear relationship (Figure 9.3) between the pK_a of the arylvanadate and the pK_a of the ligand would be expected and can be predicted from the observations of alkylvanadates. There are only minor differences that arise because of resonance electron donation and withdrawal.

9.2 GLYCOLS, α-HYDROXY ACIDS, AND OXALATE

Ethylene glycol and related 1,2-diols give rise to alkylvanadates from monodentate reaction at the individual OH groups but also form complexes via a bidentate reaction. The latter complexes are bisligand binuclear complexes with a pentacoordinate geometry similar to that depicted in Scheme 9.1a [5–7]. The monomeric precursor is highly unfavored relative to the dimer, the dimerization constant for nucleosides for the reaction 2VL V_2L_2 being 10^6 to 10^7 [7]. However, if the ligand is oxidized to an α-hydroxycarboxylic acid, the dimerization constant is 3 to
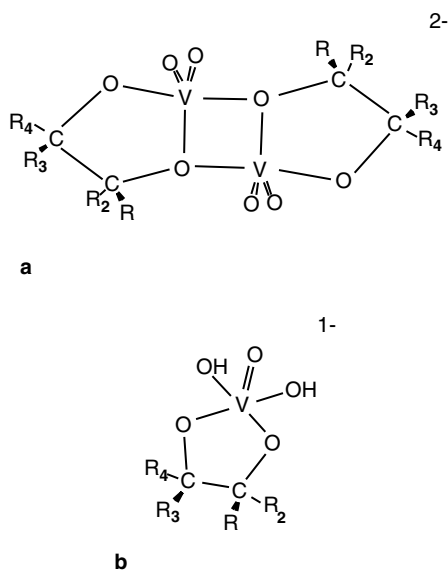
SCHEME 9.1

4 orders of magnitude smaller [8,9]. Further oxidation to oxalate provides only monomeric forms of the complex.

It is possible to rationalize these findings by extending the arguments concerning the influences of alkyl alcohol complexation on electron distribution in the coordination sphere of vanadate. The monomeric (VL) complexes of α-hydroxy acids have a pK_a of about 6.5, depending on the ligand, for the deprotonation VL^- $\rightleftharpoons$ VL^{2-} + H^+. Because VL^- has protons, it must have incorporated water during its formation and, at minimum, have a pentacoordinate geometry. Presumably, the coordination is similar to that depicted in Scheme 9.1b. If the electron density at vanadium is high, then excess density can be shed by forming a dimer like that shown in Scheme 9.1a. In this coordination mode, electron density is distributed between the vanadium nuclei, and overall there are two fewer ligands. The glycols, not being as acidic as the α-hydroxy acids, more effectively donate electron density and by doing so shift the equilibrium toward the dimeric form of the complex. The situation is reversed with the oxalate ligand, which is more effective than α-hydroxy acids in withdrawing electrons. Both mono- and bisoxalato vanadates (Scheme 9.2) are readily formed.
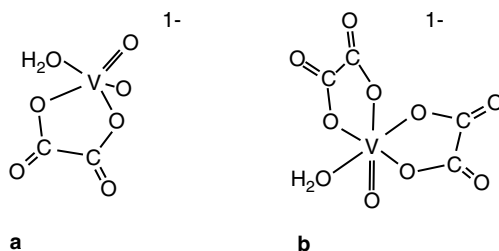
SCHEME 9.2

It is not known what the coordination geometry of the monooxalato complex is, although pentacoordinate geometry seems likely and has been proposed from ^{13}C and ^{17}O NMR studies [10]. This geometry is depicted in Scheme 9.2a. Additional electrons are introduced into the coordination sphere by the incorporation of a second ligand, and bisoxalato complexes in hexacoordinate geometry are readily formed (Scheme 9.2b). Solution studies have not revealed compounds of VL_2 stoichiometry, either with glycols or α-hydroxycarboxylates. Thus, for these types of bidentate ligands (L), the primary coordination sequence goes as (X = H_2O or OH): V_2L_2; VLX and V_2L_2; VLX and VL_2 for glycols, α-hydroxycarboxylates and oxalate, respectively.

These observations lead to an interesting question concerning monodentate complexation. A monodentate ligand (XOH) is generally assumed to complex via the reaction $H_nVO_4^{(3-n)-}$ + XOH $\longrightarrow$ $H_{(n-1)}VO_3(OX)^{(3-n)-}$ + H_2O. If the monodentate ligand is a good enough electron withdrawer, will the coordination sphere expand from the normally tetrahedral coordination to a higher coordination?

9.3 BISPEROXO AND BISHYDROXAMIDO VANADATES: HETEROLIGAND REACTIVITY

A dependence of product coordination is also observed for reactions of heteroligands with peroxo and hydroxamido vanadates. Peroxide, which complexes as O_2^{2-}, is a much better electron donor than is hydroxamido, which complexes as H_2NO^{1-}. Bis complexes from these two ligand types can have very similar coordination, as depicted in Scheme 9.3. In fact, there are two distinct types of bishydroxamido

a

b

SCHEME 9.3

complexes (Sections 5.2, 5.3), one of which apparently has water incorporated into the coordination sphere [11], perhaps as shown in Scheme 9.3b. The vanadium center can compensate for the comparatively strong electron-withdrawing property of the hydroxylamine ligand by drawing a water into the coordination sphere. The stabilization afforded by incorporation of water is not large enough that the equilibrium is shifted fully toward the hydrate. However, it can be expected that the peroxo and hydroxamido complexes will show distinct differences in their reactions with other types of heteroligands.

Both aliphatic carboxylic acids and aliphatic amines react readily with bisperoxovanadates in aqueous solution (Table 9.1 gives a compilation of ^{51}V NMR chemical shifts observed for various ligands). It is, therefore, not surprising that dipeptides and amino acids both readily form similar products with bisperoxovanadates. Even though these heteroligands have multidentate functionality, they react only in a monodentate fashion, and both carboxylate- and amino-derived products are found in aqueous solution [12,13]. There is little evidence to suggest that these types of heteroligands react in a bidentate fashion except with loss of one of the peroxo groups to form a monoperoxo product, though such bidentate complexes can be obtained as crystalline materials [14,15]. This behavior is quite different from that of the bishydroxamido complexes.

According to the thesis advanced here, the bishydroxamido ligands should be more susceptible to bidentate reaction than bisperoxovanadate. This behavior is exemplified by the reaction of glycylglycine. Glycylglycine forms two products with bisperoxovanadate (Scheme 9.4a) that derive from independent reaction at either the carboxylate or the amine groups. With bishydroxamidovanadate, a single type of product is formed where the ligand is bidentate, as depicted in Scheme 9.4b [16,17]. Of course, examples from the solid state show that bidentate ligands such as oxalate

SCHEME 9.4

[15] and various picolinates [14] react in a bidentate manner with bisperoxovanadate. However, it is not evident that those structures are retained in aqueous solution. It is interesting that for oxalate, the VO bond length to the apical carboxylate oxygen is quite long, being about 2.25 Å compared to 2.06 Å for the corresponding equatorial oxygen. The apical VO distances for similar picolinato ligands are close to 2.20 Å. In comparison, for a monoperoxo picolinato complex, the VO distance is 2.016 Å [18] and is close to 2.06 Å for the two carboxylate oxygens of a pyridine-2,6-dicarboxylato (dipic) complex [19].

These distances suggest that the apical group of these bidentate ligands in bisperoxo complexes is not strongly bonded. Also, in the case of the bisperoxo picolinato derivatives, ^{51}V NMR studies showed there was significant hydrolysis in aqueous solution, again suggesting that the ligand is not tightly bound. Unlike picoline, the glycine complex of bisperoxovanadate in the solid state has been found to complex in a monodentate fashion through the carboxylate group [20]. This is to be compared to the corresponding complex with bishydroxamidovanadate, where the glycine acts as a bidentate ligand with one oxygen of the carboxylate group in the apical position [16], as shown in Scheme 9.4b for glycylglycine. The propensity of the reactions toward expansion of the coordination sphere, therefore, follows the pattern expected on the basis of the electron-withdrawing ability of the primary ligands, hydrogen peroxide or hydroxylamine.

9.4 PHENOLS

Ligands with a pK_a close to that of vanadate will have a minimal influence on the electron distribution about the nucleus. Therefore, it might reasonably be expected that ligands with a pK_a that matches that of vanadate will exhibit selective reactive properties. In 42% by volume of acetone in water, the second pK_a of vanadate rises to about 9.5 [4]. Numerous phenols are soluble in this solvent, and they provide a convenient probe of the influence of ligand pK_a on product formation when the ligand pK_a values span the pK_a of vanadate. Figure 9.4 shows the influence of ligand pK_a on formation of the arylvanadate, where the formation constant for the aqueous acetone solution is defined by Equation 9.1.

$$H_2VO_4^- + ArOH \qquad HVO_3OAr^- + H_2O \qquad (9.1)$$

$$K = [H_2VO_4^-][ArOH] / [HVO_3OAr^-]$$

It is seen from Figure 9.4 that product formation is near a minimum over a range of about 1 pH unit either side of the vanadate pK_a. Despite this, a linear relationship (Figure 9.3) between the ligand pK_a and the pK_a of the product complex indicates there is a smooth transfer of electron density to the OH on vanadate. If the ligand has a pK_a significantly below that of the vanadate monoanion, it can transfer its proton to an OH of vanadate to form water and, in the subsequent complex, retain
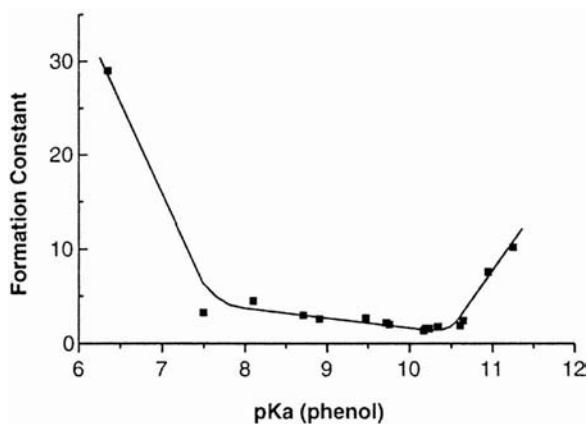
FIGURE 9.4 The relationship between the pK_a of the phenolic ligands and the formation constant of the arylvanadate ($VO_4H_2^-$ + ArOH $\rightleftharpoons$ ArOVO$_3$H$^-$) is shown. The values are for 42% by volume of acetone in water. Data taken from Galeffi and Tracey [4].

much of its ArO$^-$ character. When the pK_a of the ligand is significantly higher than that of vanadate, it can transfer electron density to the vanadium center and thus retain covalent character. Under the matched conditions, neither the ligand nor vanadate gains significantly by forming a complex, and product formation is minimized. The situation changes dramatically, however, if complexation imposes a change in coordination number.

9.5 DIETHANOLAMINES

Vanadate undergoes facile condensation reactions with a number of diethanolamines to form pentacoordinate complexes of the form depicted in Scheme 9.5 [21]. The pK_a values of the protonated forms of these ligands span the pK_a of the vanadate monoanion ($H_2VO_4^-$), which is about 8.0 in water but dependent on ionic properties of the solution [22–24]. Product formation follows according to Equation 9.2, but as is evident from Figure 9.5, it changes in accord with a systematic variation of the acidity constant of the protonated ligand. Formation of a product is greatly enhanced when the pK_a of vanadate and that of the ligand are matched.

$$H_2VO_4^- + RN(CH_2CH_2OH)_2 \rightleftharpoons RN(CH_2CH_2O)_2VO_2^- + 2H_2O \qquad (9.2)$$

$$K = [H_2VO_4^-][RN(CH_2CH_2OH)_2] \, / \, [RN(CH_2CH_2O)_2VO_2^-]$$

The formation of the diethanolamine complexes can be thought of as a three-step process, with the reaction of an alcoholic function to initially form an alkoxo complex. At this stage, there will be little perturbation of the electronic environment around the vanadium nucleus. As described previously, electron density at vanadium
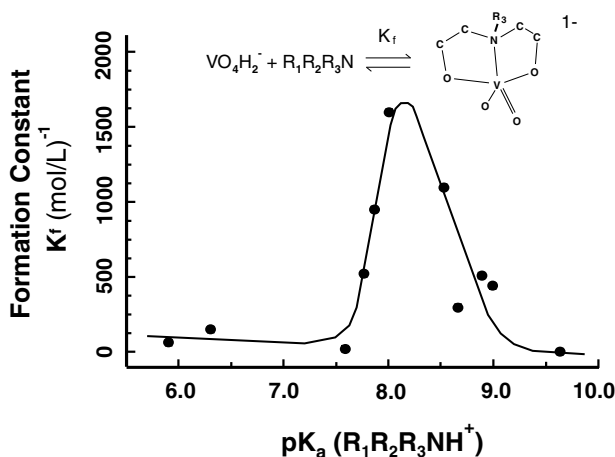
FIGURE 9.5 The formation constants ($VO_4H_2^-$ + H_2L $\quad$ VO_2L^-) for various diethanola-mine vanadate complexes are shown as a function of the pK_a of the ligand. The solid line is provided as a guide and has no theoretical significance. The values are for 0.40 M KCl solutions at room temperature and are taken from the work of Crans and Boukhobza [21].

is maintained by donating or withdrawing electron density from the ligating groups. When the vanadium coordination sphere is expanded, the nucleus will attempt to maintain that electron density. Ligands with a pK_a closest to that of vanadate have the most favorable electronic characteristics. In the second step of the complexation reaction, the amine functionality binds to vanadate and does so in a preferential manner according to its pK_a. Finally, the remaining hydroxyl group enters into the coordination sphere with elimination of a second molecule of water. Of course, the actual stepwise process of complexation is not known, but the end result is independent of that process. The result of this selectivity towards a matched pK_a is a factor of more than 2 orders of magnitude in the formation constant. Of course, other factors deriving from the properties of sidechains and the R group on the nitrogen will exert selective influences on the chemistry.
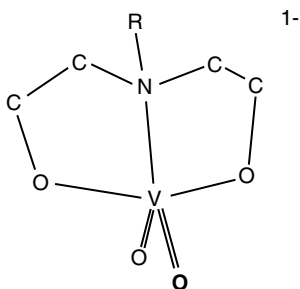
SCHEME 9.5

9.6 PATTERN OF REACTIVITY

The common thread throughout this discussion of the chemistry of monoanionic vanadate ($VO_4H_2^-$) is that the vanadium nucleus has associated with it a preferential electron density that is not readily influenced by ligands. Electrons are either withdrawn from or transferred to the ligating groups as reflected by the influence of pK_a on vanadate esters and their ^{51}V chemical shifts. When the electronic properties are forcibly changed, as in the bisperoxo and bishydroxamido complexes, there is a selective reactivity towards complexation of heteroligands that reflect and compensate for that change. This influence is then reflected in preferential reaction with heteroligands in a manner that leads to a rebalance of the charge density at the nucleus. For instance, because the hydroxamido ligand is a relatively good electron-withdrawing ligand, both ligating groups of bidentate heteroligands are drawn into the coordination sphere of bishydroxamidovanadate. This contrasts with the situation with bisperoxovanadate, where the same ligands react in a monodentate fashion.

Expansion of the coordination geometry proceeds readily but in a selective manner when diethanolamine complexes form. Here, the electron density at the vanadium nucleus is maintained by a matching of ligand pK_a to the pK_a of vanadate. In this example, the behavior is observed where two ligand alkyl hydroxyl oxygens replace vanadate hydroxyl oxygens and thus have a minimal influence on electronic properties. This observation leads to the expectation that the situation will change if complexation is by other classes of ligands with different ligating groups, for instance, sulfhydryl. Because the electronic properties of vanadium have been influenced by the different type of primary ligating group, a preference will then be shown for heteroligands with a pK_a that matches the different electronic properties of the complex.

It is evident that there is a common underlying basis to a number of chemical reactions observed for vanadium(V) and suggests that vanadate reactivity can be moderated and directed. The chemical properties described here indicate that, for certain types of reactions and with judicious choice of ligands, it should be possible to selectively enhance specific functionality of a vanadate complex. For example, it seems likely that selectivity of oxidative reactions by peroxo heteroligand complexes can be improved if appropriate heteroligands are employed. Indeed, such functionality is known for peroxocompounds, and a good example is provided by the substrate thianthrene 5-oxide, where oxidation at the sulfide or at the sulfoxide sulfur can be directed by choice of heteroligand [25]. Development of mimics of the vanadium-dependent nitrogenase will be dependent on the properties of the ancillary ligands employed, and it seems evident that a rational basis can be employed in order to enhance the desired properties. Synthesis of specific types of complexes may well be simplified by taking into account ligand properties that will favor formation of such compounds. However, as graphically illustrated by the reactions of vanadate with diethanolamine ligands, more (in this example, more basicity or more acidity) is not better, and favorable complexation by these ligands is critically dependent on matching the electron donating properties of the ligand to the require-

ments of vanadium. By deliberately mismatching properties, it should be possible to manipulate and enhance reactivity toward desired goals.

REFERENCES

1. Tracey, A.S. and M.J. Gresser. 1988. The characterization of primary, secondary, and tertiary vanadate alkyl esters by 51-V nuclear magnetic resonance spectroscopy. *Can. J. Chem.* 66:2570–2574.
2. Crans, D.C., S.M. Schelble, and L.A. Theisen. 1991. Substituent effects in organic vanadate esters in imidazole-buffered aqueous solutions. *J. Org. Chem.* 56:1266–1274.
3. Tracey, A.S., B. Galeffi, and S. Mahjour. 1988. Vanadium(V) oxyanions. The dependence of vanadate ester formation on the pK_a of the parent alcohols. *Can. J. Chem.* 66:2294–2298.
4. Galeffi, B. and A.S. Tracey. 1988. The dependence of vanadate phenyl ester formation on the acidity of the parent phenols. *Can. J. Chem.* 66:2565–2569.
5. Ray, W.J., Jr., D.C. Crans, J. Zheng, J.W. Burgner, II, H. Deng, and M. Mahroof-Tahir. 1995. Structure of the dimeric ethylene glycol-vanadate complex and other 1,2-diol-vanadate complexes in aqueous solution: Vanadate-based transition-state analog complexes of phosphotransferases. *J. Am. Chem. Soc.* 117:6015–6026.
6. Zhang, B., S. Zhang, and K. Wang. 1996. Synthesis, characterization and crystal structure of cyclic vanadate complexes with monosaccharide derivatives having a free adjacent diol system. *J. Chem. Soc., Dalton Trans.* 3257–3263.
7. Angus-Dunne, S.J., R.J. Batchelor, A.S. Tracey, and F.W.B. Einstein. 1995. The crystal and solution structures of the major products of the reaction of vanadate with adenosine. *J. Am. Chem. Soc.* 117:5292–5296.
8. Gorzsas, A., I. Andersson, and L. Pettersson. 2003. Speciation in the aqueous $H^+/H_2VO_4^-/H_2O_2$/L-(+)-lactate system. *J. Chem. Soc., Dalton Trans.* 2503–2511.
9. Hati, S., R.J. Batchelor, F.W.B. Einstein, and A.S. Tracey. 2001. Vanadium(V) complexes of α-hydroxycarboxylic acids in aqueous solution. *Inorg. Chem.* 40:6258–6265.
10. Ehde, P.M., L. Pettersson, and J. Glaser. 1991. Multicomponent polyanions. 45. A multinuclear NMR study of vanadate(V)-oxalate complexes in aqueous solution. *Acta Chem. Scand.* 45:998–1005.
11. Angus-Dunne, S.J., P.C. Paul, and A.S. Tracey. 1997. A [51]V NMR investigation of the interactions of aqueous vanadate with hydroxylamine. *Can. J. Chem.* 75:1002–1010.
12. Tracey, A.S. and J.S. Jaswal. 1993. Reactions of peroxovanadates with amino acids and related compounds in aqueous solution. *Inorg. Chem.* 32:4235–4243.
13. Tracey, A.S. and J.S. Jaswal. 1992. An NMR investigation of the interactions occurring between peroxovanadates and peptides. *J. Am. Chem. Soc.* 114:3835–3840.
14. Shaver, A., D.A. Hall, J.B. Ng, A.-M. Lebuis, R.C. Hynes, and B.I. Posner. 1995. Bisperoxovanadium compounds: Synthesis and reactivity of some insulin mimetic complexes. *Inorg. Chim. Acta* 229:253–260.
15. Begin, D., F.W.B. Einstein, and J. Field. 1975. An asymmetrical coordinated diperoxo compound. Crystal structure of $K_3[VO(O_2)_2(C_2O_4)]\cdot H_2O$. *Inorg. Chem.* 14:1785–1790.
16. Keramidas, A.D., W. Miller, O.P. Anderson, and D.C. Crans. 1997. Vanadium(V) hydroxylamido complexes: Solid state and solution properties. *J. Am. Chem. Soc.* 119:8901–8915.

17. Paul, P.C., S.J. Angus-Dunne, R.J. Batchelor, F.W.B. Einstein, and A.S. Tracey. 1997. Reactions of hydroxamidovanadate with peptides: Aqueous equilibria and crystal structure of oxobis(hydroxamido)glycylglycinatovanadium(V). *Can. J. Chem.* 75:183–191.

18. Mimoun, H., L. Saussine, E. Daire, M. Postel, J. Fischer, and R. Weiss. 1983. Vanadium(V) peroxo complexes. New versatile biomimetic reagents for epoxidation of olefins and hydroxylation of alkanes and aromatic hydrocarbons. *J. Am. Chem. Soc.* 105:3101–3110.

19. Drew, R.E. and F.W.B. Einstein. 1973. Crystal structure at –100° of ammonium oxoperoxo(pyridine-2,6-dicarboxylato)vanadate(V) hydrate, $NH_4[VO(O_2)(H_2O)$ $(C_5 H_3N(CO_2)_2)]xH_2O$ ($x \approx 1.3$). *Inorg. Chem.* 12:829–835.

20. Bhattacharjee, M., M.K. Chaudhuri, N.S. Islam, and P.C. Paul. 1990. Synthesis, characterization and physiochemical properties of peroxo-vanadium(V) complexes with glycine as the heteroligand. *Inorg. Chim. Acta* 169:97–100.

21. Crans, D.C. and I. Boukhobza. 1998. Vanadium(V) complexes of polydentate amino alcohols: Fine-tuning complex properties. *J. Am. Chem. Soc.* 120:8069–8078.

22. Pettersson, L., B. Hedman, A.-M. Nenner, and I. Andersson. 1985. Multicomponent polyanions. 36. Hydrolysis and redox equilibria of the H^+-HVO_4^{2-} system in 0.6 M Na(Cl). A complementary potentiometric and 51-V NMR study at low vanadium concentrations in acid solution. *Acta Chem. Scand.* A 39:499–506.

23. Pettersson, L., I. Andersson, and B. Hedman. 1985. Multicomponent polyanions. 37. A potentiometric and 51-V NMR study of equilibria in the H^+-HVO_4^{2-} system in 3.0 M Na(ClO_4) medium covering the range $1 < -\lg[H^+] < 10$. *Chem. Scr.* 25:309–317.

24. Tracey, A.S., J.S. Jaswal, and S.J. Angus-Dunne. 1995. Influences of pH and ionic strength on aqueous vanadate equilibria. *Inorg. Chem.* 34:5680–5685.

25. Ligtenbarg, A.G.L., R. Hage, and B.L. Feringa. 2003. Catalytic oxidations by vanadium compounds. *Coord. Chem. Rev.* 237:89–101.

26. Conte, V., F. Di Furia, and S. Moro. 1994. [51]V NMR investigation on the formation of peroxo vanadium complexes in aqueous solution: Some novel observations. *J. Mol. Catal.* 94:323–333.

27. Andersson, I., S.J. Angus-Dunne, O.W. Howarth, and L. Pettersson. 2000. Speciation in vanadium bioinorganic systems. 6. Speciation study of aqueous peroxovanadates, including complexes with imidazole. *J. Inorg. Biochem.* 80:51–58.

28. Jaswal, J.S. and A.S. Tracey. 1993. Reactions of mono- and diperoxovanadates with peptides containing functionalized side chains. *J. Am. Chem. Soc.* 115:5600–5607.

29. Gorzsas, A., I. Andersson, H. Schmidt, D. Rehder, and L. Pettersson. 2003. A speciation study of the aqueous $H^+/H_2VO_4/L$-α-alanyl-L-serine system. *J. Chem. Soc., Dalton Trans.* 1161–1167.

30. Schmidt, H., I. Andersson, D. Rehder, and L. Pettersson. 2001. A potentiometric and [51]V NMR study of the aqueous $H^+/H_2VO_4^-/H_2O_2/L$-α-alanyl-L-histidine system. *Chem. Eur. J.* 7:251–257.

10 Vanadium in Biological Systems

Vanadium is abundant in the biosphere, where it has a well-defined function in some biological systems. It also has pharmacological effects in other systems (see Chapter 11) and is listed in modern nutrition books as being a required ultra trace metal. This chapter focuses on vanadium in the biosphere and on naturally occurring compounds or proteins that interact with vanadium or have vanadium in a structural role. Although vanadium concentrations exceeding 350 mmol/L have been reported in the blood cells of ascidians, concentrations of vanadium in mammals are on average in the 10 nmol/L range.

In biological systems, vanadium interacts with small ligands and binds to transport and binding proteins. Specialized nitrogenases and haloperoxidases exist with vanadium as the structural metal. In order to illustrate how the aqueous chemistry of vanadium contributes to life processes in the biosphere, vanadium interactions in biological systems are described below. The role of vanadate as a phosphate analogue in enzyme reactions is a subject of considerable importance, both in its roles as transition-state and ground-state analogues [1]. In its function as a transition-state analogue, it has influence on the behavior of numerous important enzymes such as phosphorylases, mutases, phosphatases, ribonucleases, and ATPases [2].

10.1 DISTRIBUTION IN THE ENVIRONMENT

Vanadium is widely distributed throughout the Earth's crust and is generally found in low concentrations in both fresh and seawaters. The average concentration in the Earth's crust is about 300 μmol/kg, but concentrations may be up to 20 times this in clays and shales. Freshwater concentrations are highly variable but are in the order of 0.1 μmol/L, whereas ocean water concentrations are about one third of this. In fresh water, the levels typically vary from 0.1 μmol/L by a factor of about 5 higher or lower, though levels can be much higher. At such concentrations, vanadium(V) will exist almost exclusively as monomeric species, either as free vanadate or as ligated complexes. Concentrations such as this will not sustain appreciable levels of any of the oligomeric forms, including decavanadate if the conditions are mildly acidic. In the absence of ligation, the protonation state will vary. Under strongly basic conditions, above a pH of about 12, vanadate will almost exclusively exist as the trianionic species, VO_4^{3-}. Under moderately basic conditions between the pH values of 8.2 and 12, it will be predominantly present as the dianionic compound, VO_4H^{2-}. The principal form will be the monoanionic derivative from pH 8.2 until close to a pH of 3, when it will be protonated to become neutral. However, a second protonation step occurs concurrently with this latter protonation, and the

observed species will be cationic. The second protonation is accompanied by incorporation of water to give an octahedrally coordinated compound. This changes the chemistry somewhat, and the pK_a of the cationic species is actually higher (pK_a 3.88) than that of VO_4H_3 (pK_a 3.08) [3]. All species except the cationic derivative have tetrahedral coordination. Ligand complexes will impose a coordination geometry specific to the ligand, but most such complexes will have five or six coordination. Under mild to strongly acidic conditions, vanadate will be readily reduced to vanadyl if the conditions are suitable for reduction, for instance, the presence of reducing ligands and low water oxygen content. Conversely, both high oxygen levels in the water and high pH will favor a shift of the redox equilibrium toward V(V) species.

In the biosphere, vanadium can be considered to be of two forms, one of which is highly mobile, whereas the other is a virtually immobile form. These are closely connected to the oxidation state of vanadium, where the mobile chemically reactive form conforms more or less, but certainly not exclusively, to the V(V) oxidation state. This is the state that vanadium will predominantly have in gas effluents; in ash from oil, coal, and gas burners; in some minerals; and in surface water. Vanadium(IV) complexes of the types found in minerals will often be relatively immobile but, if subjected to an oxidative environment, can enter the mobile phase in the V(V) oxidation state. Sequestered forms of vanadium can be transported by mechanical processes such as by movements of suspended materials in creeks and rivers, where translocation from terrestrial to lake or marine environments accounts for a high percentage of the movement of vanadium. This procedure does not release the vanadium into the environment in the sense that release from the substrate does; rather, the vanadium is simply redeposited as the sediments settle. However, because of the high surface area of the suspended materials, vanadium can efficiently be removed from the suspended material by chemical reactions and enter into the environment as active species by this process.

The low levels of vanadium in ocean waters clearly show that vanadium is constantly being sequestered and deposited into ocean sediments. Uptake by some algae species and by other vanadium-accumulating organisms might account for much of this removal. In lakes and ponds, vanadium(V) will be complexed by components in sediments, often humic acid materials, and subjected to a reducing environment. Conversion to V(IV) results, and in this state, it will remain for extended time periods unless the sediments are disturbed. Conversely, redox reactions in oxygen-rich ground water moving through or over vanadium-rich materials such as vanadium-containing ore bodies or mine and other industrial wastes can lead to high V(V) levels in those waters. For instance, although it is a solid in ash wastes from coal-burning equipment, if the vanadium is not recovered, it will be rapidly leached into the environment when exposed to water from rain, snow-melt, flood, or other sources. Similarly, vanadium deposited by effluent gases will rapidly find its way into the surface and subsurface waters. Such waters may enter aquifers or appear in surface water, where they present a pollution hazard. Thus, mine tailings and contaminated mill sites are common sources of aquifer and surface water contamination. An example is contamination of the Colorado River. Water moving through mill wastes from an abandoned reduction plant near the Matheson Wetlands

of the Colorado River in Utah enters the ground water and ultimately contaminates the river itself. Examination of flathead minnows in the Colorado River adjacent to and downstream from the mill site revealed vanadium levels at about 8 times the normal levels. Numerous other metals, a number at many times the normal concentrations, were also found in the fish.

Extraction of vanadium from ores and wastes is highly dependent on how the vanadium is bound in the immobile substrate and on the properties of the water itself. The redox rates are strongly dependent on the pH of the aqueous medium, the oxygen levels, and the surface properties of the binding substrate. Interestingly, although rates of oxidation are fast when the vanadyl ion is hydrolyzed, the rates are also fast when the ion is complexed to surfaces via substrate surface hydroxyl groups [4]. On the other hand, oxidation to V(V) can be exceedingly slow or might not occur at all when the V(IV) is complexed by porphyrin ligands and various other organic compounds that are expected to occur in coal or oil deposits. Vanadium(V) can be efficiently removed from water by using zero-valent iron in permeable barriers through which V(V)-contaminated water flows. Such a barrier provides a good reducing environment that converts V(V) to V(IV). Not only vanadium but other metals have been effectively removed from water by this technique. It is not evident, however, what the fate of the vanadium will be once the iron in the barrier is fully oxidized. Iron can form heterometal complexes with vanadium(IV) [5], but whether such complexes are stable enough to prevent oxidation to V(V) is not known. The surface phenomenon discussed above could come into play, and water not depleted in oxygen would quickly release the vanadium. It is likely, therefore, that barriers based on iron/vanadium redox chemistry would have to be replaced. Presumably, proper design would involve recovery of the vanadium, if not the iron, from such barriers.

10.2   VANADIUM-LIGAND COMPLEXES

Vanadium-ligand complexes have been used to probe the structure and activity of many proteins, taking advantage of spectroscopic techniques [6]. There are naturally occurring ligands that bind vanadium, such as the iron binding siderophores. Siderophores are involved in iron homeostasis, and their binding of vanadium appears to be a secondary function [7]. Vanadate does inhibit the transport of iron-siderophore complexes [8], showing there is interaction of vanadium with iron transport systems.

Many natural metabolites, including glutathione, cysteine, ascorbic acid, nucleotides, and carbohydrates, form complexes with vanadium that have been characterized [9–11] (See Chapter 4). The interactions of vanadium and GSH, a particularly well-defined system, could be intimately involved in the interactions of cellular vanadium and redox properties [12]. Early studies of the V(IV)-GSH complex showed that the main binding site for the metal were the two carboxyl groups [13]. Equilibrium studies of the $V(IV)O_2^+$-GSH system in aqueous solution was studied in the pH range of 2 to 11. VL_2H_2 was the predominant species found at physiological pH [14]. Study of the interactions of synthetic analogues of glutathione with oxovanadium V(IV/V) [15] and of the V(V) complexes of cysteine [16], β-mercaptoet-

hanol [17], and dithiothreitol [18] are consistent with the formation of glutathione complexes of V(V). Such complexes might not be oxidatively stable for extended periods of time, but in the presence of oxygen, a redox equilibrium will be established. By this process, some level of the V(V) GSH complex will be maintained until either the glutathione or oxygen is depleted.

10.2.1 AMAVADINE

Amavadine is a naturally occurring vanadium complex that is found only in the *Aminita* mushroom genus. In amavadine, vanadium as V(IV) is complexed to two *N*-hydroxyl-2,2′-iminodipropionic acid ligands. These ligands are unique in that *N*-hydroxyl-2,2′-iminodipropionic acid is the only known naturally occurring ligand that has a higher affinity for vanadium than other metal [19]. The structure of amavadine has been completely elucidated. The vanadium-amavadine complex has four chiral carbons with an **S** configuration and a fifth chiral center generated by how the ligands wrap around the vanadium [20]. The coordination of one of its forms is displayed in Scheme 10.1. This complex has great hydrolytic stability and also exhibits reversible one-electron redox properties. In acidic solutions, amavadine will electrocatalytically oxidize thiols, including naturally occurring cysteine and glutathione [2]. It has been proposed that amavadine serves as an electron-transfer agent in the mushroom.
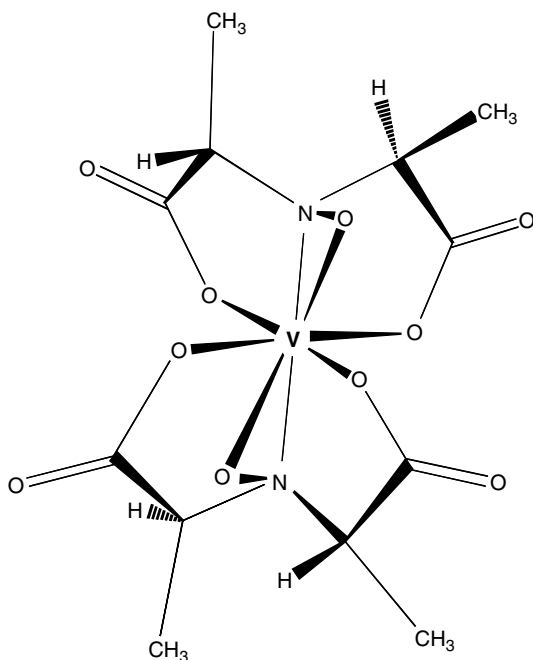
SCHEME 10.1 Coordination of one form of amavadine.

10.3 VANADIUM TRANSPORT AND BINDING PROTEINS

Vanadium can enter cells in anionic or cationic oxygenated forms, via facilitated diffusion or high-affinity energy-dependent protein systems. In the fungus *Neurospora*, vanadate-resistant mutants were isolated with defects in the single phosphate transport system present in that organism. This implies that vanadium was entering the cell as a vanadate analogue of phosphate [21]. The affinity of this high-affinity phosphate transport system for vanadate was 8.2 μM in the normal fungus [22].

Vanadate transport in the erythrocyte was shown to occur via facilitated diffusion in erythrocyte membranes and was inhibited by 4,4'-diisothiocyanostilbene-2,2'-disulfonic acid (DIDS), a specific inhibitor of the band 3 anion transport protein [23]. Vanadium is also believed to enter cells as the vanadyl ion, presumably through cationic facilitated diffusion systems. The divalent metal transporter 1 protein (called DMT1, and also known as Nramp2), which carries iron into cells in the gastrointestinal system and out of endosomes in the transferrin cycle [24], has been proposed to also transport the vanadyl cation. In animal systems, specific transport protein systems facilitate the transport of vanadium across membranes into the cell and between cellular compartments, whereas the transport of vanadium through fluids in the organism occurs via binding to proteins that may not be specific to vanadium.

The ability to transport vanadium is a key factor in the accumulation of vanadium by various organisms. Although vanadium does not appear to be concentrated by higher terrestrial plants, it is accumulated by certain terrestrial fungi, mosses, and lichens. The amanita mushroom, *Amanita muscaria*, concentrates vanadium to levels of about 100 times (2 mmol/kg dry weight) that typically are found in other mushrooms and higher plants. Some freshwater plants also accumulate vanadium to similar levels. In the ocean, a number of marine algae accumulate vanadium, where it is utilized in the function of their vanadium-dependent haloperoxidases. Perhaps the greatest accumulators of all are various ascidians that concentrate vanadium to very high levels, up to about 350 mmol/L in vanadocyte cells. Apparently, the evolutionary development of this enrichment capability is associated with protective mechanisms.

The steps in the accumulation of vanadium in ascidian vanadocyte vacuoules have been well described [25,26] and involve the reduction of the V(V) present in seawater to the V(III) found in the vacuoles (Figure 10.1). The concentration of vanadium in the marine ascidians first involves transport into the bronchial sac in the V(V) form, which crosses the plasma membrane of the vanadocyte using transport systems analogous to the divalent metal transport systems of mammalian systems. Inside the vanadocytes, V(V) is reduced to V(IV) and is shepherded into the vacuole by the vanabins. Within the vacuole, the V(IV) is further reduced to V(III). The vanabins (Section 10.3.1) are a class of vanadium binding proteins whose only function appears to be to chaperone the vanadocyte V(IV) and help it to enter the vanadocyte vacuole. It seems there may be other proteins directly involved in vanadium transport. Vanadium binding proteins with high homology to mammalian glutathione transferases (GST) and having glutathione transferase activity have been isolated from the digestive tract of ascidians [27] and proposed to be involved in
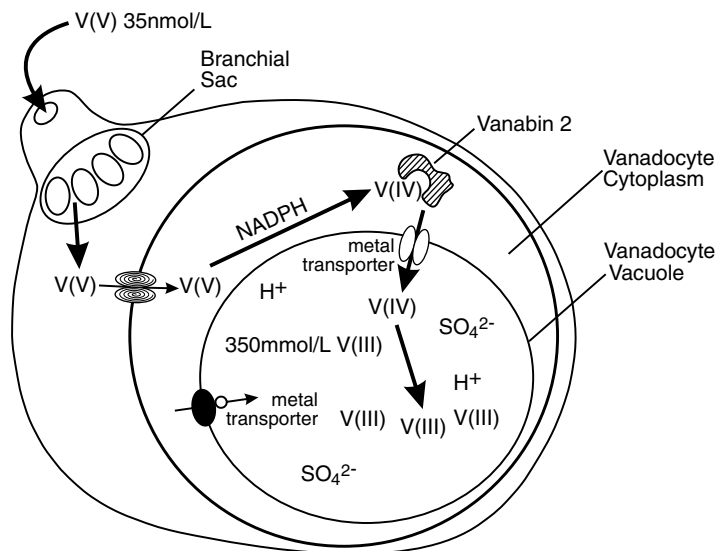
FIGURE 10.1 Ascidian vanadocyte. Modified from Reference 26.

vanadium transport in the digestive systems. The reason for V(III) concentrations in excess of 350 mmol/L in the vanadocyte vacuole is unclear.

There are other proteins that could be involved in the movement of vanadium through the body that do not appear to be specifically designed for the transport of vanadium. Interest in naturally occurring vanadium-binding proteins has increased now that vanadium is widely taken at microgram concentrations in multiple vitamins and at milligram quantities by bodybuilders and other athletes, and is being considered as a therapeutic agent for diabetes and cancer. Such proteins, which in normal metabolism have other functions, do have an affinity for vanadium and could aid in the movement of vanadium through the body. Metallothionein, transferrin, ferritin, and serum albumin are the major metal-binding proteins that are candidates for helping vanadium move throughout a mammal. Because vanadium has been used as a probe of protein structure, there has been much work on the binding of vanadium to these and other proteins [2,6]. Serum albumin, whose major function is to transport free fatty acids in the blood, has multiple binding sites for vanadium. V(V) has been observed in commercial preparations of serum albumin, and up to 20 molecules of V(IV) can be found associated with 1 molecule of this protein. Transferrin, an iron transporting protein found in blood, binds both V(IV) and V(V). It binds the vanadyl cation (VO^{2+}) 10 times more strongly than does serum albumin. The vanadium-transferrin complex is stable enough to withstand analytical treatments, such as HPLC or gel electrophoresis, and transferrin has been found to contain vanadium when isolated from animal tissues [2].

The binding of the insulin-enhancing compound bis(maltolato)oxovanadium (IV) (BMOV) to transferrin and albumin has been studied using EPR and compared to the binding of $VOSO_4$ with these proteins [28,29]. Both proteins could be impor-

tant in the delivery of vanadium metabolites to tissues in mammals. Ferritin is the main iron storage protein in the body, and the amount of ferritin in serum is a direct indicator of how much iron is present in the body. Vanadium has been found to be associated with this protein that binds the vanadium as the cation VO^{2+} [30,31]. Metallothionein is a metal binding protein shown to have antioxidant status [32]. The expression of RNA transcripts encoding metallothionein proteins has been found to be modified by vanadium treatment of normal rats [33] and decreased in diabetic rats [34].

10.3.1 Vanabins

Vanabins are the only proteins currently known whose physiological functions involve the binding of vanadium. These proteins function in binding V(IV) in the ascidians. Much insight into the function of these proteins has come from molecular biology [25,35] and structural studies [26]. Five vanabins have been isolated in *Ascidia sydneinsis samea*, four are associated with the ascidian blood cell, whereas one appears to function in the serum of the ascidian [36]. When originally isolated, BLAST searches of existing genetic sequence databases for the genes encoding the vanabin proteins showed that this was a unique family of proteins in the databases at that time. Further work showed that similar, though not identical, proteins could be isolated from the ascidian *Ciona intestinalis* [37]. These results suggest that the vanabin family of proteins are a special metallochaperone protein family that developed to assist in the accumulation of vanadium from seawater in ascidians. The vanabins have affinities for V(IV) of approximately 2×10^{-5} M. Determination of the 3D solution structure of vanabin(II) using NMR (Figure 10.2) has provided much insight into the function of these proteins [26]. This vanabin has 91 amino acids with 18 cysteines. The structure was found to be bow shaped and contains four α helical sections linked by nine disulfide bonds. Similarly to the gene sequence, there are no structural homologues found in the databases for this protein structure. The 10 to 20 bound VO^{2+} cations seem to be present on the same side of the molecule and are coordinated to amine nitrogens found on amino acids that include lysine, arginine, and histidine, confirming previous EPR studies [26].
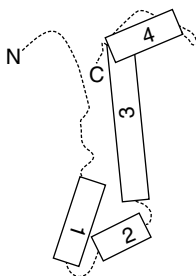
FIGURE 10.2 Structure of Vanabin2. Structural information taken from Reference 26. The rectangular blocks represent the four α helical regions of the protein.

10.4 VANADIUM-CONTAINING ENZYMES

Vanadium-containing nitrogenases have been isolated from bacteria, whereas haloperoxidases have been obtained from marine algae and terrestrial fungi and lichens. The nitrogenases have vanadium incorporated as part of a cofactor, whereas haloperoxidases have vanadate incorporated into the active site. The discovery of these naturally occurring vanadium-containing enzymes is widely quoted in discussions concerning whether or not vanadium is a trace element required for life.

10.4.1 NITROGENASES

The vanadium-dependent nitrogenase can serve as an alternative to the molybdenum nitrogen-fixing enzyme [38], particularly in molybdenum-depleted environments, but has not been as well studied as the peroxidases. However, this enzyme is attracting increasing attention, as the coordination within the active site of the enzyme is increasingly well known. The cofactor for nitrogenase activity is an iron-sulfur-vanadium cluster (Scheme 10.2) that is structurally and functionally analogous to the better-characterized FeMo-cofactor of the Mo-dependent system. The vanadium oxidation state in the cluster appears to be V(III) [39], although assignment of oxidation state in clusters such as this is difficult because of electron delocalization [39,40]. This enzyme probably does not utilize the V(V) oxidation state. On the other hand, the haloperoxidases exclusively use the V(V) oxidation state, and there does not appear to be any evidence that lower oxidation rates are involved in the catalytic process.

10.4.2 VANADIUM-DEPENDENT HALOPEROXIDASES

The haloperoxidases are a class of enzymes that catalyze the oxidation of halides via a reactive peroxometal active site. These enzymes are named according to the most electronegative halide they are able to oxidize. Hence, a bromoperoxidase can oxidize bromide and iodide but not chloride, whereas a chloroperoxidase can oxidize all three. Haloperoxidases are found in most living organisms and predominately fall into two classes: the iron heme-based and vanadium-dependent enzymes. Of these, heme-based enzymes are found in mammals, where they provide a vital
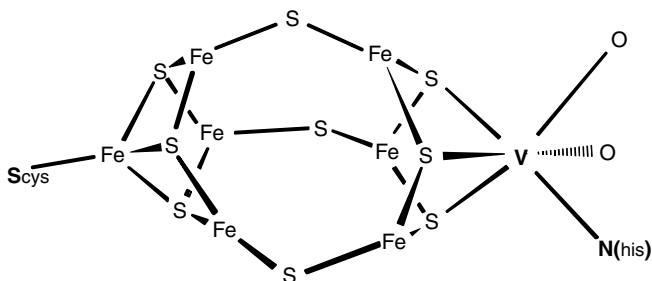
SCHEME 10.2 The cofactor for nitrogenase activity, an iron-sulfur-vanadium cluster.

protective function against pathogenic materials. An iron-based peroxidase, originating from a fungus, is commercially available.

The vanadium-dependent haloperoxidases have been receiving increasing attention since their original discovery in marine algae [41] and later in a variety of terrestrial fungi and lichens [42–45]. Of this latter group of enzymes, the bromoperoxidases occur predominantly in the marine algae, whereas chloroperoxidases are generally found in the terrestrial environment.

There is no redox cycling of vanadium during the oxidative process: The vanadium haloperoxidases catalyze the oxidation of halides by hydrogen peroxide by means of a two-electron donation to generate reactive halogen species, which can subsequently be incorporated into organic substrates to provide halogenated products (Scheme 10.3). As a consequence, the haloperoxidases are responsible for many naturally occurring organic halides [46]. In particular, the marine algae are a major source of halogenated compounds in the environment. In a recent (2004) Euro Chlor workshop on soil chlorine chemistry, a rough estimation gave production of HOBr at about 500,000 tons annually by marine algae, together with another 200,000 tons of $CHBr_3$ [47]. The haloperoxidases are also responsible for numerous other biotransformations such as oxidation of organic precursors, epoxidation, and sulfoxidation [48]. Extensive studies of the structure and function of the vanadium-dependent haloperoxidases have provided detailed information that has been utilized in the synthesis and study of model systems.

Interestingly, there is a close structural correspondence between the active sites of the haloperoxidases and the acid phosphatases that allows both peroxidase and phosphatase activity from the two types of enzymes [49–51]. For instance, recombinant acid phosphatases from both *Shigella flexneri* and *Salmonella enterica* ser. *typhimurium*, when substituted by vanadate, are able to oxidize bromide when in the presence of hydrogen peroxide. However, the turnover rate is quite slow, which is in accord with the phosphatase active sites not being optimized for peroxidase activity [52].

R-H   R-X + H_2O

XOH

H^+, X^-

enz $(O_3N)V(O_2)$ $(O)V(O_3N)$ enz

H_2O H_2O_2

X = Cl, Br, I
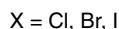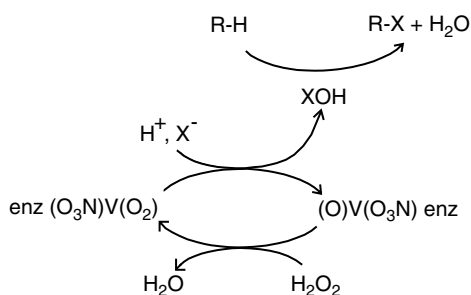
SCHEME 10.3 Halogenated products.

10.4.2.1 Haloperoxidase Active Site

Because the vanadium-dependent haloperoxidases necessarily involve vanadium(V) peroxides, the development of effective models has relied on the discovery of ligands that allow peroxidase function to be mimicked in an efficient manner. Imposition of a desired coordination geometry has been central to many of these studies. X-ray structural data for the nonperoxo form of the peroxidase has shown that the geometry about vanadium in the enzyme active site is quite simple, with vanadate being trigonal bipyramidal with coordination to four oxygens and one histidine nitrogen with the histidine in an axial position [46,50,53]. There are outer sphere hydrogen-bonding contacts between the three equatorial oxygens on the vanadium to two arginines, a lysine, and a serine that stabilize the complex and promote activity. Additionally, there is a second histidine that is within hydrogen-bonding distance of an apical hydroxo group. There is another histidine residue in the outer sphere regions of the bromoperoxidase, which is replaced by a phenylalanine in the chloroperoxidase. Additionally, a lysine has been replaced by an asparagine. Mutagenesis studies have demonstrated the importance of the histidine, arginine, and lysine groups in vanadate binding and in the function of the enzyme [49,54]. Such studies also revealed that chloroperoxidase activity can be induced in a bromoperoxidase by replacement of an arginine by a phenylalanine or tryptophan [54].

The x-ray studies are insufficiently precise to define the charge state of the vanadate in the crystalline enzyme. However, theoretical models of the resting state of the peroxidase have strongly suggested that vanadate is monoanionic with one hydroxo group axial to the N-bound imidazole ring of histidine and also one equatorial hydroxo and two equatorial oxo groups [55]. The vanadium lies at the base of an active site cleft that is about 20 Å deep. One side of the cleft is strongly hydrophobic in character, mostly being formed from proline and phenylalanine amino acid segments, whereas the other side is highly polar with arginine, aspartate, and main chain carbonyl oxygens [56,57]. The base of the cleft is lined with histidine, arginine, lysine, serine, and glycine amino acid groups that bind the vanadium in the active site. Of these groups, only a histidine forms a covalent bond, the remaining groups stabilizing the binding through hydrogen-bonding interactions.

The vanadium is not tightly held in the active site and can be rather easily removed by dialysis against phosphate. Vanadate is readily reincorporated into the enzyme, and its presence in solution will regenerate the enzyme activity. On the basis of x-ray structures and the theoretical calculations, Scheme 10.4 seems to best illustrate the structure and charge state around vanadium and also suggests that model systems might be constructed relatively easily. The theoretical calculations also suggest that the cationic arginine residues in the binding region are critical for sustaining the coordination of the imidazole of the histidine. This is not surprising, given that imidazole is known to only very weakly interact with vanadate. Although it seems that monoperoxovanadate does not bind imidazole as tightly as does the bisperoxide, it does complex imidazole much more tightly than does vanadate [58]. It therefore seems evident that in the active form of the enzyme, where vanadate carries a peroxo group, the imidazole ring will be tightly held. Even here, the cationic residues will play an important role in strengthening the imidazole reaction with
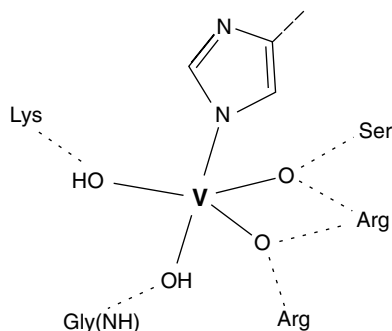
SCHEME 10.4   Structure and charge state around vanadium.

monoperoxovanadate. Also, imidazole binds strongly if it is part of a multidentate ligand, as in histidine-containing dipeptides [59–61], so, also on this basis, the cationic residues will be important in strengthening the complexation of the imidazole ring.

The active site cleft has readily distinguishable hydrophobic and hydrophilic sides. This strongly suggests that the active site will select for organic substrates with matching properties and, furthermore, will catalyze halogenation in a stereoselective manner dependent on the orientation imposed on the substrate by the interacting groups of the active site region. Indeed, it is known from competitive experiments that there is selectivity in reaction rates [57,62].

X-ray studies have revealed that a major difference between chloroperoxidase and bromoperoxidase is found in one outer sphere histidine group in the bromoperoxidase. In the chloroperoxidase, the histidine is replaced by a phenylalanine. The other two histidines are conserved. Proposals for the reaction sequence of the bromoperoxidase suggest that this histidine is involved in bromoperoxidase activity [46]. Clearly, however, it is not necessary for such activity.

10.4.2.2 Haloperoxidase Model Compounds

A detailed discussion of possible mechanisms by which bromoperoxidase functions in the marine environment [46] has revealed a little of the complex chemistry associated with this enzyme. Bisperoxovanadate is known to be able to oxidize bromide and to generate organobromides [63,64]. This particular reaction with bisperoxovanadate is not an efficient one, and considerable effort has gone into the development of effective catalytic systems. The early work on developing model haloperoxidases systems did not have the benefit of single crystal x-ray structural information on the native enzyme but relied on data from x-ray absorption studies (EXAFS, XANES) and on ^{51}V NMR spectroscopy to delineate the coordination around vanadium. The studies revealed an oxygen-rich environment supplemented by nitrogen coordination. Using this as a basis, models based on carboxylate [65], phenolate [66], imidazole [67,68], and Schiff base [69,70] precursorswere studied. Theoretical calculations, together with solution studies, have also provided insight into peroxidase activity [55,71].
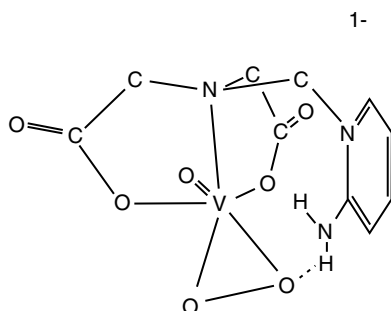
SCHEME 10.5 Hydrogen bond between one peroxo oxygen and a hydrogen of the amino group.

The advent of a well-defined structure led to rapid progress in development of model haloperoxidases systems. A wide variety of approaches were adopted. An interesting development was the finding that vanadate could be incorporated into phytase so that peroxidase activity was obtained [72]. This system catalyzed enantioselective sulfoxidation. Other model haloperoxidases based on monoperoxovanadium(V) complexes of acetic acid derivatives of ethanolamine and related compounds have also been found to effectively model the oxidation of sulfides [73]. X-ray structure and NMR studies of a related complex with an aminopyridine sidechain have revealed the presence of a rather strong hydrogen bond between one peroxo oxygen and a hydrogen of the amino group (Scheme 10.5) [74]. Hydrogen bonds similar to this may be very important for effective function of model peroxidases. This point has been emphasized by other work with similar model systems that emphasize the importance of *N*- and *O*-ligating donor groups [75]. Scheme 10.6 depicts various ligands that have been used together with hydrogen peroxide as models for peroxidase activity. Numerous other ligands have been utilized in the quest for efficient and effective models [76]. However, it does not appear that model systems where the vanadium is covalently bound only by histidine, and is stabilized by outer sphere, predominantly hydrogen-bonding, interactions have been realized.
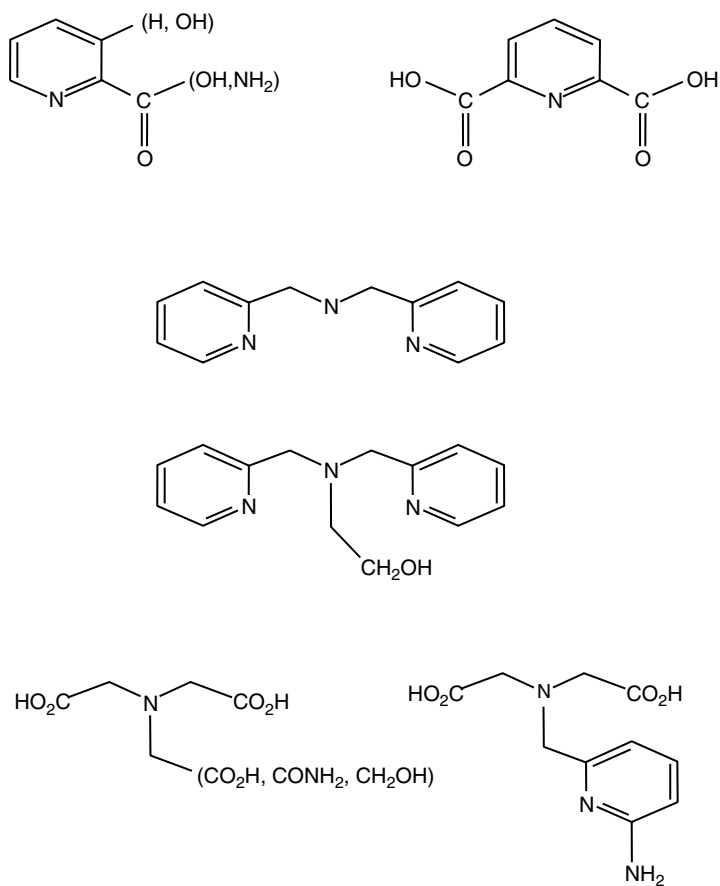
SCHEME 10.6   Ligands used with hydrogen peroxide as models of peroxidase activity.

REFERENCES

1. Gresser, M.J., A.S. Tracey, and N.D. Chasteen. 1990. Vanadates as phosphate analogs in biochemistry. Vanadium in biological systems. Dordrecht, Boston, London: Kluwer Academic Publishers. pp 63–79.

2. Crans, D.C., J.J. Smee, E. Gaidamauskas, and L. Yang. 2004. The chemistry and biochemistry of vanadium and the biological activities exerted by vanadium compounds. *Chem. Reviews* 104:849–902.

3. Pettersson, L., B. Hedman, A.M. Nenner, and I. Andersson. 1985. Multicomponent polyanions. 36. Hydrolysis and redox equilibria of the H^+-HVO_4^{2-} system in 0.6 M Na(Cl). A complementary potentiometric and 51-V NMR study at low vanadium concentrations in acid solution. *Acta Chem. Scand.* 39:499–506.

4. Wehrli, B. and W. Stumm. 1989. Vanadyl in natural waters: Adsorption and hydrolysis promote oxygenation. *Geochim. Cosmochim. Acta* 53:69–77.

5. Nunes, G.G., G.R. Friedermann, M.H. Herbst, R.B. Barthem, N.V. Vugman, J.E. Barclay, D.J. Evans, P.B. Hitchcock, G.J. Leigh, E.L. Sa, and others. 2003. The first hetero-binuclear alkoxide of iron and vanadium: Structural and spectroscopic features. *Inorg. Chem. Commun.* 6:1278–1281.

6. Chasteen, N.D. 1995. Vanadium-protein interactions. *Metal Ions in Biological Systems* 31:231–247.

7. Boukhalfa, H. and A.L. Crumbliss. 2002. Chemical aspects of siderophore mediated iron transport. *BioMetals* 15:325–339.

8. Cornish, A.S. and W.J. Page. 2000. Role of molybdate and other transition metals in the accumulation of protochelin by *Azotobacter vinelandii*. *Appl. and Environ. Microbiol.* 66:1580–1586.

9. Baran, E.J. 2000. Oxovanadium(IV) and oxovanadium(V) complexes relevant to biological systems. *J. Inorg. Biochem.* 80:1–10.

10. Ferrer, E.G., P.A.M. Williams, and E.J. Baran. 2005. On the interaction of oxovanadium(IV) with homocysteine. *Biol. Trace Elem. Res.* 105:53–58.

11. Williams, P.A.M., S.B. Etcheverry, D.A. Barrio, and E.J. Baran. 2006. Synthesis, characterization, and biological activity of oxovanadium(IV) complexes with polyalcohols. *Carbohydr. Res.* 341:717–724.

12. Macara, I.G., K. Kustin, and L.C. Cantley, Jr. 1980. Glutathione reduces cytoplasmic vanadate. Mechanism and physiological implications. *Biochim. Biophys. Acta*, 629:95–106.

13. Delfini, M., E. Gaggelli, A. Lepri, and G. Valensin. 1985. Nuclear magnetic resonance study of the oxovanadium-(glutathione)^2 complex. *Inorg. Chim. Acta* 107:87–89.

14. Pessoa, J.C., I. Tomaz, T. Kiss, E. Kiss, and P. Buglyo. 2002. The systems V(IV)O^{2+}–glutathione and related ligands: A potentiometric and spectroscopic study. *J. Biol. Inorg. Chem.* 7:225–240.

15. Tasiopoulos, A.J., A.N. Troganis, Y. Deligiannakis, A. Evangelou, T.A. Kabanos, J.D. Woollins, and A. Slawin. 2000. Synthetic analogs for oxovanadium(IV/V)-glutathione interaction: An NMR, EPR, synthetic and structural study of oxovanadium(IV/V) compounds with sulfhydryl-containing pseudopeptides and dipeptides. *J. Inorg. Biochem.* 79:159–166.

16. Bhattacharyya, S., A. Martinsson, R.J. Batchelor, F.W.B. Einstein, and A.S. Tracey. 2001. N,N-Dimethylhydroxamidovanadium(V). Interactions with sulfhydryl-containing ligands: V(V) equilibria and the structure of a V(IV) dithiothreitol complex. *Can. J. Chem.* 79:938–948.

17. Bhattacharyya, S., R.J. Batchelor, F.W.B. Einstein, and A.S. Tracey. 1999. Crystal structure and solution studies of the product of the reaction of β-mercaptoethanol with vanadate. *Can. J. Chem.* 77:2088–2094.

18. Paul, P.C. and A.S. Tracey. 1997. Aqueous interactions of vanadate and peroxovanadate with dithiothreitol. Implications for the use of this redox buffer in biochemical investigations. *J. Biol. Inorg. Chem.* 2:644–651.

19. Bayer, E. 1995. Amavadin, the vanadium compound of amanitae. *Metal Ions in Biological Systems* 31:407–421.

20. Armstrong, E.M., R.L. Beddoes, L.J. Calviou, J.M. Charnock, D. Collison, N. Ertok, J.H. Naismith, and C.D. Garner. 1993. The chemical nature of amavadin. *J. Am. Chem. Soc.* 115:807–808.

21. Bowman, B.J., K.E. Allen, and C.W. Slayman. 1983. Vanadate-resistant mutants of *Neurospora crassa* are deficient in a high-affinity phosphate transport system. *J. Bacteriol.* 153:292–296.

22. Bowman, B.J. 1983. Vanadate uptake in *Neurospora crassa* occurs via phosphate transport system II. *J. Bacteriol.* 153:286–291.

23. Yang, X., K. Wang, J. Lu, and D.C. Crans. 2003. Membrane transport of vanadium compounds and the interaction with the erythrocyte membrane. *Coord. Chem. Rev.* 237:103–111.

24. Ghio, A.J., C.A. Piantadosi, X. Wang, L.A. Dailey, J.D. Stonehuerner, M.C. Madden, F. Yang, K.G. Dolan, M.D. Garrick, and L.M. Garrick. 2005. Divalent metal transporter-1 decreases metal-related injury in the lung. *Am. J. of Physiol. Lung Cell. & Mol. Physiol.* 289:L460–7.

25. Michibata, H., N. Yamaguchi, T. Uyama, and T. Ueki. 2003. Molecular biological approaches to the accumulation and reduction of vanadium by ascidians. *Coord. Chem. Rev.* 237:41–51.

26. Hamada, T., M. Asanuma, T. Ueki, F. Hayashi, N. Kobayashi, S. Yokoyama, H. Michibata, and H. Hirota. 2005. Solution structure of vanabin2, a vanadium(IV)-binding protein from the vanadium-rich ascidian *Ascidia sydneiensis samea. J. Am. Chem. Soc.* 127:4216–4222.

27. Yoshinaga, M., T. Ueki, N. Yamaguchi, K. Kamino, and H. Michibata. 2006. Glutathione transferases with vanadium-binding activity isolated from the vanadium-rich ascidian *Ascidia sydneiensis samea. Biochim. Biophys. Acta* 1760:495–503.

28. Willsky, G.R., A.B. Goldfine, P.J. Kostyniak, J.H. McNeill, L.Q. Yang, H.R. Khan, and D.C. Crans. 2001. Effect of vanadium(IV) compounds in the treatment of diabetes: *In vivo* and *in vitro* studies with vanadyl sulfate and bis(maltolato)oxovanadium(IV). *J. Inorg. Biochem.* 85:33–42.

29. Liboiron, B.D., K.H. Thompson, G.R. Hanson, E. Lam, N. Aebischer, and C. Orvig. 2005. New insights into the interactions of serum proteins with bis(maltolato)oxovanadium(IV): transport and biotransformation of insulin-enhancing vanadium pharmaceuticals. *J. Am. Chem. Soc.* 127:5104–5115.

30. Chasteen, N.D., E.M. Lord, H.J. Thompson, and J.K. Grady. 1986. Vanadium complexes of transferrin and ferritin in the rat. *Biochim. Biophys. Acta* 884:84–92.

31. Grady, J.K., J. Shao, P. Arosio, P. Santambrogio, and N.D. Chasteen. 2000. Vanadyl(IV) binding to mammalian ferritins. An EPR study aided by site-directed mutagenesis. *J. Inorg. Biochem.* 80:107–113.

32. Cai, L., J.B. Klein, and Y.J. Kang. 2000. Metallothionein inhibits peroxynitrite-induced DNA and lipoprotein damage. *J. Biol. Chem.* 275:38957–60.

33. Chakraborty, T., S. Samanta, B. Ghosh, N. Thirumoorthy, and M. Chatterjee. 2005. Vanadium induces apoptosis and modulates the expressions of metallothionein, Ki-67 nuclear antigen, and p53 during 2-acetylaminofluorene-induced rat liver preneoplasia. *J. Cell. Biochem.* 94:744–762.

34. Willsky, G.R., L.-H. Chi, D.P. Gaile, Z. Hu, and D.C. Crans. 2006. Diabetes altered gene expression in rat skeletal muscle corrected by oral administration of vanadyl sulfate. *Physiol. Genomics* 26:192–201.

35. Yamaguchi, N., K. Kamino, T. Ueki, and H. Michibata. 2004. Expressed sequence tag analysis of vanadocytes in a vanadium-rich ascidian, *Ascidia sydneiensis samea*. *Marine Biotech.* 6:165–174.

36. Yoshihara, M., T. Ueki, T. Watanabe, N. Yamaguchi, K. Kamino, and H. Michibata. 2005. VanabinP, a novel vanadium-binding protein in the blood plasma of an ascidian, *Ascidia sydneiensis samea. Biochim. Biophys. Acta* 1730:206–214.

37. Trivedi, S., T. Ueki, N. Yamaguchi, and H. Michibata. 2003. Novel vanadium-binding proteins (vanabins) identified in cDNA libraries and the genome of the ascidian *Ciona intestinalis. Biochim. Biophys. Acta* 1630:64–70.

38. Eady, R.R. 1995. Vanadium nitrogenases of *Azotobacter. Metal Ions in Biological Systems* 31:363–405.

39. Zuo, J.L., H.C. Zhou, and R.H. Holm. 2003. Vanadium-iron-sulfur clusters containing the cubane-type [VFe$_3$S$_4$] core unit: Synthesis of a cluster with the topology of the P[N] cluster of nitrogenase. *Inorg. Chem.* 42:4624–4631.

40. Carney, M.J., J.A. Kovacs, Y.P. Zhang, G.C. Papaefthymiou, K. Spartalian, R.B. Frankel, and R.H. Holm. 1987. Comparative electronic properties of vanadium-iron-sulfur and molybdenum-iron-sulfur clusters containing isoelectronic cubane-type [VFe$_3$S$_4$]$^{2+}$ and [MoFe$_3$S$_4$]$^{3+}$ cores. *Inorg. Chem.* 26:719–724.

41. Vilter, H. 1984. Peroxidases from *Phaeophyceae*: A vanadium(V)-dependent peroxidase from *Ascophylum nodosum. Phytochem.* 23:1387–1390.

42. de Boer, E., Y. van Kooyk, M.G.M. Tromp, H. Plat, and R. Wever. 1986. Bromoperoxoperoxidase from *Ascophyllum nodosum*: A novel class of enzymes containing vanadium as a prosthetic group. *Biochim. Biophys. Acta* 869:48–52.

43. Vollenbroek, E.G.M., L.H. Simons, J.W.P.M. Schijndel, P. Barnett, M. Balzar, H. Dekker, C. van der Linden, and R. Wever. 1995. Vanadium chloroperoxidases occur widely in nature. *Biochem. Soc. Trans.* 23:267–271.

44. Soedjak, H.S. and A. Butler. 1990. Characterization of vanadium bromoperoxidase from *Macrocystis* and *Fucus*: Reactivity of vanadium bromoperoxidase toward acyl and alkyl peroxides and bromination of amines. *Biochemistry* 29:7974–7981.

45. Barnett, P., W. Hemrika, H.L. Dekker, A.O. Muijsers, R. Renirie, and R. Wever. 1998. Isolation, characterization, and primary structure of the vanadium chloroperoxidase from the fungus *Embellisia didymospor. J. Biol. Chem.* 273:23381–23387.

46. Butler, A. and J.N. Carter-Franklin. 2004. The role of vanadium peroxidase in the biosynthesis of halogenated marine natural products. *Nat. Prod. Rep.* 21:180–188.

47. Wever, R. 2004. Vanadium haloperoxidases and their role in the formation of chlorinated compounds. *Euro Chlor workshop on soil chlorine chemistry. Workshop proceedings*, Euro chlor, Brussels. pp. 29–35.

48. Littlechild, J. 1999. Haloperoxidases and their role in biotransformation reactions. *Curr. Opin. Chem. Biol*. 3:28–34.

49. Hemrika, W., R. Renirie, S. Macedo-Ribeiro, A. Messershmidt, and R. Wever. 1999. Heterologous expression of the vanadium-containing chloroperoxidase from *Curvularia inaequalis* in *Saccharomyces cerevisiae* and site-directed mutagenesis of the active site residues His(496), Lys(353), Arg(360), and Arg(490). *J. Biol. Chem.* 274:23820–23827.

50. Renirie, R., W. Hemrika, and R. Wever. 2000. Peroxidase and phosphatase activity of active-site mutants of vanadium chloroperoxidase from the fungus *Curvularia inaequalis*. *J. Biol. Chem.* 275:11650–11657.

51. Littlechild, J., E. Garcia-Rodriguez, A. Dalby, and M. Isupov. 2002. Structural and functional comparisons between vanadium haloperoxidase and acid phosphatase enzymes. *J. Mol. Recognit.* 15:291–296.

52. Tanaka, N., V. Dumay, Q. Liao, A.J. Lange, and R. Wever. 2002. Bromoperoxidase activity of vanadate-substituted acid phosphatases from *Shigella flexneri* and *Salmonella enterica ser. typhimurium*. *Eur. J. Biochem.* 269:2162–2167.

53. Messershmidt, A. and R. Wever. 1996. X-ray structure of a vanadium-containing enzyme: Chloroperoxidase from the fungus *Curvularia inaequalis*. *Proc. Natl. Acad. Sci. U. S. A.* 93:392–396.

54. Ohshiro, T., J. Littlechild, E. Garcia-Rodriguez, M.N. Isupov, Y. Iida, T. Kobayashi, and Y. Izumi. 2004. Modification of halogen specificity of a vanadium-dependent bromoperoxidase. *Protein Sci. ACS Symp. Ser. ACS Symp. Ser.* 13:1566–1571.

55. Zampella, G., J.Y. Kravitz, C.E. Webster, P. Fantucci, M.B. Hall, H.A. Carlson, V.L. Pecoraro, and L. de Gioia. 2004. Quantum mechanical models of the resting state of the vanadium-dependent haloperoxidase. *Inorg. Chem.* 43:4127–4136.

56. Messershmidt, A., L. Prade, and R. Wever. 1998. Chloroperoxidase from *Curvularia inaequalis*: x-ray structures of native and peroxide form reveal vanadium chemistry in vanadium haloperoxidases. *ACS Symp. Ser.* 711:186–201.

57. Butler, A., R.A. Tschirret-Guth, and M.T. Simpson. 1998. Reactivity of vanadium bromoperoxidase. *ACS Symp. Ser.* 711: 202–215.

58. Andersson, I., S.J. Angus-Dunne, O.W. Howarth, and L. Pettersson. 2000. Speciation in vanadium bioinorganic systems. 6. Speciation study of aqueous peroxovanadates, including complexes with imidazole. *J. Inorg. Biochem.* 80:51–58.

59. Fritzsche, M., V. Vergopoulos, and D. Rehder. 1993. Complexation of histidine and alanylhistidine by vanadate in aqueous medium. *Inorg. Chim. Acta* 211:11–16.

60. Jaswal, J.S. and A.S. Tracey. 1993. Reactions of mono- and diperoxovanadates with peptides containing functionalized side chains. *J. Am. Chem. Soc.*115:5600–5607.

61. Schmidt, H., I. Andersson, D. Rehder, and L. Pettersson. 2001. A potentiometric and ^{51}V NMR study of the aqueous $H^+/H_2VO_4^-/H_2O_2$ /L-β-alanyl-L-histidine system. *Chemistry: A European Journal* 7:251–257.

62. Tschirret-Guth, R.A. and A. Butler. 1994. Evidence for organic substrate binding to vanadium bromoperoxidase. *J. Am. Chem. Soc.* 116:411–412.

63. de la Rosa, R.I., M.J. Clague, and A. Butler. 1992. A functional mimic of vanadium bromoperoxidase. *J. Am. Chem. Soc.* 114:760–761.

64. Bhattacharjee, M. 1992. Activation of bromide by vanadium pentoxide for the bromination of aromatic hydrocarbons: Reaction mimic for the enzyme bromoperoxidase. *Polyhedron* 11:2817–2817.

65. Rehder, D., W. Priebsch, and M. von Oeynhausen. 1989. Structural characterization of a monomer V(V) and a (2+4)-nuclear V(IV)V(V) carboxylato complex. Models for vanadium-dependent peroxidases. *Angewandte Chemie* 28:1221–1235.

66. Holmes, S. and C.J. Carrano. 1991. Models for the binding site in bromoperoxidase: Mononuclear vanadium(V) phenolate complexes of the hydridotris(3,5-dimethylpyrazolyl)borate ligand. *Inorg. Chem.* 30:1231–1235.

67. Vergopoulos, V., W. Priebsch, M. Fritzsche, and D. Rehder. 1993. Binding of L-histidine to vanadium. Structure of exo-[VO$_2$\{N-(2-oxidonaphthal)-His\}]. *Inorg. Chem.* 32:1844–1849.

68. Cornman, C.R., J. Kampf, and V.L. Pecoraro. 1992. Structural and spectroscopic characterization of V(V)O-imidazole complexes. *Inorg. Chem.* 31:1981–1983.

69. Colpas, G.J., B.J. Hamstra, J.W. Kampf, and V.L. Pecoraro. 1994. Preparation of VO(3+) and VO$_2$(+) complexes using hydrolytically stable, asymmetric ligands derived from Schiff base precursors. *Inorg. Chem.* 33:4669–4675.

70. Asgedom, G., A. Sreedhara, J. Kivikoski, E. Kolehmainen, and C.P. Rao. 1996. Structure, characterization and photoreactivity of monomeric dioxovanadium(V) Schiff-base complexes of trigonal-bipyramidal geometry. *J. Chem. Soc., Dalton Trans.* 93–97.

71. Conte, V., O. Bortolini, M. Carraro, and S. Moro. 2000. Models for the active site of vanadium-dependent haloperoxidases: Insight into the solution structure of peroxovanadium compounds. *J. Inorg. Biochem.* 80:41–49.

72. van de Velde, F., L. Koneman, F. van Rantwijk, and R.A. Sheldon. 2000. The rational design of semisynthetic peroxidases. *Biotechnol. Bioeng.* 67:87–96.

73. Smith, T.S. and V.L. Pecoraro. 2002. Oxidation of organic sulfides by vanadium haloperoxidase model complexes. *Inorg. Chem.* 41:6754–6760.

74. Kimblin, C., X. Bu, and A. Butler. 2002. Modeling the catalytic site of vanadium bromoperoxidase: Synthesis and structural characterization of intramolecularly H-bonded vanadium(V) oxoperoxo complexes, [VO(O$_2$)(NH$_2$pyg$_2$)]K and [VO(O$_2$)(BrNH$_2$pyg$_2$)]K. *Inorg. Chem.* 41:161–163.

75. Casny, M. and D. Rehder. 2004. Molecular and supramolecular features of oxoperoxovanadium complexes containing O$_3$N, O$_2$N$_2$ and ON$_3$ donor sets. *J. Chem. Soc., Dalton Trans.* 839–846.

76. Ligtenbarg, A.G.L., R. Hage, and B.L. Feringa. 2003. Catalytic oxidations by vanadium compounds. *Coord. Chem. Rev.* 237:89–101.

11 The Influence of Vanadium Compounds on Biological Systems

Interest in understanding the biological effects of vanadium compounds has been stimulated by the potential uses of vanadium as a therapy for diabetes or cancer and the availability of vanadium in supplements widely taken by the general population and athletes. The first modern indications of the biological effects of vanadium compounds was the 1977 finding that vanadium found in muscle inhibited the sodium potassium ATPase [1]. This finding prompted a search into the general role of vanadium in biological systems [2]. This chapter contains an overview of recent studies involving the impact of experiments in which vanadium compounds are added to enzymes involved in phosphate metabolism, cell membranes, whole cells, and animals. Detailed studies involving the chemistry of vanadium compounds added to purified proteins and nucleic acids can be found in specialized volumes [3,4] and reviews [5]. The work described here includes descriptions of living organisms in which doses of vanadium in the mmol/L to nmol/L range are utilized experimentally. The lower range of concentrations are generally employed when vanadium compounds are added directly to cells, whereas the higher range is utilized when vanadium compounds are given orally to animals.

The effects of vanadium compounds on biological systems are presented in three parts. The first section deals with the effects of vanadium compounds on living systems and includes nutrition and basic toxicology. It provides a discussion of the important enzymes inhibited by vanadium compounds and the basic effects on growth and development observed when vanadium compounds are added to cells growing in tissue culture. The second section focuses on the pharmacological uses of vanadium compounds in cancer and diabetes. Finally, a basic overview of the oxidation-reduction processes is provided, and the biological phosphorylation/dephosphorylation signal transduction cascades that are part of the mechanism of action of vanadium-based pharmacological agents are discussed.

11.1 VANADIUM COMPOUNDS ON BIOLOGICAL SYSTEMS: CELLULAR GROWTH, OXIDATION-REDUCTION PATHWAYS, AND ENZYMES

Characteristics of biological systems, coupled with the rich chemistry of vanadium in aqueous solutions, make the study of effects of vanadium compounds in living systems difficult. The cell is divided into different organelles and vesicles by mem-

branes, and each compartment could have different pH values, different abilities to accumulate vanadium, and different natural ligands for vanadium. Combining the effects of cellular architecture with the pH and concentration-dependent equilibria that govern vanadium chemistry could likely result in different oligomeric species, with varying oxidation states, being found in different parts of the cell when a single vanadium compound is administered to that cell. For instance, as determined by EPR, V(IV) species were found inside red cells that were exposed only to the V(V) species, vanadate [6]. The V(IV) EPR resonance was also seen in spectra obtained from cells after growth in the presence of V(V) vanadate tetramer. In these experiments, the form of vanadium in the cells and growth medium was verified using EPR and ^{51}V NMR [7]. The finding of decavanadate ($V_{10}O_{25}{}^{6-}$) ^{51}V NMR resonances in yeast cells growing in 5 mM vanadate at pH 6.5 strongly implies that vanadium can be concentrated inside acidic cellular organelles, as the average cellular concentration of vanadium seems to be well below 1 mM, and the pH of the cytoplasm is usually over 6.5 [8]. In addition, these results demonstrate that vanadium speciation reactions are occurring in living cells.

It has been demonstrated that the distribution of vanadium species inside the cell can depend on the form in which the vanadium is administered, as was seen in fish where a different distribution of vanadium in red blood cells (RBCs) was found depending upon whether metavanadate or decavanadate was given. In contrast to this, a similar accumulation was found in plasma and cardiac cytosol. However, the ratio of vanadium in plasma to vanadium in RBCs increased over time with metavanadate administration and remained constant for decavanadate administration. When either of the vanadium compounds was used, most of the vanadium was first found in plasma before moving into the mitochondrial fraction [9,10]. Although one can know with some certainty what vanadium compound is given to an animal or put into a tissue culture growth medium, it is difficult to always know the identity of the active form inside the cell.

Because biological systems are highly susceptible to strong experimental variation, it is difficult to compare the effects of added vanadium compounds in studies from different laboratories. It is difficult to design an experiment that can unequivocally differentiate the effectiveness of two different vanadium compounds. These problems have frequently hampered studies of the antidiabetic properties of vanadium compounds using the noninbred Wistar rat strain in which genetic variability of each animal must be added to the list of biological variables.

Extrapolating from well-characterized enzymatic inhibition in test tubes, numerous mechanistic ideas concerning the *in vivo* effects of vanadium compounds have been advanced. The effects of vanadium compounds as transition-state analogs of certain enzymes with a phosphoprotein intermediate in their reaction scheme is proposed to account for the action of vanadium [11] in many biological systems. Unfortunately, it is often difficult to determine if the inhibition observed in the test tube occurs *in vivo*. For example, although vanadate is a potent inhibitor of plasma membrane ion pumps (such as the sodium potassium ATPase) in the test tube, it is difficult to determine if these pumps are actually inhibited in animals exposed to vanadium compounds. Currently, the role of vanadium compounds as protein phosphatase (PTP) inhibitors is believed to be related to the metabolic effects of this

metal. It is experimentally possible to determine whether or not cellular proteins are phosphorylated and whether this phosphorylation occurs at serine, threonine, or tyrosine residues. The hypothesis implies that vanadium compound treatment would increase protein phosphorylation levels if vanadium is inhibiting protein phosphatases, and that has been observed in multiple cell and animal systems [12,13].

11.1.1 VANADIUM COMPOUNDS AND OXIDATION-REDUCTION REACTIONS

Interconversion between V(III), V(IV), and V(V) vanadium species is constantly occurring inside of cells. Evidence is accumulating that ligated derivatives of vanadium are not stable in the body; the vanadium administered as a drug in any form will seek its preferred equilibrium distribution. This is inevitable because the vast majority of complexes are not hydrolytically stable so that once dissociation occurs, the vanadium will most likely complex other ligands found in its environment. The ligands available for complexation with the dissociated vanadium will be determined by the cellular compartment or body fluid in which the dissociation occurs. Therefore, understanding the oxidation-reduction interactions of vanadium with natural products is important in understanding the full effects of therapeutically administered vanadium. The natural cellular reducing compounds glutathione (GSH) and ascorbic acid bind vanadium and readily reduce V(V) to V(IV)[14]. Only in oxygen-depleted regions will reduction be complete; in the presence of oxygen, a redox equilibrium will be established.

GSH has been proposed to be part of the thiol cycling in mammalian cells that may transduce oxidative stress redox signaling into the induction of many genes involved in proliferation, differentiation, and apoptosis [15]. Studies with pure chemical systems have confirmed the reduction of V(V) maltol compounds by GSH or ascorbic acid [16]. Putative glutathione transferase enzymes that bind vanadium have been isolated from an ascidian that accumulates vanadium in specialized cells to over 350 mM [17].

H_2O_2 is part of normal signaling in cells [18]. When H_2O_2 acts as a second messenger, the mechanism is believed to involve reversible oxidation of catalytic cysteine residues in enzymes such as the protein tyrosine phosphatases (PTPases), which are also inhibited by vanadium compounds. This thiol-dependent reversible reduction can cause conformational changes in the enzyme and has been found to protect protein tyrosine phosphatase-1B (PTP1B) from irreversible oxidative inactivation by allowing redox reactions to be involved in the regulation of this enzyme [19]. The vanadate-dependent NADH oxidation activity associated with plasma membranes is one way vanadium may generate H_2O_2 and is described below.

11.1.1.1 Vanadium-Dependent NADH Oxidation Activity

Vanadate-stimulated NAD(P)H oxidation activity was first reported in the erythrocyte membrane [20] and has been found in widely diverse membranes including mammalian rat liver [21], the sugar beet plant [22], and the fungus *Saccharomyces cerevisiae* [23] membrane. The kinetics of NADH oxidation [24] observed in the presence of vanadate and plasma membranes show a variable lag, with H_2O_2 and

O_2^- being products of the reaction. The reaction is stimulated by a phosphovanadium anhydride when vanadate [V(V)] is added to yeast plasma membranes in phosphate buffer [23].

The chemical mechanism of the reaction has been proposed to be a free radical chain system [25,26] and to be a consequence of vanadate stimulation of NAD(P)H oxidation by O_2^- rather than being caused by a specific vanadate-stimulated oxygenase or dehydrogenase. It was proposed that these vanadium-dependent reactions contribute to the toxicity of vanadate [27]. Studies in *Saccharomyces cerevisiae* have demonstrated that these reactions are not involved in vanadium toxicity [28]. In fact, the kinetics of vanadium growth inhibition were the same during aerobic and anaerobic growth of the yeast, implying that no oxidative process was required for vanadium toxicity. EPR studies have implied that the vanadate-mediated hydroxyl radical generation from superoxide in the presence of NADH was due to a Fenton mechanism rather than a Haber-Weiss reaction [29].

Other forms of vanadium have been implicated in the stimulation of the plasma membrane vanadate-dependent NAD(P)H oxidation reaction. Decavanadate has been shown to be a more potent stimulator of the vanadate-dependent NADH oxidation activity than added orthovanadate [30,31]. Interestingly, decavanadate reductase activity has been found to be an alternative activity of an NADP-specific isocitrate dehydrogenase [32]. Diperoxovanadium derivatives have also been shown to be involved in this type of reaction [33,34]. Decavanadate may play a role in the biological role of vanadium, as it is found in yeast cells growing in the presence of orthovanadate [8] and is a potent inhibitor of phosphofructokinase-1, the control step of glycolysis, and other metabolic reactions [35].

The role of these interesting plasma membrane-dependent, vanadate-stimulated NAD(P)H oxidation reactions in cellular metabolism remains to be elucidated, although multiple interactions with cellular metabolism and components are possible including interactions with xanthine oxidase and lipid peroxidation [24]. Decavanadate has been shown to enhance cytochrome c reduction [31], and cytochrome c release from mitochondria is associated with initiation of apoptosis. Perhaps the reduced cytochrome c is more readily released from the mitochondria. With increasing emphasis on the redox properties of vanadium being important in its pharmacological effects, it is quite possible that these reactions, either protein dependent or not, may play a role in therapeutic actions of vanadium.

11.1.1.2 Vanadium Compounds and Cellular Oxidation-Reduction Metabolism

The influences of vanadium on a variety of cellular oxidation-reduction reactions have been reported in many cells. In addition, similar types of interactions may occur in other experimental models in which redox properties are not monitored when vanadium is added to living cells or organisms.

Oxygen and nitrogen radicals have been recently identified as important in transcriptional regulation in addition to being toxic metabolites. The aqueous chemistry of vanadium allows vanadium to interact intimately with cellular redox reactions involving both oxygen and nitrogen. The finding that nitric oxide has a

role in signal transduction pathways involved in physiological processes such as blood flow and penile erection provided the basis for the development of current drugs for erectile dysfunction [36]. In different systems, vanadium stimulates nitric oxide formation or inhibits the stimulation of nitric oxide by cellular effectors. Understanding the role of vanadium in cellular nitric oxide metabolism may shed light on how this metal may modulate processes normally controlled by the concentration of nitric oxide.

The cell membranes are very sensitive to oxidation, and the role of vanadium in causing membrane oxidation has been studied in isolated membranes. The aerobic peroxidation of liposomal membranes by vanadocene complexes has been studied. Biscyclopentadienylacetylacetonate V(IV) (acetylacetonate) has been shown to initiate oxygen-dependent lipid peroxidation [37]. The lipid peroxidation reaction correlated with a decrease in the V(IV)/V(V) redox potential and proceeded without formation of radicals. Interestingly, with a nonchelated biscyclopentadienylbischloro V(IV) dichloride, the lipid peroxidation was associated with the production of radicals. Both compounds form a vanadium(V) superoxide complex as an active oxidizing species, but the former must act directly as the active oxidizing species, whereas the latter must first decompose to form hydroxyl radicals, which are known initiators of lipid peroxidation. The lipid peroxidation seen with some transition metals is usually attributed to a Fenton-like mechanism. Hydrogen extraction initiates the reaction leading to the formation of lipid peroxyl radicals that then propagate the reaction. Vanadium compounds caused oxidation of fatty acid lipids in human erythrocytes and animals treated acutely and chronically [38].

It is possible to measure the formation of various radicals such as reactive oxygen species in cells. Reactive oxygen species (ROS) activate the nuclear factor of activated T cell transcription factor (NFAT), which is associated with its dephosphorylation, nuclear translocation, and increased affinity for DNA binding. Vanadium activation of nuclear factor of activated T cells (NFAT) was found to correlate with formation of the ROS H_2O_2 and was dependent upon the activity of calcium channels [39]. In activated human neutrophiles, vanadium(II), (III), and (IV) increased hydroxyl radical formation and attenuation of myeloperoxidase activity, whereas V(V) did not show these effects. Similar results were seen in a cell-free system [40]. Increased lipid peroxidation in liver but not in kidneys was found in normal rats treated with vanadate [41].

Formation of radicals after addition of vanadium compounds has also been looked at in tissues. In isolated perfused lungs, addition of vanadyl sulfate induced constriction of pulmonary arteries accompanied by increased threonine phosphorylation of endothelial nitric oxide synthase, which was reversed by addition of a protein kinase C inhibitor [42]. These studies directly link vanadium treatment to formation of NO via a phosphorylation mechanism. The binding of NO to soluble guanyl cyclase stimulates that enzyme to convert guanosine triphosphate (GTP) into the second messenger cGMP. Addition of peroxovanadate and bisperoxo(1,10-phenanthroline)oxovanadate (V) and H_2O_2 alone induces specific activation by tyrosine phosphorylation of soluble guanylyl cyclase subunits in PC12 cells, rat aortic smooth muscle, and rat aorta. Nitric oxide binding to guanylyl cyclase stimulates the enzyme to produce cGMP from GTP. This effect supports the hypothesis

that it may also occur in animals and provides a means of linking cellular vanadium to nitric oxide signaling. This vanadium effect could be solely related to the cellular production of H_2O_2 in these experiments [43].

11.1.2 Inhibition of Phosphate-Metabolizing Enzymes by Vanadium Compounds

Vanadium inhibition of phosphate-metabolizing reactions may be important when the metal is administered as a therapeutic agent if concentrations of inhibitory forms of the metal accumulate in the relevant biological compartments of the animal. Vanadium is believed to be a transition-state analogue for phosphate ester hydrolysis, but current evidence supports the idea that vanadium is an imperfect transition-state analogue in these systems. Details of the inorganic chemistry of vanadium inhibition of all types of phosphorylation reactions can be found in a recent review [5]. The phosphorylase reactions of biological relevance that are inhibited by vanadium compounds are ribonucleases that cleave RNA; phosphatases that cleave phosphate from small metabolites, such as alkaline and acid phosphatases; phosphatases that cleave phosphate from proteins, such as the protein tyrosine phosphatases; and plasma membrane P type ATPase ion pumps that cleave a phosphate from ATP to provide the energy to move ions against a concentration gradient.

The active sites of these enzymes can have a nitrogen ligand, usually as histidine (acid phosphatases and some protein phosphatases), a nucleophilic serine residue (alkaline phosphatases), a cysteine residue in which the thiol group can form a covalent species with the phosphate ester (protein phosphatases), or an aspartate-linked phosphate (plasma membrane ion pumps). The inhibitory form of vanadium is usually anionic vanadate V(V), but cationic vanadyl V(IV) has also shown strong inhibition of some types of phosphorylase reactions. Above neutral pH, speciation of vanadyl ions produces anionic V(IV) species capable of inhibition of enzymes in the traditional transition-state analogue manner [5].

The above enzymatic reactions involve the release of inorganic phosphate from the substrate. Vanadium also inhibits enzymes in the metabolic pathways, such as phosphoglycerate mutase, that catalyze phosphate transfer [44–46], a key step in glycolysis. A good example of the ability of vanadate to spontaneously generate an inhibitor and subsequently act as a transition-state analogue to phosphate transfer is that of vanadate in the presence of 3-phosphoglycerate in aqueous solution. 2-Vanadio-3-phosphoglycerate is spontaneously formed and, if phospho-glycerate mutase is included in the solution, inhibits this enzyme with an inhibition constant of 0.01 nM [46]. Despite this very tight binding, only about 40% of the energy available for stabilization of the transition state goes towards binding this inhibitor [47].

11.1.2.1 Inhibition of Ribonuclease

Ribonuclease A is a rather small but critically important enzyme that catalyzes the hydrolysis of ribonucleic acid and, therefore, is crucial for cell function. It has been the subject of intense study for many years [48]. As depicted in Scheme 11.1,
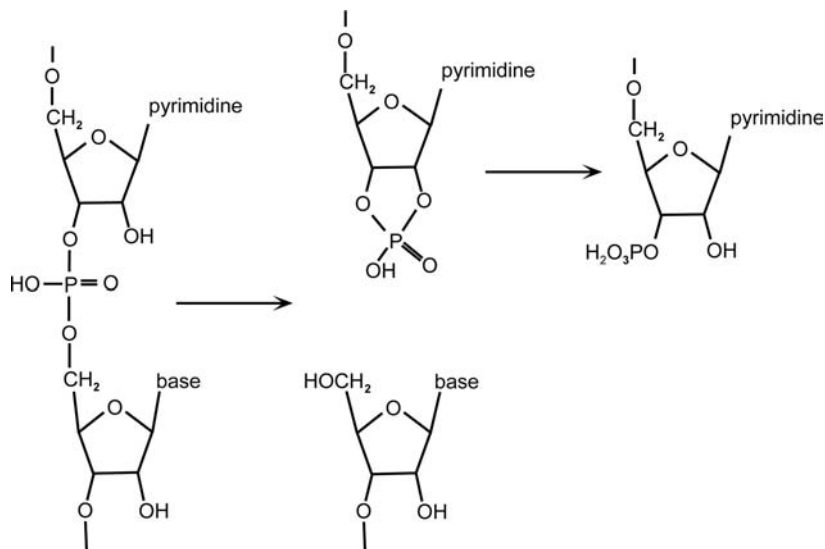
SCHEME 11.1

ribonuclease cleaves the phosphodiester bond between the 5'-ribose of a nucleotide and the phosphate group attached to the 3'-ribose of an adjacent pyrimidine nucleotide to form a 2',3'-cyclic phosphate. This cyclic phosphate can then be hydrolyzed to the corresponding 3'-nucleoside phosphate. Inhibition of this enzyme by a vanadium-uridine (VUr) complex was the first example of the inhibition of an enzyme by vanadium [49]. The complexity of the various vanadium-uridine complexation reactions was not understood at the time of this early work. The dominant product is now known to be a dimeric complex (see Section 4.1.1), and it was not until the equilibrium constant for formation of the monomer was obtained [50,51] that a good estimate for the dissociation constant of VUr from ribonuclease A was obtained, the value being close to 0.5 μM [47,52], though depending on the ionic state, the value could be as low as 20 nM [53]. From estimates of the binding energies available to the transition state in the ribonuclease A cycle, it was shown that there was a shortfall in the binding of the uridine vanadate complex of close to 60% of the energy available [47]. Similar energy shortfalls were estimated for vanadate-binding in the phosphoglucomutase system [53].

There are a number of factors that possibly contribute to the shortfall in stabilization energy available to the ribonuclease/uridine/vanadate enzyme complex. These include differences in the strength of hydrogen-bonding interactions and different bond lengths. In particular, the VO bond is in the order of 15% longer than its PO counterpart. Because the vanadium entity is three-dimensional, this translates into a requirement for a volume increase of about 50%. It is reasonable, then, that accommodation of the inhibitor will require small dislocations in the positions of the ribonuclease active site residues. Such displacements will be energetically unfavored and will be balanced by a change in structure of the vanadate complex from its optimal structure and from the structure corresponding to the transition state of
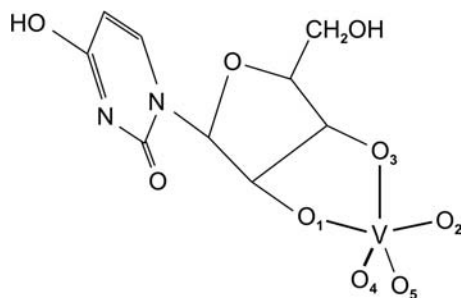
Angles

O_1VO_2	150.5	O_1VO_3	77.5
O_1VO_4	96.0	O_1VO_5	103.9
O_2VO_3	73.4	O_2VO_4	100.4
O_2VO_5	95.9	O_3VO_4	132.9
O_3VO_5	122.7	O_4VO_5	104.2

SCHEME 11.2

the phosphate-containing substrate. It is evident from crystal structure analysis that although a pentacoordinate geometry is achieved in the vanadate analogue, this geometry is only approximately trigonal bipyramidal [54,55]. This distortion from ideal geometry suggests that the inhibitor is imperfectly matched to the active site. Scheme 11.2 gives the crystal structure angles [55] found for the vanadium center. In particular, the OVO angle between the apical oxygens of the bipyramid is 150.5°, as opposed to the 180° of an undistorted OPO angle.

Detailed study of the structure of the bound inhibitor has been coupled with computational studies to provide a comprehensive mechanism for ribonuclease A function [55]. Similarly, Raman difference spectroscopic studies of the ribonuclease/VUr complex has been used as a probe of the ribonuclease active site chemistry [56]. However, strong arguments have been advanced that suggest the ribonuclease/VUr complex has properties of the ground-state complex and should not be used as a basis for analysis of the transition state [52]. Interestingly, NMR studies have shown that there is a modification of the enzyme complex from that of the solid state when it is dissolved in water. Apparently, there is a significant change in position of the sidechain of the active site histidine, his119 [57].

At first sight, it is quite surprising that decavanadate is a good inhibitor of ribonuclease A. Calorimetric binding studies gave a dissociation constant of 1.4 ±0.3 µM [58]. This is only a little poorer than inhibition by VUr, where the K_i is 0.5 µM. The active site cleft of ribonuclease A is cationic in character and has dimensions that are suitable for decavanadate binding. Decavanadate is highly anionic, typically carrying four to six negative charges, dependent on pH. This suggests that binding is coulombic. Variation of ionic strength tends to confirm this, with decavanadate binding dropping significantly with increase in salt concentration in the medium.

Vanadate itself is a much poorer inhibitor of ribonuclease A than is the VUr complex. This makes sense because vanadate alone cannot mimic the transition state. Covalently bound components, the parts of the nucleoside covalently bound to the phosphate moiety, are needed to complete the transition-state-like structure. They

undergo specific interactions within the active site pocket and position the vanadium correctly for interaction with the functional groups. It is not surprising, therefore, that a crystalline complex of vanadate in ribonuclease T_1 shows that vanadate retains tetrahedral coordination. Ribonuclease T_1 is a specific fungal enzyme that cleaves RNA at the 3′-phosphate of guanylic acid. In the vanadium-bound system, active-site sidechains undergo conformational changes from the free enzyme, and there is considerable movement in at least one peptide bond [59]. These changes are important to the binding of vanadate but may equally well contribute to its comparatively weak binding.

11.1.2.2 Inhibition of Protein Tyrosine Phosphatase

Vanadate strongly influences a number of enzymes that are responsible for phosphate transfer reactions. For instance, it is a strong inhibitor of protein tyrosine phosphatase [60–62]. The PTPases are a class of enzymes that can regulate tyrosine kinase activity by removing a phosphate and are critical to cell function. They crucially influence numerous cellular processes such as mitosis, T cell activation, and insulin-receptor signaling [63]. Unlike ribonuclease, during their catalytic cycle, the PTPases specifically attack at the phosphorous center. Vanadate, being a good analogue of phosphate, is similarly attacked and forms a high affinity transition-state-like enzyme complex. This reaction is reversible, which shows that the sulfhydryl group of the active site cysteine is not oxidized by vanadate. Bisperoxovanadate, which also is a potent inhibitor of PTPase activity, inhibits in a nonreversible fashion. This is because peroxovanadate is a good oxidizing agent and causes irreversible oxidation of the active site sulfhydryl group, thus deactivating the enzyme. Heteroligand complexes of monoperoxovanadate also can readily oxidize the cysteine sulfhydryl group and are often effective nonreversible inhibitors.

Another highly effective reversible inhibitor of PTPase function is the vanadate complex bis(*N,N*-dimethylhydroxamido)hydroxooxovanadate, which inhibits LAR and PTP1B with K_i values of 1 and 2 μM, respectively [49,69]. Furthermore, this complex is an effective inhibitor of PTPase activity in an intact cell, whereas this is not true for vanadate [65]. This is a structural analogue of bisperoxovanadate but differs from it in two highly significant ways: by not carrying a charge under most physiological conditions and because it is a poor oxidant. However, it fits very well into the reactive site cavity of PTPases where, as suggested by molecular modelling studies, it strongly interacts with active site residues by hydrogen bonding and hydrophobic interactions [64,66]. However, the vanadium is not within bonding distance of the active site cysteine-*S*. Interestingly, though, the monoligated complex also fits well into the active site cavity, where molecular modelling studies suggest it is well situated to form a sulfur-vanadium bond and, as well, still retain the stabilizing hydrogen bonding and hydrophobic interactions [66]. Both mono- and bishydroxamidovanadate readily form V-S bonds [67] (also see Section 7.1).

An interesting facet of the molecular modelling studies [66] was that they suggested that one methyl group of the hydroxylamine ligand was in an orientation suitable for replacement by other functionality. This is potentially important because PTPase active site residues are highly conserved, and enzyme selectivity is conferred

by surface recognition elements. Appropriate modification of the methyl group provides the opportunity to build in selectivity of inhibition by reaching toward specific surface recognition elements [68].

11.1.3 EFFECT OF VANADIUM COMPOUNDS ON GROWTH AND DEVELOPMENT

During normal cell growth or mitosis, mammalian cells undergo a defined cycle of events. After cell division in the mitotic or M phase is the G1 (first gap) phase. At this point, the cell contains two copies of each chromosome, the normal diploid state of a cell. When certain signals are received, the cell enters the S, or synthesis, phase of the cycle, during which DNA replication occurs. There is then a second gap, or G2 phase, in the cycle. At the end of G2, the cell enters mitosis or the M phase, during which the replicated DNA segregates in opposite parts of the cell. After cell division, the cycle returns to G1. After completing the cell cycle, two identical cells have now been produced. Many proteins and enzymes orchestrating the transition from one growth phase to another control the cell cycle. The most important class of cell cycle regulatory proteins is the cyclins, controlling a family of protein kinases called the cyclin-dependent kinases.

Stimulation or inhibition of cell growth can be described with various terms in cell biology [69]. Inducing mitosis or cell division results in two similar cells and an increase in cell number, sometimes referred to as proliferation. The receipt of certain signals by a cell can cause it to change into a different type of cell, or to differentiate. All cells in an organism are believed to have the genetic blueprints needed to make every cell type present in that organism. Differentiation occurs when a fertilized egg develops into an embryo. Cells that can differentiate into other types of cells are called stem cells.

Growth inhibitory responses can be classified into necrosis for general death, in which an injured cell swells, without any changes in the appearance of the nucleus, and eventually the plasma membrane ruptures. Apoptosis is caused by activation of specific signal transduction processes, causing membrane blebbing (formation of small vesicle outgrowths, or blebs) and nuclear fragmentation [70]. Caspases are cellular proteases having an active site cysteine residue. Caspases cleave proteins C-terminal to aspartate residues and are activated during apoptosis. Another family of proteins having both pro- and antiapoptotic effects are encoded by the *bcl* genes originally isolated as B cell lymphoma genes. Genes are traditionally referred to in small italicized letters, whereas proteins are referred to in capital letters. BCL proteins are controlled by phosphorylation of protein kinase B (see Section 11.3.2).

The mechanism of vanadium interaction with growth and differentiation pathways has been extensively studied [70]. In tissue culture systems, vanadium has been shown to inhibit growth and, in some cases, modify DNA synthesis to block the G2-to-M transition. Cells blocked at M phase are susceptible to apoptosis, which can be stimulated by vanadium compounds. Vanadium compounds have also been shown to have mitotic effects stimulating growth, cell proliferation, or cell transformation. In some cases, vanadium compounds were able to promote cellular differentiation. Clearly, the addition of vanadium compounds would not have all of these

effects in any one cell. The mechanism of action of vanadium in all of these growth processes is thought to be inhibition of protein tyrosine phosphatases. To that end, vanadate-induced changes in the phosphorylation of component proteins in the implicated signal transduction pathways have been monitored [70], which is further discussed in Section 11.3.2. Although not monitored in most studies, changes in the phosphorylation of these proteins could also be caused by slight vanadium-induced increases in ROS or NOS formation. Vanadate formation of H_2O_2 has been shown to mediate apoptosis through the activation of p53 [71].

Vanadium can also cause DNA damage outside of the apoptosis pathways, as measured by the appearance of DNA lesions in normal mice treated with vanadate [72]. A bis(peroxo)vanadium(V) complex has been shown to catalyze a nonspecific single-strand nicking of DNA [73]. The nuclease activity of oxovanadium(IV) complexes of hydroxylsalen derivatives in the presence of 3-mercaptopropionic acid occurs at guanine residues [74]. Care must be taken in interpreting vanadium compound-caused cell death as to whether it results from apoptosis or general genotoxicity. Vanadate inhibited the DNA binding activity of the tumor suppressor protein p53 in irradiated MOLT-4 cells (a human acute lymphoblastic leukemia cell line) [75], showing another type of vanadium-induced modulation of DNA function.

Vanadate compound addition to Syrian hamster embryo cells initiated some steps in the pathway leading to neoplasmic progression [76]. Perhaps, this is caused by the growth advantage conferred by vanadate to cells undergoing this transformation process. Vanadate addition to multiple cell lines increased phosphotyrosine levels and induced reversible transformation, defined as the development of cancer-associated uncontrolled growth, without causing increases in phosphoinositol turnover [77].

Experiments on the proliferative effects of vanadium compounds are not always clear. Results on the effect of vanadium compound administration on erythropoiesis, or development of red blood cells, have been mixed. A recent report has shown that orthovanadate stimulated erythropoiesis by stimulating the maturation of red blood cell precursors [78]. Peroxovanadate addition is reported to stimulate neurite outgrowth in PC12 cells [79], whereas vanadate causes growth inhibition in these cells [70].

11.1.4 Nutrition and Toxicology of Vanadium

Compared to a number of other metals, vanadium appears to be relatively innocuous when ingested in low concentrations by animals; however, it is by no means certain that this will be true for chronic exposure, as toxic effects have been reported [80]. The nutrition community treats vanadium as a member of the ultra trace metals, which have a nutritional requirement of less than 1 mg/kg diet and are present in tissues in the range of micrograms per kg [81]. Although evidence suggests that vanadium is beneficial to human health, its mechanism of action remains obscure. No specific dietary recommendations have been made, in part, because there is controversy surrounding whether or not vanadium is an essential element.

Studies in which vanadium was injected into veins of dogs and sheep using [48]V as a tracer demonstrated that vanadium was poorly absorbed into the tissues

and that the primary excretion route was in urine. The absorption of orally ingested vanadium is approximately 1 to 10% and is dependent on a variety of factors, including whether the metal is complexed to a ligand. Vanadium is relatively quickly eliminated from body organs and excreted. In a classical pharmacokinetic study, the excretion was modeled by first order kinetics after an initial distribution phase [82,83].

The concentration of vanadium in animal tissue is about 8 μmol/(kg dry weight) which, when corrected for dehydration, will be similar to the concentration typically found in fresh water. Levels are highly variable and may be as low as a few nmol/(kg tissue). A majority of the vanadium body burden in the rat was found to be in fat and bone [84]. Interestingly, the absorption, distribution, and excretion of organovanadium compounds were found to differ from that observed for inorganic vanadium compounds in the rat [85]. Rats orally treated with approximately 1 mg/ml of oral vanadium in the drinking water have vanadium concentrations in tissue in the range of 20 to 200 μmol/L [86]. Assuming that the animals are drinking about 20 ml and weigh about 250 g, this is a dose of about 80 mg/kg. Humans treated with 100 mg/V per day accumulated 1 to 2.5 μmol/L vanadium in serum after 6 weeks [87]. Using the average standard weight of 70 kg, the humans would be ingesting about 1.25 mg/kg of vanadium. The dosing levels for rodents are much higher than that given to humans, in part explaining the elevated amount of vanadium found in the serum of rodents compared to that found in humans.

Residence lifetime measurements after an extensive feeding regime have shown that the half-life for elimination of vanadium from the kidney of rats is about 12 days [88]. To the extent that this reflects excretion from the animal, then it is evident that the elevated levels will return to close to normal within a month or so after a single dose. However, this is perhaps not a valid assessment when repeated dosage occurs, even at low levels. Even if ingested as a vanadium(V) compound, significant amounts of the metal will be converted to vanadium(IV) within an animal's body. As vanadium(IV), it can be incorporated into bone [89]. Chronic exposure over the long term, therefore, leads to the possibility of vanadium concentrating to high, potentially problematic concentrations.

To date, there is limited published material concerning the pharmacokinetics of vanadium compounds in humans. The concentration of vanadium in humans not dosed with the metal is extremely low and at the limits of detection of many of the analytical techniques used. It is not possible to ascertain if the large differences observed in different populations are the result of environmental exposure or experimental variability. Studies using blood have shown vanadium levels of 0.4 to 2.8 μg/L in normal people. The serum contains the largest amount of vanadium with concentration values ranging from 2 to 4 μg/L using atomic absorption spectroscopy [90]. The upper limit of vanadium in the urine of normal people was reported to be 22 μg/L, with excretion values averaging below 8 μg/24 h. Vanadium is widely available in nutrition stores for athletes, who believe it to be a nonsteroidal compound that increases muscle mass at a dose of approximately 7 to 10 mg day, without any reports of toxicity [91].

The toxicology of vanadium compounds is beyond the scope of this volume. Comprehensive summaries are available from the World Health Organization[1] [92, 93]. A major area of concern is exposure through the lungs of workers in the vanadium industry [92]. Significant deposition of inhaled vanadium has been found in mouse lungs, resulting in significant lung pathology [94]. Inhaled vanadium has also been associated with effects on the cytokine activity of the immunesystem [95]. Of more relevance to the therapeutic role of vanadium explored in this chapter is the toxicity observed when vanadium is injected or given in the drinking water or food [86]. The role of production of reactive nitrogen species and reactive oxygen species in metal toxicity, including vanadium, has also been reviewed [96]; however, as seen below, these radical species are also important in normal metabolism.

11.2   PHARMACOLOGICAL PROPERTIES OF VANADIUM

Vanadium compounds are actively being studied as pharmacological agents for diabetes and cancer. Research directed toward specific and selective functionality of vanadium complexes of numerous types may well lead to potent drugs for the treatment of these diseases. Also, as more is learned about the effects of vanadium in biological systems, other applications in medicine may be found for the metal [70,97], including the development of vanadium-based drugs for the treatment of burn victims. This is an area in which silver-containing compounds have achieved great success as an antibacterial agent [98].

Efforts directed towards devising ligated species that have functional activity that is complementary to, and takes advantage of, site-specific interactions within the targeted enzymes will, in the long term, provide a successful strategy for obtaining selectivity of function. In this way, it seems quite possible that both a high degree of enzyme selectivity and high activity can be obtained simultaneously. Computer-assisted molecular modelling has the potential to provide invaluable insight towards such an objective. For instance, although the active sites of protein tyrosine phosphatases are highly conserved, surface recognition elements provide possibilities for developing selective inhibitors of these enzymes [66,68]. In these enzymes, there are significant differences in the amino acid residues that surround the active site. Cationic groups are replaced by neutral or anionic groups in ways that clearly differentiate these enzymes and provide selectivity to their function. It seems evident that exploitation of such differences and, indeed, similar variations in other enzyme systems provide great potential for future drug development. In order to maximize therapeutic value and decrease toxic side effects, successful use of vanadium in pharmaceuticals will require enzyme specificity and stability of the administered drug to speciation reactions in the body. Ligated complexes of vanadium, designed with full knowledge of the aqueous chemistry of the metal, appear to have the best chance of achieving these goals.

---

[1] www.inchem.org/documents/cicads/cicads/cicads/cicad29/htm and www.inchem.org/documents/ehc/ehc/ehc81/htm.

Vanadium is being proposed as a therapy for both diabetes and cancer. The signaling pathways involved in promoting growth by hormones such as insulin and killing cells by apoptosis have much in common. ROS in small amounts can induce transcription factors, stimulating the formation of messenger RNA that encodes proteins known to be induced by vanadium; however, in large amounts, ROS are toxic to the cell and will trigger apoptosis. Many of the vanadium compounds proposed for use against diabetes have shown cytotoxic effects against tumor cell lines, whereas ROS and reactive nitrogen species (RNS) have been shown to be produced from the administration of vanadium as an antidiabetes agent. The similarities of the metabolic processes involved in both diabetes and cancer need to be considered when evaluating the potential therapeutic use of this metal for either disease.

In evaluating the pharmacological properties of vanadium, the vagaries of biological systems must be considered. Compared to chemical systems, biological systems have a much greater amount of inherent variability. In addition to experimental variability, the same agent may trigger different biological actions in different cells, in animals, or even in different parts of the same cells. In fact, due to the difficulty of maintaining animals or cells in a totally chemically defined system, different results may be obtained in different laboratories using the same cell line or animal. Therefore, descriptions of biochemical alterations obtained upon adding vanadium to a biological system must be interpreted as being specific to the experimental system described. In addition, results obtained using cell culture systems and animal models cannot be directly extrapolated to human forms of disease.

11.2.1 Vanadium as a Therapeutic Agent for Diabetes: Overview

Diabetes is a multifaceted disease having many forms. Although originally recognized as a disease of carbohydrate metabolism, diabetes is now recognized as also being the result of altered lipid or fat metabolism. Type 1 diabetes results in a requirement for insulin after extended hyperglycemia, which is associated with progressive β cell death in the pancreas. Type 2 diabetes involves increasing insulin resistance, caused by an inability of insulin to be utilized [13]. Defects at many levels cause this resistance, including decreases in receptor concentration, phosphatidylinositol-3-kinase (PI-3K) activity, and glucose transporter translocation [99]. Insulin levels rise initially, but eventually the pancreas is exhausted and stops producing insulin. Type 2 diabetic patients eventually require insulin therapy. There are many other forms of diabetes, such as gestational diabetes, which occurs in pregnancy, but the vast majority of diabetic patients have either type 1 or type 2 diabetes.

A major problem in treating patients with insulin is the risk of hypoglycemia, or low blood glucose. Clinical hypoglycemia can lead to loss of consciousness and death. Insulin lowers blood glucose levels whenever administered, even if the patient's blood glucose level is at a normal level. Oral administration to normal animals of the same amount of vanadium that lowers diabetic hyperglycemia does not substantially lower blood glucose levels to cause clinical hypoglycemia, a major advantage for vanadium therapy [100,101]. Coadministration of vanadium with

insulin has been suggested to help maintain tight control of blood glucose levels without causing hypoglycemia. Vanadium administration alleviates many diabetes-altered changes in enzyme activity or gene expression without significantly affecting these processes in normal animals [13,101]. The lack of deleterious effect of vanadium compounds on normal metabolism makes these compounds attractive as adjuvant therapies for diabetes in conjunction with insulin or other drugs.

The role of oxidative stress in the etiology of diabetes and progression of diabetic complications is now well established. A unifying mechanism for the pathobiology of diabetic complications has been proposed to be hyperglycemia-induced production of superoxide in the mitochondria [102]. Diabetes increases the production of ROS and mitochondrial antioxidant defense systems in rats with streptozotocin (STZ)-induced diabetes [103]. The oxidant stress caused by glucose-induced free radical formation is implicated in the development of insulin resistance in both type 1 [104] and type 2 diabetes [105]. The presence of antioxidants such as glutathione (GSH) protects against the development of both diabetes and diabetic complications [106,107]. Because low levels of ROS are both critical in normal metabolism and involved in insulin signaling, it is difficult to correlate ROS levels with the pathophysiology of diabetes [108]. This apparent paradox in the role of ROS in insulin action is currently being widely investigated [109]. Any consideration of vanadium compounds as antidiabetic agents must also consider the effect of the compound on the formation of ROS and RNS.

In addition to vanadium, other early transition metals have been shown to have antidiabetic properties, which is not surprising, as this class of compounds would be expected to share some chemical functionality. Chromium [110–112], tungsten [113,114], and molybdenum [115,116] all have demonstrated insulin-like properties.

The ligand can have a strong influence on whether antidiabetic or cytotoxic properties are observed with vanadium complexes. The vanadium complex (4-hydroxypyridine-2,6-dicarboxylato)oxovanadate(V) was reported to have antidiabetic properties in rats and also cytotoxic effects in *Saccharomyces cerevisiae* [117]. The insulin-enhancing activity in rats and the ability to inhibit rat cell myoblast growth in tissue culture was determined for dipicolinic acid complexes of transition metals (cobalt, chromium, iron, molybdenum, manganese, nickel, tungsten, and vanadium). Unexpectedly, dipicolinic acid transition metal complexes showing the greatest cytotoxic effects on rat myoblasts also have the greatest insulin-enhancing effect in rats with STZ-induced diabetes.[1] It should be noted that vanadyl curcumin complexes were strongly cytotoxic to mouse lymphoma cells and had no insulin-enhancing or toxic effects in diabetic rats [118]. The design of ligated vanadium complexes that maintain insulin-enhancing activity and have lower toxicity in animals should be possible, applying our current knowledge of vanadium chemistry.

Vanadium was first used in France in 1899 as a therapeutic agent for diabetes [119]; however, this experimental result was buried with time. The modern era of studying the antidiabetic properties of vanadium began in 1979, when it was shown that vanadium was present in muscle and inhibited plasma membrane ion pumps [1]. Experiments were then done in tissue culture experiments, where vanadium

---

[1] Willsky and Crans, unpublished observations.

addition was shown to have insulin-like effects on glucose metabolism [120,121]. This was surprising, as the effects of vanadate on cells were expected to be due to the inhibition of plasma membrane ion pumps, which would not cause insulin-like action. The demonstration of insulin-like activity in cell culture experiments prompted the testing of oral administration of vanadium compounds on diabetes in animals [122,123], triggering an avalanche of projects involving the antidiabetic properties of vanadium compounds.

Vanadium has effects similar to and different from that of insulin [100,101,124]. The antidiabetic influence of the metal can be considered insulin-enhancing, rather than insulin-mimetic, because vanadium compounds cannot totally substitute for insulin in any model of diabetes that strictly requires insulin, such as the BB rat [125], a model of type 1 diabetes. In addition, vanadium can exert its antidiabetic effects via a mechanism or combination of mechanisms distinct from that of insulin. The metabolic actions of vanadium on metabolism do not include all of the actions of insulin, yet normal animals produce less serum insulin when given vanadium. The terms *insulin-mimetic* or *insulin-like* frequently appear in the literature for actions of vanadium that cannot be classified as similar to or different from that of insulin in the experimental system utilized.

When considering vanadium as part of a therapeutic regimen for diabetes, extreme care must be taken with regard to issues of toxicity. The effort to achieve more potent vanadium drugs and widen the therapeutic window (the difference between the dose required for therapeutic effects and the dose that elicits toxic symptoms) prompted the investigation into using ligated derivatives of vanadium to treat diabetes. Researchers have also looked into other ways of diminishing adverse effects. The toxicity of vanadate and the amount of vanadium found in tissues was lowered after administration of the metal compounds to rats with STZ-induced diabetes (a model of type 1 diabetes) in a tea decoction [126]. The overall biodistribution of the metal was not affected by this form of administration [127]. The tea decoction was also effective when used in the treatment of the type 2 diabetic Zucker diabetic fatty (ZDF) rat with vanadium. Another way of diminishing the toxicity of vanadium is to administer it in coated capsules [128].

11.2.1.1 Vanadium Compounds Used for Treatment of Diabetes: Salts, Chelate Complexes, and Peroxovanadium Compounds

The first vanadium compounds to be tested for insulin-like activities were the simple salts, the V(IV) vanadyl sulfate and the V(V) vanadates. In an effort to increase efficacy and decrease toxicity, organic ligated derivatives of vanadium have been developed. The coordination chemistry of various V(III, IV, and V) compounds that have antidiabetic properties has been reviewed and discussed in the framework of desired chemical composition of therapeutic agents [124]. The ligands used to complex vanadium include pyronates, pyridinonates, picolinates, acetylacetonates, dicarboxylate esters, and *N,N*-disalicylidineethylenediamine (SALEN) compounds, many of which are natural derivatives. Some sulfur-containing compounds have also been made as ligands for vanadium. Natural occurring compounds with strong

binding affinity to vanadium have also been used, with the L-isomer of glutamic acid γ-monohydroxymate being particularly successful [129]. The insulin-like activities of mono- and diperoxovanadates, potent inhibitors of protein-tyrosine phosphatases, have also been studied [130]. The lack of hydrolytic stability and the formation of significant free radicals with these agents limit the therapeutic applications of these compounds [131]. Macrocyclic binuclear oxovanadium complexes have been found to correct diabetic alterations of lipid metabolism in STZ-induced diabetic rats without any observed toxicity [132].

11.2.1.2 Effects of Vanadium Compounds in Biological Models

The following sections describe effects seen when administering vanadium compounds to cells, animals, or humans. Vanadium compounds can bind to components of biological systems, potentially change oxidation state, and dissociate from any associated ligand. Therefore, the exact chemical form of vanadium having an insulin-like effect is difficult to determine in any biological system. The administered form of vanadium, given in the following sections, may not be the active form of the metal in the cell.

Specific vanadium-induced alterations in the activity or expression level of components of metabolic pathways are described here. Many of these changes are not caused by alterations in the pathway enzymes themselves but in enzymes and factors involved in regulation, commonly referred to as signal transduction systems. Section 11.3 will discuss the alterations described in this section in the context of general signal transduction processes affected by vanadium.

11.2.1.2.1 Cellular Systems

Much effort has gone into the comparison of vanadium compounds and insulin on carbohydrate, lipid, and protein metabolism in cell culture systems [133,134]. All of insulin's effects on glucose uptake and metabolism have been seen in some tissue culture system. Vanadate inhibited lipolysis and stimulated lipogenesis and other reactions of lipid metabolism in adipocytes. The only area of insulin action not routinely seen with vanadium treatment is affects on nitrogen metabolism. Results obtained for both anabolic effects on protein synthesis and stimulation of amino acid uptake are inconsistent and vary according to experimental conditions. In other studies, vanadium compounds and insulin show different effects when added separately to a cell system. The addition of vanadate or insulin to primary rat hepatocytes in culture-enhanced ApoproteinB, a component of the lipid transporting lipoprotein system, secretion and increased intracellular glycogen accumulation, whereas addition of vanadate only stimulated intracellular lipogenesis [135]. Other specific areas where vanadium and insulin differ in their cellular effects are described below.

The fact that vanadium compounds were found to stimulate various biochemical pathways provided specific targets to monitor in studying the mechanism of action of vanadium compounds. In Chinese hamster ovary cells, the effects of a number of organo-vanadium compounds were examined for their effects on protein kinase B signaling and the activity of glycogen synthetase kinase 3 (GSK-3). GSK-3 is the kinase responsible for stimulating glycogen metabolism. It is a downstream target

for PI-3K (see Section 11.3). The phosphorylation of all of these proteins was determined with biochemical techniques, and these results contribute to the control of glucose homeostasis by vanadium compounds [136].

As work with vanadium compounds and diabetes in cell system has continued, it has become clear that there are also insulin-independent mechanisms at work. One insulin-independent signal transduction pathway appears to be involved in glycogen metabolism reactions in rat adipocytes [137] that also involve PI-3K. A major difference was that only vanadate promoted glycogenesis through the activation of a cytosolic protein tyrosine kinase, which was mediated in an insulin receptor-independent manner.

Simulation of glucose transport and glucose transporter translocation from intra-cellular stores to the plasma membrane in muscle cells by vanadate and peroxovan-adate involve a mechanism independent of PI-3K and protein kinase C systems utilized for stimulation of these processes by insulin. The transport of GLUT4 to the plasma membrane in muscle cells growing in culture after stimulation by van-adate, peroxovanadate, or insulin all require an intact actin network [138]. Some-times, the insulin-like action of vanadium is accompanied by overall stimulation of actual metabolic pathways. One example of this is the stimulation of the pentose phosphate pathway observed when vanadate promotes the incorporation of glucose into lipids, an antilipogenic effect [139].

Vanadate stimulates protein kinases in the cytosol, as demonstrated in adipose cells and extracts. The activation of a membrane and cytosolic protein tyrosine kinase have been demonstrated in adipocytes, and the membranous enzyme has been pos-tulated to be a way to involve PI-3K actions without activation of insulin receptor substrate-1 (IRS-1) in the insulin signal transduction pathway [140]. It is always difficult to determine if protein kinase activation is direct or the result of stimulation of a protein phosphatase. The fact that kinase stimulation was seen in isolated extracts after cell disintegration in this adipocyte cell system supports the idea that vanadium addition to cells could directly stimulate kinases via an as-yet-undetermined mech-anism. In other experiments with 3T3-L1 adipocytes bis(acetylacetonato)oxovana-dium (IV) BMOV and bis(1-N-oxide-pyridine-2thiolato)oxovanadium (IV) caused increased tyrosine phosphorylation of both the insulin receptor and IRS-1 in a synergistic way with insulin, as measured by antibodies to phosphotyrosine residues [141].

Monitoring the release of free fatty acids from adipocytes in a cell culture assay has been successfully used to test the antidiabetic properties of vanadium compounds prior to animal testing. The addition of epinephrine to adipocytes stimulates the release of free fatty acids. If vanadium is added to epinephrine-stimulated cells, the free fatty acid release is inhibited. A detailed structure activity relationship study of insulinomimetic vanadyl-picolinate complexes has been carried out using this sys-tem. The seven compounds used in this study were ordered by apparent IC_{50} values, showing that the introduction of an electron-withdrawing halogen atom or an elec-tron-donating methyl group at the fifth or third position on the picolinate ligand improved activity over the original complex [142]. These same compounds were effective in lowering blood glucose levels in the STZ-induced diabetic rat model, although the results obtained did not allow for ordering the compounds by effec-

tiveness. The release of free fatty acids has recently been used to investigate the effect of vanadyl complexes of 1 hydroxy-4,5,6 substituted 2(1H)-pyrimidinones before carrying out studies in rats with STZ-induced diabetes that demonstrated the ability of these compounds to lower blood glucose in diabetic animals [143].

11.2.1.2.2   Animal Models

In order to fully understand the antidiabetic effects of vanadium, or any other drug, cellular studies are extended to mammalian models of diabetes, frequently in rodents. Models exist and have been used for vanadium studies of both type 1 and type 2 diabetes. Below, general results observed with vanadium compounds in the various model systems are described. More detailed descriptions of the molecular signal transduction systems affected are given in references [12,13,100,133].

The ability of streptozotocin to destroy the pancreatic β cells that produce insulin makes an STZ-induced diabetic animal a good model for type 1 diabetes. However, these animals do not become insulin dependent, as human type 1 patients do. In the STZ-treated outbred Wistar rat model, only about 40 to 70% of the animals display antidiabetic responses to vanadium [100]. Nevertheless, this type 1 diabetic model is widely used to study the antidiabetic properties of vanadium compounds.

The influences of vanadium compounds on cardiovascular function, a major complication of diabetes, has been reviewed [144]. One of the first papers on the antidiabetic effects of oral administration of vanadium compounds (vanadyl sulfate) to rats with STZ-induced diabetes showed improvement of diabetes-impaired cardiac function [122]. Recent work has focused on the correction of metabolic defects of diabetes by vanadium and learning more about the immediate mechanism of the antidiabetic effect. The assumption is made that amelioration of the basic metabolic problems of diabetes by vanadium or any other drug will alleviate the long-term complication arising from disease. Diet supplementation with minerals, such as chromium, appears to complement traditional treatments of diabetes to slow the development of complications. Mineral supplementation is believed to be most effective when dietary supplementation is used to correct a deficiency of a mineral [145].

Comparison of V(IV,V) hydroxamic acid complexes showed the V(V) complex induced a stronger insulin-enhancing effect than the V(IV) complex, and both complexes were better than either of the salts, vanadyl sulfate or sodium vanadate, in relieving the symptoms of mice with STZ-induced diabetes. The distribution of vanadium in tissues was the same irrespective of the complex administered; however, the tissue distribution of vanadium when the salts were administered was different from that seen after vanadium complex administration [146]. These results suggest that the difference in the antidiabetic activity of the hydroxaminic acid V complexes is related to the different oxidation state, although there was no difference in the final tissue distribution of these complexes.

Not all vanadium chelates have antidiabetic properties in animals. For instance, four mixed *O,S* binding bidentate ligand precursors were derived from maltol to yield four new complexes, two pyranthiones and two pyridinethiones. These complexes are hydrolytically stable and had no observable insulin-enhancing properties [147]. The ultimate effectiveness of a vanadium-complex as an antidiabetic drug

depends upon its association with the appropriate biological target. In many cases, this cannot happen if the bonds keeping the complex together are too strong and effectively prevent dissociation of the complex. However, ligands that have characteristics that are complementary to those of the binding site may promote binding and enhance the effectiveness of the complex. Comparison of chemical properties of these ineffective vanadium compounds and other unsuccessful transition-state metal complexes with all successful antidiabetic transition-state metal complexes could help unravel the basis of the antidiabetic action of these complexes, particularly the very potent vanadium compounds.

Work with the type 1 models of diabetes in animals has provided evidence that there is also an insulin-independent mechanism of action for vanadium. The normal control animals in these experiments make less insulin when treated with vanadium, implying that vanadium can partially substitute for insulin. Vanadium has also been tested in the BB rat model, a genetic type 1 model in which diabetes develops with age and insulin treatment subsequently is required. Treatment with vanadyl sulfate was not able to completely substitute for insulin in the diabetic BB rat, but it did lower the amount of insulin needed to keep the animals alive [125]. This observation that vanadium compounds cannot completely substitute for insulin in the BB rat supports other data that imply that vanadium is insulin enhancing [100]. Interestingly, the insulin-enhancing antidiabetic effects of chromium are well studied and appear to be the only antidiabetic mechanism of action of this metal [148]. In the STZ-induced model of diabetes, chromium is completely ineffective, which would be expected if a certain level of insulin, below that found in the STZ-diabetic rat, is needed for the antidiabetic effect of chromium. In the STZ diabetic rat, significant numbers of animals respond to vanadium treatment, although the response of the animals to vanadium is linked to residual insulin [100], implying that an insulin-independent mechanism of action of vanadium exists.

Vanadium compounds have also been shown to be effective in animal models of insulin resistance and type 2 diabetes. Oral administration of vanadium compounds lowered blood glucose levels to near normal in the *ob/ob* and *db/db* mouse and *fa/fa* rat [149–151]. These rodent models are homozygous for the indicated gene and are characterized by obesity, hyperglycemia, and hyperinsulinemia [12]. The *ob* allele is the gene for leptin, whereas *db* and *fa* are the genes for the leptin receptor in the mouse and rat, respectively. Leptin is one of the cytokine hormones that are produced in fat cells and act on receptors in the central nervous system. Its effects involve inhibition of food intake and promotion of energy expenditure [99].

Treatment with either vanadium salts or organic complexes of vanadium have decreased plasma insulin levels and improved insulin sensitivity in animal models of both insulin resistance and type 2 diabetes. This work has recently been reviewed [13]. The Zucker Diabetic Fatty (ZDF) rat develops overt hyperglycemia in the presence of hyperinsulinemia followed by β-cell depletion. This is a type 2 diabetic rat model developed from the Zucker Fatty (*fa/fa*) rat. In these animals, chronic treatment with vanadium reduced the elevated plasma glucose levels [152,153]. The effect in the type 2 models of diabetes can take weeks to develop, whereas the effect in the type 1 models of diabetes are seen within 3 to 4 days.

In diabetic rat models, homocysteine levels are elevated in the serum. This is a predictor of cardiac dysfunction, and the heart is a target organ for diabetic complications. Oral treatment with BMOV and BEOV lowered the elevated homocysteine levels in the Zucker Fatty (ZF) but not the ZDF rat [154]. Administration of these compounds did lower the elevated homocysteine levels found in the STZ-induced type 1 model of diabetes [155]. The effects of BEOV and rosiglitazone malate (RSG), a known insulin sensitizer, were compared for their ability to prevent the development of diabetes in the ZDF rat. Treatment with both compounds prevented the development of hyperglycemia and caused improvement in insulin sensitivity and the retention of normal pancreatic islet morphology [156]. The circulating levels of adiponectin, a hormone secreted by the adipose tissue, did vary in the two treatments. ZDF rats usually develop decreased levels of adiponectin compared to lean controls, whereas the BMOV-treated rats maintained normal levels of the hormone. In contrast, the RSG-treated rats had nearly a fourfold increase in circulating adiponectin. This study shows that vanadium therapy can be advantageous in conjunction with other treatments for diabetes.

11.2.1.2.3   Human Clinical Studies

Limited human trials of vanadium salts (sodium orthovanadate and vanadyl sulfate) have been carried out with diabetic patients having both type 1 and type 2 diabetes, with a 2- to 6-week dosing regimen using 25 to 100 mg of vanadium per day [11,157–160]. These doses were lower than those used in rodents and caused some gastrointestinal distress, but were generally well tolerated. Improvements in insulin sensitivity, nonoxidative glucose production, glycogen synthesis, and insulin suppression of hepatic glucose production have been observed in some, but not all, of the studies. The amount of vanadium taken up in serum was variable in these patient populations and did not correlate with clinical efficacy. Vanadium treatment was shown to increase protein tyrosine phosphorylation of the insulin receptor, insulin responsive substrate 1, and PI-3K [11]. Interestingly, insulin administration did not increase the level of phosphorylation of these proteins, implying that the vanadium and insulin responses in these patients were mediated via the same general signal transduction pathways. Given the variability of the human response to vanadium, larger sample sizes will be required to demonstrate significant effects of vanadium. With respect to clinical trials in humans of the less toxic liganded vanadium compounds, to date only the bis(ethylmaltolato)oxovanadium (IV) complex has completed phase 1 clinical trials [124].

11.2.2   VANADIUM AS THERAPEUTIC AGENT FOR CANCER

The antineoplastic activity of vanadium compounds has been studied for some time. In 1979, the metalocene compound, biscyclopentadienyldichloro-Vanadium(IV), $(C_5H_5)VCl_2$, was found to have antitumor activity [161]. The compound inhibited the growth of various cancer cell lines and the growth of solid tumors *in vivo*. Vanadium(V) peroxocomplexes with known insulin-mimetic activity were shown to have antitumor activity against murine leukemia cells at that time. Vanadocene compounds are now known to induce apoptosis in cell lines. The apoptotic signal

of vanadocene complexes appears to be distinct from that of cisplatin, the most widely used metal cancer therapeutic agent, because it triggers primary DNA damage and involves p53 induction [162]. The p53 protein is a tumor suppressor with molecular mass of 53 kilodaltons that normally functions in the processes of apoptosis, cell cycle control, and maintenance of genomic stability. In a comparison with four other metallocene dichlorides (titanium, zirconium, molybdenum, and hafnium), vanadium(IV) metallocenes were the most potent cytotoxic compounds when tested against human testicular cancer cell lines [163].

Recent work on the antineoplastic effect of vanadium in cell lines has tried to link the anticancer properties to signal transduction processes. COX-2 is an enzyme necessary for prostaglandin formation, and it is inhibited by nonsteroidal antiinflammatory drugs (NSAIDs). In a lung carcinoma cell line, vanadate induced COX-2 expression. Other kinase markers of cell stress, extracellular signal-regulated protein kinase (ERK), cJun N-teminal protein kinase (JNK), and p39 of the mitogen activated protein kinase (MAPK) pathway, were also activated. Catalase, an H_2O_2 scavenger, decreased the vanadate enhancement of COX2 expression [164]. The antiproliferative effects of many vanadium compounds in the cancer cell line K562 were examined and found to be associated with the initiation of apoptosis. Further work looked at the binding of the transcription factors GATA-1 and NF-κβ to target DNA elements. These experiments showed that the presence of anionic units in the vanadium compound were necessary for effects on K562 cells, whereas the V(IV) oxidation state was important in inhibiting transcription factor DNA interactions [165].

Evidence is accumulating that vanadium interferes with the proper functioning of the cell cytoskeleton, which could also be involved in its antineoplastic effects. Taxol, a very successful chemotherapeutic drug, inhibits the function of microtubules in the cytoskeleton. In hepatomoa Morris 5123 cells, V(III) complexed with cysteine and derivatives inhibited the growth of these tumor cells and participated in the rearrangement of actin cytoskeleton architecture [166].

Vanadium treatment in animals has been shown to interfere with the development of malignant tumors. In 1984, oral treatment with vanadyl sulfate was shown to decrease the induction of mammary carcinoma [167]. New experiments have involved treatment to induce a mammary carcinoma in rats started on oral vanadate treatment that continued for 35 weeks. Vanadium treatment protected the rat from development of cancer as determined histologically. In addition, a significant reduction in incidence of total number of tumors and a delay in time to tumor appearance was observed. Vanadium-treated animals had lower tissue distribution of metallothionein, a prognostic marker for breast cancer. The mammary tissue in the vanadium-treated group showed increased apoptosis, which could be related to the anticarcinogenic effect [168].

Vanadium compounds have an inhibitory effect against induced rat hepatocarcinogenesis by limiting cell proliferation and chromosomal aberrations in the preneoplastic stages of the development of this cancer [169]. These antineoplastic effects of vanadium could be related to the induction of apoptosis and selective DNA damage in tumor cells [170]. Vanadate has also proven effective against induction of colon carcinomas [171]. A vanadium(III) cysteine compound has been shown to

have antimetastatic effects against lung metastases in Wistar rats that had been treated with 3,4 benzopyrene [172].

Metvan, bis(4,7-dimethyl-1,10-phenanthroline)sulfatooxovanadium(IV), is a promising new broad spectrum anticancer vanadium drug with favorable pharmacodynamic features and relatively little toxicity [173]. In primary human leukemia cells, it was more effective in inducing apoptosis than the standard chemotherapeutic agents, dexamethasone and vincristine. Vanadium compounds induce antineoplastic cell-cycle arrest or cytotoxic effects through DNA cleavage and fragmentation and plasma membrane lipoperoxidation reactions [174], presumably mediated via the effects on cellular redox chemistry previously described.

The success of vanadium compounds in these experiments argue for a future role of vanadium in chemoprotection. Studies showing the inhibition of the growth of cancer cell lines are more problematic, as the antidiabetic vanadium compounds also inhibit mammalian cell growth. It is necessary to evaluate the antineoplastic growth activity comparing effects in neoplastic and related nontransformed cell lines. This has been done in studies with osteosarcoma [175], where organic V(IV) complexes have been shown to have a much stronger inhibition of cell proliferation, in the osteosarcoma cells increasing in oxidative stress markers such as thiobarbituric acid reactive substrates (TBARS), inducing apoptosis and activating of extracellular signal-regulated protein kinase.

11.3 MECHANISM OF THERAPEUTIC AND APOPTOTIC EFFECTS OF VANADIUM

Diabetes results from alterations in amounts or usage of the growth hormone insulin, whereas cancer results from the uncontrolled activation of normal growth pathways. Both diseases are actually a family of diseases with different metabolic alterations. Both processes involve many of the same phosphorylation cascades and utilize transcription factors that can be controlled by variations in low levels of reactive oxygen and nitrogen species, ROS and RNS. These species can initiate apoptosis when administered as a therapeutic agent for both diseases. The following sections overview the altered signal transduction processes involved when vanadium compounds are given as a therapeutic agent for these diseases. For diabetes, the major signal transduction pathway are the growth hormone pathways; for killing of cancer cells, it is the apoptotic pathway. The particular signal transduction pathways involved when vanadium is used to protect from the induction of a carcinoma are not yet characterized, but would probably include the growth hormone pathways.

11.3.1 CELLULAR OXIDATION-REDUCTION REACTIONS AS PART OF THE THERAPEUTIC EFFECT OF VANADIUM

The insulin-enhancing activity of vanadium compounds is likely to be related to their interactions with cellular redox chemistry and ROS formation, in addition to direct inhibition of PTP-1B and other protein phosphatases as a transition-state analogue [100]. Differences in the effects of V (III, IV or V)-dipicolinic acid complexes on blood glucose and absorption of V into serum after chronic oral admin-

istration in rats with STZ-induced diabetes has been reported, which would be expected if interactions with cellular redox reactions are important in the therapeutic action. The V(V) dipicolinc acid complex was most successful in lowering blood glucose, while there was much less V found in the serum after administration of the V(III) dipicolinc acid complex compared to after administration of the other complexes [176]. PTP-1B, a current potential drug target in diabetes research, is important in the development of insulin resistance, resistance to obesity, and activity of the lipoprotein system [177]. Vanadium could affect the activity of this PTP-1B by two different mechanisms, as the transcription of PTP-1B is proposed to be controlled by redox regulation [19]. The insulin-stimulated formation of H_2O_2, modulated by NAD(P)H oxidase homologue Nox 4, is believed to play an integral role in insulin signal transduction; perhaps in part by affecting the transcription of PTP-1B [178]. The vanadium-dependent formation of H_2O_2 by plasma membrane NADH oxidation activity described earlier has been extensively characterized [24]. Perhaps the H_2O_2, formed intracellularly by vanadium-stimulated NADH oxidation reactions, further inhibits PTP-1B and other enzymes in addition to direct vanadium compound inhibition of the active site of the enzyme.

When the production of ROS and RNS reach high enough levels, cells can be irreversibly damaged. The body needs to get rid of these damaged cells, and apoptosis is one way to accomplish this purpose. It is now known that apoptosis is tightly controlled by phosphorylation/dephosphorylation cascades, and possible vanadium influences on cascades are described below in Section 11.3.2. In addition to the release of reactive species that have both positive and negative cellular effects, the ability of vanadium to stimulate apoptosis via interference with phosphorylation signal cascades can be beneficial both by removing damaged cells in diabetes and by destroying tumor cells. The following general discussion does not differentiate the effects of vanadium compounds in different cells such as liver and muscle; however, the tissue-specific effects of vanadium compounds on signal transduction pathways have been reviewed [13].

11.3.2 Vanadium Interaction with Signal Transduction Cascades as Part of the Therapeutic Effect

Regulation of metabolism is extremely important in biology, and approximately 90% of the proteins found in a cell are involved in regulatory processes rather than catalyzing the reactions of the metabolic pathways *per se*. The most common signal transduction systems controlling metabolism involve phosphorylation/dephosphorylation reactions, and detailed descriptions of these processes can be found in a biochemistry textbook [179]. Phosphorylation by a kinase can either activate or inhibit an enzyme. The dephosphorylation part of a signal transduction pathway is mediated by protein phosphatases [180]. If the phosphorylated form of the enzyme is active, then the dephosphorylated form is inactive, and *vice versa*. The common protein phosphatases are tyrosine protein phosphatases [181] and serine/threonine protein phosphatases [182]. Dual-specificity phosphatases, a subset of the tyrosine protein phosphatases, can also dephosphorylate serine and threonine residues of proteins [183]. Many protein kinases, and a smaller number of phosphatases, are

also part of protein receptors in the plasma membrane. The insulin receptor has a tyrosine phosphatase domain facing the cytoplasm.

Vanadium compounds are believed to exert their effects on signal transduction pathways as transition-state analogues of the tyrosine protein phosphatases. The signal transduction pathways affected by vanadium can be broadly divided into hormonal pathways, controlling normal metabolic processes, and stress-induced pathways. There are numerous crossover points for interactions among these paths. In metabolism, the effects of a signal transduction pathway can be reversed in minutes, halting the biosynthesis or breakdown of a metabolite. The stress pathways can often be quickly switched from apoptosis to mitosis by subtle changes in the cell environment.

Hormonal systems involve the amplification of an extracellular signal initiated by a small metabolite or protein binding to the external portion of a membrane receptor. Frequently, a small metabolite, or second messenger, helps with the amplification process. The hormone-sensitive cAMP system acts via a pathway in which an external hormonal signal, such as glucagon or epinephrine, interacts with a membrane receptor, eventually leading to the production of cAMP and finally the activation of protein kinase A (PKA). In this system, cAMP is considered a second messenger because one molecule can activate many PKA molecules. The phosphoinositol system involves the release of inositol phosphates from phospho-inositol by membrane phospholipase C, activation of protein kinase C, and changes in intracellular distribution of calcium. Like the hormone-sensitive cAMP-producing system, G proteins convey the signal that an agonist (for example, acetyl choline) has bound to the receptor phospholipase C. The second messengers in this system are inositol phosphates and calcium. Inositol 1,4,5 triphosphate causes the release of internal calcium stores to the cytoplasm. Cytosolic calcium activates protein kinase C, starting a number of phosphorylation cascades, and binds to calmodulin, causing a structural change that increases the affinity of calmodulin for target regulatory proteins.

Growth hormones, important in diabetes and cancer, activate a receptor with an intrinsic intracellular tyrosine protein kinase activity that passes on the signal by phosphorylating other proteins, often kinases themselves. To date, no specific second messengers have been associated with these systems. The amplification occurs by the turn-on of the receptor-associated protein kinase activity that can phosphorylate many proteins.

The stress or growth pathways modulated by vanadium involve specialized effectors and often can be activated by excess ROS. Cytokines, small proteins that effect communication between cells or cell behavior, can be involved in the cellular stress response. Tumor necrosis factor α (TNFα) is a cytokine stress signal that binds to a membrane receptor (tumor necrosis factor receptor, or TNFR). This interaction stimulates kinase activity that leads to cell injury and inflammation and also to the activation of caspases, a family of cysteine-dependent aspartate-directed proteases that are involved in apoptosis. The mitogen-activated protein (MAP) kinase cascade regulates both mitosis and apoptosis signaling pathways.

Vanadium compounds interact with insulin-activated signal transduction pathways by inhibiting protein phosphatases, as shown in Figure 11.1 for the insulin
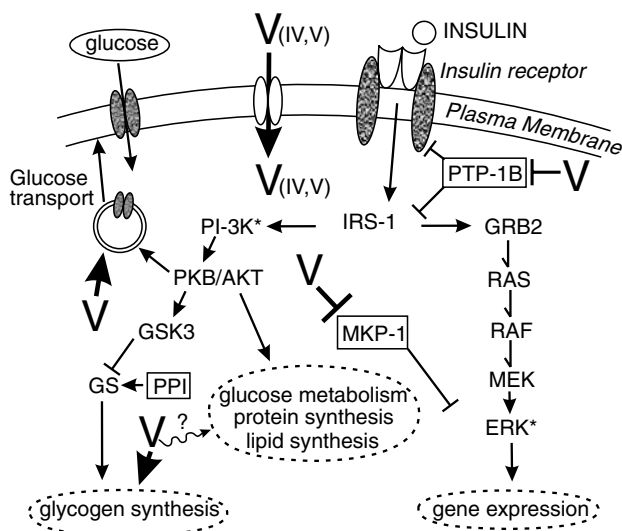
FIGURE 11.1 Interactions of vanadium with insulin signal transduction cascades. Bold lines with arrows at the end leading away from V represent stimulation, blunt-ended lines represent inhibition. The squiggly line leading from V to different metabolic processes represents the fact that vanadium is known to have both positive and negative effects in different biological systems, the "?" indicates that most of the specific proteins involved remain to be elucidated. ERK; extracellular signal-related protein kinase, GRB2: adaptor protein, GS:glycogen synthase, GSK3:glycogen synthase kinase 3, IRS 1: insulin receptor substrate 1, MEK: Mitogen activated protein kinase/ERK kinase, MKP:mitogen kinase phosphatase, RAF: serine/threonine kinase, RAS: GTP binding protein, PI-3K: phosphatidylinositol 3 kinase, PKB/AKT: protein kinase B (also called AKT), PP1:protein phosphatase 1, PTP-1B; protein tyrosine phosphatase 1B, This figure was taken from information in the following references [12,13,99,184].

pathway. Vanadium compounds will cross the cell membrane as V(IV) or V(V), mainly through passive protein facilitated diffusion systems. After insulin binding, the receptor and specific insulin response substrates are phosphorylated. Most of the effects observed with adding vanadium to such systems occur through IRS-1. A major place for intracellular vanadium to interact with the insulin signal transduction pathway is the inhibition of PTP-1B. Inhibition of PTP-1B activity effectively raises the concentration of phosphorylated insulin receptor and IRS-1. If it remains phosphorylated, IRS-1 will activate glucose, lipid, and glycogen biosynthesis by activating PI-3K [99]. Some PI-3K-activated reactions are also important in the stress responses described below. Having components of one signal transduction pathway involved in controlling more than one biological process is an example of the cross talk frequently found in signal transduction pathways.

The mitogen-activated protein kinase pathway (MAPK) on the right side of Figure 11.1 is also activated via the adaptor protein GRB-2 after insulin binds to its receptor. This activated kinase pathway eventually leads to the phosphorylation of

transcription factors regulating mitosis or apoptosis. Vanadium has been proposed to interact with the MAPK pathway by inhibition of the MAPK phosphatase family [12,70] and has been shown to inhibit mitogen kinase phosphase-1 (MKP-1) [184]. These MAP kinase phosphatases are dual-specificity protein phosphatases. These phosphatases show the most activity towards the threonine-X-tyrosine activation motif, which is found only in the MAPKs. Three of the MAPK proteins, ERK, JNK and p38, can be associated with both mitogenic and apoptotic events. Insulin causes the stimulation of the mitotic portion of MAPK pathway. It is possible that vanadium can shift this pathway toward carcinogenic or apoptotic endpoints by inhibiting protein phosphatases of the MKP family.

After phosphorylation by PI-3K, protein kinase B (PKB) is activated to phosphorylate many enzymes and factors, including those involved in glycogen biosynthesis. PKB has been shown to be modulated by vanadium [185]. Vanadium can interfere with protein phosphatases such as protein phosphatase 1, which activates glycogen synthetase, causing the stimulation of glycogen synthesis. In Zucker fatty rats, administration of BMOV stimulated glycogen synthesis [186]. However, in both the ZF rat and the STZ-diabetic rat, BMOV treatment had no influence on the function of protein phosphatase 1 or glycogen synthetase kinase 3, an inhibitor of glycogen synthesis [13]. Another aspect of PKB regulation involves the movement of glucose transporters in vesicles to the plasma membrane, which is the basis for insulin stimulation of glucose transport. Vanadium is also known to help stimulate the movement of the transporters, presumably by promoting the activity of PI-3K [13]. Experimenters looking for direct effects of vanadium compounds on the activity or expression of PI-3K have had variable results in different biological systems.

There are other types of hormone systems affected by vanadium besides the growth hormone pathways shown for insulin in Figure 11.1. Vanadium compounds also interact with hormone-sensitive G protein-modulated systems, in which cyclic nucleotides such as cAMP and cGMP, which act as second messengers, are produced. A diagram of the cAMP producing system is shown in Figure 11.2. The agonists, i.e., epinephrine or glucagon, bind to different receptors that interact with G proteins. This binding results in activation of adenylate cyclase, the formation of the second messenger cAMP, and the activation of protein kinase A. Vanadium compounds can influence this system by inhibition of phosphodiesterase IV (PDE-IV), which catalyzes the breakdown of cAMP [13]. Activation of PKA leads to increases in activity of many proteins including phosphoenolpyruvate carboxykinase (PEPCK) and glucose-6-phosphatase (G6P), enzymes important in gluconeogenesis in the liver. Vanadium is also known to inhibit the production of the mRNA encoding these proteins in rat liver [13]. The cAMP producing system also plays a role in the action of insulin through crosstalk with the growth hormone signal transduction cascade.

Vanadium compounds are also believed to interact with cellular stress pathways that lead to apoptosis [70], as shown in Figure 11.3. One way vanadium compounds can influence these processes is by catalyzing the formation of intracellular ROS and NOS. All of the phosphorylation/dephosphorylation reactions eventually activate transcription factors that move to the nucleus to initiate the DNA breakdown characteristic of apoptosis. Vanadium is postulated to interfere with the dephosphorylation of some of these proteins by inhibition of various protein phosphatases. The
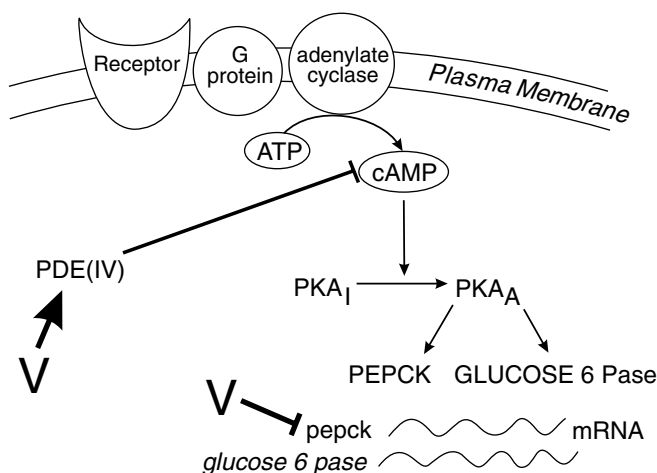
FIGURE 11.2 Interactions of vanadium with the hormone-sensitive G protein modulated cAMP producing signal transduction system. Bold lines with arrows leading away from V represent stimulation, blunt-ended lines represent inhibition. V shows where vanadium inter- actions have geen found. Pase: phosphatase, PDE(IV): phosphodiesterase (IV), PEPCK: phosphoenolpyrurate carboxykinase, PKA$_I$: protein kinse A inactive, PKA$_A$: PKA active. This figure was adapted from [13].

asterisks in the diagram indicate proteins whose level of phosphorylation in one system or another has been shown to be affected by vanadium addition.

The presence of tumor necrosis factor α directly leads to apoptosis via interaction with the tumor necrosis factor receptor, one of a class of receptors referred to as death receptors. NF-κB, which must enter the nucleus to initiate apoptosis, is a transcription factor sequestered in the cytoplasm by inhibitor of κB (IκB). The binding of TNFα to its receptor leads to the ubiquitin-dependent proteolysis of IκB, allowing NF-kB to enter the nucleus. The activation of apoptosis results directly from the stimulation of NF-κB, a transcription factor whose phosphorylation is controlled by vanadium compounds. In a global gene expression study, it was found that diabetes increased the formation of IκB, whereas vanadium compound treatment lowered the production of this inhibitor [101]. The activation of the TNFR also activates the caspase proteins, a class of proteases that cleave proteins after specific aspartate residues.

The target of the caspase proteins are nuclear, regulatory, and cytoskeleton proteins, whose degradation triggers the apoptotic response. The proteins of the *bcl* gene family modulate caspase activity and are divided into proapoptotic and anti- apoptotic fractions (see Figure 11.3). The BCL-associated death (BAD) protein is one of the proapoptotic proteins, whereas BCL-2 is one of the antiapoptotic proteins. The BCL proteins that interact with the caspases to determine whether apoptosis occurs are themselves phosphorylated by PI-3K.

As mentioned above, there is a lot of crosstalk in the stress pathways in Figure 11.3. ERKs, JNKs, and p38 are all kinases that are part of the MAPK system shown in Figure 11.1. Likewise PKB, shown in Figure 11.1, does phosphorylate the proap-
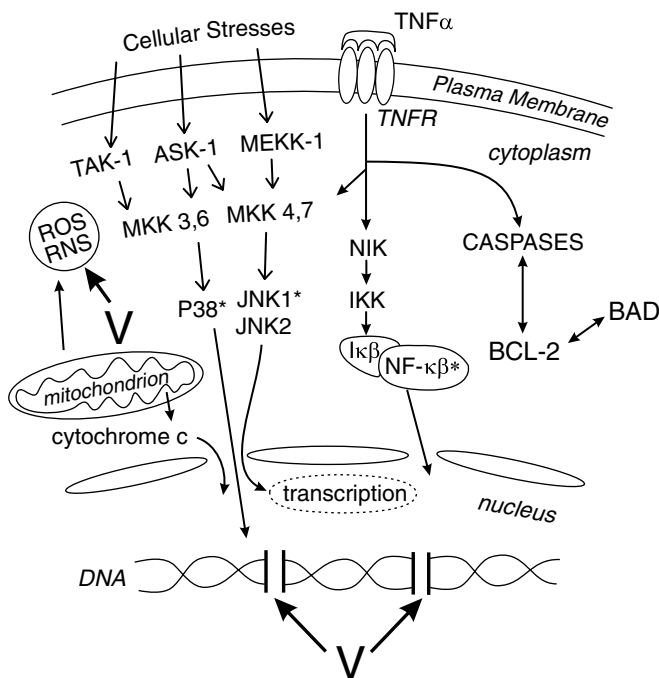
FIGURE 11.3 Vanadium interactions with some apoptotic signal transduction pathways. Bold lines with arrows leading away from the V represent stimulation of ROS,RNS production or stimulation of DNA breakdown. Vanadium modulates extent and duration of phosphorylation of proteins marked with an asterisk. ASK-1: apoptosis signal-regulating kinase 1, BCL-2: one of the family of apoptosis controlling proteins first isolated from a B-cell lymphoma, ERK: extracellular signal-regulated protein kinase, IκB: inhibitor of κB transcription factor, IKK: IκB kinase, JNK: cJun N-terminal protein kinase, MEK: MAPK/ERK kinase, MEKK: MAPK/ERK kinase kinase, MKK: MAP kinase kinase, NIK: NF-κB -inducing kinase, p38: a mitogen activated protein kinase, TAK-1: Transforming Growth Factor β-activated kinase 1, RNS: reactive nitrogen species, ROS: reactive oxygen species, This diagram was adapted from ref [70].

optotic protein (BAD) of the BCL family of proteins, which is represented in Figure 11.3 by BCL-2. The MAPK pathway affects the mitogenic processes, whereas PI-3K effects are more related to the growth hormone pathways [187].

11.4 SUMMARY

Vanadium has marked influences on cellular growth, cellular oxidation-reduction, and enzyme function. The metal is part of the active site of some enzymes, widely believed to be a required ultra trace nutrient, and is toxic in large amounts. The development of vanadium complexes as therapeutic agents for diabetes and cancer is being actively pursued. Much of the influence of vanadium on biological processes

arises from specific interactions with cellular components, including elements of the signal transduction pathway.

The interactions of vanadium compounds with the proteins of the signal transduction pathways are complex, invoking roles of the compounds as transition-state analogues of phosphatase reactions and as modulators of cellular redox reactions. A unifying concept is that vanadium compounds are predominantly involved with the growth hormone, apoptotic, MAP kinase, and hormone-sensitive G protein modulated cAMP pathways. In the literature, effects of vanadium on regulatory proteins are often discussed without any reference to signal transduction pathways involved. When examining specific regulatory proteins controlling metabolism or cell growth, where phosphorylation or other activity is modulated by a vanadium compound, it is useful to place that protein in the appropriate generalized pathway in order to elucidate the general mechanism of action of that vanadium compound.

Many of the effects that vanadium has on metabolic and growth processes appear to result from nonspecific effects on both inhibition of enzymes such as PTPs and interactions with cellular redox systems, potentially leading to the formation of reactive oxygen and reactive nitrogen species. The currently used therapeutic vanadium complexes appear to dissociate under physiological conditions inside the animal or living cell. It is very likely that success in developing vanadium therapeutic agents that target diabetes or cancer in humans will depend upon the ability to design vanadium complexes that are specific to desired biological targets. They must then have the ability to interact with that target or the ability to dissociate to a form that can interact with the specified target. The design of such vanadium compounds depends on the ability to build vanadium complexes that not only target specific enzymes or metabolic pathways but also have the requisite stability to reach the target. This requires a detailed knowledge of both the chemical and redox activity of vanadium compounds, and on the ability to build in factors that appropriately influence those functions.

ABBREVIATIONS

AKT: another name for PKB
ASK: apoptosis signal-regulating kinase
ATP: adenosine triphosphate
BAD: BCL-associated death
BCL:B cell lympohoma refers to a class of proteins regulating apoptosis
BEOV: bis(ethylmaltolato)oxovanadium(IV)
BMOV: bis(maltolato)oxovandium (IV)
cAMP: cyclic AMP
db: leptin receptor gene in mice
DNA: Deoxyribonucleic acid
ERK: extracellular signal-regulated protein kinase
fa: leptin receptor gene in rats
G proteins: guanine nucleotide binding regulatory proteins
G1: first gap in mitotic cell cycle
G2: second gap in mitotic cell cycle

GLUT4: glucose transporter 4
GRB2: an adaptor protein linking IRS-1 to the MAPK pathway with src oncogene homology
       domains 2 and 3
GS: glycogen synthase
GSH: glutathionine
GSK3: glycogen synthetase kinase 3
GTP; guanosine triphoshate
IκB: Inhibitor of ∫B transcription factor
IKK: I∫B kinase
IRS-1: insulin receptor substrate-1
JNK: cJun N-terminal protein kinase
M phase: portion of mitotic cell cycle including mitosis and cytokinesis during which the
       cell separates the duplicated genome into two identical halves
MAPK: mitogen activated protein kinase
MEK: MAPK/ERK kinase
MEKK; MAPK/ERK kinase kinase
Metvan: bis(4,7-dimethyl-1,10-phenanthroline)sulfatooxovanadium (IV)
MKK: mitogen activated protein kinase kinase
MKP: Mitogen kinase phosphatase
mRNA: messenger RNA
NAD(P)H: Nicotinamide adenine dinucleotide (phosphate)
NFAT: nuclear factor of activated T cells
NF-κB: nuclear factor κB
NIK: NF-∫B-inducing kinase
NSAIDS: non-steroidal anti-inflammatory drugs
ob: leptin gene in mice
p38: a MAPK activated by cytokines and stress
p53: a transcription factor regulating the cell cycle that functions as a tumor suppressor
Pase: phosphatase
PDE(IV): phosphodiesterase(IV)
PEPCK: phosphoenolpyruvate carboxykinase
PI-3K: phosphatidylinositol 3-kinase
PKA: protein kinase A
PKB: protein kinase B
PP1: protein phosphatase 1
PTP: Protein tyrosine phosphatase
RAF: a family of serine/threonine protein kinases involved in mitogen signal transduction.
RAS: a family of guanine nucleotide binding proteins.
RBC: red blood cell
RNS: reactive nitrogen species
ROS: reactive oxygen species
RSG: rosiglitazone malate
SALEN: Disalicylidineethylenediamine
S phase: synthesis portion of mitotic cell cycle during which DNA is duplicated.
STZ: streptozotocin, a drug used to induce diabetes by destroying pancreatic β cells
TAK-1: Transforming growth factor β-activated kinase is a MAPK kinase kinase
TBARS: thiobarbituric acid reactive substrates
TNFα: tumor necrosis factor α
TNFR: tumor necrosis factor receptor
V: vanadium

VUr: Vanadium-uridine
ZF: Zucker Fatty
ZDF: Zucker Diabetic Fatty

REFERENCES

1. Cantley, L.C., Jr., L. Josephson, R. Warner, M. Yanagisawa, C. Lechene, and G. Guidotti. 1977. Vanadate is a potent (sodium, potassium ion)-dependent ATPase inhibitor found in ATP derived from muscle. *J. Biol. Chem.* 252:7421–3.

2. Boyd, D.W. and K. Kustin. 1984. Vanadium: A versatile biochemical effector with an elusive biological function. *Adv. Inorg. Biochem.* 6:311–65.

3. Sigel, H. and A. Sigel (Eds.). 1995. *Vanadium and its role in life*. Marcel Dekker, New York.

4. Tracey, A.S. and D.C. Crans (Eds.). 1998. *Vanadium compounds: Chemistry, biochemistry, and therapeutic applications.* American Chemical Society, Washington, D.C.

5. Crans, D.C., J.J. Smee, E. Gaidamauskas, and L. Yang. 2004. The chemistry and biochemistry of vanadium and the biological activities exerted by vanadium compounds. *Chem. Reviews* 104:849–902.

6. Degani, H., M. Gochin, S.J.D. Karlish, and Y. Shechter. 1981. Electron paramagnetic resonance studies and insulin-like effects of vanadium in rat adipocytes. *Biochemistry* 20:5795–9.

7. Willsky, G.R., D.A. White, and B.C. McCabe. 1984. Metabolism of added orthovanadate to vanadyl and high-molecular-weight vanadates by *Saccharomyces cerevisiae*. *J. Biol. Chem.* 259:13273–81.

8. Willsky, G.R., A.B. Goldfine, and P.J. Kostyniak. 1998. Pharmacology and toxicology of oxovanadium species: Oxovanadium pharmacology. *ACS Symp. Ser.* 711:278–296.

9. Soares, S.S., H. Martins, and M. Aureliano. 2006. Vanadium distribution following decavanadate administration. *Arch. Environ. Contam. Toxicol.* 50:60–4.

10. Aureliano, M. and R.M. Gandara. 2005. Decavanadate effects in biological systems. *J. Inorg. Biochem.* 99:979–85.

11. Goldfine, A.B., M.E. Patti, L. Zuberi, B.J. Goldstein, R. LeBlanc, E.J. Landaker, Z.Y. Jiang, G.R. Willsky, and C.R. Kahn. 2000. Metabolic effects of vanadyl sulfate in humans with non-insulin-dependent diabetes mellitus: *In vivo* and *in vitro* studies. *Metabolism:* 49:400–10.

12. Goldfine, A.B., D.C. Simonson, F. Folli, M.E. Patti, and C.R. Kahn. 1995. *In vivo* and *in vitro* studies of vanadate in human and rodent diabetes mellitus. *Mol. Cell. Biochem.* 153:217–31.

13. Marzban, L. and J.H. McNeill. 2003. Insulin-like actions of vanadium: Potential as a therapeutic agent. *J. Trace Elem. Med. Biol.* 16:253–267.

14. Baran, E.J. 2000. Oxovanadium(IV) and oxovanadium(V) complexes relevant to biological systems. *J. Inorg. Biochem.* 80:1–10.

15. Biswas, S., A.S. Chida, and I. Rahman. 2006. Redox modifications of protein-thiols: Emerging roles in cell signaling. *Biochem. Pharmacol.* 71:551–564.

16. Song, B., N. Aebischer, and C. Orvig. 2002. Reduction of $[VO_2(ma)_2]-$ and $[VO_2(ema)_2]-$ by ascorbic acid and glutathione: Kinetic studies of pro-drugs for the enhancement of insulin action. *Inorg. Chem.* 41:1357–1364.

17. Yoshinaga, M., T. Ueki, N. Yamaguchi, K. Kamino, and H. Michibata. 2006. Glutathione transferases with vanadium-binding activity isolated from the vanadium-rich ascidian *Ascidia sydneiensis samea. Biochim. Biophys. Acta* 1760:495–503.

18. Stone, J.R. and S. Yang. 2006. Hydrogen peroxide: A signaling messenger. *Antiox. Redox Signal.* 8:243–270.

19. Salmeen, A., J.N. Andersen, M.P. Myers, T.C. Meng, J.A. Hinks, N.K. Tonks, and D. Barford. 2003. Redox regulation of protein tyrosine phosphatase 1B involves a sulphenyl-amide intermediate. *Nature.* 423:769–73.

20. Vijaya, S., F.L. Crane, and T. Ramasarma. 1984. A vanadate-stimulated NADH oxidase in erythrocyte membrane generates hydrogen peroxide. *Mol. Cell. Biochem.* 62:175–85.

21. Coulombe, R.A.J., D.P. Briskin, R.J. Keller, W.R. Thornley, and R.P. Sharma. 1987. Vanadate-dependent oxidation of pyridine nucleotides in rat liver microsomal membranes. *Biochim. Biophys. Acta* 255:267–273.

22. Briskin, D.P., W.R. Thornley, and R.J. Poole. 1985. Vanadate-dependent NADH oxidation in microsomal membranes of sugar beet. *Biochim. Biophys. Acta* 236:228–237.

23. Minasi, L.A. and G.R. Willsky. 1991. Characterization of vanadate-dependent NADH oxidation stimulated by *Saccharomyces cerevisiae* plasma membranes. *J. of Bacteriol.* 173:834–41.

24. Liochev, I.S. and I. Fridovich. 1990. Vanadate-stimulated oxidation of NAD(P)H in the presence of biological membranes and other sources of O_2^-. *Arch. Biochem. Biophys.* 279:1–7.

25. Liochev, S. and I. Fridovich. 1986. The vanadate-stimulated oxidation of NAD(P)H by biomembranes is a superoxide initiated free radical chain reaction. *Biochim. Biophys. Acta* 250:139–145.

26. Liochev, S.I. and I. Fridovich. 1989. Vanadate-stimulated oxidation of NAD(P)H. *Free Rad. Biol. Med.* 6:617–622.

27. Liochev, S. and I. Fridovitch. 1987. The oxidation of NADH by tetravalent vanadium. *Biochim. Biophys. Acta* 255:274–278.

28. Minasi, L.A., A. Chang, and G.R. Willsky. 1990. Plasma membrane-stimulated vanadate-dependent NADH oxidation is not the primary mediator of vanadate toxicity in *Saccharomyces cerevisiae. J. Biol. Chem.* 265:14907–10.

29. Shi, X. and N.S. Dalal. 1993. Vanadate-mediated hydroxyl radical generation from superoxide radical in the presence of NADH: Haber-Weiss vs. Fenton mechanism. *Arch. Biochem. Biophys.* 307:336–341.

30. Kalyani, P. and T. Ramasarma. 1993. A novel phenomenon of burst of oxygen uptake during decavanadate-dependent oxidation of NADH. *Mol. Cell. Biochem.* 121:21–9.

31. Ramasarma, T. and A.V.S. Rao. 2006. Decavanadate interacts with microsomal NADH oxidation system and enhances cytochrome c reduction. *Mol. Cell. Biochem.* 281:139–144.

32. Rao, A.V.S. and T. Ramasarma. 2000. NADH-dependent decavanadate reductase, an alternative activity of NADP-specific isocitrate dehydrogenase protein. *Biochim. Biophys. Acta* 1474:321–330.

33. Ravishankar, H.N. and T. Ramasarma. 1995. Requirement of a diperoxovanadate-derived intermediate for the interdependent oxidation of vanadyl and NADH. *Biochim. Biophys. Acta* 316:319–26.

34. Ramasarma, T. and H.N. Ravishankar. 2005. Formation of an oxo-radical of peroxovanadate during reduction of diperoxovanadate with vanadyl sulfate or ferrous sulfate. *Biochim. Biophys. Acta* 1722:30–35.

35. Willsky, G.R. 1990. Vanadium in the biosphere. In *Vanadium in biological systems. Physiology and biochemistry,* N.D. Chasteen (Ed.), Kluwer, Dordrecht. pp. 1–24.

36. Lowenstein, C.J., J.L. Dinerman, and S.H. Snyder. 1994. Nitric oxide: A physiologic messenger. *Ann. Intern. Med.* 120:227–37.

37. Kotchevar, A.T., P. Ghosh, D.D. DuMez, and F.M. Uckun. 2001. Induction of aerobic peroxidation of liposomal membranes by bis(cyclopentadienyl)-vanadium(IV) (acety-lacetonate) complexes. *J. Inorg. Biochem.* 83:151–160.

38. Keller, R.J., R.P. Sharma, T.A. Grover, and L.H. Piette. 1988. Vanadium and lipid peroxidation: Evidence for involvement of vanadyl and hydroxyl radical. *Biochim. Biophys. Acta* 265:524–533.

39. Huang, C., M. Ding, J. Li, S.S. Leonard, Y. Rojanasakul, V. Castranova, V. Vallyathan, G. Ju, and X. Shi. 2001. Vanadium-induced nuclear factor of activated T cells activation through hydrogen peroxide. *J. Biol. Chem.* 25:22397–22403.

40. Fickl, H., A.J. Theron, H. Grimmer, J. Oommen, G.J. Ramafi, H.C. Steel, S.S. Visser, and R. Anderson. 2006. Vanadium promotes hydroxyl radical formation by activated human neutrophils. *Free Radic. Biol. Med.* 40:146–55.

41. Scibior, A., H. Zaporowska, J. Ostrowski, and A. Banach. 2006. Combined effect of vanadium(V) and chromium(III) on lipid peroxidation in liver and kidney of rats. *Chem.-Biol. Interact.* 159:213–22.

42. Li, Z., J.D. Carter, L.A. Dailey, and Y.C. Huang. 2004. Vanadyl sulfate inhibits NO production via threonine phosphorylation of eNOS. *Environ. Health Persp.* 112:201–6.

43. Meurer, S., S. Pioch, S. Gross, and W. Muller-Esterl. 2005. Reactive oxygen species induce tyrosine phosphorylation of and Src kinase recruitment to NO-sensitive guanylyl cyclase. *J. Biolog. Chem.* 280:33149–56.

44. Carreras, J., R. Bartrons, and S. Grisolia. 1980. Vanadate inhibits 2,3-bisphospho-glycerate dependent phosphoglycerate mutases but does not affect the 2,3-bisphos-phoglycerate independent phosphoglycerate mutases. *Biochem. Biophys. Res. Commun.* 96:1267–1273.

45. Carreras, J., F. Climent, R. Bartrons, and G. Pons. 1982. Effect of vanadate on the formation and stability of the phosphoenzyme forms of 2,3-bisphosphoglycerate-dependent phosphoglycerate mutase and of phosphoglucomutase. *Biochim. Biophysic. Acta* 705:238–242.

46. Liu, S., M.J. Gresser, and A.S. Tracey. 1992. 1-H and 51-V nmr studies of the reaction of vanadate and 2-vanadio-3-phosphoglycerate with phosphoglycerate mutase. *J. Biochem.* 31:2677–2685.

47. Leon-Lai, C.H., M.J. Gresser, and A.S. Tracey. 1996. Influence of vanadium(V) complexes on the catalytic activity of ribonuclease A. The role of vanadate complexes as transition state analogues to reactions at phosphate. *Can. J. Chem.* 74:38–48.

48. Raines, R.T. 1998. Ribonuclease A. *Chem Rev.* 98:1045–1065.

49. Lindquist, R.N., J.L. Lynn, Jr., and G.E. Lienhard. 1973. Possible transition-state analogs for ribonuclease. The complexes of uridine with oxovanadium(IV) ion and vanadium(V) ion. *J. Am. Chem. Soc.* 95:8762–8768.

50. Tracey, A.S., J.S. Jaswal, M.J. Gresser, and D. Rehder. 1990. Condensation of aqueous vanadate with the common nucleosides. *Inorg. Chem.* 29:4283–4288.

51. Tracey, A.S. and C.H. Leon-Lai. 1991. 1-H and 51-V NMR investigation of the complexes formed between vanadate and nucleosides. *Inorg. Chem.* 30:3200–3204.

52. Messmore, J.M. and R.T. Raines. 2000. Pentavalent organo-vanadates as transition state analogues for phosphoryl transfer reactions. *J. Am. Chem. Soc.* 122:9911–9916.

53. Ray, W.J., Jr. and C.B. Post. 1990. The oxyvanadium constellation in transition-state-analogue complexes of phosphoglucomutase and ribonuclease. Structural deductions from electron-transfer spectra. *J. Biochem.* 29:2779–2789.

54. Borah, B., C.W. Chen, W. Egan, M. Miller, A. Wlodawer, and J.S. Cohen. 1985. Nuclear magnetic resonance and neutron diffraction studies of the complex of ribonuclease A with uridine vanadate, a transition-state analogue. *J. Biochem.* 24:2058–2067.

55. Wladkowski, B.D., L.A. Svensson, L. Sjolin, J.E. Ladner, and G.L. Gilliland. 1998. Structure (1.3 A) and charge state of a ribonuclease A-uridine vanadate complex: Implications for the phosphate ester hydrolysis mechanism. *J. Am. Chem. Soc.* 120:5488–5498.

56. Deng, H., J.W. Burgner, II, and R.H. Callender. 1998. Structure of the ribonuclease A-uridine-vanadate transition state analogue complex by Raman difference spectroscopy: Mechanistic implications. *J. Am. Chem. Soc.* 120:4717–4722.

57. Veenstra, T.D. and L. Lee. 1994. NMR study of the positions of his-12 and his-119 in the ribonuclease A-uridine vanadate complex. *Biophys. J.* 67:331–335.

58. Messmore, J.M. and R.T. Raines. 2000. Decavanadate inhibits catalysis by ribonuclease A. *Biochim. Biophys. Acta* 381:25–30.

59. Kostrewa, D., H.W. Choe, U. Heinemann, and W. Saenger. 1989. Crystal structure of guanosine-free ribonuclease T¹, complexed with vanadate(V), suggests conformation change upon substrate binding. *Biochemistry* 28:7592–7600.

60. Swarup, G., S. Cohen, and D.L. Garbers. 1982. Inhibition of membrane phosphotyrosyl-protein phosphatase activity by vanadate. *Biochem. Biophys. Res. Commun.* 107:1104–1109.

61. Huyer, G. 1997. Mechanism of inhibition of protein tyrosine phosphatases by vanadate and pervanadate. *J. Biolog. Chem.* 272:843–851.

62. Denu, J.M., D.L. Lohse, J. Vijayalakshmi, M.A. Saper, and J.E. Dixon. 1996. Visualization of intermediate and transition-state structures in protein-tyrosine phosphatase catalysis. *Proceedings of the National Academy of Sciences of the U.S.A.* 93:2493–2498.

63. Goldstein, B.J. 1998. *Tyrosine phosphoprotein phosphatases.* Oxford University Press, Oxford, U.K., New York.

64. Nxumalo, F., N.R. Glover, and A.S. Tracey. 1998. Kinetics and molecular modelling studies of the inhibition of protein tyrosine phosphatases by N,N-dimethylhydroxylamine complexes of vanadium(V). *Journal of Biological Inorg. Chem.* 3:534–542.

65. Cuncic, C., N. Detich, D. Ethier, A.S. Tracey, M.J. Gresser, and C. Ramachandran. 1999. Vanadate inhibition of protein tyrosine phosphatases in Jurkat cells: Modulation by redox state. *J. Biolog. Inorg. Chem.* 4:354–359.

66. Bhattacharyya, S. and A.S. Tracey. 2001. Vanadium(V) complexes in enzyme systems: Aqueous chemistry, inhibition and molecular modeling in inhibitor design. *J. Inorg. Biochem.* 85:9–13.

67. Bhattacharyya, S., A. Martinsson, R.J. Batchelor, F.W.B. Einstein, and A.S. Tracey. 2001. N,N-dimethylhydroxamidovanadium(V). Interactions with sulfhydryl-containing ligands: V(V) equilibria and the structure of a V(IV) dithiothreitol complex. *Can. J. Chem.* 79:938–948.

68. Tracey, A.S. 2000. Hydroxamido vanadates: Aqueous chemistry and function in protein tyrosine phosphatases and cell cultures. *J. Inorg. Biochem.* 80:11–16.

69. Alberts, B., A. Johnson, J. Lewis, K. Roberts, and P. Walter. 2002. *Molecular biology of the cell.* Garland Science Taylor & Francis Group, New York.

70. Morinville, A., D. Maysinger, and A. Shaver. 1998. From Vanadis to Atropos: Vanadium compounds as pharmacological tools in cell death signalling. *Trends Pharmacol. Sci.* 19:452–60.

71. Huang, C., Z. Zhang, M. Ding, J. Li, J. Ye, S.S. Leonard, H.-M. Shen, L. Butterworth, Y. Lu, M. Costa and others. 2000. Vanadate induces p53 transactivation through hydrogen peroxide and causes apoptosis. *J. Biol. Chem.* 275:32516–32522.

72. Leopardi, P., P. Villani, E. Cordelli, E. Siniscalchi, E. Veschetti, and R. Crebelli. 2005. Assessment of the *in vivo* genotoxicity of vanadate: Analysis of micronuclei and DNA damage induced in mice by oral exposure. *Toxicol. Lett.* 158:39–49.

73. Sam, M., J.H. Hwang, G. Chanfreau, and M.M. Abu-Omar. 2004. Hydroxyl radical is the active species in photochemical DNA strand scission by bis(peroxo)vanadium(V) phenanthroline. *Inorg. Chem.* 43:8447–55.

74. Verquin, G., G. Fontaine, M. Bria, E. Zhilinskaya, E. Abi-Aad, A. Aboukais, B. Baldeyrou, C. Bailly, and J.-L. Bernier. 2004. DNA modification by oxovanadium(IV) complexes of SALEN derivatives. *J. Biol. Inorg. Chem.* 9:345–353.

75. Morita, A., J. Zhu, N. Suzuki, A. Enomoto, Y. Matsumoto, M. Tomita, T. Suzuki, K. Ohtomo, and Y. Hosoi. 2006. Sodium orthovanadate suppresses DNA damage-induced caspase activation and apoptosis by inactivating p53. *Cell Death Differ.* 13:499–511.

76. Afshari, C., S. Kodama, H. Bivins, T.B. Willard, H. Fujiki, and J.C. Barrett. 1993. Induction of neoplastic progression in Syrian hamster embryo cells treated with protein phosphatase inhibitors. *Cancer Res.* 53:1777–1782.

77. Klarlund, J.K. 1985. Transformation of cells by an inhibitor of phosphatases acting on phosphotyrosine in proteins. *Cell* 41:707–17.

78. Aguirre, M.V., J.A. Juaristi, M.A. Alvarez, and N.C. Brandan. 2005. Characteristics of *in vivo* murine erythropoietic response to sodium orthovanadate. *Chemico-Biolog. Interact.* 156: 55–68.

79. Rumora, L., A. Shaver, T.Z. Grubisic, and D. Maysinger. 2001. MKP-1 as a target for pharmacological manipulations in PC12 cell survival. *Neurochem. Int.* 39:25–32.

80. Domingo, J.L. 2002. Vanadium and tungsten derivatives as antidiabetic agents: A review of their toxic effects. *Biol. Trace Elem. Res.* 88:97–112.

81. Eckhert, C.D. 2006. Other trace elements. In *Modern nutrition in health and disease.* 10th ed. Shils, M.E., M. Shike, A.C. Ross, C. Benjamin, and R.J. Cousins (Eds.). Lippincott Williams and Wilkins, Philadelphia. pp. 338–350.

82. Harris, W.R., S.B. Friedman, and D. Silberman. 1984. Behavior of vanadate and vanadyl ion in canine blood. *J. Inorg. Biochem.* 20:157–69.

83. Patterson, B.W., S.L. Hansard, II, C.B. Ammerman, P.R. Henry, L.A. Zech, and W.R. Fisher. 1986. Kinetic model of whole-body vanadium metabolism: Studies in sheep. *Am. J. Physiol.* 251:R325–32.

84. Sabbioni, E., E. Marafante, L. Amantini, L. Ubertalli, and C. Birattari. 1978. Similarity in metabolic patterns of different chemical species of vanadium in the rat. *Bioorg. Chem.* 8:503–15.

85. Setyawati, I.A., K.H. Thompson, V.G. Yuen, Y. Sun, M. Battell, D.M. Lyster, C. Vo, T.J. Ruth, S. Zeisler, J.H. McNeill and others. 1998. Kinetic analysis and comparison of uptake, distribution, and excretion of 48V-labeled compounds in rats. *J. Appl. Physiol.* 84:569–575.

86. Thompson, K.H., M. Battell, and J.H. McNeill. 1998. Toxicology of vanadium in mammals. In *Vanadium in the environment.* Part 2. Health effects, Nriagu, J.O. (Ed.). John Wiley and Sons, Ann Arbor, MI. pp. 21–37.

87. Goldfine, A.B., G. Willsky, and C.R. Kahn. 1998. Vanadium salts in the treatment of human diabetes mellitus. *ACS Symposium Series* 711:353–368.

88. Ramanadham, S., C. Heyliger, M.J. Gresser, A.S. Tracey, and J.H. McNeill. 1991. The distribution and half-life for retention of vanadium in the organs of normal and diabetic rats orally fed vanadium(IV) and vanadium(V). *Biol. Trace Elem. Res.* 30:119.

89. Dikanov, S.A., B.D. Liboiron, and C. Orvig. 2002. Two-dimensional (2D) pulsed electron paramagnetic resonance study of VO_{2+}-triphosphate interactions: Evidence for tridentate triphosphate coordination, and relevance to bone uptake and insulin enhancement by vanadium pharmaceuticals. *J. Am. Chem. Soc.* 124:2969–2978.

90. Stroop, S.D., G. Helinek, and H.L. Greene. 1982. More sensitive flameless atomic absorption analysis of vanadium in tissue and serum. *Clin. Chem.* 28:79–82.

91. Leibovitz, B. 1993. Vanadium (vanadyl): Does it really increase anabolism? *Musc. Develop.* October:74–75,191.

92. Costigan, M., R. Cary, and S. Dobson. 2001. Vanadium pentoxide and other inorganic vanadium compounds. *Concise International Chemical Assessment Document* 29:i–v, 1–53.

93. Anonymous. 1988. *Environmental Health Criteria 81. Vanadium.* World Health Organization, Geneva.

94. Ress, N.B., B.J. Chou, R.A. Renne, J.A. Dill, R.A. Miller, J.H. Roycroft, J.R. Hailey, J.K. Haseman, and J.R. Bucher. 2003. Carcinogenicity of inhaled vanadium pentoxide in F344/N rats and B6C3F1 mice. *Toxicol. Sci.* 74:287–96.

95. Cohen, M.D, Z. Yang, J. Zelikoff and R.B. Schlesinger. 1996. Pulmonary immunotoxicity of inhaled ammonium metavanadate in Fischer 344 rats. *Fundam. Appl. Toxicol.* 33: 254-263.

96. Valko, M., H. Morris, and M.T.D. Cronin. 2005. Metals, toxicity and oxidative stress. *Curr. Med. Chem.* 12:1161–1208.

97. Hulley, P.A., F. Gordon, and F.S. Hough. 1998. Inhibition of mitogen-activated protein kinase activity and proliferation of an early osteoblast cell line (MBA 15.4) by dexamethasone: Role of protein phosphatases. *Endocrinology* 139:2423–31.

98. Silver, S., L.T. Phung, and G. Silver. 2006. Silver as biocides in burn and wound dressings and bacterial resistance to silver compounds. *J. Ind. Microbiol. Biotechnol.* 33:627–634.

99. Saltiel, A.R. and C.R. Kahn. 2001. Insulin signalling and the regulation of glucose and lipid metabolism. *Nature.* 414:799–806.

100. Cam, M.C., R.W. Brownsey, and J.H. McNeill. 2000. Mechanisms of vanadium action: Insulin-mimetic or insulin-enhancing agent? *Can. J. Physiol. Pharmacol.* 78:829–847.

101. Willsky, G.R., L.-H. Chi, D.P. Gaile, Z. Hu, and D.C. Crans. 2006. Diabetes altered gene expression in rat skeletal muscle corrected by oral administration of vanadyl sulfate. *Physiol. Genom.* 26:192–201.

102. Brownlee, M. 2005. Banting Lecture 2004: The pathophysiology of diabetic complications, a unifying mechanism. *Diabetes* 54:1615–1625.

103. Raza, H. P., S.K. Prabu, M.A. Robin, and N.G. Avadhani. 2004. Elevated mitochondrial cytochrome P450 2E1 and glutathione S-transferase A4-4 in streptozotocin-induced diabetic rats. *Diabetes* 53:185–194.

104. Tabatabaie, T., A. Vasquez-Weldon, D.R. Moore, and Y. Kotake. 2003. Free radicals and the pathogenesis of type 1 diabetes: Beta-cell cytokine-mediated free radical generation via cyclooxygenase-2. *Diabetes.* 52:1994–9.

105. Robertson, R.P., J. Harmon, P.O. Tran, Y. Tanaka, and H. Takahashi. 2003. Glucose toxicity in beta-cells: Type 2 diabetes, good radicals gone bad, and the glutathione connection. *Diabetes.* 52:581–7.

106. Thornalley, P.J., A.C. McLellan, T.W. Lo, J. Benn, and P.H. Sonksen. 1996. Negative association between erythrocyte reduced glutathione concentration and diabetic complications. *Clin. Sci.* 91:575–82.

107. Yoshida, K., J. Hirokawa, S. Tagami, Y. Kawakami, Y. Urata, and T. Kondo. 1995. Weakened cellular scavenging activity against oxidative stress in diabetes mellitus: Regulation of glutathione synthesis and efflux. *Diabetologia.* 38:201–10.

108. Rusnak, F. and T. Reiter. 2000. Sensing electrons: Protein phosphatase redox regulation. *Tr. Biochem. Sci.* 25:527–9.

109. Goldstein, B.J., K. Mahadev, X. Wu, L. Zhu, and H. Motoshima. 2005. Role of insulin-induced reactive oxygen species in the insulin signaling pathway. *Antiox. Redox Signal.* 7:1021–1031.

110. Anderson, R.A. 2000. Chromium in the prevention and control of diabetes. *Diabetes Metabol.* 26:22–7.

111. Clodfelder, B.J., R.G. Upchurch, and J.B. Vincent. 2004. A comparison of the insulin-sensitive transport of chromium in healthy and model diabetic rats. *J. Inorg. Biochem.* 98:522–33.

112. Brautigan, D.L., A. Kruszewski, and H. Wang. 2006. Chromium and vanadate combination increases insulin-induced glucose uptake by 3T3-L1 adipocytes. *Biochem. Biophys. Res. Commun.* 347:769–773.

113. Fernandez-Alvarez, J., A. Barbera, B. Nadal, S. Barcelo-Batllori, S. Piquer, M. Claret, J.J. Guinovart, and R. Gomis. 2004. Stable and functional regeneration of pancreatic beta-cell population in STZ-rats treated with tungstate. *Diabetologia.* 47:470–7.

114. Dominguez, J.E., M.C. Munoz, D. Zafra, I. Sanchez-Perez, S. Baque, M. Caron, C. Mercurio, A. Barbera, R. Perona, R. Gomis and others. 2003. The antidiabetic agent sodium tungstate activates glycogen synthesis through an insulin receptor-independent pathway. *J. Biol. Chem.* 278:42785–42794.

115. Ozcelikay, A.T., D.J. Becker, L.N. Ongemba, A.M. Pottier, J.C. Henquin, and S.M. Brichard. 1996. Improvement of glucose and lipid metabolism in diabetic rats treated with molybdate. *J. Am. J. Physiol.* 270:E344–52.

116. Thompson, K.H., J. Chiles, V.G. Yuen, J. Tse, J.H. McNeill, and C. Orvig. 2004. Comparison of anti-hyperglycemic effect amongst vanadium, molybdenum and other metal maltol complexes. *J. Inorg. Biochem.* 98:683–90.

117. Crans, D.C., L. Yang, J.A. Alfano, L.-H. Chi, W. Jin, M. Mahroof-Tahir, K. Robbins, M.M. Toloue, L.K. Chan, A.J. Plante, R.Z. Grayson, and G.R. Willsky. 2003. (4-Hydroxypyridine-2,6-dicarboxylato)oxovanadate(V)—a new insulin-like compound: Chemistry, effects on myoblast and yeast cell growth and effects on hyperglycemia in rats with STZ-induced diabetes. *Coord. Chem. Rev.* 237:13–22.

118. Thompson, K.H., K. Boehmerle, E. Polishchuk, C. Martins, P. Toleikis, J. Tse, V. Yuen, J.H. McNeill, and C. Orvig. 2004. Complementary inhibition of synoviocyte, smooth muscle cell or mouse lymphoma cell proliferation by a vanadyl curcumin complex compared to curcumin alone. *J. Inorg. Biochem.* 98:2063–2070.

119. Lyonnet, M. and E. Martin. 1899. L'emploi therapeutique des derives du vanadium. *La Presse Medicale* 32:191–192.

120. Dubyak, G.R. and A. Kleinzeller. 1980. The insulin-mimetic effects of vanadate in isolated rat adipocytes. Dissociation from effects of vanadate as a (Na+-K+)ATPase inhibitor. *The J. Biol. Chem.* 255:5306–12.

121. Shechter, Y. and S.J.D. Karlish. 1980. Insulin-like stimulation of glucose oxidation in rat adipocytes by vanadyl (IV) ions. *Nature* 284:556–8.

122. Heyliger, C.E., A.G. Tahiliani, and J.H. McNeill. 1985. Effect of vanadate on elevated blood glucose and depressed cardiac performance of diabetic rats. *Science*. 227:1474–7.

123. Meyerovitch, J., Z. Farfel, J. Sack, and Y. Shechter. 1987. Oral administration of vanadate normalizes blood glucose levels in streptozotocin-treated rats. Characterization and mode of action. *J. Biol. Chem.* 262:6658–62.

124. Thompson, K.H. and C. Orvig. 2001. Coordination chemistry of vanadium in metallopharmaceutical candidate compounds. *Coor. Chem. Rev.* 219–221:1033–1053.

125. Battell, M.L., V.G. Yuen, and J.H. McNeill. 1992. Treatment of BB rats with vanadyl sulphate. *Pharmacol. Commun.* 1:291–301.

126. Edel, A.L., M. Kopilas, T.A. Clark, F. Aguilar, P.K. Ganguly, C.E. Heyliger, and G.N. Pierce. 2006. Short-term bioaccumulation of vanadium when ingested with a tea decoction in streptozotocin-induced diabetic rats. *Metabol.* 55:263–70.

127. Clark, T.A., A.L. Edel, C.E. Heyliger, and G.N. Pierce. 2004. Effective control of glycemic status and toxicity in Zucker diabetic fatty rats with an orally administered vanadate compound. *Can. J. Physiol. Pharm.* 82:888–94.

128. Fugono, J., H. Yasui, and H. Sakurai. 2005. Improvement of diabetic states in streptozotocin-induced type 1 diabetic rats by vanadyl sulfate in enteric-coated capsules. *Can. J. Physiol. Pharm.* 57:665–669.

129. Shechter, Y., I. Goldwaser, M. Mironchik, M. Fridkin, and D. Gefel. 2003. Historic perspective and recent developments on the insulin-like actions of vanadium; toward developing vanadium-based drugs for diabetes. *Coor. Chem. Rev.* 237:3–11.

130. Bevan, A.P., P.G. Drake, J.F. Yale, A. Shaver, and B.I. Posner. 1995. Peroxovanadium compounds: Biological actions and mechanism of insulin-mimesis. *Mol. Cell. Biochem.* 153:49–58.

131. Thompson, K.H., J.H. McNeill, and C. Orvig. 1999. Vanadium compounds as insulin mimics. *Chem. Rev.* 99:2561–2571.

132. Ramachandran, B. and S. Subramanian. 2005. Amelioration of diabetic dyslipidemia by macrocyclic binuclear oxovanadium complex on streptozotocin induced diabetic rats. *Mol. Cell. Biochem.* 272:157–64.

133. Tsiani, E. and I.G. Fantus. 1997. Vanadium compounds. Biological actions and potential as pharmacological agents. *Tr. Endo. Metabol.* 8:51–58.

134. Shechter, Y., G. Eldberg, A. Shisheva, D. Gefel, N. Sekar, S. Qian, R. Bruck, E. Gershonov, D.C. Crans, Y. Goldwasser and others. 1998. Insulin-like effects of vanadium; reviewing *in vivo* and *in vitro* studies and mechanisms of action. *ACS Symposium Series* 711:308–315.

135. Jackson, T.K., A.I. Salhanick, J.D. Sparks, C.E. Sparks, M. Bolognino, and J.M. Amatruda. 1988. Insulin-mimetic effects of vanadates in primary cultures of rat hepatocytes. *Diabetes* 37:1234–1240.

136. Mehdi, M.Z. and A.K. Srivastava. 2005. Organo-vanadium compounds are potent activators of the protein kinase B signaling pathway and protein tyrosine phosphorylation: Mechanism of insulinomimesis. *Biochim. Biophys. Acta* 440:158–164.

137. Sekar, N., J. Li, Z. He, D. Gefel, and Y. Shechter. 1999. Independent signal-transduction pathways for vanadate and for insulin in the activation of glycogen synthase and glycogenesis in rat adipocytes. *Endocrinology* 140:1125–1131.

138. Tsiani, E., E. Bogdanovic, A. Sorisky, L. Nagy, and I.G. Fantus. 1998. Tyrosine phosphatase inhibitors, vanadate and pervanadate, stimulate glucose transport and GLUT translocation in muscle cells by a mechanism independent of phosphatidylinositol 3-kinase and protein kinase C. *Diabetes* 47:1676–1686.

139. Duckworth, W.C., S.S. Solomon, J. Lepnieks, F.G. Hamel, S. Hand, and D.E. Peavy. 1988. Insulin-like effects of vanadate in isolated rat adipocytes. *Endocrinology* 122:2285–2289.

140. Elberg, G., Z. He, J. Li, N. Sekar, and Y. Shechter. 1997. Vanadate activates membranous nonreceptor protein tyrosine kinase in rat adipocytes. *Diabetes* 46:1684–1690.

141. Ou, H., L. Yan, D. Mustafi, M. Makinen, M.J. Brady. 2005. The vanadyl (VO2+)chelate bis(acetylacetonato)oxovanadium (IV) potentiates tyrosine phosphorylation of the insulin receptor. *J. Biolog. Inorg. Chem.* 10: 874-886.

142. Sakurai, H. and H. Yasui. 2003. Structure-activity relationship of insulinomimetic vanadyl-picolinate complexes in view of their clinical use. *J. Trace Elem. Med. Biol.* 16:269–280.

143. Yamaguchi, M., K. Wakasugi, R. Saito, Y. Adachi, Y. Yoshikawa, H. Sakurai, and A. Katoh. 2006. Syntheses of vanadyl and zinc(II) complexes of 1-hydroxy-4,5,6-substituted 2(1*H*)-pyrimidinones and their insulin-mimetic activities. *J. Inorg. Biochem.* 100:260–9.

144. Coderre, L. and A.K. Srivastava. 2005. Vanadium and the cardiovascular functions. *Can. J. Physiol. Pharm.* 82:833–9.

145. Bonnefont-Rousselot, D. 2005. The role of antioxidant micronutrients in the prevention of diabetic complications. *Treat. Endo.* 3:41–52.

146. Haratake, M., M. Fukunaga, M. Ono, and M. Nakayama. 2005. Synthesis of vanadium(IV,V) hydroxamic acid complexes and *in vivo* assessment of their insulin-like activity. *J. Biol. Inorg. Chem.* 10:250–258.

147. Monga, V., K.H. Thompson, V.G. Yuen, V. Sharma, B.O. Patrick, J.H. McNeill, and C. Orvig. 2005. Vanadium complexes with mixed O,S anionic ligands derived from maltol: Synthesis, characterization, and biological studies. *Inorg. Chem.* 44:2678–88.

148. Sun, Y., B.J. Clodfelder, A.A. Shute, T. Irvin, and J.B. Vincent. 2002. The biomimetic [Cr(3)O(O(2)CCH(2)CH(3))(6)(H(2)O)(3)](+) decreases plasma insulin, cholesterol, and triglycerides in healthy and type II diabetic rats but not type I diabetic rats. *J. Biol. Inorg. Chem.* 7:852–62.

149. Brichard, S.M., A.M. Pottier, and J.C. Henquin. 1989. Long term improvement of glucose homeostasis by vanadate in obese hyperinsulinemic fa/fa rats. *Endocrinology* 125:2510–16.

150. Brichard, S.M., C.J. Bailey, and J.C. Henquin. 1990. Marked improvement of glucose homeostasis in diabetic ob/ob mice given oral vanadate. *Diabetes* 39:1326–32.

151. Meyerovitch, J., P. Rothenberg, Y. Shechter, S. Bonner-Weir, and C.R. Kahn. 1991. Vanadate normalizes hyperglycemia in two mouse models of non-insulin-dependent diabetes mellitus. *J. Clin. Invest.* 87:1286–94.

152. Yuen, V.G., R.A. Pederson, S. Dai, C. Orvig, and J.H. McNeill. 1996. Effects of low and high dose administration of bis(maltolato)oxovanadium(IV) on fa/fa Zucker rats. *Can. J. Physiol. Pharmacol.* 74:1001–9.

153. Yuen, V.G., E. Vera, M.L. Battell, W.M. Li, and J.H. McNeill. 1999. Acute and chronic oral administration of bis(maltolato)oxovanadium(IV) in Zucker diabetic fatty (ZDF) rats. *Diabetes Res. Clin. Pract.* 43:9–19.

154. Wasan, K.M., V. Risovic, V.G. Yuen, and J.H. McNeill. 2006. Differences in plasma homocysteine levels between Zucker fatty and Zucker diabetic fatty rats following 3 weeks oral administration of organic vanadium compounds. *J. Tr. Elem. Med. Biol.* 19:251–8.

155. Wasan, K.M., V. Risovic, V.G. Yuen, A. Hicke, and J.H. McNeill. 2004. Effects of three and eight weeks oral administration of bis(maltolato)oxovanadium(IV) on plasma homocysteine and cysteine levels in streptozotocin-induced diabetic rats. *Exp. Clin. Cardiol.* 9:125–129.

156. Winter, C.L., J.S. Lange, M.G. Davis, G.S. Gerwe, T.R. Downs, K.G. Peters, and B. Kasibhatla. 2005. A nonspecific phosphotyrosine phosphatase inhibitor, bis(malto-lato)oxovanadium(IV), improves glucose tolerance and prevents diabetes in Zucker diabetic fatty rats. *Exp. Biol. Med.* 230:207–16.

157. Cohen, N., M. Halberstam, P. Shlimovich, C.J. Chang, H. Shamoon, and L. Rossetti. 1995. Oral vanadyl sulfate improves hepatic and peripheral insulin sensitivity in patients with non-insulin-dependent diabetes mellitus. *J. Clin. Invest.* 95:2501–9.

158. Boden, G., X. Chen, J. Ruiz, G.D.V. van Rossum, and S. Turco. 1996. Effects of vanadyl sulfate on carbohydrate and lipid metabolism in patients with non-insulin-dependent diabetes mellitus. *Metabol.* 45:1130–1135.

159. Halberstam, M., N. Cohen, P. Shlimovich, L. Rossetti, and H. Shamoon. 1996. Oral vanadyl sulfate improves insulin sensitivity in NIDDM but not in obese nondiabetic subjects. *Diabetes* 45:659–666.

160. Cusi, K., S. Cukier, R.A. DeFronzo, M. Torres, F.M. Puchulu, and J.C.P. Redondo. 2001. Vanadyl sulfate improves hepatic and muscle insulin sensitivity in type 2 diabetes. *J. Clin. Endo. Metabol.* 86:1410–1417.

161. Djordjevic, C. 1995. Antitumor activity of vanadium compounds. *Metal Ions in Biological Systems* 31:595–616.

162. Aubrecht, J., R.K. Narla, P. Ghosh, J. Stanek, and F.M. Uckun. 1999. Molecular genotoxicity profiles of apoptosis-inducing vanadocene complexes. *Toxicol. Appl. Pharm.* 154:228–235.

163. Ghosh, P., O.J. D'Cruz, R.K. Narla, and F.M. Uckun. 2000. Apoptosis-inducing vana-docene compounds against human testicular cancer. *Clin. Can. Res.* 6:1536–1545.

164. Chien, P.-S., O.-T. Mak, and H.-J. Huang. 2006. Induction of COX-2 protein expression by vanadate in A549 human lung carcinoma cell line through EGF receptor and p38 MAPK-mediated pathway. *Biochem. Biophys. Res. Commun.* 339:562–568.

165. Lampronti, I., N. Bianchi, M. Borgatti, E. Fabbri, L. Vizzielo, M.T.H. Khan, A. Ather, D. Brezena, M.M. Tahir, and R. Gambari. 2005. Effects of vanadium complexes on cell growth of human leukemia cells and protein-DNA interactions. *Oncol. Rep.* 14:9–15.

166. Osinska-Krolicka, I., H. Podsiadly, K. Bukietynska, M. Zemanek-Zboch, D. Nowak, K. Suchoszek-Lukaniuk, and M. Malicka-Blaszkiewicz. 2004. Vanadium(III) complexes with L-cysteine–stability, speciation and the effect on actin in hepatoma Morris 5123 cells. *J. Inorg. Biochem.* 98:2087–2098.

167. Thompson, H.J., N.D. Chasteen, and L.D. Meeker. 1984. Dietary vanadyl (IV) sulfate inhibits chemically-induced mammary carinogenesis. *Carcinogenesis* 5:849–851.

168. Ray, R.S., S. Roy, S. Samanta, D. Maitra, and M. Chatterjee. 2005. Protective role of vanadium on the early process of rat mammary carcinogenesis by influencing expression of metallothionein, GGT-positive foci and DNA fragmentation. *Cell Biochem. Funct.* 23:447–456.

169. Chakraborty, T., A. Chatterjee, M.G. Saralaya, D. Dhachinamoorthi, and M. Chatter-jee. 2006. Vanadium inhibits the development of 2-acetylaminofluorene-induced pre-malignant phenotype in a two-stage chemical rat hepatocarcinogenesis model. *Life Sciences* 78:2839–2851.

170. Mukherjee, B., B. Patra, S. Mahapatra, P. Banerjee, A. Tiwari, and M. Chatterjee. 2004. Vanadium—an element of atypical biological significance. *Toxicol. Let.* 150:135–43.

171. Kanna, P.S., M.G. Saralaya, K. Samanta, and M. Chatterjee. 2005. Vanadium inhibits DNA-protein cross-links and ameliorates surface level changes of aberrant crypt foci during 1,2-dimethylhydrazine induced rat colon carcinogenesis. *Cell Biol. Toxicol.* 21:41–52.

172. Papaioannou, A., M. Manos, S. Karkabounas, R. Liasko, A.M. Evangelou, I. Correia, V. Kalfakakou, J.C. Pessoa, and T. Kabanos. 2004. Solid state and solution studies of a vanadium(III)-L-cysteine compound and demonstration of its antimetastatic, antioxidant and inhibition of neutral endopeptidase activities. *J. Inorg. Biochem.* 98:959–68.

173. D'Cruz, O.J. and F.M. Uckun. 2002. Metvan: A novel oxovanadium(IV) complex with broad spectrum anticancer activity. *Expert Opinion on Investigational Drugs* 11:1829–1836.

174. Evangelou Angelos, M. 2002. Vanadium in cancer treatment. *Crit. Rev. Oncol. Hematol.* 42:249–65.

175. Molinuevo, M.S., D.A. Barrio, A.M. Cortizo, and S.B. Etcheverry. 2004. Antitumoral properties of two new vanadyl(IV) complexes in osteoblasts in culture: Role of apoptosis and oxidative stress. *Can. Chemo. Pharm.* 53:163–172.

176. Buglyo, P., D.C. Crans, E.M. Nagy, R.L. Lindo, L. Yang, J.J. Smee, W. Jin, L.-H. Chi, M.E. Godzala, III, and G.R. Willsky. 2005. Aqueous chemistry of the vanadiumIII (VIII) and the VIII-dipicolinate systems and a comparison of the effect of three oxidation states of vanadium compounds on diabetic hyperglycemia in rats. *Inorg. Chem.* 44:5416–5427.

177. Qiu, W., R.K. Avramoglu, N. Dube, T.M. Chong, M. Naples, A. C., K.G. Sidiropoulos, G.F. Lewis, J.S. Cohn, M.L. Tremblay, and K. Adeli 2004. Hepatic TRP-1B expression regulates the assembly and secretion of apolipoprotein B-containing lipoproteins. Evidence from protein tyrosine phosphatase-1B overexpression knockout and RNAi studies. *Diabetes* 53:3057–3066.

178. Mahadev, K., H. Motoshima, X. Wu, J.M. Ruddy, R.S. Arnold, G. Cheng, J.D. Lambeth, and B.J. Goldstein. 2004. The NAD(P)H oxidase homolog Nox4 modulates insulin-stimulated generation of H_2O_2 and plays an integral role in insulin signal transduction. *Mol. Cell. Biol.* 24:1844–1854.

179. Mathews, C.K., K.E. Van Holde, and K.G. Ahern. 2000. *Biochemistry.* Benjamin/Cummings, San Francisco.

180. Hunter, T. 1995. Protein kinases and phosphatases: The yin and yang of protein phosphorylation and signalling. *Cell.* 80:225–236.

181. Fauman, E.B. and M.A. Saper. 1996. Structure and function of the protein tyrosine phosphatases. *Tr. Biochem. Sci.* 21:413–417.

182. Barford, D. 1996. Molecular mechanisms of the protein serine/threonine phosphatases. *Tr. Biochem. Sci.* 21:407–412.

183. Denu, J.M. and J.E. Dixon. 1995. A catalytic mechanism for the dual-specific phosphatases. *Biochemistry* 92:5910–5914.

184. Hulley, P. and A. Davison. 2003. Regulation of tyrosine phosphorylation cascades by phosphatases: What the actions of vanadium teach us. *J. Trace Elem. Med. Biol.* 16:281–290.

185. Li, J., Q. Tong, X. Shi, M. Costa, and C. Huang. 2005. ERKs activation and calcium signaling are both required for VEGF induction by vanadium in mouse epidermal Cl41 cells. *Mol. Cell. Biochem.* 279:25–33.

186. Semiz, S. and J.H. McNeill. 2002. Oral treatment with vanadium of Zucker fatty rats activates muscle glycogen synthesis and insulin-stimulated protein phosphatase-1 activity. *Mol. Cell. Biochem.* 236:123–131.

187. Mehdi, M.Z., S.K. Pandey, J.-F. Theberge, and A.K. Srivastava. 2006. Insulin signal mimicry as a mechanism for the insulin-like effects of vanadium. *Cell Biochem. Biophys.* 44:73–81.

12 Technological Development

12.1 MOLECULAR NETWORKS AND NANOMATERIALS

Many of the reactions that vanadate undergoes suggest that by making use of solution-phase self-assembly processes, it might be possible to form supramolecular vanadium-anchored chains and networks when appropriate ligands are used. It seems that for this to succeed, bidentate building blocks will generally be required. Vanadium does not easily forgo the oxo (V=O) bond, and therefore, complexation by two tridentate ligands is not generally a favored coordination, though the situation might well be different in an anhydrous oxygen-free environment. Surprisingly enough, aqueous surfactant solutions provide a medium for self-assembly of nanowires and nanotubes. This opens up the possibility of using the unique flow and magnetic self-alignment properties of lyotropic liquid crystals for imposing specific physical characteristics on such entities.

It has been shown that a phenanthroline/tartrate-based dinuclear complex of chromium in aqueous solution spontaneously forms a self-organized ribbon structure that aggregates into a lyotropic liquid crystal [1]. This suggests similar self-arrayed materials could be formed if appropriate vanadate ligands were utilized. Picolinic acid, bipyridine, and other bidentate ligands react in a highly favorable manner to form bis complexes. If these ligands are modified to types such as displayed in Scheme 12.1a, it seems possible that simple networks would be formed in the presence of vanadate. More extensive networks might be formed if the ligand is extended to include more ligating groups. Scheme 12.1b depicts a couple of possibilities. With the appropriate choice of ligating group positions on a fixed ligand template, it is possible that selection between different types of networks might be possible. For instance, one would be able to select between linear, ladder-like, and extended networks. Even helical schemes can be envisioned. If such materials can be formed, unique chemical properties can be expected, and they may provide a basis for the development of useful nanomaterials.

Cooperative organization of vanadium(V) complexes is certainly not unknown and, for instance, has been observed in reactions of vanadium pentoxide (V_2O_5), boric acid, and phosphoric acid, together with other reactants to form vanadium borophosphate networks [2]. A particularly interesting templated self-assembly process has been observed in the reaction of tris(isopropoxo)oxovanadate in aqueous reverse micellar solution to form nanomaterials of V_2O_5 stoichiometry. Within a day of the preparation, nanorods of about 90 nm in length were obtained. Aging the preparations for 100 days led to the formation of much elongated rods, actually nanowires of about 1000 nm in length [3].
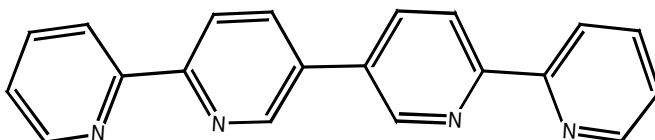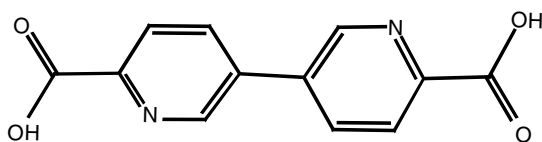
a
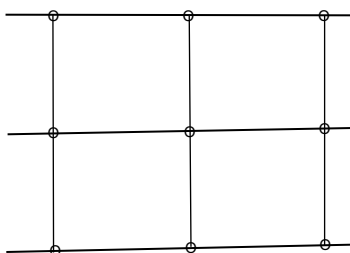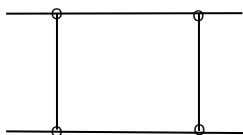
b

SCHEME 12.1

Reverse micelles have many features in common with nematic lyotropic liquid crystals. Because of cooperative effects, the micelles of nematic lyotropic liquid crystals spontaneously and homogeneously align when a magnetic field is applied, as for instance in an NMR spectrometer. Flow alignment also occurs with nematic liquid crystals. Techniques developed from these observations, therefore, offer a reasonable possibility of obtaining bulk homogeneously aligned nanowire aggregates, for which useful applications might be developed. Highly aligned single-crystal-like nanorods and nanotubes can be obtained by electrophoretic deposition, invoking template-based growth of nanoclusters from V_2O_5 sols. Uniformly sized

V_2O_5 nanorods of approximately 10 μm in length and about 200 nm in diameter can be obtained that have a nearly unidirectional alignment. Nanotubes obtained by similar methods also have comparable outer dimensions, with an inner diameter of 100 nm [4].

It is also possible to prepare V_2O_5–based vanadium nanotubes from surfactant solution. They are formed using oxotriisopropoxovanadium(V) and have been found to have unique electronic properties that can be controlled by electron doping [5]. In fact, these tubes offer the possibility of spin control and, therefore, have significant potential in the development of spintronic devices.

The vanadium isopropoxide has proven to be quite a versatile reactant. In addition to the above, in other applications, it has been used to generate V_2O_5 nanowires on metallic film over silica. The V_2O_5 nanowires then serve as a mask in the preparation of metallic nanowires by protecting the underlying film during ion beam etching. Removal of the V_2O_5 mask by dissolution in acidic medium affords the desired metallic nanowire. This process offers very fine control over the dimensions of the metal wires, which are in the order of 6 nm thick and 15 to 20 nm wide [6].

Polyoxometalates are important catalysts but they are also finding application in optical, electrical, and magnetic devices. Mixed-metal polyoxometalates with vanadium(V) in the polyoxoanion core confers enhanced properties to such structures, principally in their ability to form essentially infinite networks that can be utilized as coatings or as other thin film materials. Additionally, these materials have tunable electromagnetic and photochromic properties. In combination with organic polymers, so-called hybrid polymers, special electrochemical properties are conferred, making possible such electrical storage devices such as capacitors and batteries that utilize the redox properties of the polyoxometalate [7].

These areas of vanadium research are in their infancy, but clearly, there is great potential in the applications of vanadium nanomaterials.

12.2 THE VANADIUM REDOX BATTERY

A ubiquitous characteristic of vanadium chemistry is the fact that vanadium and many of its complexes readily enter into redox reactions. Adjustment of pH, concentration, and even temperature have often been employed in order to extend or maintain system integrity of a specific oxidation state. On the other hand, deliberate attempts to use redox properties, particularly in catalytic reactions, have been highly successful. Vanadium redox has also been successfully utilized in development of a redox battery. This battery employs the V(V)/V(IV) and V(III)/V(II) redox couples in 2.5 M sulfuric acid as the positive and negative half-cell electrolytes, respectively. Scheme 12.2 gives a representation of the battery. The vanadium components in both redox cells are prepared from vanadium pentoxide. There are two charge-discharge reactions occurring in the vanadium redox cells, as indicated in Equation 12.1 and Equation 12.2. The thermodynamics of the redox reactions involved have been extensively studied [8].

V(II)/V(III)   Cell Stack   V(IV)/V(V)

Vanadium half-cell   Vanadium half-cell
storage tank   storage tank
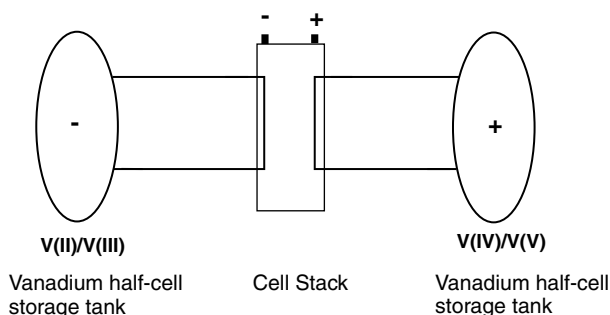
SCHEME 12.2

At the positive electrode:

$$VO_2^+ + 2H^+ + e^- \xrightarrow[\text{charge}]{\text{discharge}} VO^{2+} + H_2O \quad E^\circ = 1.00 \text{ V} \tag{12.1}$$
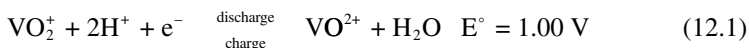
At the negative electrode:

$$V^{3+} + e^- \xrightarrow[\text{discharge}]{\text{charge}} V^{2+} \quad E^\circ = -0.26 \text{ V} \tag{12.2}$$
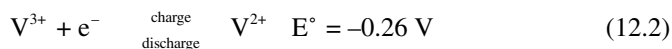
Because an identical electrolyte is used in both halves of the battery, if any inadvertent mixing of the charged electrolytes occurs, there is an energy loss as heat. As the electrolyte reverts to its uncharged state. It is then recycled without detriment to the battery. During the next battery cycle, the electrolyte is simply recharged. An important aspect of this battery is that hydrogen is not generated during a battery cycle.

One unique property of this battery is the fact that the capacity of the battery is limited by the volume of the two redox cells. A second unique property is that the battery can be recharged simply by replacing the discharged electrolytic solutions by fully charged ones. The depleted solutions can then be recharged in an appropriate holding tank. The capacity of the battery is simply a function of the volume of the cell, and this means that large electrical storage capacities are relatively easily obtained; these batteries have great potential as storage facilities for cyclical generating devices such as wind power, solar power, or similar electricity-generating power stations. A large system, for instance, has recently been installed by the Huxley Hill Wind Farm of Hydro Tasmania for use in its King Island generation plant. Because of the long-term stability and recyclability of the electrolytic materials, the virtually nonexistent emissions and other factors, this redox battery has the lowest ecological impact of all energy-storage technologies.

The battery can simply be regenerated by replacing the discharged fluids with recharged ones. As a consequence of this, there are many potential applications of this technology to mobile devices. Proof of concept has been demonstrated, and virtually all mobile battery-driven devices are suitable for this new technology. Because of the corrosive nature of the electrolyte and expense of small units, this battery will probably not be made available for domestic use soon, though future changes in technology may allow such applications.

Developments in the technology of this battery have led to a second type of redox battery that employs a vanadium bromide electrolyte but otherwise functions similarly to the above battery [9]. This battery improves on the vanadium redox battery design by using a combination of a vanadium-bromide solution, improved cell design, and membranes to improve electron exchange between the half cells. This battery employs V(III) (VBr_3) and V(IV) (VBr_4) bromides in a 50:50 mixture as the electrolyte. Because an identical electrolyte is used in both halves of the battery, there are no cross-contamination problems. Up to twice the energy density of existing systems is expected for this battery. This is mainly because the vanadium concentration in this battery can range up to 3 or 4 mol/L, so that smaller volumes than required for the original battery are achievable, providing benefits for stationary applications such as wind and solar energy storage systems and for electric vehicle applications including on-road buses and trucks as well as delivery vans and vehicles for urban areas.

12.3 THE SILVER VANADIUM OXIDE BATTERY

The reactions of silver with vanadate and vanadium pentoxide have been the subject of investigation for three-quarters of a century. One aspect of this work was the development of silver vanadium oxide batteries. Lithium silver vanadium oxide (Li/SVO) batteries are typically manufactured for small-scale applications where highly reliable long-term functionality over several years is required, such as for medically implantable devices like cardioverter defibrillators, neurostimulators, atrial defibrillators, and drug infusion devices. These batteries have a lithium anode, a liquid organic electrolyte, a cathode composed of conductive additives, a binder, and silver vanadium oxide, which is a bronze produced by the reaction of vanadium oxide and a silver compound, typically silver nitrate or silver oxide. Because of the demonstrated value of the silver/vanadium oxide batteries, they are under continuous development, with modifications being made to the materials within the battery. It has, for instance, recently been suggested that improvements to the battery might possibly be obtained if silver fluoride (AgF_2) is incorporated into the battery matrix [10]. Other work has suggested that vanadium pentoxide ribbon-carbon nanotubes be utilized in the electrodes in lithium vanadium oxide batteries [11]. Chapter 13 gives a detailed summary of the development of silver/vanadium oxide batteries and their potential, particularly as implantable medical devices.

REFERENCES

1. Imae, T., Y. Ikeda, M. Iida, N. Koine, and S. Kaizaki. 1998. Self-organization of a dinuclear metal complex in lyotropic liquid crystal: Ribbonlike supramolecular assemblies. *Langmuir* 14:5631–5635.
2. Wang, Y., J. Yu, Q. Pan, Y. Du, Y. Zou, and R. Xu. 2004. Synthesis and structural characterization of 0D vanadium borophosphate $[Co(en)_3]_2[V_3P_3BO_{19}][H_2PO_4].H_2O$ and 1D vanadium oxides $[Co(en)_3][V_3O_9].H_2O$ and $[Co(en)_2][V_3O_9].H_2O$ templated by cobalt complexes: Cooperative organization of the complexes and the inorganic networks. *Inorg. Chem.* 43:559–565.
3. Pinna, N., M. Willinger, K. Weiss, J. Urban, and R. Schlogl. 2003. Local structure of nanoscopic materials: V_2O_5 nanorods and nanowires. *Nano Lett.* 3:1131–1134.
4. Wang, Y., K. Takahashi, H. Shang, and G. Cao. 2005. Synthesis and electrochemical properties of vanadium pentoxide nanotube arrays. *J. Phys. Chem. B* 109:3085–3088.
5. Kruslin-Elbaum, L., D.M. Newns, H. Zeng, V. Derycke, J.Z. Sun, and R. Sandstrom. 2004. Room-temperature ferromagnetic nanotubes controlled by electron or hole doping. *Nature* 431:672–676.
6. Sordan, R., M. Burghard, and K. Kern. 2001. Removable template route to metallic nanowires and nanogaps. *Appl. Phys. Lett.* 79:2073–2075.
7. Casan-Pastor, N. and P. Gomez-Romero. 2004. Polyoxometalates: From inorganic chemistry to materials science. *Front. Biosci.* 9:1759–1770.
8. Heintz, A. and Ch. Illenberger. 1998. Thermodynamics of vanadium redox flow batteries: Electrochemical and calorimetric investigations. *Ber. Bunsenges. Phys. Chem.* 102:1401–1409.
9. M. Skyllas-Kazacos. 2004. New vanadium bromide redox fuel cell. In P.D. Bourkas, P. Halaris (Eds.), Power and energy systems (442): EuroPES 2004, 226. Calgary, Acta Press.
10. Sorensen, E.M., H.K. Izumi, J.T. Vaughey, C.L. Stern, and K.R. Poeppelmeier. 2005. $Ag_4V_2O_6F_2$: An electrochemically active and high silver density phase. *J. Am. Chem. Soc.* 127:6347–6352.
11. Sakamoto, J.S. and B. Dunn. 2002. Vanadium oxide-carbon nanotube composite electrodes for use in secondary lithium batteries. *J. Electrochem. Soc.* 149:A26–A30.

13 Preparation, Characterization, and Battery Applications of Silver Vanadium Oxide Materials

13.1 INTRODUCTION

This brief review contains some literature references involving the preparation, characterization, and battery applications of silver vanadium oxide, hereafter referred to as SVO. For this review, the term *SVO* is used to describe a family of materials containing silver, vanadium, and oxygen in stoichiometric or nonstoichiometric ratios. The published history of SVO is long, initially involving the synthesis and characterization of the various phases of SVO. However, with the discovery of SVO as an important electrode material in batteries, the number of SVO publications and patents has increased markedly within the past 20 years. Although not comprehensive, this review is designed to provide the reader with an overall appreciation of the initial research efforts involving SVO, leading up to the more recent battery chemistry of SVO.

13.2 PREPARATION, STRUCTURE, AND REACTIVITY OF SILVER VANADIUM OXIDE AND RELATED MATERIALS

Notably, SVO can display a variety of phases, both stoichiometric and nonstoichiometric. Thus, variations in reaction conditions, starting materials, and reagent stoichiometries for the preparation of SVO can result in a wealth of products that display different structures and different properties. In addition, the variety of oxidation states available to the silver and especially the vanadium components of SVO, plus the open structure of some of the SVO materials, suggest that these materials are well suited for electron transfer applications. It is thus logical and not surprising that reports of SVO battery applications and SVO redox catalyst applications appear within similar time frames. Some reports involving the structure of SVO solids and the catalysis of organic substrate oxidation by SVO-based catalysts will be described in Section 13.2, due to their possible relevance to the SVO battery chemistry described in Section 13.3.

In this section, select literature reports of the chemistry of SVO will be presented chronologically. Please note the historical evolution of SVO chemistry, from the variety of phases of SVO discovered, to the synthetic strategies necessary for specific phase preparation, then the proposed structures of the various forms of SVO, and finally the chemical reactivities of SVO (especially the redox catalysis activity).

Some of the earliest published work on SVO compounds was authored by Briton and Robinson in 1930 [1]. Electrochemical titrations of aqueous silver nitrate with aqueous sodium vanadate were conducted using silver electrodes, where vanadates of silver of various Ag:V ratios were formed as precipitates, with the 3:1 and 1:1 precipitates being orange and the 2:1 precipitate being light yellow. In addition, the solubility products of the vanadates were determined, ranging from 1×10^{-24} for the 3:1 compound to 2×10^{-14} for the 2:1 silver vanadate to 5×10^{-7} for the 1:1 compound. Subsequently, in 1933, Briton and Robinson reported some of the experimental details associated with the isolation of the stoichiometric solids $AgVO_3$, $Ag_4V_2O_7$, and Ag_3VO_4 by various precipitation methods from cold $AgNO_3$/alkali vanadate solutions [2]. The importance of aging or boiling the aqueous reactant solutions in order to obtain stoichiometric solids was emphasized.

In 1964, Deschanvres and Raveau reported preparation of three phases of SVOs, obtained through the reaction of silver powder with V_2O_5 powder in the presence of a vacuum or air [3]. Distinct phases and phase mixtures were defined for $Ag_xV_2O_5$ over several ranges of x. From $0.17 \leq \times \leq 0.45$, a homogeneous nonstoichiometric β phase was observed. A homogeneous nonstoichiometric δ phase was observed from $0.6 \leq \times \leq 0.8$, and a biphasic region of β plus δ occurred when $0.45 \leq \times \leq 0.6$. For reactions in the presence of air, a nonstoichiometric ε phase was generated, homogeneous from $1 \leq \times \leq 1.15$. In the case where $\times = 1$, the stoichiometric product from the air reaction was described as $Ag_2V_4O_{11}$, observed as shiny clear blue crystals. At still higher levels of silver, $AgVO_3$ was obtained. Finally, it was noted that the δ phase undergoes a complex air oxidation at 500ºC, yielding a mixture of β and ε phases.

In 1965, Andersson combined water and V_2O_5 powder in silver capsules and heated the sealed capsules at temperatures between 300 and 700ºC under applied pressures of 2000 atm [4,5], obtaining $Ag_{1-x}V_2O_5$ as blue-black crystals after 3 days of heating and pressure. The crystals were sometimes rod-shaped and sometimes plate-like. Using x-ray powder diffraction, the crystal was assigned a space group of C2/m, and a value for $\times$ of approximately 0.32 was determined after least-squares treatment. A monoclinic unit cell was determined, with a = 11.742 Å, b = 3.667 Å, c = 8.738 Å, β = 90.48º. Two independent vanadium atoms, V_1 and V_2, were resolved, each one displaying distorted octahedral geometry. Five V_1-O distances ranged from 1.42 to 1.95Å and five V_2-O distances ranged from 1.54 to 2.10Å. For both V_1 and V_2, there was one further oxygen at the distances of 2.43 and 2.35Å to complete the distorted octahedron around each V. The silver cation displayed a coordination number of five, with Ag-O distances ranging from 2.48 to 2.68 Å. The overall structure was described as double zigzag ribbons of distorted VO_6 octahedra, sharing edges and corners with silver cations sandwiched between the V_2O_5 layers. Finally, the structure of $Ag_{1-x}V_2O_5$ was compared to the structure of $Na_xTi_4O_8$.

In 1966, Hagenmuller et al. prepared and reported on a series of vanadium bronzes, including $Ag_xV_2O_5$ [6]. Four phases were reported, an orthorhombic α phase from $0 \le \times \le 0.01$, a monoclinic β phase from $0.29 \le \times \le 0.41$, and a monoclinic δ phase from $0.67 < \times < 0.86$. Above $\times = 0.86$, silver metal and the δ phase were observed. For $\times = 0.86$, the parameters of a unit cell were determined, with a = 11.73 ±0.03 Å, b = 3.66 ±0.02 Å, c = 8.75 ±0.02 Å, β = 91°30' ±30', the space group = C^3_{2h} and Z = 4. These cell dimensions are similar to the cell dimensions reported by Andersson for $Ag_{1-x}V_2O_5$ where $\times = 0.32$ (*vide supra*), but the space group differed. Conductivity for the α phase is reported to be in the magnitude of 10^{-3} ∫$^{-1}$cm^{-1} (T = 300 K), whereas the conductivities of the β and δ phases are reported to be in the order of 10^0 ∫$^{-1}$cm^{-1} (T = 300 K).

Also in 1966, Fleury et al. used thermal analysis on the Ag_2O-V_2O_5 system to construct a phase diagram from the combination of the two solid oxides in five distinct stoichiometric ratios: 1:7, 1:2, 1:1, 2:1, and 3:1 [7]. The first four compounds, AgV_7O_{18}, $Ag_2V_4O_{11}$, $AgVO_3$, and $Ag_4V_2O_7$, displayed melting points that ranged from 732ºC for AgV_7O_{18} to 392ºC for $Ag_4V_2O_7$, where the decrease in melting point corresponded to an increase in Ag:V ratio. The thermal analyses were conducted under flowing oxygen in order to avoid the *in-situ* formation of nonstoichiometric bronzes.

In 1967, Galy et al. related the range of phases associated with nonstoichiometric vanadium bronzes of the general formula $M_xV_2O_5$ (where M = monovalent, divalent, or trivalent metals) to the ionic radius and insertion rate of M [8]. Included in this analysis was the δ phase $Ag_{1-x}V_2O_5$ characterized by Andersson (*vide supra*). The structure of this monoclinic C2/m crystal was compared to the structures of five other $M_xV_2O_5$ phase types, namely $\alpha, \beta, \gamma, \alpha'$, and 0 phases. In all cases, the V_2O_5 part of the $M_xV_2O_5$ phases consists of distorted octahedra and bipyramids, forming parallel chains arranged two or three dimensionally within the solid. The metal cations are positioned between or among the V_2O_5 chains.

Also in 1967, Casalot and Pouchard prepared a phase diagram for the Ag_2O-V_2O_5-VO_2 system through the reaction of silver powder with V_2O_5 powder and $AgVO_3$ powder with V_2O_5 powder [9]. Through the reaction of silver with V_2O_5 at 600ºC, three successive phases of $Ag_xV_2O_5$ were observed: an α phase from $0 \le \times \le 0.01$ consisting of a solid solution of Ag^+ ions in V_2O_5, a monoclinic β phase from $0.29 \le \times \le 0.41$, and a δ phase from $0.67 \le \times \le 0.86$. The melting points of the phases were determined: α phase m.p. = 672ºC, β phase m.p. = 715ºC, δ phase m.p. = 690ºC. The α and β phases were stable with melting, whereas upon melting and subsequent cooling, the δ phase transformed into a mixture of β phase, VO_2, and $AgVO_3$. At $\times$ values between phases, both adjoining phases were observed. Four successive phases were prepared via the reaction of $AgVO_3$ with V_2O_5 under an oxygen atmosphere at temperatures ranging from 350 to 640ºC: Phase I was the β phase of $AgVO_3$, phase II corresponded to an "oxygen deficient" phase of $Ag_2V_4O_{11-e}$, phase III coexisted with phase IV, where phase III was described by the $Ag_{1+x}V_3O_8$, and phase IV appeared when the V:Ag ratio was greater than 2.5, where for V:Ag = 6, phase IV was pure and appeared to be the β phase of $Ag_{0.33}V_2O_5$.

Also in 1967, Lukacs et al. heated solid mixtures of $AgVO_3$ and V_2O_5 powders to form SVO, where the reaction temperatures ranged from 450 to 600ºC [10]. A

mixture of two nonstoichiometric phases of $Ag_xV_m^{4+}V_n^{5+}O_y$ were initially obtained: phase I, where $0.29 \leq \times \leq 0.43$, $0.32 \leq m \leq 0.44$, $1.56 \leq n \leq 1.68$, $4.96 \leq y \leq 5.05$, and phase IIA, where $0.80 \leq \times \leq 0.99$, $0.06 \leq m \leq 0.20$, $1.90 \leq n \leq 1.94$, $5.32 \leq y \leq 5.46$. This mixture was treated with HNO_3, and a third nonstoichiometric phase of $Ag_xV_m^{4+}V_n^{5+}O_y$ was obtained: phase IIB, where $0.67 \leq \times \leq 0.77$, $0.05 \leq m \leq 0.09$, $1.91 \leq n \leq 1.95$, $5.22 \leq y \leq 5.36$. Notably, phase IIB was V^{4+} deficient, possibly due to HNO_3 oxidizing any V^{4+} to V^{5+}. The mixtures were characterized via TGA, IR spectroscopy, x-ray diffraction, and redox titrations.

Also in 1967, Raveau investigated some of the chemical reactivities of SVO materials derived from the combination of V_2O_5 powder with Ag_2O powder [11]. In his studies, the rich and varied chemistry of SVO was demonstrated. First, Raveau studied the effects of heating SVO *in vacuo*, in an inert atmosphere, and in an oxygen atmosphere, where in some cases interconversion among some SVO phases was observed. For example, β-$Ag_xV_2O_5$ was stable under air or oxygen, but unstable *in vacuo*, whereas δ-$Ag_xV_2O_5$ oxidized in air at 500ºC to form $Ag_2V_4O_{11}$ and β-$Ag_xV_2O_5$. Further, $Ag_2V_4O_{11-y}$ was formed from the decomposition of $Ag_2V_4O_{11}$ at 450ºC *in vacuo*, and $Ag_2V_4O_{11-y}$ decomposed *in vacuo* at 550ºC into δ-Ag_xV_2O, silver, and oxygen. In addition, $Ag_2V_4O_{11-y}$ was formed from γ-$AgVO_3$ at 450ºC, whereas $Ag_2V_4O_{11}$ and $Ag_2V_4O_{11-y}$ reacted with VO_2 at 500ºC to form δ-$Ag_xV_2O_5$. Second, Raveau studied the reaction of gaseous ammonia with δ-$Ag_xV_2O_5$ and liquid ammonia with β– and δ-$Ag_xV_2O_5$. In general, in the presence of humidity, ammonium vanadate and silver were reaction products.

In 1974, Drozdov et al. reported the crystal structure of $Ag_{4-x}V_4O_{12}$ ($\times = 1.05$), where the authors noted that the deviation from stoichiometry by the Ag ions complicated the structural analysis [12]. The structure is described in terms of V_4O_{12} repeat units, consisting of V-centered octahedra, which form infinite isolated vanadium-oxygen rods ($[V_4O_{12}]_\infty$). The authors suggest that the infinite rod structures determine the fibrous character of the $Ag_{4-x}V_4O_{12}$ ($\times = 1.05$) crystals. Notably, the infinite vanadium-based rods of previously reported nonstoichiometric vanadium bronzes are not isolated but rather are parts of more complex two- and three-dimensional structures. It is interesting that from the stoichiometry of the title compound, $Ag_{4-x}V_4O_{12}$ ($\times = 1.05$), in order to have charge balance, either the charge of at least one of the Ag ions is more positive than +1 or the charge of at least one of the O ions is less negative than –2.

Ten years after the phase diagram study by Fleury (*vide supra*), Volkov et al. reported in 1976 an equilibrium phase diagram of the V_2O_5-$AgVO_3$ system [13]. Powder mixtures of V_2O_5 with $AgVO_3$ were heated for 200 h in an atmosphere of air where the temperatures ranged from 400 to 450ºC. Chemical analysis and x-ray diffraction measurements of the products revealed three materials: β-$Ag_xV_{12}O_{30}$ ($1.7 \leq \times \leq 2.0$), γ-$Ag_{1.12}V_3O_{7.8}$, and ϵ-$Ag_2V_4O_{10.85}$, which were characterized via x-ray diffraction. Both Fleury and Volkov noted that the compositions of the SVO products were functions of the oxygen reaction pressure, so it is important to note the specific equilibrium conditions when an equilibrium phase diagram of V_2O_5-$AgVO_3$ is constructed. Because Fleury used oxygen gas and Volkov used air in the production of the SVO compounds, the resultant phase diagrams differed.

Also in 1976, Scholtens measured the diffusion constants of silver in solid $Ag_xV_2O_5$ as a function of × in a temperature range from 200 to 450ºC [14]. $Ag_xV_2O_5$ was prepared in three ways: silver + V_2O_5 solids at 650ºC, $Ag_2CO_3 + V_2O_4 + V_2O_5$ solids at 650ºC, and AgI + V_2O_5 solids above 300ºC. The silver diffusion constant (D_{Ag+}) in $Ag_xV_2O_5$ varied with x: for × = 0.30, $D_{Ag+} = 10^{-13}$, whereas for × = 0.70, $D_{Ag+} = 10^{-16}$. When × = 0.30, $Ag_xV_2O_5$ is in the β phase, whereas when × = 0.70, $Ag_xV_2O_5$ is in the δ phase. Because the tunnels in both phases were almost the same size, the authors proposed that diffusion was faster in the β phase because there were more energetically equivalent sites unoccupied by silver cations.

In 1981, Andreikov and Volkov reported the oxidation of *o*-xylene and napthalene by solid heterogeneous SVO catalysts [15]. To prepare the catalysts, mixtures of silver nitrate and vanadium oxide solids in 12 different ratios were fused at 750ºC in an atmosphere of air, producing several nonstoichiometric and stoichiometric phases of SVO. x-ray diffraction was used to identify α phase material, $Ag_xV_2O_5$, obtained when silver concentration was low ($0 \leq × \leq 0.02$), and β phase material, obtained for $Ag_xV_6O_{15}$ where $0.85 \leq × \leq 1.0$. Silver vanadates $Ag_{1.2}V_3O_7$ (γ) and $Ag_2V_4O_{10.5}$ (ε), as well as the silver metavanadate $AgVO_3$, were also observed. Regarding the SVO catalyst activity, a molar concentration of 20 to 30 atomic % Ag in the catalyst appeared to optimize target oxidation. Notably, the catalyst compositions changed during the course of the catalyses, with the following exceptions: β phase $Ag_xV_6O_{15}$, where the Ag/Ag+V ratio = 0.14, and $AgVO_3$ did not decompose.

In 1983, Van Den Berg et al. conducted a thermal analysis study comparing $Ag_{0.35}V_2O_5$ powder with a mixture of 0.35 Ag + V_2O_5 powders, in the presence of a variety of inert, oxidizing, and reducing atmospheres, using DTA, TGA, and DTG techniques [16]. The presence of silver catalyzed the gaseous reduction of vanadium in V_2O_5 and the mixture of 0.35 Ag + V_2O_5 displayed initial reduction DTG curves that differ from the initial reduction DTG curves of $Ag_{0.35}V_2O_5$. Also, the second reduction DTG curve of the mixture was similar in appearance to the first reduction DTG curve of $Ag_{0.35}V_2O_5$, possibly implying that the mixture after the initial heating curve formed $Ag_{0.35}V_2O_5$.

Nine years after the Volkov study, Wenda investigated the V_2O_5-Ag_2O system in 1985 [17]. Powdered samples of V_2O_5 and Ag_2O were mixed and heated under air in a quartz tube at temperatures ranging from 380 to 640ºC, with a variety of reaction times. The materials were characterized by DTA, TGA, and x-ray powder diffractometry. Seven phases were observed including V_2O_5, solid Ag or Ag_2O in V_2O_5, β-$Ag_{0.30}V_{1.7}O_{4.25}$, $Ag_2V_4O_{11}$, β-$AgVO_3$, Ag_3VO_4, and Ag. A phase diagram was presented in partial agreement with both the work of Fleury and Volkov. However, unlike Fleury, the thermal transitions from α to β (372ºC) and β to γ (473ºC) phase were not observed, the shape of the liquidus from 12 to 35 mol % Ag_2O was different, and thermal effects at 400ºC for samples with more than 66 mol % Ag_2O were not observed.

Galy et al. conducted several studies concerning the structure of V_2O_5 and the related structural chemistry of MV_2O_5 phases (*vide infra*). In 1986, a refinement of the structure of V_2O_5 was reported, where the structure of V_2O_5 was described as a layered structure, involving VO_5 square pyramids sharing edges and corners, with V_2O_5 sheets held together via weak vanadium–oxygen interactions (V-O distance =

2.791(3) Å) [18]. This report was important because previously, the VO_5 polyhedra in V_2O_5 were described as trigonal bipyramids instead of square pyramids.

In 1989, Znaidi et al. synthesized monoclinic β-phase SVO via a sol gel process involving V_2O_5 xerogels [19]. V_2O_5 gels were formed via acidification of aqueous vanadium, where the resulting V_2O_5 fibers took on the appearance of entangled flat ribbons of dimensions 1000 Å long, 100 Å wide, and 10 Å thick. The V_2O_5 gels were dried to form a thin xerogel film, which was soaked in a solution 0.1 M in silver cation for a few minutes. The intercalation compound obtained from the soaking process was $Ag_{0.36}V_2O_5$•$1.17H_2O$, with a d-spacing of 10.9 Å. By dehydration and subsequent heating of the intercalated xerogel, the bronze $Ag_{0.36}V_2O_5$ was formed. X-ray powder diffraction, coupled with thermogravimetric and differential thermal analysis, was used to characterize the bronze formation.

In 1991, Vassileva et al. reported the complete air oxidation of benzene by SVO catalysts supported on Al_2O_3 [20]. Catalysts were prepared by first combining $AgNO_3$ and NH_4VO_3 in ratios from 1:71 to 1:1 in aqueous solution, then the water was removed by heating, with the solid product calcined in air at 500 to 520ºC. The catalysts were characterized via V^{5+}, V^{4+}, and V^{3+} composition (wt %) as a function of catalysis time. In general, the V^{5+} composition decreased as the catalysis progressed, whereas the V^{4+} and V^{3+} compositions both increased. Catalysts with small (<< 1:1) silver:vanadium ratios displayed the highest and most prolonged catalytic activity, whereas the 1:1 catalyst showed the lowest activity. The authors rationalized the catalyst activity by suggesting that an optimal V^{5+}/V^{4+} ratio was maintained when silver was not chemically bound to the vanadium oxides and when a distinct phase of silver was not formed during catalysis.

In 1992, structural changes in the structure of V_2O_5 due to metal cation insertion were investigated and rationalized by Galy [21]. In 1994, Deramond et al. investigated silver cation insertion into a β-$Ag_xV_2O_5$ tunnel structure, where $0.29 \leq \times \leq 0.41$ [22]. Recalling the study by Casalot and Pouchard (*vida supra*) regarding the phases of $Ag_xV_2O_5$, Deramond et al. confirmed the structure of β-$Ag_xV_2O_5$ and rationalized why the value of $\times$ in β-$Ag_xV_2O_5$ can exceed the theoretical limit of β phases (x = 0.33). The large values of $\times$ in β-$Ag_xV_2O_5$ occur because silver cations can distribute over more sites than previously observed for other metal cations, resulting in a new upper limit for the β phase of $M_xV_2O_5$ of 0.66 instead of 0.33.

In 1993 and 1994, Crespi et al. and Zandbergen et al. used high-resolution electron microscopy (HREM) and x-ray powder diffractometry (XRD) to characterize $Ag_{2-x}V_4O_{11}$ [23,24]. The SVO sample was prepared by the solid-state reaction of Ag_2O powder with V_2O_5 powder in a 1:2 ratio at 500ºC under oxygen atmosphere for 6 h. Notably, small particles of silver were observed via HREM on the SVO surface; thus, the authors suggested the formulation for SVO was more appropriately $Ag_{2-x}V_4O_{11}$ than $Ag_2V_4O_{11}$. Two phases were observed via HREM, phase I and phase II. Phase I, the majority phase, was a two-dimensional cell with a = 0.77, c = 0.90 nm, β = 125º, which corresponded to a C-centered monoclinic unit cell (a = 1.53 nm, b = 0.360 nm, c = 0.95 nm, and β = 125º). Phase II, differing from phase I only in the stacking along the c^* axis, was a two-dimensional cell with a = 0.77 nm, c = 0.72 nm, β = 102º, where the authors propose a C-centered monoclinic cell (a = 1.53 nm, b = 0.36 nm, c = 0.76 nm, and β = 102º). Several possible structures of

$Ag_{2-x}V_4O_{11}$ were proposed, based on the shifting of V_4O_{11} slabs. The V cations in these slabs exhibited distorted six coordination, whereas the Ag cations displayed irregular oxygen coordination.

In 1996, Rozier et al. determined the structure of β-$AgVO_3$, using single crystal x-ray diffraction, and compared it to the reported structures of $Ag_2V_4O_{11}$ and δ-$Ag_xV_2O_5$ [25]. β-$AgVO_3$ crystals were prepared by 1) heating a 1:1 mixture of Ag_2O and V_2O_5 powders in a gold crucible at 420ºC for 12 h under a stream of oxygen gas, then 2) reheating the product from step 1 under the same conditions, then 3) heating the product from step 2 in a gold crucible under an oxygen atmosphere at 500ºC for 10 h, cooling to 450ºC at a rate of 2ºC/h, then quenching to room temperature. After several crystals were examined, the structure of β-$AgVO_3$ was assigned to the monoclinic system, space group Cm, and the structure consisted of infinite $[V_4O_{12}]_n$ double zigzag chains of edge shared distorted VO_6 octahedra, with four different V-O bond lengths ranging from 1.67(4) to 2.44(8) Å. The four silver cations were distributed in three types of geometries: The first Ag cation geometry was a weakly distorted octahedron (typical bond distance = 2.43(4) Å); the second and third Ag cation geometries were square pyramids (typical bond distance = 2.40 Å); and the fourth Ag cation geometry was a monocapped trigonal prism, where the Ag-O bond lengths ranged from 2.22 to 2.89 Å. Because the fourth Ag cation monocapped trigonal prism was the largest site and shared faces along the [010] direction, the authors proposed that these Ag cations might be particularly mobile within the crystalline lattice. Also, the authors proposed that β-$AgVO_3$ can be envisioned structurally as $Ag[Ag_3V_4O_{12}]$, where the Ag^+ is the fourth silver cation. Finally, the authors also discussed the structural similarities among β-$AgVO_3$, $Ag_2V_4O_{11}$, and δ-$Ag_xV_4O_{10}$, and proposed possible routes of interconversion via loss of Ag_2O or O.

In 1997, Rozier and Galy followed up on the 1996 Rozier report, detailing a proposed sprouting mechanism for the transition of $Ag_2V_4O_{11}$ to $Ag_{1+x}V_3O_8$ via loss of oxygen through $Ag_2V_4O_{11-y}$ [26]. A polycrystalline sample of ϵ-$Ag_2V_4O_{11}$ was prepared by heating a 1:2 molar mixture of Ag_2O and V_2O_5 in a sealed quartz ampule at 450ºC for 10 h, followed by reheating at 500ºC for 10 h. To obtain single crystals of ϵ-$Ag_2V_4O_{11}$, the polycrystalline sample was heated in a sealed quartz ampule at 560ºC for 5 h, cooled at 2ºC/h to 540ºC, and quenched to room temperature. An ϵ-$Ag_2V_4O_{11}$ crystal was subjected to complete single crystal x-ray analysis, and the chemical formula of the crystal was determined as $Ag_{1+x}V_3O_8$ instead of $Ag_2V_4O_{11}$; the space group was determined to be $P2_1/m$. The $[V_3O_8]_n$ chain framework was built around three independent vanadium sites: V1 exhibited a five-coordinate, trigonal bipyramidal coordination environment of oxygen atoms, whereas V2 and V3 exhibited a six-coordinate, octahedral coordination environment of oxygen atoms. The Ag^+ ions resided mainly in weakly distorted octahedral sites (typical Ag-O distance = 2.438(8) Å), whereas some of the Ag^+ ions were in sites described by the authors as having tetrahedral and trigonal prismatic limiting forms. The Ag-O distances in these sites varied from 2.09(1) to 3.30(1) Å. The authors proposed that the electrochemical results of Leising and Takeuchi [55] (*vida infra*), as well as Tarascon and Garcia Alverado [71] (*vida infra*), regarding SVO prepared in air or an inert atmosphere could be rationalized if the material prepared under inert atmo-

sphere was $Ag_{1+x}V_3O_8$. Finally, an Ag_2O-V_2O_5-V_2O_4 ternary diagram was proposed and sprouting phenomenon discussed as a possible means of rationalizing an ε-$Ag_2V_4O_{11}$-to-$Ag_{1+x}V_3O_8$ transition.

In 1998, Ge and Zhang prepared V-Ag catalysts according to V/Ag ratios of 1/0, 9/1, 3/1, 2.16/1, 1.5/1, 1/1, and 0/1, and studying the reduction behavior of these materials via temperature programmed reduction in an H_2/N_2 atmosphere, x-ray diffraction, and ultraviolet diffuse reflectance spectra [27]. Reminiscent of the 1991 study by Vassileva et al., the Zhang catalysts were prepared by combining aqueous solutions of silver nitrate and ammonium metavanadate in the presence of a small amount of oxalic acid. The water was removed by evaporation and the dried product was calcined in a muffle furnace at 450ºC for 9 h. Interestingly, the surface area of the products was largest with a V/Ag ratio = 1/0 and smallest with a V/Ag ratio = 0/1. The first step of reduction of $Ag_2V_4O_{11}$, $Ag_2V_4O_{10.84}$, and $Ag_{1.2}V_3O_8$ all formed Ag metal, V_6O_{13}, and H_2O. V_6O_{13} was then reduced to VO_2, which was then reduced to V_2O_3.

In 2000, Rozier et al. studied lithium insertion into V_2O_5 and $Ag_2V_4O_{11-y}$, using solid-state chemistry and x-ray diffractometry measurements [28]. The starting γ-LiV_2O_5 was prepared by the solid-state reaction between $LiVO_3$ and VO_2, and lithium insertion into γ-LiV_2O_5 to produce $Li_{x'}V_2O_5$ was accomplished chemically using C_4H_9Li or $Li_2C_2O_4$. For the $Li_{x'}V_2O_5$ materials, when x' > 1, several phases are observed by XRD. Thus, the stepped discharge profile obtained during discharge of an Li/V_2O_5 cell was rationalized as the demixing of the several phases until $LiVO_2$ is obtained. Regarding the oxygen-deficient $Ag_2V_4O_{11-y}$, because it had an identical x-ray diffraction pattern to that predicted for $Ag_{1+x}V_3O_8$, the electrochemistry associated with oxygen-deficient $Ag_2V_4O_{11-y}$ was interpreted in terms of addition of lithium to $Ag_{1+x}V_3O_8$. The proposed mechanism involved lithium first inserting into $Ag_{1+x}V_3O_8$ to create $(Li,Ag)^+_{1+x}V_3O_8$ and then, finally, $Li_{1+x}V_3O_8$. This mechanism accounts for the similarity in discharge curves between $Ag_{1+x}V_3O_8$ and $Li_{1+x}V_3O_8$. Finally, lithium was inserted into $Ag_{1+x}V_3O_8$ by reacting $Li_2C_2O_4$ with $Ag_{1.2}V_2O_8$; a mixture of $Li_{1+x}V_3O_8$ and silver metal was obtained, consistent with the proposed mechanism.

In 2003, a mechanistic study of SVO synthesis was reported by Takeuchi and coworkers [29]. Thermal analyses were undertaken using Ag_2CO_3 or Ag(0) powders, with V_2O_5 to elucidate the mechanism of SVO formation using these starting materials. Reaction of $AgCO_3$ and V_2O_5 proceeded via a two-step decomposition/combination reaction, in the temperature range of 150 to 400ºC. Consistent with these results, reaction of Ag(0) powder with V_2O_5 under an air or oxygen atmosphere generated ε-phase $Ag_2V_4O_{11}$ at 350ºC. In contrast, reaction of Ag(0) and V_2O_5 under an inert atmosphere generated the oxygen-deficient bronze AgV_2O_5.

In 2005, Mao and coworkers reported hydrothermal synthesis of single-crystal-line $Ag_2V_4O_{11}$ nanobelts [30]. $AgNO_3$, V_2O_5, and 1,6-hexanediamine were dissolved in water and heated in a Teflon-lined stainless-steel autoclave at 180ºC for 2 days. SEM and TEM showed the SVO products to have widths of 70 to 200 nm, and lengths of 2 to 5 microns. The SVO product was characterized by XRD and XPS, where no impurities could be detected. Thermogravimetric analysis showed some weight loss below 486ºC, which was attributed to decomposition of residual organic

templates and the loss of water between vanadium oxide layers. Magnetic measurements showed the nanobelts to be paramagnetic, which was attributed to the oxygen deficiencies.

In 2005, Sharma and coworkers reported ion exchange synthesis of silver vanadates from organically templated layered vanadates ($(org)_xV_2O_5$) [31]. Layered vanadates were prepared using a previously reported procedure [32], then stirred with 1 M solution of $AgNO_3$ for ion exchange. The progress of the ion exchange reaction was monitored by the color of the reaction medium, with a color change from green to yellow observed. It was suggested from XRD data that the parent layered structure of $(org)_xV_2O_5$ was destroyed within a few hours of mixing with silver nitrate, with a gradual evolution of a β-$AgVO_3$ phase after 36 to 48 h. The product was observed via TEM to consist of $AgVO_3$ nanorods covered with small spherical silver nanoparticles with diameters of 2 to 5 nm.

13.3 BATTERY APPLICATIONS OF SILVER VANADIUM OXIDE

Advanced batteries with lithium metal anodes possess high energy density, due to the high electrochemical equivalence (or high coulombic output for a given weight of material) of lithium. Lithium metal has an electrochemical equivalence of 3860 mAh/g and a standard potential of –3.05 V at 25ºC [33]. These values are the highest for any of the metals and make lithium an excellent anode material. One characteristic associated with lithium anode batteries is the need to use nonaqueous electrolyte solutions due to the reactivity of lithium metal with water. The lower conductivity of organic-based electrolytes compared to aqueous electrolytes can limit current, or rate capability, that a battery can provide. However, high-performance lithium batteries have been designed that display utility in special applications where high power and high battery capacity are needed. It is in this area that SVO has found its niche as a cathode material for lithium batteries and has been enthusiastically studied as such over the past 2 decades.

Commercially, it has been as a cathode material in a primary (nonrechargeable) lithium anode cell that SVO has made the largest impact, mainly associated with batteries for implantable medical devices. Specifically, lithium/SVO batteries are able to produce the high pulse currents that are required for the operation of implantable cardiac defibrillators (ICDs) [34]. ICDs monitor the patient's heart and provide a high-energy electrical shock to a patient experiencing ventricular fibrillation, which allows the heart to return to normal rhythm. During the functional use of the device, continuous low-current drain is required over the entire life of the device (several years) to power the monitoring circuitry. In addition, when fibrillation is detected, the battery must rapidly deliver a series of high-current pulses, typically on the order of 2 to 3 A [35,36]. In addition, the lithium/SVO battery has demonstrated the safety and reliability needed for an implantable battery. In 1991, Holmes and Visbisky reported on the reliability of SVO-based cells used in implantable defibrillators [37]. A total of 788 cells were tested at 37ºC under both constant resistive load and pulse discharge. Although none of the cells had reached premature end of test, a maximum

TABLE 13.1

The gravimetric capacities of cathode materials for lithium and lithium ion batteries tabulated from the literature

Cathode material	Capacity (mAh/g)	Ref.
$LiWO_2$	120	84
$LiMn_2O_4$	123	39
$LiCoO_2$	131	39
$LiNi_{0.5}Co_{0.5}O_2$	147	39
$LiNiO_2$	160	83
$LiMoO_2$	199	84
TiS_2	226	84
MnO_2	308	85
SVO ($Ag_2V_4O_{11}$)	315	51
CF_x	860	86

random rate of failure of 0.0167% per month was calculated ($\alpha = 0.90$). Reliability and quality assurance programs for the construction of implantable-grade lithium/SVO cells were also outlined by Takeuchi [38]. Data from the testing of over 3800 cells indicated a maximum random failure rate of 0.005% at a 90% confidence interval, demonstrating the successful deployment of the technology.

There have been several papers and patents related to the use of SVO as a high-rate cathode material for the ICD application. In addition to the high-rate capability displayed by SVO as a cathode, this material also displays high-energy density relative to other solid cathode materials used in lithium batteries (see Table 13.1). Additionally, there has also been interest in SVO and related materials as rechargeable cathode materials for lithium and lithium-ion type cells. Literature related to both of these intended applications are reviewed in the following sections.

13.3.1 PRIMARY SILVER VANADIUM OXIDE CELLS

In 1978, the first reference was made regarding the use of SVO as a battery cathode material, when Scholtens and coworkers investigated solid electrolyte cells of the type $Ag/Ag-\beta-alumina/Ag_xV_2O_5$, where silver metal was used as the anode and $Ag_xV_2O_5$ as the cathode with a range of $\times$ values [39]. Partial thermodynamic enthalpic and entropic functions of silver within the compound were calculated using galvanic cell measurements. Compounds in the range $0.1 < \times < 0.7$ were studied, where conductivity was successfully measured in the region $0.29 < \times < 0.41$. This region was denoted the β phase and was determined to be most stable from the thermodynamic measurements. With the benefit of hindsight, it is interesting to note that the authors had commented that $Ag_xV_2O_5$ bronzes (used in conjunction with a silver ion electrolyte) offered no possibilities for practical storage cells.

History began for the lithium/SVO cell in 1982, when the first of two U.S. patents for the use of metal vanadium oxides as cathodes in electrochemical cells was granted to Liang et al. [40]. Thermal decomposition methods were utilized to

react vanadium oxides with several elements, including silver, to prepare the SVO. The use of $Ag_2V_4O_{11}$ as a cathode in a lithium battery with a nonaqueous liquid electrolyte was disclosed by this patent, and this system was originally targeted for use in high-temperature (~150ºC) battery application.

In 1984, Keister et al. proposed the use of Li/SVO-based systems to power implantable devices [41]. The SVO material was designated AgV_2O_5 in this paper, although the actual elemental analysis indicated a formula of $AgV_2O_{5.5-6.0}$, suggesting that the material was actually the ε-phase of SVO ($Ag_2V_4O_{11}$). The cell construction included a single central lithium anode enveloped by an SVO cathode, limiting the area of contact between the electrodes and thus the rate capability of the cell. Pulse testing was performed at a current density of 0.8 mA/cm^2, corresponding to an overall low current of 10 mA. The electrochemical cell consisted of SVO cathode, lithium anode, and 1 M $LiBF_4$ electrolyte salt in propylene carbonate. Although the low conductivity of the liquid electrolyte also limited the rate capability of this cell, the high boiling point of the solvent provided the cell the ability to tolerate autoclave temperatures of around 125ºC.

In 1986, Keister et al. detailed the first implantable-grade commercial cell based on SVO chemistry, a significant milestone concerning the use of Li/SVO cells in implantable cardiac defibrillators [42]. The system employed $Ag_2V_4O_{11}$ cathode material with a liquid organic electrolyte and lithium anode, all contained in a prismatic-shaped hermetically sealed stainless-steel case. Extensive safety and performance testing was conducted on this cell, demonstrating the cell's ability to withstand abusive conditions as well as the ability to function at both low continuous currents and high-current pulsitile loads. The large increase in rate capability of this cell was due in part to the use of a multiplate cell design. By connecting several cathode plates in a parallel configuration, the effective surface area of the cathode was increased, allowing higher currents to be drawn from the cell. The cell was pulse tested using 2 A pulse currents, considerably higher than the 10 mA pulse testing conducted in the previous study.

In 1986, Takeuchi et al. further improved the performance of the lithium/SVO system under high-current discharge conditions [43]. A nonaqueous electrolyte consisting of lithium salt ($LiSO_3CF_3$ or $LiAsF_6$) in a 50:50 mix of propylene carbonate and dimethoxyethane was developed for this system, which demonstrated high conductivity and good stability toward the anode and cathode materials. Up to 76% of theoretical capacity was obtained when the cell was discharged using high-current density pulses at 20 mA/cm^2 of cathode area. In 1987, Holmes et al. also reported on the performance of this newly developed cell [44].

Detailed electrochemical characterization of the lithium/SVO battery system continued in several publications. The synthesis and characterization of $Ag_2V_4O_{11}$–based cathode material for lithium cells was further investigated by Takeuchi and Piliero in 1987 [45]. SVO cathode materials with silver-to-vanadium ratios of 0:10 to 1.1 were prepared via thermal decomposition of $AgNO_3$ and V_2O_5 mixtures. Lithium anode batteries were built using the materials, and the batteries were discharged under several different loads. Cathodes containing primarily V_2O_5 gave the lowest capacity, whereas material containing mainly $AgVO_3$ was slightly higher. The $Ag_2V_4O_{11}$ cathodes showed the highest capacity and the lowest resistance under

pulsed discharge conditions of any of the materials tested. Chemical lithiation of the cathode materials using n-butyllithium was conducted, and these experiments indicated that $Ag_2V_4O_{11}$ provided the highest theoretical volumetric energy density, in agreement with the actual electrochemical cell data. It is interesting to note that very different discharge curves were observed for the different cathode materials. Because the voltage of the lithium metal anode is nearly constant during discharge, the cathode plays a dominant role in determining the voltage of the cell as the battery is drained. The dependence of the cell voltage on the ratio of silver to vanadium in the cathode of these cells illustrates the differences in electrochemical behavior displayed by the different phases of SVO.

The electrochemical reduction of SVO during discharge of $Li/Ag_2V_4O_{11}$ cells was explored in greater detail by Thiebolt and Takeuchi in 1987. In this work, they identified five voltage plateaus throughout the electrochemical discharge of SVO [46,47]. $Li/Ag_2V_4O_{11}$ cells were discharged to various stages and disassembled to investigate the cathode composition at each plateau region. Chemical titration and atomic absorption were used to reveal the total amount and oxidation state of the silver and vanadium present in each sample. Most notably, low-rate cyclic voltammetry on lithium/SVO was reported for the first time in this paper. Electrodes were prepared using the $Ag_2V_4O_{11}$ analyte, graphite conductive additive, and polyacrylic acid as binder. A low scan rate of 0.08 mV/sec was used for this experiment, resulting in well-resolved peaks in the voltammogram.

In 1987, Bergman et al. presented calorimetric analysis of lithium/SVO cells [48]. Heat dissipation during cell discharge was characterized under several resistive loads, where these experiments were undertaken to determine the long-term stability of the cells. Although calorimetric measurements suggested a self-discharge rate as high as 3.4% per year, analysis of residual lithium present after discharge suggested that the actual self-discharge rate was less than 1% per year. The difference was attributed to parasitic side reactions of lithium and non-Faradaic contributions, as heat dissipation due to cell polarization and entropy were determined to be small.

In 1988, Takeuchi and Thiebolt measured the diffusion rate of lithium in SVO electrodes [49]. Cells were discharged to various depths of discharge, allowed to equilibrate, and then pulsed at high current. Subsequent to the pulse, voltage recovery was monitored to determine lithium diffusion rates. It was determined that the rate and magnitude of voltage recovery was not constant at all depths of discharge, suggesting that the electrochemical characteristics of SVO change as the material is reduced.

In 1989, Bergman and Takeuchi investigated the complex impedance characteristics of lithium/SVO cells [50]. Complex impedance responses were generated at various levels of discharge, and the cells were repeatedly stored and pulsed to determine voltage delay. Voltage delay refers to a transient initial drop in voltage after a cell is subjected to a high-current pulse after a long storage period. Subsequent pulses are not expected to show the same voltage drop. Voltage drops of 850 to 905 mV were recorded in this study, with 100 to 150 mV due to voltage delay.

In 1990, Takeuchi et al. investigated the low-temperature performance of Li/SVO batteries for potential nonmedical specialty applications [51]. Twenty-three percent of theoretical capacity was obtained under constant resistive load at –40ºC, and

seventy percent theoretical capacity at 0ºC. Under pulsitile discharge, 40% of theoretical capacity was obtained at –40ºC. In addition to the electrochemical testing, cells were safety-tested under short-circuit and crush conditions. An aggressive crush test was designed to generate an internal short circuit, and no violent cell behavior was observed.

In 1991, Takeuchi and Thiebolt investigated the nature and mechanism of lithium deposition inside sealed Li/SVO cells [52]. Case-neutral cells were constructed, and the current flow between the case and anode was measured following intermittent high-current discharges. This current was correlated with the amount of deposited lithium measured via destructive analysis of the cell. Small clusters of lithium metal were observed to deposit on nonactive components inside the cell during discharge. This study concluded that inhomogeneous discharge of the cathode under high rates could induce lithium deposition, where cell orientation during discharge, current level, and frequency of pulse discharge all played an important role in determining the amount of lithium deposited.

Starting in 1993, several published reports appeared that examined in greater detail the influence of the synthesis method of $Ag_2V_4O_{11}$ on the performance of cells using this cathode material. Leising and Takeuchi studied the effects of synthesis temperature on SVO [53]. The reaction of $AgNO_3 + V_2O_5$ was used to prepare $Ag_2V_4O_{11}$ at temperatures ranging from 320 to 540ºC. The morphologies of the materials showed a temperature dependence, where the material synthesized at 320 and 375ºC displayed irregularly shaped particles, whereas the 450ºC material displayed small (< 1 µm in diameter) acicular nanoparticles. Although the results of a rapid discharge test were very similar for cathodes containing materials prepared at 320 to 450ºC, the physical characterization indicated that the temperature of synthesis played an important role in determining the properties of the solid product. The material prepared at 540ºC was found to be very different from all of the other materials. At 540ºC, the $Ag_2V_4O_{11}$ material began to soften and, on cooling, yielded large plate-like particles, which contained a mixture of phases.

In 1993, Crespi was granted a U.S. patent for Li/SVO cells constructed with SVO cathodes prepared via an addition reaction of $AgVO_3$ or Ag_2O with V_2O_5 [54]. The inventor maintained that the chemical addition reaction conducted at 520ºC produced $Ag_2V_4O_{11}$, which performed differently electrochemically than material prepared by the prior art outlined by Liang et al. in the 1982 patent [40]. The $Ag_2V_4O_{11}$ material described by Liang et al. was prepared at 360ºC by a thermal decomposition of $AgNO_3$ and V_2O_5. It was shown that the cathode material prepared by chemical addition at 520ºC displayed higher rate capability than the 360ºC thermal decomposition material, when test cells were pulsed using current densities of 12 or 19 mA/cm^2. The 520ºC chemical addition material also displayed greater crystallinity, as measured by x-ray powder diffraction, than the 360ºC thermal decomposition material.

In 1994, Leising and Takeuchi investigated the synthesis of SVO under both air and argon at 500ºC from many different silver precursors including silver nitrate, silver nitrite, silver vanadate, silver oxide, silver carbonate, and silver metal [55]. Materials prepared under air at the same temperature using either the thermal decomposition reaction ($AgNO_3$) or the chemical addition reaction (Ag_2O or $AgVO_3$)

appeared similar in terms of morphology, thermal properties, and electrochemical performance. Interestingly, the crystallinity of the $Ag_2V_4O_{11}$ synthesized at 500ºC by the thermal decomposition reaction was actually higher than the $Ag_2V_4O_{11}$ prepared at 500ºC by the chemical addition reaction, as illustrated by x-ray powder diffraction patterns. The increased crystallinity of $Ag_2V_4O_{11}$ prepared at higher temperature (500 to 520ºC) via the thermal decomposition route is reiterated in a 1999 U.S. patent issued to Crespi and Chen [56]. In this patent, the inventors claim the use of $Ag_2V_4O_{11}$ prepared by the thermal decomposition route at 360ºC, according to the Liang et al. method, which is then reheated to a higher temperature to give a more crystalline material.

In 1994, a detailed characterization of the SVO discharge reaction in lithium batteries was published by Leising et al. [57]. In this study, $Li_xAg_2V_4O_{11}$ products were prepared and isolated over the range of $0 < \times < 6.6$, and a combination of physical and wet chemical characterization techniques were used to identify the composition of the product cathode materials. X-ray powder diffraction experiments demonstrated that the reduction of SVO in the process $Li + Ag_2V_4O_{11} \rightarrow Li_xAg_2V_4O_{11}$ resulted in a loss of crystallinity over the range $0 < \times < 2.4$, with the concurrent reduction of Ag^+ to Ag^0. The reduction of silver to the metallic form was found to play an important role in the battery chemistry, accounting for approximately 30% of the overall capacity of the SVO cathode material, and a 5 orders of magnitude increase in conductivity between the starting $Ag_2V_4O_{11}$ and the material containing reduced silver. The enhanced conductivity of the reduced cathode material contributes to the high-rate capability displayed by the lithium/SVO system, which is a key property of the material. At $\times$ values > 2.4 in $Li_xAg_2V_4O_{11}$, the reduction of V^{5+} to V^{4+} and V^{3+} was identified. It was found that the reduction of V^{4+} to V^{3+} competed with the reduction of V^{5+} to V^{4+} at $\times > 3.8$, resulting in the formation of mixed-valent materials, where vanadium (III), (IV), and (V) were found in the same sample.

In 1995, Crespi et al. used high-resolution electron microscopy to investigate the structure of slightly silver-deficient $Ag_{2-y}V_4O_{11}$ [58]. During the discharge reaction, silver particles were observed on the outside of the needle-shaped SVO particles, which confirmed that the first step in the lithiation of this material was reduction of silver. The stacking of the vanadium oxide layers was also found to become random in this process.

New approaches to the synthesis of SVO cathode material have been reported. In 1995, Takeuchi and Thiebolt patented a new preparation for SVO cathodes prepared via addition of elemental silver to vanadium compounds present in an anhydrous mixture. Oxygen-deficient SVO compounds were found, as well as compounds designed to provide a desired shape in the electrical discharge curve of the cell [59]. Following this work in 1996, Takeuchi and Thiebolt patented several methods for the preparation of amorphous SVO prepared by chemical addition reaction at temperatures high enough to melt the mixture, coupled with rapid cooling [60]. The use of a phosphorus pentoxide dopant was also discussed.

New approaches to battery design have also been described. A wound-electrode design has been proposed to improve design efficiency, as reported by Crespi et al. [61] and Skarstad [62] in 1995 and 1997, respectively. The cell was capable of consuming 6.67 equivalents of lithium per $Ag_2V_4O_{11}$ formula unit. The crystalline

SVO material utilized was prepared via a combination reaction. A spirally wound lithium/SVO cell was also described in 1998 by Takeuchi et al. [63]. This cell achieved a volumetric energy density of 540 Wh/l, delivered greater than 50% of theoretical capacity under loads greater than 3 $\int$, and was successfully pulse discharged at 2.0 A. Several safety tests were conducted, including short-circuit, forced overdischarge, crush, and charging tests, and the cells did not rupture, vent, or leak under these abusive conditions.

In 1998, Gan and Takeuchi identified a key role of anode surface film composition in SVO cell performance [64]. The addition of carbon dioxide synthons such as dibenzyl carbonate and benzyl succinimidyl carbonate was found to reduce resistance build-up and alleviate voltage delay in silver vanadium oxide cells.

There has been some very recent interest in utilizing new synthetic approaches to make SVO with improved electrochemical performance. In 2004, Xie and coworkers reported an ultrasonic sol-gel synthesis of $Ag_2V_4O_{11}$ from V_2O_5 gel [65]. V_2O_5 gel was prepared by polycondensation of vanadic acid, then mixed directly with Ag_2O powder, using ultrasonic treatment to disperse the powder in the gel. The resulting $Ag_2V_4O_{11}$ gel was dried *in vacuo* at 50ºC, then heated for 10 h in air at 150 to 450ºC. X-ray powder diffraction showed the SVO to be fully crystallized at 350ºC. The SVO synthesized using sol-gel methods showed a higher capacity when discharged versus metallic lithium at 30 mA/g than SVO made using a standard solid-state high-temperature synthesis [24].

Xie and coworkers continued their work on sol-gel synthesis of silver vanadium oxides, with additional results reported in 2005 [66]. Ag_2O powder was added to the V_2O_5 gel at Ag/V ratios of 1:1, 1:2, and 1.2:3, producing products of $AgVO_3$, $Ag_2V_4O_{11}$, and $Ag_{1.2}V_3O_8$, respectively. Similar to the previous results for $Ag_2V_4O_{11}$, the $Ag_{1.2}V_3O_8$ prepared using sol-gel synthesis showed higher discharge capacity than $Ag_{1.2}V_3O_8$ prepared by a standard solid-state approach [24].

In 2006, Zhou and coworkers reported synthesis of $Ag_2V_4O_{11}$ via a rheological phase method [67]. Stoichiometric amounts of Ag_2CO_3 and NH_4VO_3 were mixed and heated with water in a Teflon-lined stainless autoclave at 90 to 120ºC, then removed and heated in air at 400 to 500ºC to form the $Ag_2V_4O_{11}$ product. For comparison, SVO was also synthesized using a previously reported solid-state method [24]. Particle sizes for the rheologically formed SVO were smaller on average and had a narrower distribution than those of the solid-state product. The rheologically formed SVO had higher specific capacity than the solid-state product when discharged in coin cells versus Li foil at 30 to 120 mA/g.

In 2006, Popov and coworkers studied discharge characteristics of silver vanadium oxide cathodes [68]. Commercial Li-$Ag_2V_4O_{11}$ cells were studied under various operating conditions, including galvanostatic discharge at a 0.08 mA/cm^2 discharge current. Three distinct plateaus were identified under this discharge condition and attributed to silver and vanadium species reduction. Batteries were disassembled at various depths of discharge and studied by scanning electron microscopy. Below 2.8 V, the ohmic resistance increased, which the authors attributed to formation of less-conductive vanadium oxides and the erosion of silver, increasing the electronic and particle-to-particle resistance.

13.3.2 RECHARGEABLE SILVER VANADIUM OXIDE CELLS

The use of SVO as a rechargeable cathode material is enticing due to the high-energy density (> 300 mAh/g) of this material. However, during the discharge reaction of a lithium/SVO cell, the reduced silver is replaced by lithium in the vanadium oxide matrix. Therefore, the reversibility of this lithium for silver substitution under charge conditions is still a matter of debate, as will be outlined below.

In 1991, Takada et al. investigated the reversibility of silver intercalation in silver vanadium bronzes ($Ag_xV_2O_5$), where materials were prepared in the range $0.3 \leq \times \leq 1.0$ [69]. Silver ion conductive solid electrolytes were used to study the electrochemistry of the bronzes versus a silver powder anode. The δ-phase ($0.67 \leq \times \leq 0.86$) material was found to be electroactive, whereas the β-phase ($0.29 \leq \times \leq 0.41$) was not. Characterization of the silver vanadium bronzes obtained by electrochemical intercalation and deintercalation of silver was accomplished by x-ray diffraction. It was proposed that new phases of SVO were obtained by the electrochemical reaction, which were structurally distinct from those synthesized at high temperature. Rechargeable cells were fashioned using $Ag_{0.7}V_2O_5$ for both the anode and the cathode, with $Ag_6I_4WO_4$ as the solid-state electrolyte. By using twice as much $Ag_{0.7}V_2O_5$ in the anode as the cathode, the battery was configured such that the silver composition would vary between 0.81 and 0.90 for $\times$ in $Ag_xV_2O_5$ in the anode, and 0.30 and 0.47 for $\times$ in $Ag_xV_2O_5$ for the cathode. This produced a cell with a running voltage between 0.5 and 0.25 V, which was charged and discharged (cycled) over 600 times. However, it should be noted that aside from the low voltage produced by the cell, the capacity of the cathode was found to be only 5 to 10 mAh/g.

In 1992, Garcia-Alvarado et al. reported use of the δ-phase silver vanadium bronze $Ag_{0.68}V_2O_5$ to produce cathode materials for rechargeable lithium batteries [70]. $Ag_xV_2O_5$ with $\times = 0.4$, 0.15, and 0.04 was formed by reacting δ-$Ag_{0.68}V_2O_5$ with NO_2BF_4 oxidizing agent to remove silver. Cells containing $Ag_xV_2O_5$ cathodes with $\times = 0.68$ and 0.4 incorporated 2.9 and 2.7 equivalents of lithium, respectively, on the first discharge. In comparison, cells using cathodes containing lower silver contents ($\times = 0.15$ and 0.04) displayed large polarization, decreased initial capacities of 2.3 and 2.1 equivalents of lithium, and large decreases in capacity on the second cycle.

In 1994, Garcia-Alvarado et al. continued their studies of silver vanadium oxide secondary batteries, investigating $Ag_2V_4O_{11}$ and $Ag_2V_4O_{11-y}$ [71]. The same synthetic approach was used as in their earlier study [70], where oxidation of the SVO starting material by NO_2BF_4 produced new cathode materials with decreased silver contents. Multiple phases were observed and characterized during charge and discharge of the samples between 3.6 and 1.5 V. The formation of $Li_xAg_2V_4O_{11}$ was characterized as reversible over the range of $0 \leq \times \leq 7$, although the replacement of silver by lithium from $0 \leq \times \leq 2$ was reported as irreversible. The oxygen-deficient material, $Ag_2V_4O_{11-y}$, was found to incorporate a maximum of 5.7 equivalents of lithium, yielding a lower capacity. These new cathode materials all displayed a maximum capacity of 5.7 Li per unit formula, similar to the oxygen-deficient material.

In 1995, West and Crespi studied the reversibility of the lithium insertion process in a polymer electrolyte $Li/Ag_2V_4O_{11}$ cell, cycled between 2.2 and 3.5 V at 100ºC

[72]. The formation of metallic silver was identified in the x-ray diffraction patterns for the reduced cathodes, consistent with the earlier findings of Leising et al. [57] and Garcia-Alvarado et al. [71]. However, this study also showed that at high temperature (100ºC), some reversible formation of $Ag_2V_4O_{11}$ takes place at the cathode when charged to 3.5 V. It was proposed that silver was oxidized and re-entered the vanadium oxide matrix upon charge. Based on the shape of the charge/discharge curves for an $Li/Ag_2V_4O_{11}$ cell using propylene carbonate liquid electrolyte at 25ºC, the authors maintained that silver also reinserts into the vanadium oxide framework at ambient temperatures. The reversibility of the $Li/Ag_2V_4O_{11}$ system was poor, where 80% capacity fade was reported for 25 cycles when the system was charged to 3.5 V, and 45% capacity fade for 25 cycles when charged to 3.25 V. Capacity fade is defined as the percentage loss of capacity during cycling as compared to the starting capacity of the cell.

In 1997, Kawakita et al. investigated the performance of $Ag_{1+x}V_3O_8$ cathode material, prepared via an exchange reaction of $Na_{1+x}V_3O_8$ with Ag^+ ions or the solid-state reaction of Ag_2O and V_2O_5 [73]. Discharge of the material against a lithium anode resulted in displacement of the silver ions and their reduction to silver metal upon discharge. In contrast to the work of West and Crespi [72], oxidation and reinsertion of silver was not observed during charge. No anodic peaks corresponding to $Ag(0) \rightarrow Ag(I)$ were observed in cyclic voltammetry of the system, confirming that silver was not returned to the vanadium oxide matrix. In addition, silver metal was identified in x-ray diffraction patterns of the charged cathode.

Kawakita et al. continued their studies of the reversibility of silver vanadium oxide systems, reporting on the use of δ-AgV_2O_5 in 1998 [74]. Approximately three equivalents of lithium were inserted into the material over three distinguishable voltage plateaus. In the first region, $Ag(I)$ is reduced to $Ag(0)$. In the second region, the δ-phase $Ag_yV_2O_5$ changes to ϵ-phase $Li_xV_2O_5$, and in the third region, additional lithium ions are inserted into the ϵ material. Once again, $Ag(I)$ did not return to the vanadate on charge once $Ag(0)$ was formed during discharge.

Also in 1998, Kawakita et al. prepared layered sodium SVOs of the formula $(Na_yAg_{1-y})_2V_4O_{11}$ by substituting part of the silver ions in $Ag_2V_4O_{11}$ with sodium [75]. Discharge curves similar to that obtained with pure SVO were obtained, and reduction of $Ag(I)$ was observed in competition with $V(V)$ reduction. Unlike $Ag_2V_4O_{11}$, which becomes amorphous on discharge, $Na_{1.54}Ag_{0.46}V_4O_{11}$ still displayed x-ray diffraction corresponding to the starting material upon deep discharge to 2 V. This material was cycled successfully with less capacity loss than that observed with pure SVO, indicating the sodium may have stabilized the structure. The authors maintained that substituting some silver with sodium results in a pillar effect, in which sodium ions continue to connect adjacent layers in the material.

Coustier et al. have investigated reacting $Ag(0)$ powder with vanadium pentoxide hydrogels to produce silver-doped vanadium oxides [76,77,78]. Mixtures of V_2O_5 hydrogels were vigorously mixed with silver powder until the silver was completely oxidized. The addition of a full equivalent of silver to vanadium oxide resulted in a material that displayed several x-ray diffraction peaks corresponding to those found in $Ag_2V_4O_{11}$. The addition of silver increased the V_2O_5 conductivity threefold. Cathodes were constructed from the material and discharged against lithium, intercalating

a maximum of four equivalents of lithium. No silver loss occurred during cycling. Samples of $Ag_{0.3}V_2O_5$ were shown to retain a capacity of over 250 mAh/g after 65 cycles at a C/4 rate.

Chu and Qin have investigated the synthesis of silver-V_2O_5 thin films and their use as electrodes in secondary lithium batteries [79]. Targets with a molar ratio for Ag/V_2O_5 of 0.1 to 0.7 were prepared by mixing stoichiometric amounts of silver powder and V_2O_5 powder. The pulsed laser deposition method was used, with 355 nm laser irradiation in an ambient oxygen atmosphere. Deposition time was found to impact the crystallinity of the thin films, where the $Ag_{0.3}V_2O_5$ thin film deposited at a substrate temperature of 300°C for 0.5 h was amorphous by x-ray diffraction and showed little structure, with only sparse 100 to 200 nm grains by scanning electron microscopy. In contrast, the $Ag_{0.3}V_2O_5$ thin film deposited at 300°C for 2 h showed distinct x-ray diffraction peaks indicative of a polycrystalline phase, and large, regular 20 to 30 nm grains by scanning electron microscopy. The amorphous $Ag_{0.3}V_2O_5$ thin film electrode exhibited the best electrochemical performance, with a specific capacity of 396 mAh/g at 4.0 to 1.0 V at a 2°C rate, and a capacity of 260 mAh/g at a 20°C rate with no obvious fading after more than 1000 cycles.

Huang and coworkers continued their work on thin film silver vanadium oxide composite cathodes, reporting on synthesis and electrochemistry of an $Li_2Ag_{0.5}V_2O_5$ cathode in 2003 [80]. Pulsed laser deposition was used, with targets prepared from a mixture of lithium carbonate, silver, and vanadium pentoxide with molar ratio of x:1:2 (x = 0, 1, 2, 3, 4). XRD suggested the $Li_xAg_2V_2O_5$ (x = 2, 3, 4) composite films to have a framework similar to β-$Li_{0.33}V_2O_5$. The electrochemical property of the $Li_xAg_{0.5}V_2O_5$ (x = 2) cathode was found to be better than that of pure V_2O_5, $Ag_{0.5}V_2O_5$, and $Li_xAg_{0.5}V_2O_5$ (x = 1, 3, 4) films, exhibiting a capacity of 60 µA/µm cm^2 at a current density of 7 µA/cm^2 in an all solid-state thin film lithium battery. The battery exhibited some reversibility issues, with sharp capacity fade on initial cycles attributed to the phase change of the film cathode from crystalline to amorphous composite film, and more gradual fade over the subsequent 40 cycles attributed to the *ex situ* film deposition process used in the fabrication of the thin film battery.

In 2004, Huang and coworkers reported synthesis and characterization of 0.5 Ag:V_2O_5 thin-film electrodes [81]. The films were fabricated by pulsed laser deposition in oxygen ambient using 355 nm laser irradiation of a target made from mixing silver and V_2O_5 powders with a molar ratio of 0.5 for Ag/V_2O_5. A rocking chair-type battery was assembled using 0.5 Ag:V_2O_5 films with and without lithiation as anode and cathode electrodes, respectively. The discharge capacity reached 22 µA/µm-cm^2, with low capacity fading up to 100 cycles at a current of 10 µA/cm^2.

In 2004, Hwang and coworkers reported synthesis and characterization of silver doped vanadium oxide thin films for thin film batteries [82]. Amorphous V_2O_5 thin films were simultaneously cosputtered with a high-purity metal silver target. By ICP-AES analysis, the compositions were determined to be $Ag_{0.1}V_2O_5$, $Ag_{0.3}V_2O_5$, $Ag_{0.8}V_2O_5$, and $Ag_{1.8}V_2O_5$ for silver target at rf power of 10, 20, 30, and 40 W, respectively. X-ray diffraction showed no characteristic peaks for V_2O_5 or SVO, indicating that both undoped and Ag cosputtered films were amorphous. By scanning electron microscopy, the surface grain size of the as-deposited films was found to become larger as the amount of doped Ag increased. All solid-state batteries were

prepared with undoped V_2O_5, $Ag_{0.1}V_2O_5$, $Ag_{0.8}V_2O_5$, and $Ag_{1.8}V_2O_5$ thin film cathodes versus lithium metal. The $Ag_{1.8}V_2O_5$ film showed lower discharge capacity than the undoped V_2O_5 film, which the authors attributed to the large grain size of the $Ag_{1.8}V_2O_5$ film. The $Ag_{0.8}V_2O_5$ showed the highest discharge capacity, delivering ~80 µAh/cm²-µm with little fade over 200 cycles at a current density of 20 µA/cm² and a cut-off voltage of 1.5 to 3.6 V.

13.4 SUMMARY

Silver vanadium oxide is a material of rich synthetic and electrochemical history. Early papers reported on materials synthesis and characterization, with particular emphasis on the several different phases of SVO. Products with varying properties were synthesized via variation in reaction conditions, starting materials, and reagent stoichiometries. As an example of the materials available, in the presence of air, the combination of silver with vanadium oxides in different ratios yielded β ($Ag_{0.3}V_2O_5$), γ($Ag_{1.12}V_3O_{7.8}$), and ε ($Ag_2V_4O_{11}$) phases as well as $AgVO_3$, $Ag_4V_2O_7$, and Ag_3VO_4. In addition, the combination of these starting materials in inert atmospheres yielded mainly different products, including materials of the general formula $Ag_xV_2O_5$, where the α phase ($0 \leq \times \leq 0.01$), β phase ($0.29 \leq \times \leq 0.41$), and δ phase ($0.67 \leq \times \leq 0.86$) were formed. Besides the physical characterization of SVO, there have also been several reports on the chemical reactivity of these materials. Some of these reports focused on the interconversion of phases with variation in temperature and atmosphere, whereas others reported the use of SVO as a catalyst for the oxidation of organic substrates. Taken together, the characterization of SVO materials in these earlier studies provided an important foundation for the successful commercial use of SVO.

The focus of much of the research on SVO shifted to the ε-phase when this material was discovered to be a useful cathode material for advanced lithium batteries. SVO was found to possess high-rate capability and capacity as a cathode material, and Li/SVO batteries have since been commercially successful in powering implantable medical devices. The importance of this application and the key role played by the SVO cathode material has led to a large increase in the number of reports on SVO in recent years. Li/SVO batteries have demonstrated high reliability and safety, which has been documented in several references. Much of the work surrounding SVO cathode materials has also focused on the electrochemical characterization of the material, where lithiation of SVO has been analyzed and described in detail. Likewise, a number of synthetic routes to prepare SVO have been described in publications and patents to optimize the ability of the material to function as a primary cathode material. As an extension of the work on nonrechargeable Li/SVO batteries, several studies have also looked at the ability of SVO to act as a rechargeable cathode material. There is still some controversy in the literature concerning the reversibility of silver oxidation/reduction in SVO during the charge and discharge of the material. This issue may require further study to bring agreement on the subject. Due to the complexity of SVO chemistry as well as the subtle and sometimes not-well-understood structural-functional relationships between the chemistry of

SVO and the electrochemical performance parameters of batteries utilizing SVO electrodes, the future for SVO research remains bright.

REFERENCES

1. Briton, H.T.S. and R.A. Robinson. 1930. Physicochemical studies of complex acids. Part IV. The vanadates of silver. *J. Chem. Soc. London.* 2328–2343.
2. Briton, H.T.S. and R.A. Robinson. 1933. Physicochemical studies of complex acids. Part X. The precipitation of metallic vanadates, with a note on Moser and Brandl's method of estimating vanadium. *J. Chem. Soc. London.* 512–517.
3. Deschanvres, A. and B. Raveau. 1964. V-Ag-O-system. *C. R. Acad. Sc. Paris.* 259: 3553–3554.
4. Andersson, S. 1965. Hydrothermally grown crystals of silver vanadium oxides bronzes. *Acta Chem. Scand.* 19: 269–270.
5. Andersson, S. 1965. The crystal structure of a new silver vanadium oxide bronze, $Ag_{1-x}V_2O_5$ (x. approx. 0.32). *Acta Chem. Scand.* 19: 1371–1375.
6. Hagenmuller, P., J. Galy, M. Pouchard, and A. Casalot. 1966. Recent research on vanadium bronzes. I. Monovalent interstitial elements. *Mat. Res. Bull.* 1: 45–54.
7. Fleury, P., R. Kohlmuller, and M.G. Chaudron. 1966. System Ag_2O-V_2O_5. *C. R. Acad. Sc. Paris.* 262: 475–477.
8. Galy, J., M. Pouchard, A. Casalot, and P. Hagenmuller. 1967. Oxygenated vanadium bronzes. *Bull Soc. Fr. Mineral. Cristallogr., XC.* 544–548.
9. Casalot, A. and M. Pouchard. 1967. New nonstoichiometric phases of the silver oxide-vanadium pentoxide-vanadium dioxide system. I. Chemical and chrystallographic study. *Bull. Soc. Chim.* 10: 3817–3820.
10. Lukas, I., C. Strusievici, and C. Liteanu. 1967. Vanadate compounds. VIII. Formation of bronzes in the silver vanadate-vanadium oxide system. *Z. Anorg. Alg. Chem.* 349: 92–100.
11. Raveau, B. 1967. Studies in the systems vanadium-silver-oxygen and vanadium-copper-oxygen. *Rev. Chim. Min.* 4: 729–758.
12. Drozdov, Y.N., E.A. Kuzmin, and N.V. Belov. 1974. Determination of the crystal structure of silver vanadate ($Ag_{4-x}V_4O_{12}$) (x = 1.05) by Shenk's method. *Kristal-lografiya.* 19: 36–38.
13. Volkov, V.L., A.A. Fotiev, N.G. Sharova, and L.L. Surat. 1976. Phase diagram of the vanadium pentoxide-silver metavanadate system. *Russian J. Inorg. Chem.* 21: 1566–1567.
14. Scholtens, B.B. 1976. Diffusion of silver in silver vanadium bronzes. *Mat. Res. Bull.* 11: 1533–1538.
15. Andreikov, E.I. and R.L. Volkov. 1981. Catalytic properties of vanadium oxide compounds of silver in the oxidation of o-xylene and napthalene. *Kinetika i Katlitz* 4: 963–968.
16. Van Den Berg, J., A. Broersma, A.J. Van Dillen, and J.W. Geus. 1983. A thermal analysis study of vanadium pentoxide and silver vanadate ($Ag_{0.35}V_2O_5$). *Thermochim. Acta.* 63: 123–128.
17. Wenda, E. 1985. Phase diagram of vanadium pentoxide-molybdenum trioxide-silver oxide. I. Phase diagram of vanadium pentoxide-silver oxide system. *J. Therm. Anal.* 30: 879–887.
18. Enjalbert, R. and J. Galy. 1986. A refinement of the structure of vanadium pentoxide. *Acta Cryst.* C42: 1467–1469.

19. Znaidi, L., N. Baffier, and M. Huber. 1989. Synthesis of vanadium bronzes $M_xV_2O_5$ through sol-gel processes. I. Monoclinic bronzes (M = sodium, silver). *Mat. Res. Bull.* 24: 1501–1514.

20. Vassileva, M., A. Andreev, and S. Dancheva. 1991. Complete catalytic oxidation of benzene over supported vanadium oxides modified by silver. *Appl. Catal.* 69: 221–234.

21. Galy, J. 1992. Vanadium pentoxide and vanadium oxide bronzes — structural chemistry of single (S) and double (D) layer $M_xV_2O_5$ phases. *J. Solid State Chem.* 100: 229–245.

22. Deramond, E., J.-M. Savariault, and J. Galy. 1994. Silver insertion mode in β-$Ag_xV_2O_5$ tunnel structure. *Acta Cryst.* C50: 164–166.

23. Crespi, A.M., P.M. Skarstad, H.W. Zandebergen, and J. Schoonman. 1993. *Proc. Symp. Lithium Batt.* 93–94: 98–105.

24. Zandbergen, H.W., A.M. Crespi, P.M. Skarstad, and J.F. Vente. 1994. Two structures of $Ag_{2-x}V_4O_{11}$, determined by high resolution electron microscopy. *J. Solid State Chem.* 110: 167–175.

25. Rozier, P., J.M. Savariault, and J. Galy. 1996. β-$AgVO_3$ crystal structure and relationships with $Ag_2V_4O_{11}$ and δ-$Ag_xV_2O_5$. *J. Solid State Chem.* 122: 303–308.

26. Rozier, P. and J. Galy. 1997. $Ag_{1.2}V_3O_8$ crystal structure: Relationship with $Ag_2V_4O_{11-y}$ and interpretation of physical properties. *J. Solid State Chem.* 134: 294–301.

27. Ge, X. and H. Zhang. 1998. Temperature programmed reduction studies of V-Ag catalysts. *J. Solid State Chem.* 141: 186–190.

28. Rozier, P., J.M. Savariault, and J. Galy. 2000. *Mat. Res. Soc. Symp. Proc.* 575: 113–119.

29. Takeuchi, K.J., R.A. Leising, M.J. Palazzo, A.C. Marschilok, and E.S. Takeuchi. 2003. Advanced lithium batteries for implantable medical devices: Mechanistic study of SVO cathode synthesis. *J. Power Soc.* 119–121: 973–978.

30. Mao, C., X. Wu, H. Pan, J. Zhu, and H. Chen. 2005. Single-crystalline $Ag_2V_4O_{11}$ nanobelts: Hydrothermal synthesis, field emission, and magnetic properties. *Nanotechnology.* 16: 2892–2896.

31. Sharma, S., M. Panthoefer, M. Jansen, and A. Ramanan. 2005. Ion exchange synthesis of silver vanadates from organically templated layered vanadates. *Mat. Chem. and Physics.* 91: 257–260.

32. Sharma, S., A. Ramanan, and M. Jansen. 2004. Hydrothermal synthesis of new organically intercalated layered vanadates. *Solid State Ionics.* 170: 93–98.

33. Linden, D. 1984. Lithium cells. In *Handbook of batteries & fuel cells*, D. Linden (Ed.). New York: McGraw -Hill. 11.5–11.6.

34. Nelson, J.P. 1995. *Proc. 12th Int. Semin. Prim. & Sec. Batt.*, Deerfield Beach, FL.

35. Brodd, R.J., K.R. Bullock, R.A. Leising, R.L. Middaugh, J.R. Miller, and E. Takeuchi. 2004. Batteries, 1977 to 2002. *J. Electrochem. Soc.* 151: K1–K11.

36. Takeuchi, E.S. and R.A. Leising. 2002. Lithium batteries for biomedical applications. *MRS Bulletin.* August: 624–627.

37. Holmes, C.F. and M. Visbisky. 1991. Long-term testing of defibrillator batteries. *Pace.* 14: 341–345.

38. Takeuchi, E.S. 1995. Reliability systems for implantable cardiac defibrillator batteries. *J. Power. Sources.* 54: 115–119.

39. Scholtens, B.B., R. Polder, and G.H.J. Broers. 1978. Some thermodynamic, electrical, and electrochemical properties of silver vanadium bronzes. *Electrochim. Acta.* 23: 483–488.

40. Liang, C.C., E. Bolster, and R.M. Murphy. 1982. United States Patent 4,310,609.

41. Keister, P., R.T. Mead, S.J. Ebel, and W.R. Fairchild. 1984. *Proc. 31st Int. Power Sources Symp.* 331–338.
42. Keister, P.P., E.S. Takeuchi, and C.F. Holmes. 1986. *Cardiostim* 86. 463.
43. Takeuchi, E.S., M.A. Zelinsky, and P. Keister. 1986. *Proc. 32nd Int. Power Sources Symp.* 268–273.
44. Holmes, C.F., P. Keister, and E.S. Takeuchi. 1987. High-rate lithium solid cathode battery for implantable medical devices. 1987. *Prog. Batt. Solar Cells.* 6: 64–66.
45. Takeuchi, E.S. and P. Piliero. 1987. Lithium/silver vanadium oxide batteries with various silver to vanadium ratios. *J. Power Sources.* 21: 133–141.
46. Thiebolt, W.C. and E.S. Takeuchi. 1987. *Ext. Ab. Batt. Div. Electrochem. Soc.* 29.
47. Takeuchi, E.S. and W.C. Thiebolt. 1988. The reduction of silver vanadium oxide in lithium/silver vanadium oxide cells. *J. Electrochem. Soc.* 135: 2691–2694.
48. Bergman, G.M., S.J. Ebel, E.S. Takeuchi, and P. Keister. 1987. Heat dissipation from lithium/silver vanadium oxide cells during storage and low-rate discharge. *J. Power Sources.* 20: 179–185.
49. Takeuchi, E.S. and W.C. Thiebolt. 1988. *Ext. Ab. Batt. Div. Electrochem. Soc.* 47.
50. Bergman, G.M. and E.S. Takeuchi. 1989. Voltage delay and complex impedance characteristics of a high-rate lithium/silver-vanadium oxide multiplate battery. *J. Power Sources.* 26: 365–367.
51. Takeuchi, E.S., D.R. Tuhovak, and C.J. Post. 1990. *Proc. 34th Int. Power Sources Symp.* 355–358.
52. Takeuchi, E.S. and W.C. Thiebolt. 1991. Lithium deposition in prismatic lithium cells during intermittent discharge. *J. Electrochem. Soc.* 138: L44–L45.
53. Leising, R.A. and E.S. Takeuchi. 1993. Solid-state cathode materials for lithium batteries: Effect of synthesis temperature on the physical and electrochemical properties of silver vanadium oxide. *Chem. Mater.* 5: 738–742.
54. Crespi, A.M. 1993. United States Patent 5,221,453.
55. Leising, R.A. and E.S. Takeuchi. 1994. Solid-state synthesis and characterization of silver vanadium oxide for use as a cathode material for lithium batteries. *Chem. Mater.* 6: 489–495.
56. Crespi, A.M. and K. Chen. 1999. United States Patent 5,955,218.
57. Leising, R.A., W.C. Thiebolt, and E.S. Takeuchi. 1994. Solid-state characterization of reduced silver vanadium oxide from the Li/SVO discharge reaction. *Inorg. Chem.* 33: 5733–5740.
58. Crespi, A.M., P.M. Skarstad, and H.W. Zandbergen. 1995. Characterization of silver vanadium oxide cathode material by high-resolution electron microscopy. *J. Power Sources.* 54: 68–71.
59. Takeuchi, E.S. and W.C. Thiebolt. 1995. United States Patent 5,389,472.
60. Takeuchi, E.S. and W.C. Thiebolt. 1996. United States Patent 5,498,494.
61. Crespi, A.M., F.J. Berkowitz, R.C. Buchman, M.B. Ebner, W.G. Howard, R.E. Kraska, and P.M. Skarstad. 1995. The design of batteries for implantable cardiac defibrillators. *Power Sources.* 15: 349–357.
62. Skarstad, P.M. 1997. *Proc. 12th Annual Battery Conf. App. Adv.* 151–155.
63. Takeuchi, E.S. and R.T. Mead. 1988. *Proc. 33rd Int. Power Sources Symp.* 667–675.
64. Gan, H. and E. Takeuchi. 1998. *Ext. Ab. Batt. Div. Electrochem. Soc.* 332.
65. Xie, J., J. Li, Z. Dai, H. Zhan, and Y. Zhou. 2004. Ultrasonic sol-gel synthesis of $Ag_2V_4O_{11}$ from V_2O_5 gel. *J. Mat. Sci.* 39: 2565–2567.
66. Xie, J., X. Cao, J. Li, H. Zhan, Y. Xia, and Y. Zhou. 2005. Application of ultrasonic irradiation to the sol-gel synthesis of silver vanadium oxides. *Ultrasonics Sonochem.* 12: 289–293.

67. Cao, X., H. Zhan, J. Xie, and Y. Zhou. 2006. Synthesis of $Ag_2V_4O_{11}$ as a cathode material for lithium battery via a rheological phase method. *Materials Letters.* 60: 435–438.

68. Ramasamy, R.P., C. Feger, T. Strange, and B.N. Popov. 2006. Discharge characteristics of silver vanadium oxide cathodes. *J. Applied Electrochem.* 36: 487–497.

69. Takada, K., T. Kanbara, Y. Yamamura, and S. Kondo. 1991. Electrochemical studies on silver vanadium bronzes. *Eur. J. Solid State Inorg. Chem.* 28: 533–545.

70. Garcia-Alvarado, F., J.M. Tarascon, and B. Wilkens. 1992. Synthesis and electrochemical study of new copper vanadium bronzes and of two new vanadium pentoxide polymorphs: β'- and ε'-V_2O_5. *J. Electrochem. Soc.* 139: 3206–3214.

71. Garcia-Alvarado, F. and J.M. Tarascon. 1994. Lithium intercalation in $Ag_2V_4O_{11}$. *Solid State Ionics.* 73: 247–254**.**

72. West, K. and A.M. Crespi. 1995. Lithium insertion into silver vanadium oxide, $Ag_2V_4O_{11}$. *J. Power Sources.* 54: 334–337.

73. Kawakita, J., Y. Katayama, T. Miura, and T. Kishi. 1997. Lithium insertion behavior of silver vanadium bronze. *Solid State Ionics.* 99: 71–78.

74. Kawakita, J., H. Sasaki, M. Eguchi, T. Miura, and T. Kishi. 1998. Characteristics of δ-$Ag_yV_2O_5$ as a lithium insertion host. *J. Power Sources.* 70: 28–33.

75. Kawakita, J., K. Makino, Y. Katayama, T. Miura, and T. Kishi. 1998. Preparation and characteristics of $(Na_yAg_{1-y})_2V_4O_{11}$ for lithium secondary battery cathodes. *J. Power Sources.* 75: 244–250.

76. Coustier, F., S. Passerini, and W.H. Smyrl. 1997. Dip-coated silver-doped V_2O_5 xerogels as host materials for lithium intercalation. *Solid State Ionics.* 100: 247–258.

77. Coustier, F., J. Hill, S. Passerini, and W.H. Smyrl. 1998. Silver-doped vanadium oxides as host materials for lithium intercalation. *Electrochem. Soc. Proc.,* 98–16: 350–355.

78. Coustier, F., S. Passerini, J. Hill, and W.H. Smyrl. 1988. Silver-doped vanadium oxides as host materials for lithium intercalation. *Mat. Res. Soc. Symp. Proc.* 496: 353–358.

79. Chu, Y.Q. and Q.Z. Qin. 2002. Fabrication and characterization of silver-V_2O_5 composite thin films as lithium-ion insertion materials. *Chem. Mater.* 14: 3152–3157.

80. Huang, F., Z. Fu, and Q. Qin. 2003. A novel $Li_2Ag_{0.5}V_2O_5$ composite film cathode for all-solid-state lithium batteries. *Electrochem. Comm.* 5: 262–266.

81. Huang, F., Z.W. Fu, Y.Q. Chu, W.Y. Liu, and Q.Z. Qin. 2004. Characterization of composite 0.5Ag:V_2O_5 thin-film electrodes for lithium-ion rocking chair and all-solid-state batteries. *Electrochem. and Solid-State Lett.* 7: A180–A184.

82. Hwang, H.S., S.H. Oh, H.S. Kim, W.I. Cho, B.W. Cho, and D.Y. Lee. 2004. Characterization of Ag-doped vanadium oxide ($Ag_xV_2O_5$) thin film for cathode of thin film battery. *Electrochim. Acta.* 50: 485–489.

83. Huang, D. 1998. *Advanced Battery Technology.* 11: 21–23.

84. Hossain, S. 1995. Rechargeable lithium batteries (ambient temperature). In *Handbook of batteries & fuel cells*, 2nd ed. D. Linden (Ed.). New York: McGraw-Hill. 36.4.

85. Linden, D. 1995. Basic concepts. In *Handbook of Batteries & Fuel Cells*, 2nd ed. D. Linden (Ed.). New York: McGraw-Hill. 1.8.

86. Linden, D. 1995. Lithium/carbon monofluoride [(Li/(CF)$_n$] cells. In *Handbook of batteries & fuel cells*, 2nd ed. D. Linden (Ed.). New York: McGraw-Hill. 14.59.

Index

General Chemistry

VANADIUM

Chemistry, Biochemistry, Pharmacology and Practical Applications

The first comprehensive resource on the chemistry of vanadium, *Vanadium: Chemistry, Biochemistry, Pharmacology and Practical Applications* has evolved from over a quarter century of research that concentrated on delineating the aqueous coordination reactions that characterize the vanadium(V) oxidation state. The authors distill information on biological processes needed to understand vanadium effects in biological systems and make this information accessible to a wide range of readers, including chemists without extensive biological training.

Primary sources documented after each chapter minimize the need to search the literature, 80 illustrations provide structural information, reaction schemes, spectra, speciation diagrams, and biochemical schemes, and 22 tables present detailed information with references to primary sources. Packed with current and authoritative information, the book covers chemistry and bioinorganic vanadium chemistry in a broad and systematic manner that engenders comprehensive understanding.

Features

- Explores the chemistry, environmental influences, pharmacological applications, and technological uses of vanadium
- Compiles the results from research on the aqueous coordination reactions characterizing the vanadium(V) oxidation state
- Details the application of NMR spectroscopy to the speciation of vanadium compounds
- Explains signal transduction processes and related biology, biochemistry, and cell biology in a way that is accessible to chemists
- Provides detailed descriptions of vanadium batteries
- Describes recent advances in the applications of the lithium/silver vanadium oxide battery, particularly for medical applications